IL
NUOVO CIMENTO
ORGANO DELLA SOCIETÀ ITALIANA DI FISICA
SOTTO GLI AUSPICI DEL CONSIGLIO NAZIONALE DELLE RICERCHE

VOL. XIX, N. 4 *Serie decima* 16 Febbraio 1961

A Contribution to the K^+-Decay Statistics.

J. K. BØGGILD, K. H. HANSEN, J. E. HOOPER and M. SCHARFF
Institute for Theoretical Physics - University of Copenhagen, Denmark

AND

P. K. ADITYA
Panjab University - Chandigarh, India

(ricevuto il 27 Luglio 1960)

Summary. — K^+-decay events in a large block of emulsions have been studied, mainly by following the charged secondaries to the ends of their ranges. Emphasis was laid on: 1) obtaining unbiassed information on the high energy end of the spectrum of the $K_{\mu 3}$ secondary; 2) a search for a decay mode $K^+ \to \mu^+ + \mu^0$; when combined with the results of earlier experiments the data were such that it should have been possible to detect the process if the branching ratio was greater than $\approx 5\%$; no positive evidence was found; 3) a search for π^+ secondaries of energy (53÷61) MeV. Among 467 decay events there were no such secondaries. The branching ratios for the various decay modes were determined. Combining our data with those of previous experiments the following values were obtained: $B(K_{\mu 2}) = (58.6 \pm 2.6)\%$; $B(K_{\pi 2}) = (21.7 \pm 2.5)\%$; $B(K_{\pi 3}) = (7.1 \pm 0.4)\%$; $B(K'_{\pi 3}) = (2.4 \pm 0.4)\%$; $B(K_{\mu 3}) = (5.5 \pm 1.1)\%$; $B(K_{\beta 3}) = (4.7 \pm 1.1)\%$. The measured scanning efficiency in this experiment was 99%.

1. – Introduction.

It is now generally accepted that there exists only one positive K-meson, which decays in many various ways. Of these the following have been iden-

tified:

(1)

Decay scheme	Name	Branching ratio %
$K^+ \to \mu^+ + \nu$	$K_{\mu 2}$	59
$K^+ \to \pi^+ + \pi^0$	$K_{\pi 2}$	22
$K^+ \to \pi^+ + \pi^+ + \pi^-$	$K_{\pi 3}$	7
$K^+ \to \pi^+ + \pi^0 + \pi^0$	$K'_{\pi 3}$	2
$K^+ \to \mu^+ + \pi^0 + \nu$	$K_{\mu 3}$	5
$K^+ \to e^+ + \pi^0 + \nu$	$K_{\beta 3}$	5

The branching ratios are not known very precisely. This is in particular true of the branching ratios to the $K_{\mu 3}$ and $K_{\beta 3}$-decay modes, which are known only to within about 30%. The energy spectra of the charged particles from these two modes are likewise only poorly determined. This again is connected with the fact that almost all the information about the K^+-decay comes from investigations in nuclear emulsion, in which $K_{\mu 3}$ and $K_{\beta 3}$-decays are difficult to study because they must be identified against a much more intense background of $K_{\mu 2}$ and $K_{\pi 2}$-decays. At emission secondaries from the last named modes appear very similar to those $K_{\mu 3}$ and $K_{\beta 3}$-decays from which a high energy μ^+ or e^+ is emitted.

Another group of questions, to which the present experimental data can only supply a rather unsatisfactory answer, concerns the possible existence of rare decay modes other than those listed in (1).

The observation among K^+-decays of two decay events from which were emitted π^+ secondaries of energies close to 61 MeV [1,2] suggested the possible existence of a decay mode $K^+ \to \pi^+ + \pi^0 + \gamma$ or, alternatively, of a two-body decay of K^+ in which a neutral particle of mass $\approx 500\, m_e$ is emitted. However, in the light of the recently discussed evidence for the existence of a particle of mass $\approx 1400\, m_e$, the D-meson [3], these two π-secondaries are now more reasonably interpreted as decay products of the D^+-meson. The results of HARRIS *et al.* and PROWSE *et al.* have nevertheless induced us to search among the K^+-secondaries for π^+-mesons in the energy range above the maximum energy of the π^+ from the $K'_{\pi 3}$-decay (53.3 MeV).

Another possible decay mode was suggested by MARSHAK and SUDARSHAN [4] who pointed out that the K^+-decay supplies the most sensitive test for the existence of a neutral μ-meson, μ^0. If such a particle exists, it is expected to give rise to a decay

(2) $$K^+ \to \mu^+ + \mu^0$$

(1) G. HARRIS, J. LEE, J. OREAR and S. TAYLOR: *Phys. Rev.*, **108**, 1561 (1957).
(2) D. J. PROWSE and D. E. EVANS: *Nuovo Cimento*, **8**, 856 (1958).
(3) T. YAMANOUCHI: *Phys. Rev. Lett.*, **3**, 480 (1959).
(4) R. E. MARSHAK and E. C. G. SUDARSHAN: *Nuovo Cimento*, **6**, 1335 (1957).

analogous to the $K_{\mu 2}$-decay $K^+ \to \mu^+ + \nu$. The kinetic energy of the μ^+ from decay (2) would, if the μ^0 mass equals that of the charged μ-meson, be 142 MeV. Thus decay (2) will produce a monoenergetic group of μ^+-mesons which, if the branching ratio is not too small, can be separated by range measurements from the ordinary $K_{\mu 2}$ group. The separation of the mean ranges in emulsion of the two range distributions will be ≈ 2 cm, which is about three standard deviations of the range straggling for μ-mesons at these energies. Previous range data provide very little information on this point.

2. – Methods of identification of decay modes and statistical bias.

In photographic emulsion, which is the instrument of the present investigation, the mode by which a given K^+-meson decays is revealed by the appearance of the tracks of the charged secondary particles. In a study of decay statistics, errors may therefore be introduced at two stages: during the scanning, since some decay modes are more conspicuous than others, and during the identification of the various decay modes. To control the scanning error one can collect stopped K-mesons without use of the decay event. If a secondary particle is found on all these K-mesons, no scanning bias can exist. The process of identification is discussed below.

When identifying the secondary particle, the measurable quantities are ionization and multiple scattering as functions of the distance from the K-decay, and, if the particle is stopped, its total range and type of decay.

The only decay mode which is readily identified at the point of decay is the $K_{\pi 3}$-decay, which is characterized by the emission of three non-relativistic charged particles.

In Table I are listed the energy, velocity and $p\beta c$ of the single charged secondaries from the other five decay modes.

TABLE I.

	Kinetic energy of the charged secondary (MeV)	β of the charged secondary	$p\beta c$ of the charged secondary (MeV)
$K_{\mu 2}$	152	0.91	213
$K_{\pi 2}$	109	0.82	178
$K_{\mu 3}$	$0 \div 134$	$0 \div 0.89$	$0 \div 190$
$K_{\beta 3}$	$0 \div 228$	$0 \div 1$	$0 \div 228$
$K'_{\pi 3}$	$0 \div 53.3$	$0 \div 0.69$	$0 \div 91$

This table gives an idea of the degree of difficulty involved in separating the few high energy $K_{\mu 3}$ and $K_{\beta 3}$-secondaries from the intense background of

secondaries due to $K_{\mu 2}$ and $K'_{\pi 2}$-decays. In fact, complete separation cannot be obtained by measurements close to the point of emission (the immediately accessible region). On the other hand, a secondary particle can obviously be identified uniquely if its track can be traced through the emulsion stack until the particle stops.

When the particle track for some reason is not followed to the end of its range and decay, the possibility of identification depends strongly on the velocity of the particle at the point where the track is left. It is thus clear that, if the identification of the secondaries from the various decay modes is to be made with the same degree of reliability, the distance along which the secondary track must be followed varies widely. In a stack of finite size this fact tends to favour the identification of some types of decay against others.

To avoid such bias the stack must be so large that it is possible to select a suitable K-meson sample, chosen at random with respect to the type of decay and such that any secondary particle has a track length sufficient to allow unique identification by the method used. Thus, in a given stack the sample of K-decays may be increased if in return more care and labour are invested in measurements of ionization and scattering. However, this procedure is limited by the maximum available resolving power of these methods, and in practice one aims at some compromise between limited statistics and uncertainties in identification. These uncertainties, when present, will, as mentioned above, primarily affect the fast secondaries of the rare decay modes.

The above considerations may be illustrated by the work of the Berkeley and Dublin groups ([5,6]). The Berkeley investigation is based on one sample with long distance tracing and identification, partly by following to rest, and another sample which is handled by ionization measurements. The Dublin paper treats all tracks on an equal footing: *i.e.*, by very careful measurements of ionization and scattering on comparatively short segments of tracks.

In the present work emphasis was laid on resolving power rather than on large samples. Accordingly we selected a sample of K-decays in which any secondary particle was known to have all (or most) of its range in the emulsion block, even if the total range was the maximum possible (≈ 20 cm). A further reason for this type of approach was our wish to collect stopped $K_{\mu 2}$ secondaries in order to shed some light on the question of the μ^0 (*).

([5]) R. W. BIRGE, D. H. PERKINS, J. E. PETERSON, D. H. STORK and M. W. WHITEHEAD: *Nuovo Cimento*, **4**, 834 (1956).

([6]) G. ALEXANDER, R. H. W. JOHNSTON and C. O'CEALLAIGH: *Nuovo Cimento*, **6**, 478 (1957).

(*) We had also the purpose of measuring precisely the ranges of $K_{\mu 2}$ and $K_{\pi 2}$ secondaries, for use in a study of stopping power. This work will be published separately in Mat. Fys. Medd. Dan. Vid. Selsk.

In a stack of reasonable size only a very limited fraction of the K-decays contributed to the above mentioned sample. Fortunately, however, the lower energy (lower range) parts of the decay spectrum do not require to be studied on a sample defined as above. We have therefore selected two other samples of K-decay in which any secondary particle was known with near certainty to stop in the emulsion block if its total range was less than 12 cm or 6 cm, respectively. These latter samples could be used to study the medium and lower range part of the decay spectrum.

To select such samples in a given emulsion stack it is necessary to know the stopping probability for the secondaries in terms of their initial conditions (point of origin and emission direction in the stack). Of course, this stopping probability depends also on the mass and energy of the emitted particle. For the purpose of stack design the stopping probabilities were estimated from multiple scattering theory, and checked by observations on the scattering of μ-mesons from π-μ decays. A further check of these estimates was of course obtained as a result of later observations in the course of this experiment (*).

3. – Emulsion stack. Exposure and scanning.

The minimum size of the stack is determined by the requirement that it should be possible to find some K-decays, such that the secondary particle from the decay is almost certainly known to stop in the stack, even if it has the maximum possible range (≈ 20 cm).

This requirement leads to the result that the stack must be at least ≈ 10 cm thick (*i.e.*: more than 165 emulsion pellicles (600 μm)). As a reasonable compromise between cost and useful fraction of K-decays we have chosen a stack size of 200 600 μm Ilford G-5 emulsion pellicles (28×31) cm^2, giving a sensitive volume of 10.4 liters.

The stack was exposed to a K^+ beam of momentum 350 MeV/c from the Berkeley Bevatron. The K-mesons were sent into a corner of the stack with direction parallel to the 31 cm edge. The range of the K-mesons was (7 ± 1.5) cm and the width of that part of the beam which entered the stack (half of it missed the stack) was about 8 cm. The density of K-mesons is about 75 per plate.

The beam was unfortunately contaminated by protons with a continuous energy spectrum extending from 0 to 175 MeV. This background of protons made the scanning somewhat difficult. The scanning procedure used was as follows:

(*) A note on this topic will be published shortly.

Tracks with directions close to the beam direction and with the correct blob density were picked up on a line perpendicular to the beam direction, 5.5 cm inside the stack. (This is ≈ 1.5 cm before the main stopping region of the K-mesons.) The track was followed until either *a*) it appeared clear from its characteristics that it was a proton track; it was then abandoned before the end point was seen, or *b*) it stopped. Provided that the stopping point was more than 10 μm from the surfaces of the emulsion, a stopped track was examined for a secondary track connected with its end point. Such a secondary was found on 90% of the end points, thus identifying the followed track as that of a K-meson. Careful mass measurements (gap-density and range) were performed on the residual 10% of the tracks followed to rest, and in this way proton and K-meson tracks were clearly separated. The end points of the tracks thus identified as K-mesons were again scrutinized and in almost every instance the secondary track was found. Tracks whose identity remained doubtful (identified by mass measurements as K-mesons, but with no secondary track observed) constitute 1.2% of the total sample (15 without and 1257 with secondaries). The ensemble studied is thus very clean.

When a track was identified as that of a K-meson with a single charged secondary whose projected track length per plate was more than 1 mm, the direction of emission and blob density of the secondary were measured. The blob density was measured by counting the number of blobs on 500 μm projected track length in a region of the emulsion layer more than 50 μm from both the surfaces of the emulsion. If this could not be done in the plate containing the K-decay, the track was followed to the next plate, where the blob count was then made.

4. – Classification of decays.

All the K-decays, other than $K_{\pi 3}$-decays, were classified according to the position in the emulsion stack of the decay and the direction of emission of the charged secondary particle, in one of the following classes:

Class A consists of decays which occur at such a position and from which the secondary particle is emitted in such a direction that from these data alone it was known that the probability of the secondary particle stopping in the emulsion was greater than 75%, even if the secondary was a μ-meson of energy 134 MeV (range 17.8 cm), which is the highest possible energy (range) for a μ-meson from a $K_{\mu 3}$-decay.

Class B consists of decays, which are not in class A, and with secondaries whose stopping probability (in terms of the same characteristics as above) is greater than 75%, even if the secondary is a μ-meson of range 12 cm (energy

101 MeV). To avoid tracing steep tracks a further requirement for accepting a decay in class B has been that the projected track length of the secondary at emission should exceed 1 mm per plate.

It may be mentioned here that a π-meson of the same range as a μ-meson suffers less scattering along its path than does the μ-meson. The stopping probability of a π-meson from a $K_{\pi 2}$-decay (range 11.7 cm) of class B is thus much greater than 75%.

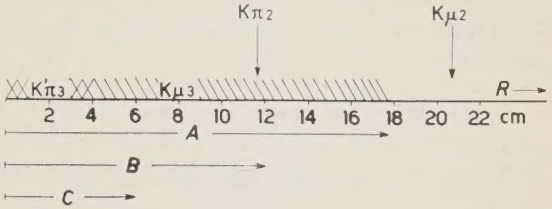

Fig. 1. – The schematic range spectrum of the secondaries from K⁺-decay is compared with the « ranges » of the three classes.

Class C consists of decays, which are not included in classes A or B, and from which any secondary has a stopping probability greater than 75%, even if it is a μ-meson of range 6 cm (energy 63 MeV). Decays with steep secondary tracks were excluded using the same criterion as for B.

Class O comprises all decays which are not in classes A, B or C. For practical reasons subclasses A′, B′ and C′ were selected as described in the next section.

The total sample of K-decays was classified as shown in Table II.

TABLE II.

	Number of decays
$K_{\pi 3}$-decays	98
Class A	80
Class B	83
Class C	268
Class O	728
Total number of identified K-decays	1257

Number of tracks of particles to which K mass was attributed but without an observed secondary: 15.

5. – Measurements on the secondary tracks.

Decays of class A. – Secondary tracks from decays of class A were followed to their end or as far as possible, if the projected angle between the starting direction of the track and the beam direction was more than 2°. This restricted class is called A′.

In some instances the tracing of a track was abandoned before the stopping point was reached. The reason was then one of those listed below:

1) The track ends in a star, so that the secondary particle is identified as a π-meson. To refer this to either $K_{\pi 2}$ or $K'_{\pi 3}$, a blob count was sometimes necessary.

2) After following for some distance the tracks showed the characteristic increase of scattering without a corresponding rise in ionization, which identified the secondary particle as a positron.

3) After some distance the track became so steep that tracing was very difficult and uncertain.

4) The track left the stack.

5) Strong, local distortion prevented tracing from one plate to the next.

On all secondary tracks which were not followed to the end, a blob count was made as far away as possible from the K-decay. Almost all these secondaries could be referred uniquely to one of the K-decay modes (1).

The results of measurements on class A′ secondaries are listed in Table III.

TABLE III. - *Class* A′.

Total number of decays	75
Decays identified by following the secondary to rest: $K_{\mu 2}$ 36; $K_{\pi 2}$ 14; $K_{\mu 3}$ 2	52
$K_{\pi 2}$ decays identified by interaction of the secondary and blob-count	3
$K_{\beta 3}$ decays identified by the scattering of the secondary	3
$K_{\mu 2}$ decays identified by blob-counting after 20.9; 20.8; 20.3; 17.3; 15.7; 15.6; 15.5; 14.7; 12; 12; 11.5; 11; 9; 9; 9 cm from K-decay	15
K-decays not identified uniquely: secondary traced 2.7 cm / secondary traced 0.3 cm both consistent with $K_{\mu 2}$-decay	2

Decays of class B. – From class B was selected a subclass B′, consisting of those decays having secondaries satisfying the two conditions: 1) the projected track length is more than 2 mm per plate, and 2) the projected angle to the beam direction is more than 10°.

The secondary tracks from class B′ have all been followed either to the stopping point or so far that it was possible, by counting 300 blobs, to be sure (3 standard deviations) that the secondary was not a μ-meson of range less than 12 cm, nor a π-meson of range less than 18 cm. All non-stopping tracks have been followed at least 6 cm (average 8 cm).

The results of measurements on class B′ secondaries are listed in Table IV.

TABLE IV. – *Class* B′.

Total number of decays		36
Decays identified by following the secondary to rest	$K_{\pi 2}$ 7 $K_{\mu 3}$ 2 $K'_{\pi 3}$ 1	
		10
$K_{\pi 2}$-decay identified by interaction of the secondary and blob-count		1
$K_{\beta 3}$-decay identified by the scattering of the secondary		1
Decays with secondary tracks followed more than 6 cm (average 8 cm) and such that ionization measurements exclude a total (μ) range less than 12 cm		24

Decays of class C. – A subclass C′, consisting of those decays with secondaries which have a projected track length of more than 2 mm per plate, was selected from class C.

In this class we were interested in selecting and identifying the few secondaries with range less than 6 cm. A considerable fraction of the large background of fast secondaries could immediately be distinguished by a low blob-density at decay. Thus, the secondaries which were known from the blob-count at decay (allowing for fluctuations of three standard deviations) to have ranges greater than 6 cm, if μ-mesons, were not followed. The remainder of the secondaries were followed to rest or until a count of 300 blobs excluded the possibility of the particle stopping within the class limit (6 cm μ range).

Table V lists the results of measurements on class C′ secondaries.

TABLE V. – *Class* C′.

Total number of decays		128
Decays identified by following the secondary to rest	$K'_{\pi 3}$ 6 $K_{\mu 3}$ 3	
		9
Decays with secondaries shown not to have (μ) ranges less than 6 cm (*)		119

(*) Of these 119 tracks 44 were followed on the average 3 cm. Three $K_{\pi 2}$ stars were observed.

6. – Grey secondaries.

The π-mesons from $K'_{\pi 3}$-decays and the 61 MeV π-mesons referred to in the introduction are so highly ionizing at their point of emission that these decays can easily be extracted from the total classes A, B and C.

To this end, secondary tracks from class A+B+C were followed if their ionization at decay was compatible with that of a π-meson of range 5 cm or

less. The cut-off was then chosen at a blob-density three standard deviations below that expected for the fastest $K'_{\pi 3}$-secondary (2.5 standard deviations below that of a π-meson with 5 cm range).

The result of this following of « grey tracks » was the observation of 6 $K'_{\pi 3}$ and one $K_{\mu 3}$-decays which were not contained in classes A′, B′ or C′. No π-meson was found which could not be attributed to the $K'_{\pi 3}$-decay mode.

7. – Results on branching ratios and energy spectra.

$K_{\pi 3}$-*decay.* – The chance of overlooking any of the secondaries from a $K_{\pi 3}$-decay is so remote that we disregard it. Thus the $K_{\pi 3}$ branching ratio is obtained from the 98 $K_{\pi 3}$-decays observed in the total simple of 1257 K-decays with observed secondaries plus 15 « K tracks » with no observed secondary,

$$B(K_{\pi 3}) = \frac{98}{1272} = (7.7 \pm 0.8)\,\% .$$

Here and in the following we write the branching ratios of the K-decay as $B(K_{\mu 2})$, $B(K_{\pi 2})$, etc.

Other decays. – An investigation of a sample of K-decays—other than $K_{\pi 3}$—chosen randomly with respect to the other decay modes gives unbiassed information on the relative frequency of a specified group of K-decays, provided that the sample is investigated to such a degree that any decay of the sample belonging to the given group is recognized as such. The largest sample which satisfies this requirement for a certain group of decays is called in the following the « proper sample » corresponding to the group in question. The proper sample is extracted from the 1159 decays which, together with the $K_{\pi 3}$-decays, constitute our experimental material.

K-*decays with a single* π^+ *secondary of energy less than* 61 MeV ($K'_{\pi 3}$-*decay*). – The proper sample corresponding to K-decays with a single π^+ secondary of energy up to 61 MeV (5 cm range) is composed of the events listed in Table VI.

TABLE VI.

	Number of decays
Class A	80
Class B	83
Class C	268
	431

Among these decays the following 13 π^+ secondaries with ranges less than 5 cm were observed (Table VII).

TABLE VII.

Range mm	2.05	2.52	2.88	4.12	4.95	5.84	8.17	9.03	9.38	9.96	19.60	22.04	24.09
Energy MeV	9.4	10.6	11.4	13.9	15.5	17.2	20.6	21.8	22.4	23.2	34.6	37.6	39.4

(No π^+ with range between 2.4 cm and the range of the $K_{\pi 2}$ (12 cm) has been observed).

None of these π^+-secondaries fall outside the energy spectrum of π^+ from $K'_{\pi 3}$. They must therefore all be interpreted as being due to $K'_{\pi 3}$-decays. The present work thus allows one to say that in the proper sample of 431 decays there are no secondary π^+-mesons emitted with energies between the upper limit of the $K'_{\pi 3}$ spectrum and 61 MeV. Taking into account the 7.7% $K_{\pi 3}$-decays which were not included in the proper sample, we obtain the branching ratio

$$B(K'_{\pi 3}) \frac{13}{167} = (2.8 \pm 0.8)\%.$$

Fig. 2 shows the energy spectrum of the π^+ from $K'_{\pi 3}$-decays, compiled from the data of Table VIII. This is compared with the calculated phase-space spectrum.

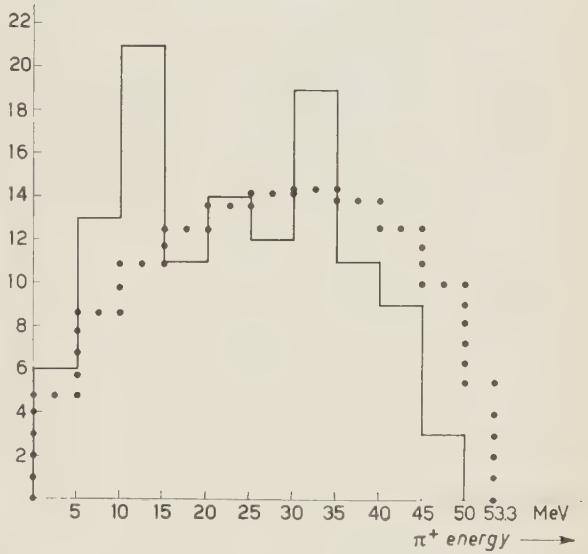

Fig. 2. – The energy spectrum of the π^+-meson from the $K'_{\pi 3}$-decay. The full line histogram shows the collected data from Columbia (7), Dublin (6), Bristol (8), and the present experiment. The dotted histogram is calculated from the phase-space distribution.

TABLE VIII.

Group	Reference	Number of $K'_{\pi 3}$-decays
Columbia	(7)	69
Dublin	(6)	26
Bristol	(8)	11
Copenhagen (present work)		13
	Total	119

(7) G. HARRIS, J. OREAR and S. TAYLOR: Roch. Conf. Rep., VIII-26 (1957).

(8) B. BHOWMIK, D. EVANS, D. J. PROWSE, F. ANDERSON and A. KERNAN: *Nuovo Cimento*, **8**, 147 (1958).

It will be noticed that there appears to be a lack of high energy secondaries as compared with the phase-space distribution.

$K_{\mu 3}$-*decay.* – Any $K_{\mu 3}$-decay of classes A′, B′, or C′ was identified if the secondary μ-meson had a total range less than 17.8 cm, 12 cm or 6 cm, respectively. These μ-ranges correspond to the kinetic energies 134 MeV (the maximum energy of a μ-meson from a $K_{\mu 3}$-decay) 101 MeV and 63 MeV. In the special investigation of the grey secondaries any $K_{\mu 3}$-decay of the total classes A, B and C has been identified if the μ-meson had a kinetic energy less than 40 MeV corresponding to a range of 3 cm. All observed $K_{\mu 3}$-decays have been identified by the range and decay of the secondary μ-meson. This ensures unique identification (*).

Thus the different parts of the $K_{\mu 3}$ spectrum have been studied without bias on different samples of K-decays. The complete $K_{\mu 3}$ spectrum can then be constructed from the observed $K_{\mu 3}$ ensemble by giving the different parts of this ensemble weights according to the size of the proper sample of K-decays contributing to the part in question.

The different energy regions, the proper samples of K-decays contributing to each region, and the corresponding weights to be given to observed $K_{\mu 3}$-decays falling in the region, are listed in Table IX.

TABLE IX.

Range region	Energy region	Proper sample of K-decays contributing	Weights
(0 ÷ 3) cm	(0 ÷ 40) MeV	A + B + C	$w_1 = 1$
(3 ÷ 6) cm	(40 ÷ 63) MeV	A′ + B′ + C′	$w_2 = \dfrac{N}{N_{A'}+N_{B'}+N_{C'}}$
(6 ÷ 12) cm	(63 ÷ 101) MeV	A′ + B′	$w_3 = \dfrac{N}{N_{A'}+N_{B'}}$
(12 ÷ 17.8) cm	(101 ÷ 134) MeV	A′	$w_4 = \dfrac{N}{N_{A'}}$

$N_{A'}$, $N_{B'}$, $N_{C'}$, (N_A, N_B, N_C) are numbers of K-decays in the classes A′, B′, C′ (A, B, C) and $N = N_A + N_B + N_C$.

The numbers are, as already quoted,

$N_A = 80$	$N_{A'} = 75$	$w_2 = 1.8$
$N_B = 83$	$N_{B'} = 36$	$w_3 = 3.9$
$N_C = 268$	$N_{C'} = 128$	$w_4 = 5.8$
$N = 431$	239	

(*) The possibility of misinterpreting a $K'_{\pi 2}$ or $K'_{\pi 3}$-secondary π-meson, decaying in flight, as a $K_{\mu 3}$-secondary is discussed later.

With one exception, described below, the $K_{\mu 3}$-decay was rejected if the emitted μ-meson from a decay of a definite class was shown on following to have a range greater than the class limit. The rule was used on one example, a $K_{\mu 3}$-decay of class C with a secondary of 8 cm range.

The total number of K-decays among which the weighted $K_{\mu 3}$-decays have been found thus consists of N plus the corresponding number of $K_{\pi 3}$-decays = = 467 K-decays.

The observed, unbiassed $K_{\mu 3}$-secondaries are listed in Table X.

TABLE X. – *Table of observed* $K_{\mu 3}$*-secondaries.*

Secondary to decay of class	Range (mm)	Energy (MeV)	Weight
C′	4.95	13.8	1
C (not C′)	5.30	14.4	1
C′	6.36	15.9	1
B′	44.6	52.2	1.8
C′	63.5 (*)	66.6	1.8
A′	63.8	66.7	3.9
B′	114.0	97.0	3.9
A′	165.0	128.0	5.8
			20.2

(*) Rigorously, this particle, which is secondary to a K-decay of class C′, should have been rejected as its range is more than 60 mm, which is the class limit for unbiassed identification. However, as its range is only very little greater than this limit, the bias introduced by including it with the weight which it would have been given if its range had turned out to be 60 mm or less, instead of the actual 63 mm, is vanishing.

The effective total number of $K_{\mu 3}$-decays among the 467 K-decays is the sum of the weights from Table X, while the corresponding statistical error is the square root of the sum of the squares of the weights. Thus the effective number of $K_{\mu 3}$-decays is 20.2 ± 8.6 and the resulting branching ratio

$$B(K_{\mu 3}) = (4.3 \pm 1.8)\ \% .$$

Returning to the question of the uniqueness of the identification of $K_{\mu 3}$-decays, it must be noted that the bare observation that the secondary track ends like that of a μ-meson of range less than 17.8 cm does not exclude the possibility of misinterpretation. A $K_{\pi 2}$ or a $K'_{\pi 3}$-decay, the secondary π^+ of which decayed in flight, could be confused with a $K_{\mu 3}$-decay.

The probability that the π-meson from a $K_{\pi 2}$ event decays in flight is 1.7 %. With a $K_{\pi 2}$ branching ratio of 22 % this process leads to secondary tracks stopping as μ-mesons in 0.4 % of all K-decays; *i.e.*, a frequency of one tenth

of the $K_{\mu 3}$ frequency. (The corresponding frequency resulting from the rarer and slower π-mesons from $K'_{\pi 3}$-decays is small enough to be neglected.) The total track length from K-decay to the stopping point of the μ-meson may vary between 3.1 cm and 17.8 cm, depending on the velocity of the π-meson at the π-μ decay point and the orientation of the π-μ decay in the centre of mass system.

Each secondary which ends like a μ-meson from a $K_{\mu 3}$-decay must therefore be investigated individually to find out whether it could be due to the above source. This possibility may sometimes be ruled out by measurement of the ionization of the secondary track close to the K-decay, while in other cases it may be necessary to study all sudden changes of direction along the track, in conjunction with the total length of the track and the position on the track of each single scatter.

All events recorded as $K_{\mu 3}$-decays have been carefully examined and it has not been possible to show that any of them could be interpreted as being due to $K_{\pi 2}$-secondaries decaying in flight.

The observation of the 128 MeV $K_{\mu 3}$-secondary shows definitely that the $K_{\mu 3}$ spectrum is not vanishing at μ energies close to the maximum energy.

Earlier information on the $K_{\mu 3}$ spectrum has been obtained from the work of the Dublin group ([6]), the Berkeley group ([5]) and the Columbia group ([9]). The results of the Columbia group are relevant to the shape of the spectrum only up to 63 MeV.

The results of the present work combined with those of the Dublin group are presented in Table XI.

TABLE XI. – *Partial branching ratios to different energy regions of the* $K_{\mu 3}$ *spectrum.*

Energy interval (MeV)	0÷26.8	26.8÷53.6	53.6÷80.4	80.4÷107.2	107.2÷134
Dublin results	2/358	5/358	5/358	5/358	3/358
Present results	3/467	1/361	2/167	1/112	1/81
Weighted mean	5/825 $= 6.1 \cdot 10^{-3}$	6/719 $= 8.3 \cdot 10^{-3}$	7/537 $= 13.0 \cdot 10^{-3}$	6/470 $= 12.8 \cdot 10^{-3}$	4/439 $= 9.1 \cdot 10^{-3}$

The partial branching ratios are given in the table as fractions n/N. Here n denotes the number of observed $K_{\mu 3}$-secondaries in the energy interval in

([9]) S. TAYLOR: Nevis Cyclotron Lab. Rep., R-223 (1958).

question, while N is the total number of K-mesons in the sample used. In the Dublin experiment a single sample is used for the complete spectrum. The various samples used in the present experiment can be found (*) from the information in Table IX. The weighted mean (combined value) is obviously $(n_D+n_d)/(N_D+N_d)$.

The combined results are compared with the phase-space spectrum in Fig. 3. The statistical errors expected from the size of the samples used have been included on the diagram. The shaded part of the experimental histogram represents two Dublin events which could not be resolved with certainty from the $K_{\mu 2}$ group. These two events are not used by the Dublin group when calculating their branching ratios, and we have not included them in Table XI.

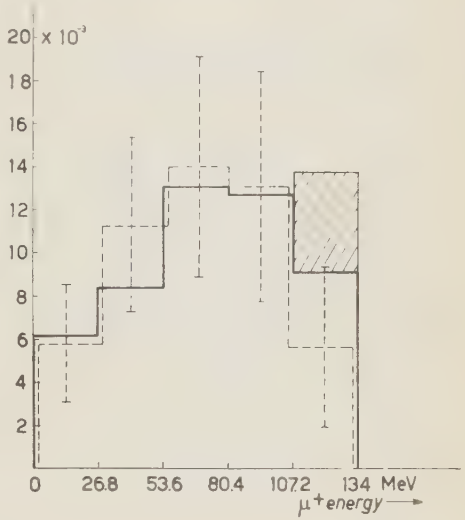

Fig. 3. – The $K_{\mu 3}$ spectrum. The combined data of Dublin ([6]) and the present experiment (full line histogram) are compared with the phase-space distribution (broken line) and the expected statistical errors (shaded region, see text).

$K_{\beta 3}$-*decay*. – On the basis of the track length of secondaries of classes A′ and B′ actually followed, we estimate that the probability that a positron secondary among these events escaped observation is less than 5%. We therefore choose as our proper sample class A′+B′, excluding the two events of class A′ whose secondaries were followed less than 3 cm.

The proper sample of K-decays relevant to the determination of the $K_{\beta 3}$ branching ratio is composed of those events listed in Table XII.

TABLE XII.

	Number of decays
Class A′ (excluding the two decays with secondaries followed only 2.7 and 0.3 cm)	73
Class B′	36
	109

(*) A special procedure is needed when an energy interval contains a boundary between two of the energy regions of Table IX. Two samples then contribute to this energy interval. If N_1 and N_2 be the sizes of these samples and Δ_1 and Δ_2 the corresponding parts of the energy interval, the denominator in Table XI is the effective sample size $N=(N_1\Delta_1+N_2\Delta_2)/(\Delta_1+\Delta_2)$.

Among these decays 4 $K_{\beta 3}$-decays were observed. Taking $K_{\pi 3}$-decay into account this leads to the branching ratio

$$B(K_{\beta 3}) = (3.4 \pm 1.7)\ \% .$$

No attempt has been made to determine the energy of emission of these $K_{\beta 3}$-secondaries.

$K_{\mu 2}$ *and* $K_{\pi 2}$*-decays.* – As the proper sample for $K_{\mu 2}$ and $K_{\pi 2}$-decays we use class A′ + B′. This procedure is not strictly correct because those decays of class B′ of whose secondaries we know only that the range is greater than 12 cm may be either $K_{\mu 2}$ or $K_{\mu 3}$-decays. Using the observed $K_{\mu 3}$ spectrum, we can estimate the ratio of $K_{\mu 3}$ to $K_{\mu 2}$-decays in this sample to be about 1 %. We neglect this small contamination—and the even smaller contamination of positron secondaries of class B′ not recognized as such—and assume that all of the 24 long range class B′ secondaries are due to $K_{\mu 2}$-decays.

The composition of the proper sample and the numbers of $K_{\mu 2}$ and $K_{\pi 2}$-decays are shown in Table XIII.

TABLE XIII.

	Number of decays	Number of $K_{\pi 2}$-decays	Number of $K_{\mu 2}$-decays
Class A′	74 (*)	17	51
Class B′	36	8	24
Class A′ + B′	110	25	75

(*) Excluding the decay whose secondary was only observed for 0.3 cm.

The ratio between the $K_{\mu 2}$ and $K_{\pi 2}$ frequencies is thus found to be

$$B(K_{\mu 2})/B(K_{\pi 2}) = 3.0 \pm 0.7 .$$

Taking the $K_{\pi 3}$ decays into account the individual branching ratios determined directly are

$$B(K_{\mu 2}) = (64 \pm 13)\ \%$$

and

$$B(K_{\pi 2}) = (21 \pm 6)\ \% .$$

These branching ratios are, however, determined with greater precision from the ratio $B(K_{\mu 2})/B(K_{\pi 2})$ and the sum

$$B(K_{\mu 2}) + B(K_{\pi 2}) = 100 - (B(K_{\pi 3}) + B(K'_{\pi 3}) + B(K_{\mu 3}) + B(K_{\beta 3})) .$$

Using this method we find

$$B(K_{\mu 2}) + B(K_{\pi 2}) = (82 \pm 3)\ \%$$
$$B(K_{\mu 2}) = (61 \pm 4)\ \%$$
$$B(K_{\pi 2}) = (20 \pm 4)\ \% .$$

K-*decay with an associated electron pair.* – Among the 1257 events examined we have found three events with an associated electron pair. Taking the branching ratios as determined into account, we would expect such pairs to be associated with 6 ± 3 events. Two were associated with $K_{\pi 2}$ and one with $K_{\mu 3}$-decays.

8. – The range distribution of $K_{\mu 2}$-secondaries and the possible existence of a neutral μ-meson.

As mentioned in the introduction, a hypothetical decay

(2) $$K^+ \to \mu^+ + \mu^0$$

would produce secondary charged μ-mesons of kinetic energy 142 MeV corresponding to a range of 188 mm. These values are derived on the assumption that $m_{\mu^0} = m_{\mu^+}$. The energy and range of the μ^+ are, however, rather insensitive to the mass of the μ^0. Thus a 5 MeV decrease of the μ^0 mass results in an increase of the μ^+ range of about 2 mm. As the range of secondaries from the ordinary $K_{\mu 2}$-decay is 207 mm, we shall disregard effects resulting from a small mass difference between the μ^+ and the hypothetical μ^0 in the following discussion.

The ranges quoted above are mean ranges. For μ-mesons of these energies the ranges are distributed with a standard deviation of 2.8% or 6 mm, corresponding to one third of the difference between the two mean ranges mentioned. Thus the range straggling is such that the secondaries from decay (2) cannot appear as a separate peak in the range distribution of K^+-secondaries. The separation of the mean ranges is nevertheless so large that there is a reasonable possibility of detecting decay mode (2) by investigating the shape of the $K_{\mu 2}$ peak.

The range distribution (normalized to standard emulsion density) of the

36 stopped $K_{\mu 2}$-secondaries is shown in Fig. 4. The observed distribution has a shape which might seem to support the existence of decay (2). However, the fact that at the velocities in question the range distribution of a monoenergetic beam of particles is somewhat skew must be taken into account. The skewness is associated with the relativistic increase of the maximum possible energy transfer to the electrons of the stopping medium (*).

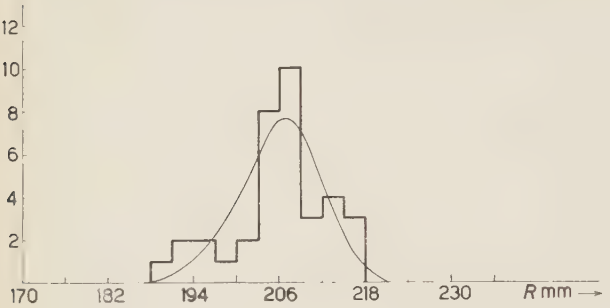

Fig. 4. – The distribution of the ranges of 36 stopped μ-mesons from $K_{\mu 2}$-decay. This is compared with a distribution calculated from the theory of range straggling, assuming a monoenergetic μ-meson source.

We have made a detailed calculation of the range distribution of the $K_{\mu 2}$-secondaries. This is shown as the smooth curve in Fig. 4. As the absolute position of the calculated curve depends on the emulsion stopping power, which is not precisely known, the curve has been drawn in such a way that its mean range is the same as the mean range of the observed distribution.

As can be seen from the figure, there is no positive evidence for decay mode (2). This negative result is not surprising, as our sample of $K_{\mu 2}$ ranges is not larger than the collection of previously published ranges. Counting only those publications which allow conversion to standard density the previous sample amounts to 33 events.

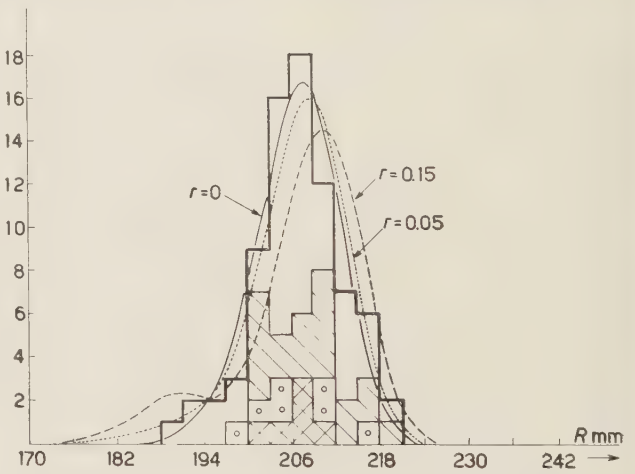

Fig. 5. – The combined range distribution of fast μ-mesons from K^+-decay. ⊠ M.I.T. ([11]); ◫ *G*-stack ([10]); ▨ Berkeley ([6]); □ present experiment plus nine unpublished Copenhagen events. The resulting histogram is compared with curves calculated on the assumption that $r = 0$, 0.05 and 0.15. The significance of r is explained in the text.

(*) This problem is discussed in greater detail in a coming paper (see footnote p. 624).

To find an upper limit for the frequency of decay (2) relative to the ordinary $K_{\mu 2}$-decay we have collected a sample consisting of the « $K_{\mu 2}$ ranges » of this experiment, 9 ranges measured previously in this laboratory (not published) and the above mentioned 33 published events, all normalized to standard emulsion density.

The combined distribution is shown in Fig. 5. It is compared with the range distributions calculated for various assumed values of the relative frequency, r (ratio of $K^+ \to \mu^+ + \mu^0$ to $K^+ \to \mu^+ + \nu$). As can be seen from the figure, the experimental range distribution is very well fitted with $r = 0$ and is hardly consistent with $r > 0.1$.

9. – Present knowledge of the branching ratios of the K+-decay.

Of the many experiments ([5-14]) yielding information on the branching ratios of the K+-decay only a few have been designed for this specific purpose. Thus the scanning efficiency of some of the experiments was low and often not known precisely. The resolution of the identification method used also differs widely among the various experiments.

If all the available information on the branching ratios is combined, the resulting statistical errors are so small that even moderate systematic errors become important. In this situation we find it most reasonable to combine only the results of those experiments known to have a high scanning efficiency.

The only published work, known to us, in which resolving power is good and the scanning efficiency is directly measured is that of ALEXANDER *et al.* ([6]) (loss of secondaries $\approx 1\%$) and that of BIRGE *et al.* ([5]) (loss of secondaries $\approx 15\%$). In the present experiment (loss of secondaries $= 1.2\%$) and in the Dublin experiment the scanning efficiency is so high that errors introduced by a scanning bias can be neglected. In the Berkeley experiment the possible error is not necessarily negligible, and the authors have made a correction for it. This correction is based on the total scanning loss which is not necessarily the same as the loss in the geometrically defined sample (flat tracks) which is actually used for the determination of the branching ratios.

([10]) G-Stack Collaboration: *Nuovo Cimento*, **2**, 1063 (1955).

([11]) D. M. RITSON, A. PEVSNER, S. C. FUNG, M. WIDGOFF, G. T. ZORN, S. GOLDHABER and G. GOLDHABER: *Phys. Rev.*, **101**, 1085 (1956).

([12]) J. CRUSSARD, V. FOUCHÉ, J. HENNESSY, G. KOYAS, L. LEPRINCE-RINGUET, D. MORELLET and F. RENARD: *Nuovo Cimento*, **3**, 731 (1956).

([13]) T. F. HOANG, M. F. KAPLON and G. YEKUTIELI: *Phys. Rev.*, **102**, 1185 (1956); **105**, 278 (1957).

([14]) M. BRUIN, D. J. HOLTHUIZEN and B. JONGEJANS: *Nuovo Cimento*, **9**, 422 (1958).

The branching ratios obtained by BIRGE *et al.* by correction of the observed frequencies may therefore be overcorrected. This suspicion is supported by the comparison of the values of the branching ratios obtained by the Berkeley group with those obtained by Dublin and ourselves.

The branching ratios to the four rarest decay modes obtained in the Dublin experiment and the present work, and the weighted means of these values, are listed in Table XIV. The values obtained by the Berkeley group are quoted for comparison.

TABLE XIV. – *Branching ratios in* %.

	$B(K_{\pi 3})$	$B(K'_{\pi 3})$	$B(K_{\mu 3})$	$B(K_{\beta 3})$
1) Dublin	6.8 ± 0.5	2.2 ± 0.4	5.9 ± 1.3	5.1 ± 1.3
2) Present work	7.7 ± 0.8	2.8 ± 0.8	4.3 ± 1.8	3.4 ± 1.7
Weighted mean	7.1 ± 0.4	2.4 ± 0.4	5.5 ± 1.1	4.7 ± 1.1
3) Berkeley	5.6 ± 0.4	2.1 ± 0.5	2.8 ± 1.0	3.2 ± 1.3

The first three decay modes listed in Table XIV can produce a slow charged secondary. The sum of the corresponding branching ratios obtained by 3), (10.5 ± 1.2)%, is seen to be scarcely consistent with the combined results of 1) and 2), (15.0 ± 1.2)%. The difference is reduced if BIRGE *et al.*'s corrections are omitted.

We therefore find it most correct to use only the combined data of ALEXANDER *et al.* and the present work when finding « best values » of the branching ratios. The two experiments lead to the values of the ratio $B(K_{\mu 2})/B(K_{\pi 2})$ given in Table XV.

TABLE XV.

	$B(K_{\mu 2})/B(K_{\pi 2})$
Dublin	2.5 ± 0.4
Present work	3.0 ± 0.7
Weighted mean	2.7 ± 0.4

For comparison the (corrected) value quoted from BIRGE *et al.* is 2.1 ± 0.3. Using the value $B(K_{\mu 2})/B(K_{\pi 2}) = 2.7 \pm 0.4$ and the sum

$$B(K_{\mu 2}) + B(K_{\pi 2}) = 100 - \left[(B(K_{\pi 3}) + B(K'_{\pi 3}) + B(K_{\mu 3}) + B(K_{\beta 2})\right] =$$

$$= (80.3 \pm 1.7)\ \%,$$

obtained from Table XIV, we find

$$B(K_{\mu 2}) = (58.6 \pm 2.6)\ \%$$

$$B(K_{\pi 2}) = (21.7 \pm 2.5)\ \%\ .$$

* * *

The authors would like to take this opportunity of thanking Dr. E. J. LOFGREN, members of Dr. R. W. Birge's group, Dr. R. KERTH and the crew of the Bevatron for the exposure. We are grateful to Mr. TOMMY BERGSTEIN, Miss JYTTE SØRENSEN, Mrs. RUTH PREBEN-JENSEN, and Mr. MOGENS HANSEN who scanned the plates and made many of the measurements. Mr. LEIF KRISTENSEN helped with the calculations of the range straggling distribution.

J.E.H. expresses his gratitude to the Ford Foundation for financial support.

P.K.A. is in particular grateful to Prof. B. PETERS for arranging his participation in the work and thanks Prof. NIELS BOHR for hospitality and financial support made available at the Institute for Theoretical Physics. Thanks are also due Prof. B. M. ANAND and the Panjab University for leave of absence and further financial support.

RIASSUNTO (*)

Si sono studiati, principalmente seguendo i secondari carichi sino alla fine dei loro percorsi, gli eventi di decadimento K^+ in un grande pacco di emulsioni. Si è messo in rilievo: 1) la possibilità di ottenere dati genuini sull'estremità di alta energia dello spettro dei secondari $K_{\mu 3}$; 2) la ricerca del modo di decadimento $K^+ \to \mu^+ + \mu^0$; se combinati con i risultati dei precedenti esperimenti, i dati avrebbero dovuto permettere di rilevare questo processo se il rapporto di branching fosse stato maggiore di $\approx 5\%$; non si sono avute prove positive; 3) la ricerca di secondari π^+ di energia $(53 \div 61)$ MeV. In 467 eventi di decadimento non vi erano di questi secondari. Si sono determinati i rapporti di branching dei vari modi di decadimento. Combinando i nostri dati con quelli degli esperimenti precedenti si sono ottenuti i seguenti valori: $B(K_{\mu 2}) = (58.6 + 2.6)\%$; $B(K_{\pi 2}) = (21.7 \pm 2.5)\%$; $B(K_{\pi 3}) = (7.2 \pm 0.4)\%$; $B(K'_{\pi 3}) = (2.4 \pm 0.4)\%$; $B(K_{\mu 3}) = (5.5 \pm 1.1)\%$; $B(K_{\beta 3}) = (4.7 \pm 1.1)\%$. In questo esperimento l'efficienza di scanning misurata è stata del 99%.

(*) *Traduzione a cura della Redazione.*

The Ground State Spin of $^{212}_{84}$Po.

F. Demichelis

Istituto di Fisica Sperimentale del Politecnico - Torino

(ricevuto il 30 Agosto 1960)

Summary. — The angular correlation between the β transitions (energy 2.27 MeV) from the ground state of $^{212}_{83}$Bi to the ground state of $^{212}_{84}$Po and the α particles (energy 8.776 MeV) from the ground state of $^{212}_{84}$Po to the ground state of $^{208}_{82}$Pb, and the angular correlation between the γ rays (energy 0.727 MeV) from the first excited state to the ground state of $^{212}_{84}$Po and the above α particles have been measured. The very short lifetime of $^{212}_{84}$Po allowed us to perform these measurements. We have found isotropic correlations in opposition to previous experimental results. Our results are in agreement with the $J=0+$ assignment to the ground state of the even-even nucleus $^{212}_{84}$Po.

1. – Introduction.

The ground state of the stable nucleus $^{208}_{82}$Pb is characterized by closed shell of both neutrons ($N=126$) and of protons ($Z=82$). The $^{212}_{84}$Po nucleus ($N=128$, $Z=84$), which is in the neighbourhood of $^{208}_{82}$Pb can be considered with almost closed shell configuration. Indeed the deformations of the spherical shape are small and one retains many of the features of the static shell model.

In the nuclear shell structure theory it is generally assumed, on the basis of the coupling rules, that the ground states of all even even nuclei have zero spin and even parity.

According to the collective model theory for even even nuclei, all rotational states have

$$J = 0,\ 2,\ 4,\ 6,\ \ldots \text{ even parity}. \tag{1}$$

Only very few exceptions have been encountered, all referring to essentially spherical nuclei, for which (1) does not apply.

The decay

$$^{212}_{83}\mathrm{Bi} \rightarrow {}^{212}_{84}\mathrm{Po} \rightarrow {}^{208}_{82}\mathrm{Pb}$$

has been investigated by many authors [1].

In Fig. 1 is reported the decay scheme which includes the results and the most reliable assignment of spins and parities of the various levels.

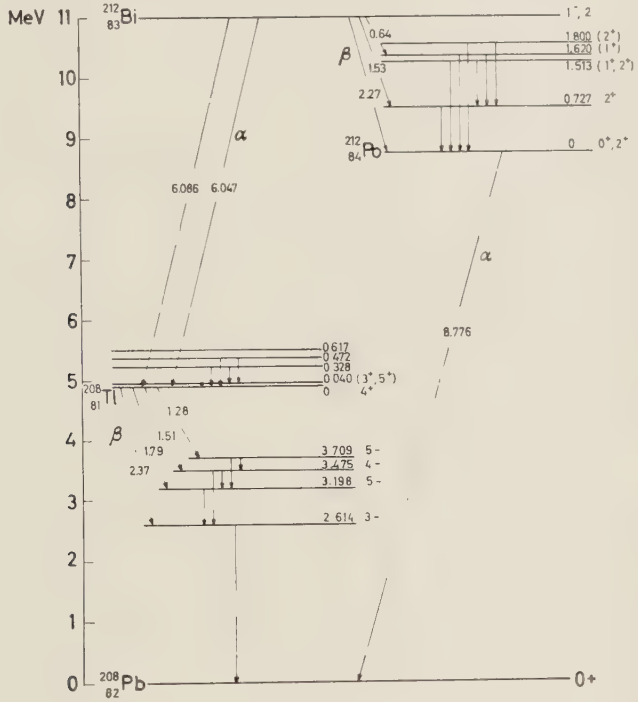

Fig. 1.

The β transition from the ground state of $^{212}_{83}$Bi to the ground state of $^{212}_{84}$Po should be first forbidden [2]; its log *ft* is in agreement with $\Delta J = 0, 1, 2$ parity change.

---

(1) F. Demichelis: *Nuovo Cimento*, **12**, 407 (1954); D. G. E. Martin and G. Parry: *Proc. Phys. Soc.*, A **68**, 1177 (1955); F. Demichelis and R. A. Ricci: *Nuovo Cimento*, **4**, 96 (1956); J. Burde and B. Rozner: *Phys. Rev.*, **107**, 531 (1957); B. Chinaglia and F. Demichelis: *Nuovo Cimento*, **8**, 365 (1958); U. Hauser and W. Kerler: *Zeits. f. Phys.*, **158**, 405 (1960).

(2) D. G. E. Martin and H. O. W. Richardson: *Proc. Roy. Soc. London*, A **195**, 287 (1949); F. Demichelis, R. A. Ricci and G. Trivero: *Nuovo Cimento*, **3**, 377 (1956); J. Burde and B. Rozner: *Phys. Rev.*, **107**, 531 (1957).

The $^{212}_{83}$Bi ground state should have $J = 1-$ or $2-$ ([3]).

The ground state of $^{208}_{82}$Pb is undoubtedly $0+$.

On the other hand MARTIN and RICHARDSON ([2]), assuming $0+$ for the ground state of $^{212}_{84}$Po, and from the measurement of the internal conversion for the 0.727 MeV transition, deduced that this transition is electric quadrupole leading to $2+$ assignment for the first excited level.

These conclusions are consistent with the supposition that the ground state of the even even nucleus $^{212}_{84}$Po is $0+$.

Experimental determination of the spin of $^{212}_{84}$Po ground state was performed by some authors. On the basis of his correlation data, A. BEISER ([4]) deduces for the ground state of $^{212}_{84}$Po the $2+$ value.

If the ground state of $^{212}_{84}$Po has spin $J = 2+$, the α particles from this level to the ground state of $^{208}_{82}$Pb must have an angular momentum greater than zero, while decays involving the ground state J_1 and J_- of even even nuclei are presumably parity favored with $J_1 = J_2 = 0$.

If the angular momentum L_α of the α-particles is greater than zero, since higher values of L_α imply lower decay probability ([5]) and therefore higher lifetime, one would expect an increased lifetime of $^{212}_{84}$Po. The Geiger-Nuttall relation shows an exception for $^{212}_{84}$Po ($T = 3.04 \cdot 10^{-7}$ s); an increased lifetime should remove this exception.

On the other hand J. W. WEALE ([3]) deduces, from his isotropic correlation obtained by coincidence measurements between all the γ-rays to the ground state of $^{212}_{84}$Po and the α-particles, the value $J = 0+$ for this state. The same result was obtained by I. I. FILIMONOV and G. A. PETROV ([6]) from coincidences between the 0.727 MeV γ-rays and the α-particles.

In the present research we have measured the angular correlation between the 2.27 MeV β-transition to the ground state of $^{212}_{84}$Po and the 8.776 MeV α-particle from the ground state of $^{212}_{84}$Po to the ground state of $^{208}_{82}$Pb and the angular correlation between the $E2$ γ-ray from the first excited state to the ground state of $^{212}_{84}$Po and the above α-particle. This was possible on account of the short lifetime of $^{212}_{84}$Po.

We will show that our angular correlation measurements can be interpreted by assuming that the ground state of $^{212}_{84}$Po has $J = 0+$ in agreement with the theoretical suggestions on even even nuclei.

([3]) R. W. KING: *Rev. Mod. Phys.*, **26**, 327 (1954); J. W. WEALE: *Proc. Phys. Soc.*, A **68**, 35 (1955); D. G. E. MARTIN and G. PARRY: *Proc. Phys. Soc.*, A **68**, 1177 (1955); F. DEMICHELIS and R. A. RICCI: *Nuovo Cimento*, **4**, 96 (1956).

([4]) A. BEISER: *Ann. of the N. Y. Acad. of Sci.*, **62**, 423 (1956).

([5]) J. M. BLATT and V. F. WEISSKOPF: *Theoretical Nuclear Physics* (New York, 1952).

([6]) I. I. FILIMONOV and G. A. PETROV: *Izvest. Akad. Nauk. SSSR Ser. Fiz.*, **20**, 1434 (1956).

2. – Experimental apparatus.

In order to measure β-α and γ-α coincidences we have used the following arrangements.

For all the measurements the source consists of a very thin layer of $^{228}_{90}$Th, in equilibrium with its decay products (intensity $\approx 10\ \mu$c).

2·1. – For the β-α angular correlation the experimental apparatus is the usual set up for coincidence measurements.

As β detector we used a stilbene crystal (thickness ≈ 6 mm, diameter ≈ 13 mm) and as α detector a CsI(Tl) crystal (thickness ≈ 0.8 mm, diameter ≈ 10 mm); both the crystals are followed by 6292 Du Mont photomultipliers.

An aluminum sheet (2.7 mm thick) is placed in front of the β detector in order to stop all the β-particles having energy lower than 1.60 MeV. Only the 2.27 MeV β transition from the ground state of $^{212}_{83}$Bi to the ground state of $^{212}_{84}$Po and the 2.37 and 1.79 MeV β transitions from the ground state of $^{208}_{81}$Tl to the first and second excited states of $^{208}_{82}$Pb whose end point energy is greater than the cut-off energy 1.60 MeV, are detected.

The background (mainly γ-rays) of the β detector and the γ-α coincidences background in the β-α measurements, were determined by placing in front of the β detector a beryllium absorber ($\approx 1.27\ g_m/cm^2$).

An aluminum absorber ($\approx 30\ \mu$m) and a cm of air between the source and the α detector were sufficient to stop all the α-particles having energy lower than 6.8 MeV. The background of the α detector (mainly β and γ-rays) was quite negligible.

The resolving time of the coincidence circuit was $\tau_2 = 1.2 \cdot 10^{-7}$ s.

Mumetal shieldings are placed all round the detectors in order to reduce the magnetic fields.

The measurements were performed with the α detector fixed and the β detector movable. The counting rate of the β detector as a function of the angle θ was constant within the statistical errors.

For the β-α coincidence rate we have:

$$n_{\beta\alpha} = (n_t - n_a) - (n'_t - n'_a)\,,$$

where: $n_{\beta\alpha}$ is the coincidence rate between the 2.27 MeV β transition and the 8.776 MeV α-particle;

n_t and n_a are the total coincidence rate and the accidental coincidence rate respectively, without beryllium;

n'_t and n'_a the total coincidence rate and the accidental coincidence rate respectively, with beryllium.

n_t' and n_a' have been measured at $\theta = 90°$, 120°, 150°, 180°, θ being the angle subtended at the source by the two detectors.

2·2. – In the γ-α angular correlation measurements the α detector was, also in this case, the same CsI(Tl) crystal used in the β-α measurements; as γ detector we used a NaI(Tl) crystal (1 in. $\times$ 1 in.); for both a 6292 DuMont photomultiplier.

In order to ensure that β-particles do not reach the γ detector, a lead sheet (1 mm thick) was placed in front of the detector.

The electronic set up was a fast-slow coincidence system. The pulses from the two detectors were fed to the fast coincidence circuit (resolving time $\tau_2 = 1.2 \cdot 10^{-7}$ s) and, at the same time, to the two single channel analyzers. Pulses coming from the two analyzers and from the coincidence circuit were fed to the triple coincidence circuit (resolving time $\tau_3 = 3.08 \cdot 10^{-6}$ s).

The two analyzers had the windows set on the peaks of the 8.776 MeV α-particles and on the photoelectric peak of the 0.727 MeV γ-rays.

Also in this set of measurements the α detector was fixed and the γ detector movable. The γ-ray rate was found to be constant with θ within the statistical errors.

All the coincidence rates were determined for the following values of θ: 90°, 120°, 150°, 180°.

We have made two sets of measurements for β-α coincidences and one set of measurements for γ-α coincidences.

We have followed the usual procedure [7] in order to correct for the asymmetry of the source, for the fluctuations with time of the detector's efficiencies.

3. – Experimental results.

In Fig. 2 and 3 are reported the experimental points and their probable errors obtained respectively in the first measurement set of β-α coincidences and in the measurement set of γ-α coincidences.

In both the diagrams we have plotted

$$\varepsilon(\theta) = (n_{c,\theta}/n_{c,90}) - 1 = W(\theta) - 1$$

against θ.

$n_{c,\theta}$ and $n_{c,90}$ are the effective β-α or γ-α coincidence rates for the values of θ and 90° respectively.

---

[7] D. T. Stevenson and M. Deutsch: *Phys. Rev.*, **83**, 1202 (1951); H. Frauenfelder: β *and* γ *Spectroscopy*, Ed. K. Siegbahn (Amsterdam), p. 531.

In every case we can observe that, within the experimental errors, there is no anisotropic correlation.

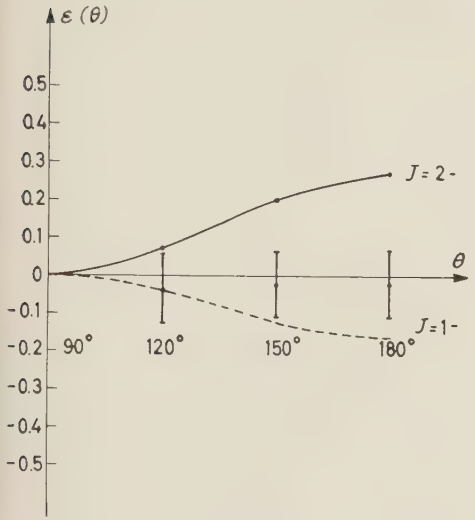

Fig. 2.

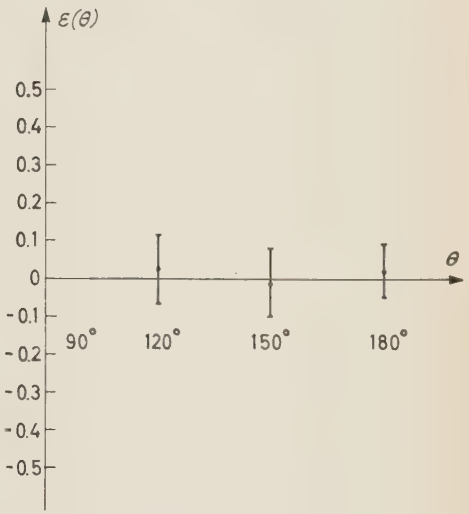

Fig. 3.

4. – Discussion.

4·1. – Let us consider first the angular correlation with the angular momentum scheme $J_1(L_1)J(L_2)J_2$, where L_1 and L_2 are the multipolarity of the two radiations in cascade.

The most convenient form of describing the correlation $W(\theta)$ is

$$W(\theta) = \sum A_\nu P_\nu(\cos\theta)\,, \tag{2}$$

where $W(\theta)$ is the probability for the angle θ to occur, A_ν a parameter, P_ν the Legendre polynomial of order ν.

The highest term in this expansion is determined by the selection rules [8]

$$\begin{cases} 0 \leqslant \nu \leqslant L_1 \\ 0 < \nu \leqslant J \\ 0 \leqslant \nu \leqslant L_2\,. \end{cases} \tag{3}$$

---

[8] C. N. Yang: *Phys. Rev.*, **74**, 764 (1948).

However in the case of $^{212}_{84}$Po it is to be expected that the angular correlations be influenced by extranuclear fields. Indeed the perturbation depends also on the mean life τ_b of the intermediate state and an angular correlation can be considered perturbed if the lifetime of the intermediate state is longer than about 10^{-10} s.

In solids the magnetic interaction can usually be neglected in comparison with the quadrupole interaction; it was experimentally verified, in some cases, that the attenuation is mostly (or entirely) due to quadrupole interaction.

If we assume pure quadrupole interaction and if the unperturbed correlation be given by (2), then the perturbed correlation can be written

$$W(\theta) = \sum G_\nu A_\nu P_\nu(\cos\theta) .$$

The attenuation factors G_ν depend on the interaction in the intermediate nuclear state (*i.e.* on J, τ_b, Q, $\partial^2 V/\partial z^2$ and other parameters); explicit expressions of these factors are given in Abragam and Pound (9).

At the present time no reliable estimate of the field gradient $\partial^2 V/\partial z^2$ in $^{212}_{84}$Po exists and it is thus impossible to calculate the quadrupole moment Q. For quadrupole interaction, values for $(eQ/h)(\partial^2 V/\partial z^2) = \Delta\nu_Q$ varying from 0.33 MHz for $^{23}_{11}$Na to 3000 MHz for $^{127}_{53}$I have been obtained; f.i. for $^{111}_{48}$Cd it is $(eQ/h)(\partial^2 V/\partial z^2) = 6.2$ MHz (10).

For $^{212}_{84}$Po, supposing the spin of the intermediate state $J = 2$, known the mean life $\tau_b = 4.38 \cdot 10^{-7}$ s and assuming for $\Delta\nu_Q$ the values 1 and 10^3 MHz respectively, we have used the formulas of Abragam and Pound to determine the attenuation factors and we have found $G_2 = 0.375$ and 0.371, $G_4 = 0.461$ and 0.460 respectively.

Taking into consideration that the attenuation factors G_ν do not depend on the parameters describing the initial and final levels of the cascade nor on the radiations, the calculated coefficients can be applied to our β-α and γ-α angular correlations.

4·2. – β-α angular correlation $J_1(\beta)J(\alpha)J_2$.

Taking into account that:

the 2.27 MeV β transition from the $^{212}_{83}$Bi ground state to the $^{212}_{84}$Po ground state is first forbidden (2),

the ground state of $^{212}_{83}$Bi has $J_1 = 1-$ or $2-$ (3),

the ground state of $^{208}_{82}$Pb has $J_2 = 0+$,

(9) A. Abragam and R. V. Pound: *Phys. Rev.*, **92**, 943 (1953).

(10) H. Albers-Schönberg, E. Heer, T. B. Novey and R. Rüetschi: *Phys. Rev.*, **91**, 199 (1953).

we may discuss the following 4 possibilities for the decay chain $^{212}_{83}\mathrm{Bi} \rightarrow {}^{212}_{84}\mathrm{Po} \rightarrow {}^{208}_{82}\mathrm{Pb}$:

	J_1	J	J_2
1)	1	0	0
2)	2	0	0
3)	1	2	0
4)	2	2	0

From the selection rules (3) we can deduce immediately that in the first two cases, $\nu = 0$, there is no anisotropic correlation.

In cases 3) and 4) it is $L_2 = 2$. If also L_1 would be equal 2 the correlation function should contain a term proportional to $\cos^4\theta$. We shall then assume that the transition is a first forbidden one.

The partial parameters b_ν for the β radiation, which appear in the $W(\theta)$ expression of Biedenharn and Rose's paper ([11]) are listed in Table X of this paper. We must note that these parameters are functions of the energy of the β particle so that they must be averaged over the whole range of energies from the cut-off energy ($E_c = 4.14\ \mathrm{mc}^2$) to the maximum energy ($E_c = 5.41\ \mathrm{mc}^2$).

The A_ν parameters are related to the coefficients F_ν by formula (69) in the paper of Biedenharn and Rose; the F_ν coefficients are tabulated in Table I of the same paper.

The results of the calculations of the anisotropy coefficient a_2 which appear in the angular correlation function $W(\theta) = 1 + a_2 \cos^2\theta$, for $L_1 = 1$ and for $J_1 = 1$ and 2 and corrected for the influence of the extranuclear fields are summarized in Table I.

If we suppose that the β interaction contains only scalar, tensor, pseudoscalar terms; (the vector and axialvector terms seem to be excluded according to the empirical evidence on the shapes of first and second forbidden spectra ([12])), the considerations on the theoretical values of a_2 allow us to deduce that:

the pseudoscalar interaction is not consistent with the odd parity of the initial state;

a tensor interaction, containing only the $\sum |B_{ij}^{\beta}|^2$ matrix element, cannot agree with the experimental results;

([11]) L. C. Biedenharn and M. E. Rose: *Rev. Mod. Phys.*, **25**, 729 (1953),
([12]) D. C. Peaslee: *Phys. Rev.*, **91**, 1447 (1953).

TABLE I (*). – *Values of the anisotropy coefficient* a_2.

Interaction \ J_1		1	2	Parity of the initial state
S	$\lvert\int\beta\boldsymbol{r}\rvert^2$	0.115	− 0.107	odd
T	$\sum\lvert B_{ij}^{\beta}\rvert^2$	− 0.340	0.440	odd
	$\lvert\int\beta\boldsymbol{\sigma}\wedge\boldsymbol{r}\rvert$	− 0 050	0.052	odd
	$\lvert\int\beta\boldsymbol{\alpha}\rvert^2+\lvert\int\beta\boldsymbol{\sigma}\wedge\boldsymbol{r}\rvert^2+$ $+\lvert\int\beta\boldsymbol{\alpha}\rvert\lvert\int\beta\boldsymbol{\sigma}\wedge\boldsymbol{r}\rvert$	− 0.047	0.049	odd
	P	0.115	− 0.107	even
V	$\lvert\int\boldsymbol{r}\rvert^2$	0.138	− 0.126	odd
	$\lvert\int\boldsymbol{\alpha}\rvert^2+\lvert\int\boldsymbol{\alpha}\rvert\lvert\int\boldsymbol{r}\rvert$	0.056	− 0.054	odd
A	$\lvert\int\boldsymbol{\sigma}\wedge\boldsymbol{r}\rvert^2$	− 0.013	0.013	odd
	$\sum\lvert B_{ij}\rvert^2$	− 0.340	0.440	odd

(*) The notations for the interaction terms are the same as those used by Biedenharn and Rose.

the matrix elements

$$\left|\int\beta\boldsymbol{\sigma}\wedge\boldsymbol{r}\right|^2, \qquad \left|\int\beta\boldsymbol{\alpha}\right|^2+\left|\int\beta\boldsymbol{\sigma}\wedge\boldsymbol{r}\right|^2+\left|\int\beta\boldsymbol{\alpha}\right|\left|\int\beta\boldsymbol{\sigma}\wedge\boldsymbol{r}\right|,$$

by themselves give a very weak correlation. Each of these operators should give a correlation which is within the experimental errors.

Furthermore, assuming $J_1=2$ — for the initial state, it happens that a suitable mixture of scalar and tensor interaction with matrix elements

$$\left|\int\beta\boldsymbol{\sigma}\wedge\boldsymbol{r}\right|^2, \qquad \left|\int\beta\boldsymbol{\alpha}\right|^2+\left|\int\beta\boldsymbol{\sigma}\wedge\boldsymbol{r}\right|^2+\left|\int\beta\boldsymbol{\alpha}\right|\left|\int\beta\boldsymbol{\sigma}\wedge\boldsymbol{r}\right|, \qquad \text{and} \qquad \left|\int\beta\boldsymbol{r}\right|^2,$$

fits the β-α correlation.

In mixing scalar and tensor terms we have left out the interference terms [7,13], whose calculation is very difficult.

On the contrary, according to the failure of parity conservation in

[13] M. MORITA: *Prog. Theor. Phys.*, **10**, 363 (1953).

β-decay ([14]), and assuming that the β interaction is composed of only vector and axialvector terms, we can deduce that:

an axial vector interaction containing only the $\sum |B_{ij}|^2$ matrix element, cannot agree with the experimental results;

the matrix elements

$$V) \quad \left| \int \boldsymbol{\alpha} \right|^2 + \int \boldsymbol{\alpha} \int \boldsymbol{r} \Big| ; \qquad A) \quad \left| \int \sigma \wedge \boldsymbol{r} \right| ,$$

by themselves give a very weak correlation; each of these operators should give a correlation which is within the experimental errors.

In mixing vector and axialvector terms, and leaving out the interference terms, we obtain the theoretical curves of Fig. 2 (full line $J_1 = 2$ —; dotted line $J_1 = 1$ —).

4·3. – γ-α angular correlation $J_1(\gamma)J(\alpha)J_2$.

In order to confirm that there is no anisotropic correlation and that the spin of $^{212}_{84}$Po is 0+, let us consider now the γ-α correlation.

Taking into consideration that:

the 0.727 MeV γ-ray from the first excited state to the ground state of $^{212}_{84}$Po is electric quadrupole ([15]) and that the ground state of $^{208}_{82}$Pb is 0+, we can discuss the following 2 possibilities:

	J_1	J	J_2
1)	2	0	0
2)	0	2	0

In the first case we have not anisotropic correlation. In the second case, the spin assignment $0(\gamma)2(\alpha)0$ leads to $A_{2\text{th.or}} = 5/7$ and $A_{4\text{theor}} = -12/7$ for the unperturbed correlation; taking the value $G_2 = 0.375$ and $G_4 = 0.461$ one finds $A_{2\,\text{theor.corr.}} = 0.268$ and $A_{4\,\text{theor.corr.}} = -0.790$.

Undoubtedly the angular correlation should be very large.

We then find that our experimental results are well in agreement with the spin assignment $2(\gamma)0(\alpha)0$.

([14]) T. D. Lee and C. N. Yang: *Phys. Rev.*, **104**, 254 (1956).

([15]) D. G. E. Martin and H. O. W. Richardson: *Proc. Roy. Soc. London*, A **195**. 287 (1949).

5. – Conclusions.

The assignment $J = 0+$ for the ground state of $^{212}_{84}$Po is consistent with our experimental results, with the log ft of the 2.27 MeV β transition, the $J_1 = 1-$ or $2-$ assignment for the ground state of $^{212}_{83}$Bi.

Moreover according to results of Martin and Richardson on multipolarity ($E2$) of 0.727 MeV γ-ray, the first excited state of even-even nucleus $^{212}_{84}$Po is $2+$.

Finally the assignment $J = 0+$ to the ground state of even even nucleus $^{212}_{84}$Po can be justified from the point of view of the nuclear shell model and of the collective model.

* * *

The author wishes to thank Prof. E. Perucca for his kind interest and Dr. C. Oldano and Dr. A. Scibilia for their collaboration in the experimental measurements.

RIASSUNTO

Si è proceduto alla misurazione della correlazione angolare tra le transizioni β (energia 2.27 MeV) dallo stato fondamentale del $^{212}_{83}$Bi allo stato fondamentale del $^{212}_{84}$Po e le particelle α (energia 8.776 MeV) dallo stato fondamentale del $^{212}_{84}$Po allo stato fondamentale del $^{208}_{82}$Pb, e della correlazione angolare tra i raggi γ (energia 0.727 MeV) dal primo stato eccitato allo stato fondamentale del $^{212}_{84}$Po e le particelle α emesse da questo nucleo. Queste misurazioni sono state possibili grazie al brevissimo periodo di dimezzamento del $^{212}_{84}$Po. Non si è trovato anisotropia contrariamente a risultati precedenti. I risultati sperimentali ottenuti sono in accordo con l'assegnazione $J = 0+$ allo stato fondamentale del nucleo pari pari $^{212}_{84}$Po.

L'effetto Bordoni nelle leghe argento-oro.

I. Barducci, M. Nuovo e L. Verdini

Istituto Nazionale di Ultracustica «O. M. Corbino» - Roma

(ricevuto il 7 Settembre 1960)

Riassunto. — Si presentano alcuni risultati relativi all'effetto Bordoni in una serie di leghe binarie del sistema Ag-Au. Si è verificata sperimentalmente la presenza di un effetto di rilassamento attivato termicamente e dovuto al moto delle dislocazioni libere, sotto l'azione combinata dell'agitazione termica e della sollecitazione meccanica impressa. Le misure sono state eseguite, in tutti i campioni esaminati, facendo uso di vibrazioni proprie estensionali, alla frequenza di circa 20 kHz. La temperatura T_m del massimo di dissipazione cresce gradualmente al variare della concentrazione ed i valori relativi alle leghe sono in ogni caso compresi fra quello dell'argento puro (71.5 °K) e quello dell'oro puro (132 °K). Il massimo di attenuazione risulta notevolmente più accentuato per leghe contenenti piccole percentuali di Au (2% Au) e tende a diminuire man mano che esse si arricchiscono di atomi di Au finchè il rapporto tra i due componenti si approssima all'unità. Anche le misure di velocità di propagazione c_0 e del coefficiente di temperatura β indicano la presenza di un numero assai elevato di dislocazioni attive nelle leghe con piccole percentuali di Au. Dai valori della temperatura T_m del massimo di attenuazione è possibile prevedere indirettamente la dipendenza dalla concentrazione dell'energia di attivazione. L'andamento di questo parametro caratteristico del processo di rilassamento, si discosta dalla legge lineare e la curva sembra presentare una concavità rivolta verso l'asse delle concentrazioni. L'energia di attivazione è stata direttamente determinata nel caso della lega al 20% di Au, misurando la temperatura del massimo per due differenti frequenze di vibrazione. Il valore che così si ottiene è in accordo con le previsioni fatte sull'andamento di W.

1. – Introduzione.

L'esistenza di un effetto di rilassamento anelastico nei metalli alle basse temperature è stato segnalato per la prima volta da P. G. Bordoni [1] il quale ha inoltre individuata la causa di questo effetto nel moto delle dislocazioni

[1] P. G. Bordoni: *Journ. Acoust. Soc. Am.*, **26**, 495 (1954).

sotto l'azione combinata dell'agitazione termica e di una sollecitazione meccanica [2].

Tra le ipotesi che in seguito sono state proposte nel tentativo di spiegare anche quantitativamente il meccanismo che regola il moto delle dislocazioni nei metalli, la più attendibile sembra quella dovuta a J. WEERTMAN [3] ed a A. SEGER [4], secondo la quale nelle dislocazioni si formerebbero coppie di flessi (*kinks*) per effetto dell'agitazione termica, mentre la sollecitazione meccanica agirebbe sulle dislocazioni allontanando tra loro i due flessi ed aumentando in tal modo la regione deformata.

L'effetto Bordoni, che sperimentalmente si manifesta con un massimo nelle curve di attenuazione ed un flesso nelle curve dei moduli al variare della temperatura, è stato sinora generalmente osservato sia nei metalli di elevato grado di purezza sia in quelli contenenti piccole percentuali di impurità, tutti appartenenti al sistema cubico a facce centrate, e precisamente nel piombo [1,5,6], nell'alluminio [1,7-9], nel rame [1,10-17], nell'argento [1,18], nell'oro [18], nel palladio [18] e nel platino [18].

Le indagini sperimentali sono state recentemente estese anche a metalli appartenenti a sistemi cristallini non cubici, come il magnesio [12] e lo zinco [19]. Mentre nel caso dello zinco l'effetto si presenta vistoso e con tutte le caratteristiche proprie di un effetto di rilassamento attivato termicamente, nel caso del magnesio sussiste tuttora qualche incertezza nell'interpretazione dei risultati sperimentali.

Con il presente lavoro gli autori si sono proposti di estendere le ricerche

[2] P. G. BORDONI: *Ric. Scient.*, **19**, 851 (1949).
[3] J. WEERTMAN: *Journ. Appl. Phys.*, **26**, 202 (1955).
[4] A. SEEGER: *Phil. Mag.*, **1**, 651 (1956).
[5] H. E. BOEMMEL: *Phys. Rev.*, **96**, 220 (1954).
[6] W. P. MASON e H. E. BOEMMEL: *Journ. Acoust. Soc. Am.*, **28**, 930 (1956).
[7] T. S. HUTCHISON e A. J. FILMER: *Can. Journ. Phys.*, **34**, 159 (1956).
[8] T. S. HUTCHISON e G. J. HUTTON: *Can. Journ. Phys.*, **34**, 1498 (1956).
[9] N. G. EINSPRUCH e R. TRUELL: *Phys. Rev.*, **109**, 652 (1958).
[10] D. H. NIBLETT e J. WILKS: *Phil. Mag.*, **1**, 415 (1956).
[11] D. H. NIBLETT e J. WILKS: *Phil. Mag.*, **2**, 1427 (1957).
[12] H. L. CASWELL: *Journ. Appl. Phys.*, **29**, 1210 (1958).
[13] V. K. PARÉ: *Experimental and theoretical study of low-temperature internal friction in copper* (Cornell University, Dept. Eng. Phys., Techn. Rep., July 1958).
[14] D. O. THOMPSON e F. H. GLASS: *Rev. Sci. Instr.*, **29**, 1034 (1958).
[15] D. O. THOMPSON e D. K. HOLMES: *Journ. Appl. Phys.*, **10**, 525 (1959).
[16] P. G. BORDONI, M. NUOVO e L. VERDINI: *Phys. Rev. Lett.*, **2**, 200 (1959).
[17] P. G. BORDONI, M. NUOVO e L. VERDINI: *Nuovo Cimento*, **14**, 273 (1959).
[18] P. G. BORDONI, M. NUOVO e L. VERDINI: *Relaxation of dislocations in face-centered cubic metals* (in corso di stampa su « Proc. 3rd I.C.A. Congress », Stuttgart, Settembre 1959).
[19] P. G. BORDONI, M. NUOVO e L. VERDINI: *Nuovo Cimento*, **16**, 373 (1960).

relative all'effetto Bordoni anche al campo delle leghe metalliche. A questo scopo si sono prescelte le leghe del sistema binario Ag-Au, la cui struttura cristallina è certamente tra le più simili a quella dei metalli costituenti cubici a facce centrate; infatti il rapporto fra le costanti reticolari dei due componenti puri è in questo caso molto prossimo all'unità (*) e pertanto la distorsione del reticolo cristallino dovuta alla differenza fra le distanze interatomiche dei due metalli risulta non troppo sensibile, mentre la solubilità reciproca nella fase solida è completa per tutte le concentrazioni. Anche la geometria degli effetti di scorrimento nelle leghe rimane identica a quella dei due metalli puri, cioè i piani e le direzioni di scorrimento mantengono inalterata la loro natura cristallografica.

Si deve infine aggiungere che in una ricerca di questo tipo è necessario poter disporre di campioni per i quali la storia dei trattamenti termici e meccanici subiti prima delle misure sia nota anche nei minimi dettagli. Inoltre, al fine di rendere paragonabili i risultati sperimentali relativi ai campioni appartenenti a leghe di differente concentrazione, tali trattamenti debbono essere mantenuti rigorosamente uguali per tutti i campioni che si vogliono esaminare. Nel caso della presente ricerca tutto questo è stato reso possibile tramite la cortese collaborazione della « Metalli Preziosi S.p.A. » di Milano, il cui Laboratorio Ricerche e Controlli ha curato la preparazione e le analisi chimiche, spettroscopiche e metallografiche dei campioni.

Una indagine preliminare sulla dipendenza dei parametri elastici ed anelastici dai trattamenti termici e meccanici compiuta in una analoga serie di leghe Ag-Au ([20]), si è dimostrata di grande ausilio e di guida sia nella progettazione degli esperimenti, sia nella interpretazione dei risultati ottenuti.

In tutte le leghe del sistema Ag-Au esaminate nel corso della presente ricerca si è trovato il massimo di attenuazione caratteristico dell'effetto Bordoni ad una temperatura compresa tra 71.5 °K (argento puro) e 132 °K (oro puro). L'ampiezza di tale massimo risulta molto diversa al variare della concentrazione; in particolare essa assume valori di poco superiori alla dissipazione di fondo nei campioni a concentrazioni intermedie.

2. – Metodo sperimentale.

I campioni su cui sono state eseguite le misure hanno la forma di sottili sbarre parallelepipede, di sezione trasversale pari a 2.0 mm × 7.0 mm; la loro lunghezza varia con il tenore dei due componenti ed è stata calcolata in modo

(*) La distanza interatomica nell'argento e nell'oro è, rispettivamente,

$$a_{Ag} = 2.888 \cdot 10^{-8} \text{ cm} \qquad \text{e} \qquad a_{Au} = 2.884 \cdot 10^{-8} \text{ cm}$$

(vedi, C. S. Barrett: *Structure of Metals* (London, 1953), pp. 647 e 648).

([20]) I. Barducci e L. Verdini: *Ric. Scient.*, **26**, 95 (1956).

che le frequenze proprie di vibrazione non siano troppo diverse al variare della concentrazione.

Le vibrazioni estensionali vengono eccitate per mezzo di forze elettrostatiche servendosi di un opportuno elettrodo, il quale è utilizzato anche per rivelare l'ampiezza di vibrazione. Questa rivelazione viene effettuata mediante un vibrometro a modulazione di frequenza e di una apparecchiatura sperimentale già ampiamente descritta in precedenti lavori ([21-23]).

Le grandezze direttamente misurate con questa tecnica sperimentale sono la prima autofrequenza estensionale f_0 e la larghezza di banda Δf della corrispondente curva di risonanza; quando lo smorzamento del sistema è sufficientemente piccolo, invece di quest'ultima grandezza si misura il tempo di decadimento t_{60}, definito come il tempo necessario affinchè l'ampiezza delle oscillazioni libere della sbarretta si riduca di 60 db, cioè ad un millesimo del suo valore iniziale.

Dalla misura di questi parametri fisici è possibile calcolare la velocità di propagazione c_e delle onde elastiche estensionali mediante la relazione:

$$c_e = \left(\frac{E}{\varrho}\right)^{\frac{1}{2}} = 2lf_0 , \tag{1}$$

dove $E =$ modulo di Young, $\varrho =$ densità, $l =$ lunghezza della sbarretta, nonchè il coefficiente di risonanza meccanica Q:

$$Q = \frac{f_0}{\Delta f} , \tag{2}$$

oppure il decremento logaritmico d:

$$d = 2.20 \frac{\pi}{t_{60} f_0} . \tag{3}$$

Questi due ultimi parametri rappresentano una misura della *dissipazione* di energia elastica o, come comunemente si dice, di *attenuazione* (*),

([21]) P. G. Bordoni: *Nuovo Cimento*, **4**, 177 (1947).

([22]) P. G. Bordoni e M. Nuovo: *Acustica*, **4**, 184 (1954); *Ric. Scient.*, **24**, 560 (1954).

([23]) P. G. Bordoni e M. Nuovo: *Acustica*, **7**, 1 (1957); *Ric. Scient.*, **27**, 695 (1957).

(*) Il coefficiente di attenuazione α di un'onda piana di lunghezza d'onda λ, misura la diminuzione dell'ampiezza di vibrazione nello spazio. Esso è legato al parametro Q^{-1}, che chiameremo *coefficiente di dissipazione* (dell'energia elastica), dalla semplice relazione:

$$Q^{-1} = \pi^{-1} \lambda \alpha .$$

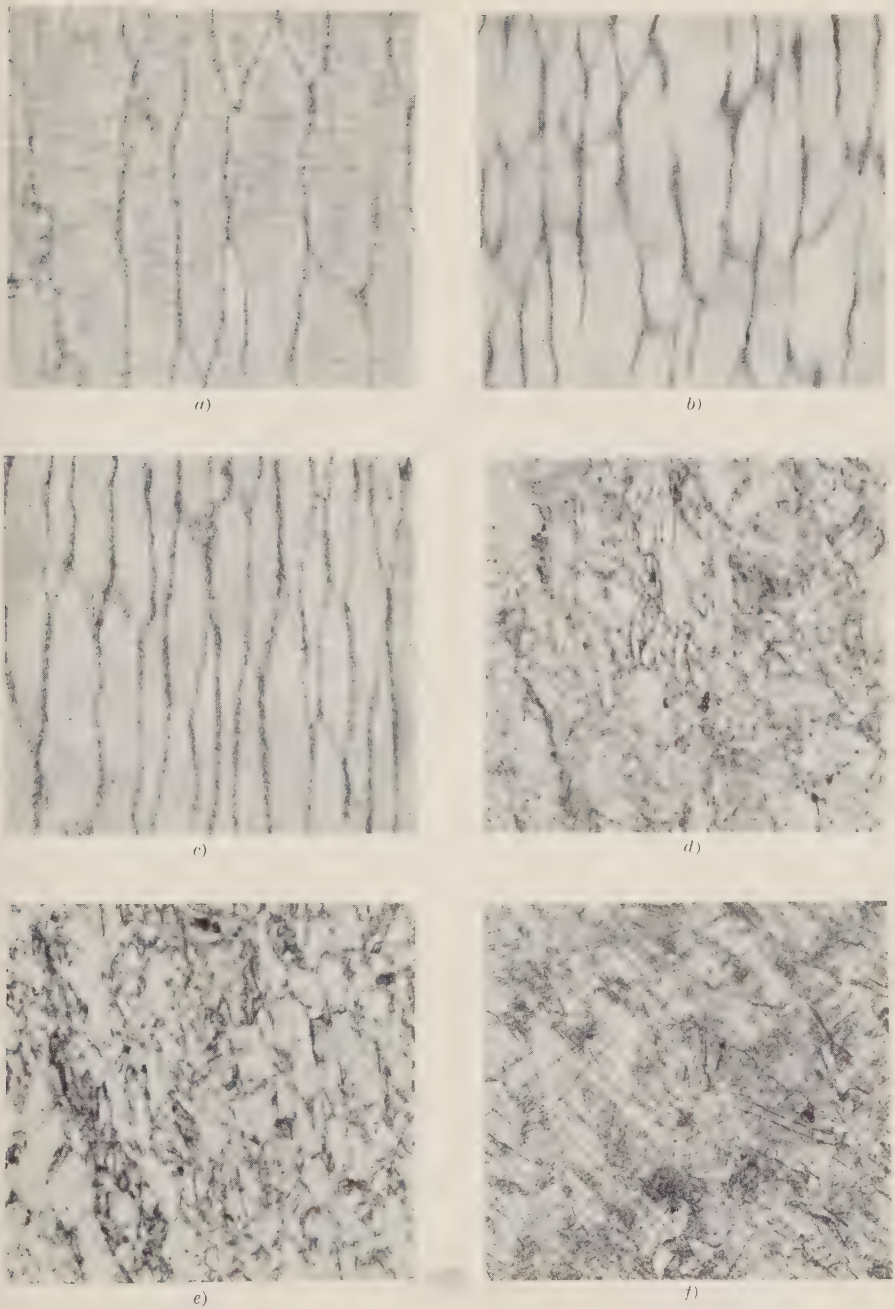

Fig. 1. – Micrografie eseguite in alcune leghe del sistema Ag-Au dopo tutti i trattamenti termici e meccanici (24 ingrandimenti): *a*) 1% Au; *b*) 5% Au; *c*) 10% Au; *d*) 40% Au; *e*) 60% Au; *f*) 80% Au.

essendo:

$$d = \pi Q^{-1} = \frac{\Delta U}{U}, \tag{4}$$

dove ΔU = energia dissipata per mezzo ciclo e U = energia elastica totale. È interessante inoltre ricordare che, per un dato sistema meccanico, il coefficiente Q^{-1} rappresenta anche la tangente dell'angolo di fase tra una sollecitazione sinusoidale e la corrispondente deformazione.

Le misure di frequenza e di dissipazione sono state eseguite variando la temperatura, in un intervallo compreso tra la temperatura ambiente e quella dell'azoto solido (~ 60 °K).

Poichè per la maggior parte dei campioni la dissipazione a temperatura ambiente risulta non troppo elevata, e poichè la loro particolare forma geometrica non rende agevole porre il giunto di una termocoppia a contatto diretto con il campione stesso senza alterare in modo eccessivo i valori del coefficiente Q^{-1} e della frequenza di risonanza, si è preferito determinare la temperatura servendosi della curva di frequenza. Quest'ultima grandezza è stata misurata con notevole precisione in tutte le sbarrette a temperatura ambiente (293 °K), alla temperatura di ebollizione dell'azoto (77.3 °K) ed al suo punto triplo (63.1 K).

Poichè per quasi tutti i metalli l'andamento della frequenza di risonanza, almeno nell'intervallo qui considerato ed in assenza di effetti di rilassamento, è lineare con la temperatura, risulta facile risalire con sufficiente precisione da misure di frequenza alla misura della temperatura. Nel presente lavoro, a causa dell'effetto Bordoni, che, come già si è accennato, si rivela nella curva frequenza-temperatura con un flesso abbastanza esteso, è stato necessario tener conto anche di questo fatto per determinare accuratamente la temperatura. L'incertezza nei valori di T così ricavati può essere stimata in ogni caso certamente non superiore a ± 1 °K.

Durante le misure, le sbarrette sono poste in un supporto metallico, particolarmente progettato per essere usato a bassa temperatura ([17]); esso può, tra l'altro, permettere l'immissione di un gas di scambio ed essere evacuato fino a pressioni di qualche micron di Hg. Ciò consente sia di stabilizzare la temperatura del campione prima e durante la misura, sia di ridurre le perdite di energia elastica dovute alla radiazione ed allo smorzamento del gas circostante.

Le principali caratteristiche dei campioni esaminati sono raccolte nella Tabella I. Come già si è accennato, una particolare cura è stata posta nella preparazione delle sbarrette affinchè la storia dei trattamenti termici e meccanici risultasse esattamente la stessa per tutti i campioni.

Nella Fig. 1 sono riportate alcune micrografie eseguite subito dopo l'ultimo trattamento meccanico (trafilatura). Esse mostrano chiaramente che, a parità di trattamenti termici e meccanici, il grado di incrudimento ottenuto è molto maggiore nelle leghe contenenti piccole percentuali di oro.

TABELLA I. – *Principali caratteristiche dei campioni esaminati.*

Atomi % Au	0.002	0.69	0.99	2.00	5.01	10.04	19.98	39.90	60.16	60.15	99.998
Analisi spettrografica	tracce di Au, Cu Mg, Ca	tracce imponderabili di Cu, Mg, Ca			tracce imponderabili di Ca, Fe, Cu				tracce di Cu, Mg, Ca		linee di Ag e tracce di Cu, Fe, Ca
Storia dei trattamenti termici e meccanici	*a*) fusione sotto vuoto in sbarrette tonde di diametro $D=10$ mm; *b*) trafilatura a quadrato sino alle dimensioni di 6 mm × 6 mm; *c*) normalizzazione sotto vuoto a 600 °C per 1 ora; *d*) laminazione a freddo del quadro sino alla sezione di 2.4 mm × 7.7 mm; *e*) trafilatura con tre passaggi sino ad ottenere la sezione finale.										
Sezione trasversale	2.0 mm × 7.0 mm										
Lunghezza (mm)	59.92	59.93	60.03	60.06	60.10	59.18	58.04	55.56	54.92	52.86	51.94

3. – Risultati sperimentali.

Le misure di dissipazione e di frequenza di risonanza del primo modo di vibrazione estensionale sono state eseguite, al variare della temperatura, su undici campioni, comprendenti i due metalli puri e nove leghe di composizione differente (v. Tabella I).

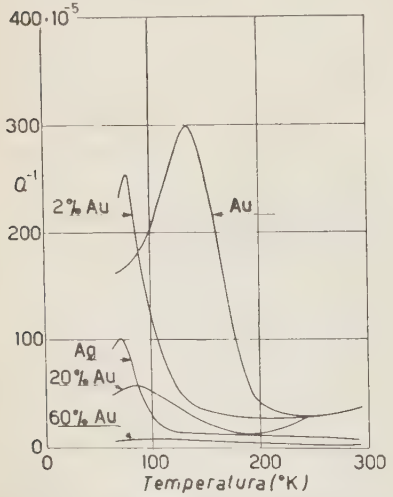

Fig. 2. – Coefficiente di dissipazione in funzione della temperatura assoluta in alcune leghe e nei due metalli puri.

I risultati sperimentali di queste misure sono stati raccolti nella Tabella II.

La Fig. 2 illustra l'andamento del Q^{-1} in funzione della temperatura assoluta, per i metalli puri e per alcune leghe fra le più caratteristiche. È evidente che l'effetto si presenta particolarmente vistoso non solo nell'argento e nell'oro, come già è stato provato in una precedente ricerca [18], ma anche nelle leghe contenenti piccole percentuali di Au. Al crescere della concentrazione di quest'ultimo, si nota una diminuzione dell'ampiezza del massimo; tuttavia l'effetto Bordoni risulta sperimentalmente accertato in tutte le leghe esaminate.

TABELLA II. – *Principali risultati sperimentali.*

Atomi % Au	f $T = 293$ °K (Hz)	c_e $T = 293$ °K (ms^{-1})	$\beta = -\frac{\partial \ln c_e}{\partial T}$ $T = 293$ °K ($°K^{-1}$)	$\beta = -\frac{\partial \ln c_e}{\partial T}$ $T = 77$ °C ($°K^{-1}$)	f_m (Hz)	T_m (°K)	Q_m^{-1}	Q^{-1} $T = 293$ °K
0.0	22 368	2 680	$2.01 \cdot 10^{-4}$	$1.92 \cdot 10^{-4}$	23 390	71.5	$103 \cdot 10^{-5}$	$33 \cdot 10^{-5}$
0.7	22 390	2 682	1.98	1.90	23 414	74	200	31
1	22 235	2 668	1.99	1.91	23 270	72	203	31
2	22 064	2 647	2.04	1.95	23 104	76.5	254	37
5	22 133	2 660	2.01	1.93	23 140	76.5	166	31
10	22 394	2 647	1.96	1.88	23 374	78	124	21
20	22 560	2 617	1.85	1.78	23 454	83	59.7	9.0
40	22 379	2 529	1.71	1.65	23 176	86.5	17.8	4.6
60	21 961	2 411	1.60	1.54	22 676	89.5	8.3	4.8
80	21 378	2 262	1.54	1.49	21 990	107	10.6	13.5
100	19 490	2 027	1.46	1.42	20 010	132	302	38

f = frequenza del primo modo estensionale.
c_e = velocità di propagazione delle onde elastiche estensionali.
β = coefficiente di temperatura della velocità.
f_m = frequenza corrispondente al massimo di dissipazione.
T_m = temperatura del massimo di dissipazione.
Q_m^{-1} = valore del massimo di dissipazione.

La Fig. 3 illustra i risultati relativi ai campioni contenenti percentuali di Au inferiori al 10%. Nella Fig. 4 sono infine riportate le misure eseguite nelle leghe a maggior tenore di Au, utilizzando una scala delle ordinate molto allargata per meglio mettere in evidenza il massimo

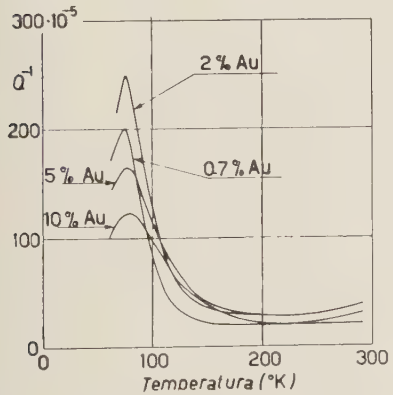

Fig. 3. – Coefficiente di dissipazione in alcune leghe ricche d'argento, in funzione della temperatura assoluta.

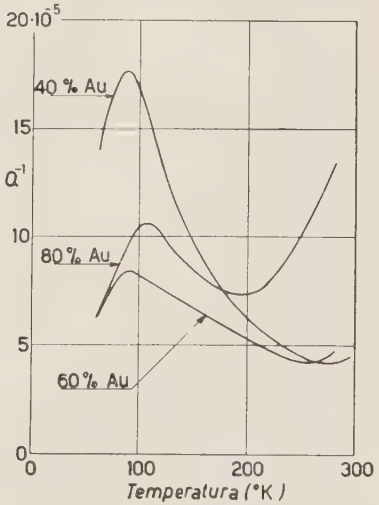

Fig. 4. – Coefficiente di dissipazione in alcune leghe a concentrazione intermedia in funzione della temperatura assoluta.

della dissipazione, che, specialmente nel campione contenente il 60% di Au, risulta poco pronunciato. Anche la temperatura T_m, cui corrisponde il massimo di attenuazione, varia con la concentrazione. Nelle Fig. 2, 3 e 4 si può infatti notare uno spostamento graduale della temperatura del picco verso valori più elevati al crescere della percentuale di Au. Le temperature T_m relative alle leghe risultano tuttavia in ogni caso comprese tra la temperatura dell'argento puro (71.5 °K) e quella dell'oro puro (132 °K).

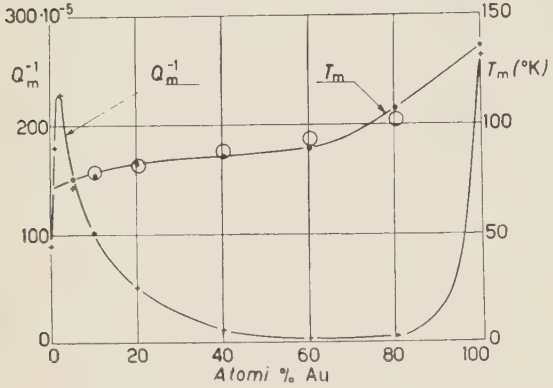

Fig. 5. – Valore del massimo di dissipazione Q_m^{-1} dovuto all'effetto Bordoni in funzione della concentrazione, senza la dissipazione di fondo. • Temperatura T_m corrispondente al massimo di dissipazione, in funzione della temperatura, determinate sperimentalmente. ○ Temperatura T_m calcolata mediante l'equazione (7).

Questi risultati sono raccolti e meglio illustrati nella Fig. 5, in cui il valore del massimo di dissipazione Q_m^{-1} e la corrispondente temperatura T_m, che si ottengono con una frequenza di vibrazione sensibilmente uguale per tutti i campioni (v. Tabella II), sono stati riportati in funzione della concentrazione. È interessante notare il comportamento del Q_m^{-1} in corrispondenza alle piccole percentuali di Au in Ag, e, in particolare, il massimo che si ha per la lega al 2% di Au. Sfortunatamente non è stato ancora possibile verificare se anche le leghe costituite da piccole percentuali di Ag in Au presentano un analogo comportamento.

Una particolarità nell'andamento della velocità di propagazione delle onde elastiche in funzione della concentrazione è già stata messa in evidenza da due degli autori in una precedente ricerca, eseguita su una serie analoga di leghe ([20]). Nella Fig. 6 è stata tracciata la curva della velocità c_e, misurata a temperatura ambiente, in funzione della concentrazione. La curva presenta una

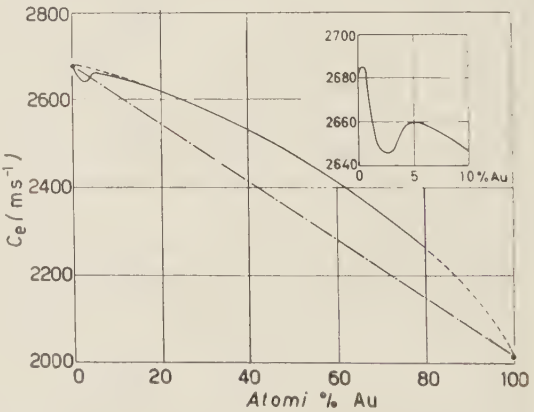

Fig. 6. – Velocità di propagazione delle onde elastiche estensionali a temperatura ambiente in funzione della concentrazione.

concavità rivolta verso l'asse delle ascisse ed il suo andamento conferma i risultati precedentemente ottenuti; in particolare, si ritrova il minimo di velocità in corrispondenza alle leghe a basso tenore di Au e precisamente per quelle che presentano valori del Q_m^{-1} più grandi del valore relativo al campione di Ag puro (v. Fig. 5).

Anche il coefficiente di temperatura della velocità:

$$(5) \qquad \beta = -\frac{\partial \ln c_e}{\partial T} \simeq -\frac{\partial \ln f}{\partial T},$$

ha un andamento piuttosto irregolare in corrispondenza alle particolarità riscontrate sia nel Q_m^{-1}, sia nella velocità c_e: La Fig. 7 presenta il coefficiente β al variare della concentrazione; i valori di β sono stati calcolati, per tutti i campioni, a due temperature molto differenti e precisamente a 293 °K ed a 77 °K. In entrambi i casi il coefficiente β presenta, nell'intervallo di concentrazione tra l'1% ed il 10% di Au, valori più elevati di quelli previsti da un andamento regolare, con un massimo in corrispondenza alla lega contenente il 2% di atomi di Au.

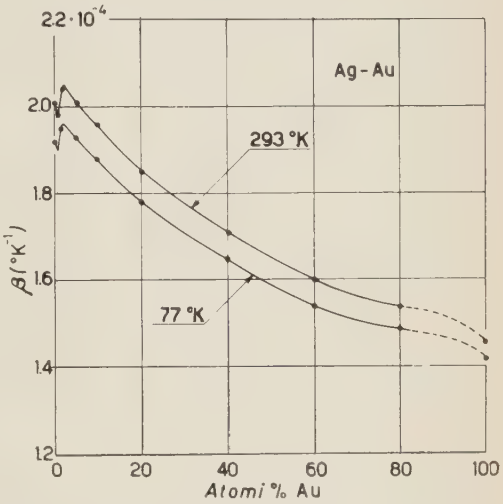

Fig. 7. – Coefficiente di temperatura della velocità a temperatura ambiente ed alla temperatura di ebollizione dell'azoto.

Una serie di misure anche a frequenza più elevata (174 kHz circa) è stata eseguita nel campione contenente il 20% di atomi di Au. Nella Fig. 8 è mostrato l'andamento del coefficiente Q^{-1}, in funzione della temperatura asso-

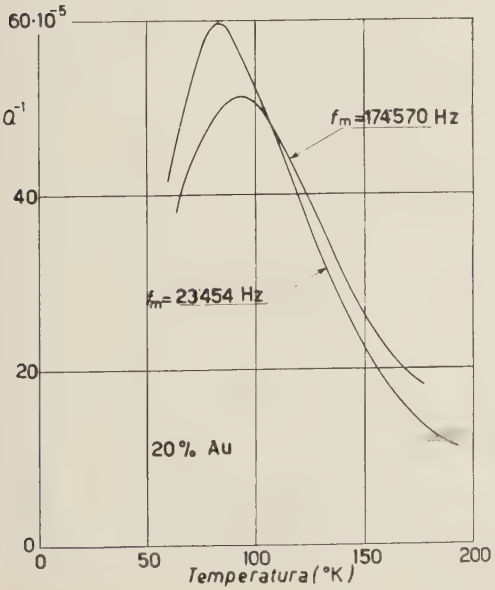

Fig. 8. – Coefficiente di dissipazione in funzione della temperatura assoluta nella lega contenente il 20% di Au, determinato per due diverse frequenze di vibrazione.

luta, per le due diverse frequenze di vibrazione. Il risultato più importante di questo confronto è certamente la verifica sperimentale dell'aumento della temperatura T_m col crescere della frequenza, come è richiesto dall'effetto di rilassamento attivato termicamente associato al moto delle dislocazioni ([17]).

Nella Tabella III sono raccolti i valori dei parametri che caratterizzano l'effetto Bordoni in questa lega, determinati in corrispondenza ai due diversi valori della frequenza.

TABELLA III. – *Valori caratteristici dell'effetto Bordoni nella lega al 20% di* Au *determinati per due frequenze diverse.*

f_m (Hz)	T_m (°K)	Q_m^{-1}	Q^{-1} per $T = 293$ °K
23 454	83 ± 0.5	$59.7 \cdot 10^{-5}$	$9.0 \cdot 10^{-5}$
174 570	92.5 ± 0.5	$51.5 \cdot 10^{-5}$	$11.7 \cdot 10^{-5}$

4. – Discussione dei risultati sperimentali.

I risultati sperimentali presentati nel paragrafo precedente indicano che nelle leghe del sistema Ag-Au si nota, a bassa temperatura, un aumento della dissipazione qualunque sia la loro composizione. Le curve delle Fig. 2, 3 e 4 mostrano il caratteristico andamento a campana della dissipazione in funzione della temperatura legato ad un fenomeno di rilassamento. Inoltre la Fig. 8 prova che l'effetto in esame è certamente dovuto ad un fenomeno di rilassamento attivato termicamente, in quanto lo spostamento della temperatura T_m del massimo di attenuazione al variare della frequenza di vibrazione è caratteristico di questo tipo di fenomeni di rilassamento.

In una ricerca precedente ([18]) è stato possibile dimostrare che nei due metalli puri questo massimo di dissipazione è dovuto ad un effetto di rilassamento legato al moto delle dislocazioni presenti nel reticolo cristallino, sotto l'azione combinata della sollecitazione meccanica e della agitazione termica. Si è potuto constatare sperimentalmente che tra la temperatura del massimo di dissipazione T_m e la frequenza f_m della sollecitazione meccanica, sussiste la relazione esponenziale di tipo Arrhenius:

$$f_m = f_A \exp\left[-Wk^{-1} \cdot T_m^{-1}\right], \tag{6}$$

dove k = costante di Boltzmann, f_A rappresenta il valore limite, per $T \to \infty$, della frequenza di vibrazione e W l'energia di attivazione del moto delle dislocazioni.

Nella Tabella IV sono stati raccolti i valori dei parametri caratteristici del processo di rilassamento determinati nei due metalli puri.

TABELLA IV. – *Alcuni parametri caratteristici relativi ai due componenti puri* [18].

Metallo	W (eV)	f_A (s^{-1})	ν_D (s^{-1})	ϱ (g cm^{-3})	ϱc_t (g cm^{-2} s^{-1})	$\frac{\sigma_p^0}{\mu}$
Ag	0.124 ($\pm$0.005)	$40 \cdot 10^{11}$	$45 \cdot 10^{11}$	10.50	$2.814 \cdot 10^6$	$6.0 \cdot 10^{-4}$
Au	0.158 ($\pm$0.002)	$0.7 \cdot 10^{11}$	$35 \cdot 10^{11}$	19.32	$3.916 \cdot 10^6$	$8.6 \cdot 10^{-4}$

ν_D = frequenza limite di Debye.
σ_p^0 = sforzo di Peierls.
μ = modulo elastico di scorrimento.

Per ottenere questi stessi parametri per le varie leghe Ag-Au qui esaminate, è necessario determinare la temperatura T_m, al variare della frequenza di vibrazione f_m, per ogni campione della serie considerata.

Questa misura, a causa della impossibilità di determinare con sufficiente precisione la temperatura dei campioni (v. Sezione 2), è stata eseguita solo sulla lega contenente il 20% di Au.

È tuttavia possibile prevedere l'andamento di W in funzione della concentrazione anche servendosi dei dati sperimentali ottenuti nella presente ricerca e dei valori di W e di f_A relativi ai due metalli puri.

Si supponga che l'energia di attivazione W dipenda dalla concentrazione come il prodotto ϱc_t, dove ϱ è la densità della lega e c_t la velocità di propagazione delle onde elastiche estensionali. Questa ipotesi è confortata dal fatto che il rapporto delle energie di attivazione W_{Au}/W_{Ag} è praticamente uguale al rapporto dei corrispondenti valori di ϱc_t, nonchè di σ_p^0/μ, essendo σ_p^0 lo sforzo di Peierls e μ il modulo elastico di scorrimento (v. Tabella IV). Nella Fig. 9 è stato rappresentato, in funzione della concentrazione, l'andamento dell'energia di attivazione W che così si ottiene.

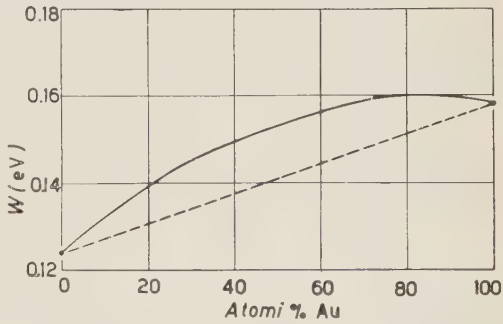

Fig. 9. Dipendenza dell'energia di attivazione W dalla concentrazione: *a*) linea a tratti: dipendenza lineare; *b*) linea continua: dipendenza suggerita dalle considerazioni svolte nel testo.

Conviene inoltre osservare che un andamento del genere viene suggerito anche dallo scostamento negativo che la costante reticolare presenta al variare della concentrazione, rispetto alla legge lineare di Vegard ([24]).

Supposto infine che la frequenza limite f_A vari come la velocità c_s al variare della concentrazione (*), è possibile determinare i valori della temperatura T_m del massimo di dissipazione per tutte le leghe mediante la relazione

$$T_m(p) = \frac{W(p)}{k[\ln f_A(p) - \ln f_m]}, \tag{7}$$

in cui W ed f_A dipendono dalla concentrazione p secondo le due ipotesi dianzi fatte ed f_m è la frequenza della sollecitazione meccanica, che, in questo caso, è praticamente uguale per tutti i campioni. In questo modo sono stati calcolati i valori di T_m che si trovano riportati nel diagramma di Fig. 5 con cerchi vuoti. L'accordo tra i risultati sperimentali ed i valori così determinati è soddisfacente e rappresenta una prova indiretta della bontà delle ipotesi avanzate circa la dipendenza di W ed f_A dalla concentrazione. Come ulteriore prova, l'energia di attivazione della lega contenente il 20% di atomi Au è stata direttamente calcolata servendosi dei dati sperimentali della Fig. 8, raccolti nella Tabella III.

L'energia di attivazione W si calcola mediante la

$$W = k \frac{\ln f_{m2} - \ln f_{m1}}{T_{m1}^{-1} - T_{m2}^{-1}}, \tag{8}$$

in cui T_{m1} e T_{m2} sono le temperature del massimo di attenuazione ottenute rispettivamente alle frequenze di vibrazione f_{m1} ed f_{m2}, e $k = 8.615$ eV grado^{-1}.

Il valore che così si ottiene:

$$W = (0.14 \pm 0.01) \text{ eV}$$

è in buon accordo con il valore previsto dal diagramma di Fig. 9. L'imprecisione che si ha in questo risultato (si confrontino, ad esempio, i valori di W riportati nella Tabella IV e nella citazione ([18])) dipende essenzialmente dalla scarsa precisione con cui è stato possibile determinare le due temperature T_m nel campione esaminato.

Un altro risultato particolarmente interessante che si può trarre dall'analisi delle Fig. 2, 3 e 4, è rappresentato dalla progressiva diminuzione del valore del massimo di dissipazione Q_m^{-1} all'aumentare della concentrazione degli atomi di oro. Questo massimo, che è particolarmente accentuato nelle leghe con pic-

([24]) C. S. BARRETT: *Structure of Metals*, (London, 1953), p. 222.

(*) Ciò equivale a supporre che f_A dipenda dalla concentrazione come la frequenza caratteristica di Debye ν_D.

cole percentuali di oro, si riduce ad un lieve ingobbamento della curva dissipazione-temperatura quando il rapporto tra il numero di atomi dei due costituenti si avvicina al valore unitario (v. Fig. 5). Contemporaneamente si può notare anche una progressiva diminuzione della dissipazione a temperatura ambiente; per le leghe centrali essa assume dei valori minimi dell'ordine di $4.6 \cdot 10^{-5}$ (v. Tabella II).

Questi risultati sembrano indicare che, a parità di trattamenti meccanici e termici, le leghe contenenti piccole percentuali di oro sono molto più ricche di dislocazioni attive. Le micrografie riportate nella Fig. 1 mostrano effettivamente che in queste leghe il grado di incrudimento raggiunto è maggiore rispetto a quello delle leghe contenenti maggiori percentuali di oro. Infatti, nelle prime tre micrografie, che si riferiscono rispettivamente alle leghe con l'1, il 5 e 10% di oro, è possibile distinguere chiaramente i grossi grani cristallini fortemente deformati secondo la direzione di laminazione. Le altre micrografie, al contrario, mostrano una struttura granulare molto irregolare e più finemente suddivisa, senza particolari effetti legati alla direzione di laminazione. Anche il minimo di velocità trovato in corrispondenza alla lega contenente il 2% di atomi di oro (v. Fig. 6), nonchè l'andamento anomalo del coefficiente di temperatura (v. Fig. 7), indicano senza dubbio la presenza di un più elevato numero di dislocazioni attive, cioè capaci di muoversi liberamente sotto l'azione combinata dell'agitazione termica e della sollecitazione periodica esterna.

In una precedente ricerca [20] è stato dimostrato sperimentalmente che, dopo opportuni trattamenti termici, è possibile ridurre sensibilmente tale minimo, come conseguenza della eliminazione, per effetto dell'agitazione termica, di buona parte delle dislocazioni attive. Dopo tali trattamenti, si è inoltre constatato che la curva velocità-concentrazione tende a perdere la concavità rivolta verso l'asse delle ascisse per assumere invece un andamento lineare.

La progressiva diminuzione dell'ampiezza del massimo di dissipazione all'aumentare della percentuale di oro è accompagnata da un allargamento delle curve dissipazione-temperatura assoluta, come si può chiaramente vedere nelle Fig. 2, 3 e 4. Questo allargamento delle curve a campana indica un progressivo aumento della larghezza dello spettro delle frequenze di rilassamento (o, se si vuole, dei tempi di rilassamento), dovuto, come si può facilmente intuire dopo quanto è stato sin qui detto, al minor grado di incrudimento che sembra sia stato introdotto nelle leghe a composizione intermedia, cioè ad un esiguo numero di dislocazioni attive tra cui non riesce a prevalere un certo tipo di dislocazioni. Anche il rapporto prossimo all'unità del numero degli atomi dei due metalli è certamente responsabile del gran numero di dislocazioni presenti che sono bloccate in più punti e rese inattive (diminuzione del massimo di dissipazione) oppure ridotte a segmenti attivi di lunghezza molto diversa (allargamento dello spettro delle frequenze di rilassamento).

5. – Conclusioni.

Con la presente indagine sperimentale è stato provato che anche nelle leghe la dissipazione di energia elastica presenta un massimo a bassa temperatura. È stata presa in esame una serie completa di leghe del sistema binario Ag-Au, che, per le particolari caratteristiche fisico-chimiche dei due componenti, meglio di ogni altro si presta ad una indagine di questo tipo. Il massimo di dissipazione, trovato in tutti i campioni esaminati, presenta senza possibilità di dubbio le caratteristiche dell'effetto Bordoni, sinora accertato sperimentalmente solo in alcuni metalli puri o contenenti piccolissime percentuali di impurità.

A parità di frequenza di vibrazione, la temperatura T_m del massimo di attenuazione cresce gradualmente al variare della concentrazione e per ogni lega essa risulta compresa tra i valori relativi ai due metalli puri.

Dall'andamento della temperatura del massimo in funzione della concentrazione è stato possibile prevedere i valori dell'energia di attivazione W per le diverse concentrazioni e dimostrare che essa non varia linearmente, ma piuttosto secondo una curva che presenta una concavità rivolta verso l'asse delle concentrazioni. Nel caso della lega contenente il 20% di atomi di Au, il valore di W è stato determinato direttamente, ed esso risulta in buon accordo con l'ipotesi dianzi avanzata.

La progressiva diminuzione dell'ampiezza del massimo ed il graduale allargamento delle curve a campana all'aumentare del numero di atomi di Au, sembrano indicare la presenza di un numero di dislocazioni attive che va man mano diminuendo. In particolare, le anomalie riscontrate in corrispondenza alle leghe con piccole percentuali di Au sia nei valori della dissipazione, sia in quelli della velocità di propagazione e del coefficiente di temperatura β, suggeriscono l'ipotesi che, a parità di trattamenti termici e meccanici, queste leghe risultino notevolmente più ricche di dislocazioni attive, cioè di dislocazioni libere di muoversi sotto l'azione delle onde termiche e delle vibrazioni elastiche impresse.

L'aumento graduale della temperatura del massimo dovuto all'effetto Bordoni al crescere del numero di atomi di Au, rappresenta infine una nuova prova del carattere intrinseco dei due parametri W ed f_A che compaiono nell'equazione (6). Essi risultano lievemente influenzati sia dal grado di incrudimento, sia dalla presenza di atomi di natura diversa in seno ai cristalli. Questi atomi infatti sembrano controllare principalmente il numero delle dislocazioni attive presenti e, di conseguenza, il valore del massimo di dissipazione Q_m^{-1}.

La misura della velocità di propagazione delle onde elastiche di tipo estensionale in funzione della concentrazione, ha confermato i risultati sperimentali di una precedente ricerca. In particolare si è ritrovato un minimo per la velocità in corrispondenza alle leghe meno ricche in oro, dovuto alla presenza di un gran numero di dislocazioni attive.

* * *

Gli autori desiderano ringraziare vivamente la « Metalli Preziosi S.p.A. » di Milano, il cui Laboratorio ricerche e controlli ha curato con tanta perizia la preparazione dei campioni e la loro analisi chimica, spettrografica e metallografica.

Ci è gradito ringraziare il prof. P. G. BORDONI per le utili discussioni e gli incoraggiamenti avuti durante il lavoro di ricerca e di stesura.

SUMMARY

A new set of experiments carried out in the alloys of the Ag-Au system has shown the existance of the Bordoni peak in a temperature range between 71.5 °K (pure silver) and 132 °K (pure gold), for a vibration frequency of about 20 kHz. The peak is clearly exhibited by the alloys with a small concentration of foreign atoms, but it is reduced to a nearly flat curve when the atomic concentration approches the one to one ratio. The experimental curve of the extensional velocity measured at room temperature and that of the velocity temperature coefficient β measured at 293 °K and 77 °K, show an anomalous behaviour for atomic concentrations of gold less than 10%. These effects are related to a high number of active dislocations present in these specimens. For alloys containing more than 10% of gold, the velocity curve is concave towards the concentration axis. The activation energy W for the alloys has not yet been measured directly. An estimate for the values of W has however been obtained assuming that the curve of W as a function of concentration is not a straight line, but a curve with its concavity towards the abscissa as it is suggested by the negative deviation from the Vegard's law shown by the lattice constant of the Ag-Au system.

Heisenberg Representation in Classical General Relativity.

R. Arnowitt (*), S. Deser (**) and C. W. Misner (***)

Department of Physics, Syracuse University - Syracuse, N.Y.
and Department of Physics, Brandeis University - Waltham, Mass.

(ricevuto l'8 Ottobre 1960)

Summary. — The energy of the gravitational field (as of any other system) is not always the numerical value of the Hamiltonian (for example, not in a Hamilton-Jacobi formulation). We define a classical « Heisenberg representation » which excludes Hamilton-Jacobi-like canonical transformations. Ordinarily, within the Heisenberg representation, there remains only the possibility of time-independent canonical transformation among the dynamical variables. However, the freedom of co-ordinate transformations in general relativity allows many extra « canonical » transformations not found in conventional Lorentz covariant theory. This wider class of canonical formalisms possess all the properties usually associated with the Heisenberg picture in that in each formalism the measurable quantities, $g_{\mu\nu}(t)$, are obtained from knowledge of the canonical variables at the same time without any explicit co-ordinate dependence. Further, the Hamiltonian is a constant of motion. Only in Heisenberg frames is the Hamiltonian to be associated with the energy of the system. In spite of the additional freedom of canonical transformations (due to the freedom of co-ordinate change mentioned above), it is shown that the Hamiltonian is numerically the same for a fixed state of the gravitational field in any Heisenberg representation. The energy is then a uniquely definable quantity in the theory. In the process, it is established that two Heisenberg frames can differ by co-ordinate transformations that depend only on the canonical variables and not explicitly on the co-ordinates. These transformations must also preserve the property that at spatial infinity the metric become Lorentz so that the physical boundary conditions be unaltered.

(*) Research supported in part by the United States Air Force through The Aeronautical Research Laboratory, WADD and Contract AF49(638)-636 of the Air Force Office of Scientific Research.

(**) Research supported in part by The National Science Foundation and Air Force Office of Scientific Research under Contract AF49(638)-636.

(***) Alfred P. Sloan Research Fellow. On leave from Palmer Physical Laboratory Princeton University, Princeton, N. J..

1. – Introduction.

As is well known, the canonical variables arising in the Hamiltonian formulation of mechanical systems and conventional Lorentz covariant field theories are not unique. The freedom of canonical transformations among these variables corresponds to the possibility of different descriptions of the same physical system. In previous work [1], the gravitational field has been cast into canonical form in terms of two explicitly-defined pairs of conjugate field variables. These four quantities may be specified arbitrarily at an initial time, and their subsequent motion is governed by a non-vanishing Hamiltonian depending only on these canonical variables. Within this framework, unique and physically correct definitions have been given of such quantities as the total energy, total momentum and flux of radiation in the wave zone. The theory, then, has the physical properties of an ordinary classical field.

The freedom of canonical transformations among the canonical variables of ordinary theories is found for our four variables as well. In general relativity, however, a second class of transformations arises due to the general covariance, which have no counterpart in ordinary field theories. The process of reducing the gravitational system to canonical form involves choosing four invariant functionals of the metric as co-ordinates. For any choice of co-ordinates (obeying the physical requirement of being asymptotically Lorentz at spatial infinity), it has been shown that a set of canonical variables can be obtained (see III). A change from one co-ordinate system to another (with a concomitant change of the canonical variables) can also be regarded as a « canonical » transformation in that it can be generated by adding a time derivative of the original Lagrangian. However, this time derivative depends, in general, on all eight variables, *i.e.*, on the four quantities that become the canonical variables *and* on those four which are eventually chosen to be the space-time co-ordinates. Thus, the transformation falls outside the range of the conventional canonical ones. It is therefore necessary to investigate what changes in the physical description of the system may be involved in such transformations.

One does not, of course, expect that in every canonical form of a theory the energy be the numerical value of the Hamiltonian. Hamilton-Jacobi transformations, for example, will alter this relationship, without affecting the value

---

[1] Other papers in this series will be referred to by Roman numerals: I - *Phys. Rev.*, **113**, 745 (1959); II - *Phys. Rev.* **116**, 1322 (1959); III - *Phys. Rev.*, **117**, 1595 (1960); IV - *Phys. Rev.*, **118**, 1100 (1960); V - *Phys. Rev.*, **120**, 313 (1960); IIIa - *Journ. Math. Phys.*, **1**, 434, (1960); IVb - *The Wave Zone in General Relativity, Phis. Rev.* (to be published); IVc - *Co-ordinate Invariance and Energy Expressions in General Relativity*, sub. to *Phys. Rev.* — This paper is IVa.

of the (physically-defined) energy. For the Hamiltonian to yield the energy, the theory must be expressed in one of a particular set of canonical forms, which we call the « Heisenberg representation » in analogy with quantum mechanical usage. In Section 3, we shall explicitly define the Heisenberg representation precisely as is done in other branches of physics. We shall then see that, in general relativity, two canonical forms within the Heisenberg set will, in general, correspond to different co-ordinate conditions. Thus, unlike the usual situation, canonical transformations among Heisenberg forms may involve a *change of co-ordinate frame*. In spite of this, it will be seen in Section 4 that the energy (which is the numerical value of the Hamiltonian in any Heisenberg form) has the same value in all such frames (as is physically required). Identical results hold for the momentum of the gravitational field.

In Section 2 we shall investigate the formal aspects of the generalized canonical transformations. The underlying physics will be clarified by discussing the analogous freedom which exists in the simple case of parametrized particle mechanics.

2. – Generalized canonical transformations.

Since the generalized class of transformations that we must discuss is a consequence of co-ordinate invariance, a simple analogue arises in parametrized particle (or field) mechanics. (Such systems are also invariant under an arbitrary change of the parameters.) The particle example will provide a good illustration of the main features to be analyzed below in general relativity. The action for a mechanical system,

$$I=\int \mathrm{d}t\,[p\dot{q}-H(p,q)]\,, \tag{2.1}$$

may be parametrized by adding the extra variables p_t and $q_t = t$, and by using τ as the independent co-ordinate:

$$I=\int \mathrm{d}\tau[pq'+p_tq_t'-N(\tau)R]\,. \tag{2.2}$$

In eq. (2.2), $q'\equiv \mathrm{d}q/\mathrm{d}\tau$ and R is any function of p, q, p_t such that $R=0$ has the solution $p_t=-H(p,q)$. The quantity $N(\tau)$ is an arbitrary Lagrange multiplier whose variation enforces the constraint $R=0$. Thus, elimination of p_t *and* imposition of the *particular* co-ordinate condition $\tau=q_t$ returns I to the original form. [We might note that the action for general relativity is of precisely the type (2.2) without any preferred pre-existing form (2.1), since eq. (2.1) singles out a particular co-ordinate frame.] The generator asso-

ciated with the action of eq. (2.2) (arising due to end point variations) becomes (after elimination of p_t)

$$G = p\ \delta q - H\ \delta q_t\,. \tag{2.3}$$

The general class of « canonical » transformations which do not alter the Lagrange equations of motion are obtained by adding a term $\mathrm{d}W/\mathrm{d}\tau$ to the Lagrangian, and corresponding, δW to the generator. Three types of transformations can be distinguished. First, within a given co-ordinate frame, *e.g.* $\tau = q_t$ there exist the « simple canonical transformations » characterized by the relation

$$p\ \delta q + \delta W(p, q) = P\ \delta Q \tag{2.4}$$

where P and Q are functions of p and q only. Such transformations therefore take place entirely within the $2N$ dimensional phase space (N being the number of canonical pairs q and p). Such a « recanonization » of the form on the left-hand side of eq. (2.4) to obtain the right-hand side can, of course, be carried out for any $W = W(p, q)$. A transformation of this type maintains the numerical value of the Hamiltonian, H, as well as the co-ordinate condition $q_t = t$.

Second, still within a given co-ordinate frame, one can consider transformations characterized by

$$p\ \delta q - H\ \delta t + \delta W(p, q, t) = P\ \delta Q - \bar{H}(P, Q, t)\ \delta t\,, \tag{2.5}$$

where P and Q are functions of p, q and t. Here we are performing a transformation in the $2N+1$ dimensional space, the Hamilton-Jacobi transformation being a familiar example.

The third class of transformations, which we shall call generalized canonical (G.C.) transformations, goes beyond these two well-known types in allowing changes of the co-ordinate frame as well. Here we have

$$p\ \delta q - H\ \delta q_t + \delta W(p, q, q_t) = P\ \delta Q - \bar{H}\ \delta Q_t\,. \tag{2.6}$$

If the original co-ordinate system was $q_t = t = \tau$ the new frame may be chosen to be $Q_t(p, q, q_t) = \bar{t} = \tau$ to reinstate canonical form. This relation may be rewritten $\bar{t} = \bar{t}(p, q, t)$, an equation which represents the co-ordinate transformation between the two frames. The Hamiltonian $\bar{H}$ may or may not be numerically equal to H. It generates time motion in the $\bar{t}$ frame according to

$$\mathrm{d}Q/\mathrm{d}\bar{t} = [Q, \bar{H}]\,, \qquad \mathrm{d}P/\mathrm{d}\bar{t} = [P, \bar{H}]\,, \tag{2.7a}$$

$$[Q, P] = 1\,, \qquad [Q, Q] = [P, P,] = 0\,. \tag{2.7b}$$

The Poisson bracket (P.B.) relations (2.7*b*) are valid in the $\bar{t}$ frame. For example, they may be used to evaluate the P.B.'s in eq. (2.7*a*) to obtain the correct equations of motion in this frame. The G.C. transformation gives the relation between $P, Q, Q_{\bar{t}} = \bar{t}$ and p, q and $q_t = t$. However, if these relations were substituted into the left-hand side of eq. (2.7*b*) and the P.B. evaluated in the t frame where $[q, p] = 1$, one would *not*, in general, obtain unity for $[Q, P]$. Thus this class of transformations is not of the usual type.

A simple example illustrates the above points. For a free particle, $H = \frac{1}{2}p^2$, we choose as a new frame $\bar{t} = t + q(t)$. This corresponds to a G.C. transformation with $W = 0$, $P(\bar{t}) = p(t) + \frac{1}{2}p^2(t)$, $Q(\bar{t}) = q(t)$ and $\bar{H}(P, Q) = H(p, q) = 1 + P - (1 + 2P)^{\frac{1}{2}}$. It is clear that $[Q(\bar{t}), P(\bar{t})]_{pq} = [q(t), p(t) + \frac{1}{2}p^2(t)] = 1 + p \neq 1$. However, the equations of motion, calculated by eq. (2.7), are indeed the valid ones.

While, in the particle case, there is no mathematical inconsistency in using the $\bar{t}$ frame [2], such $\bar{t}$ clocks are not employed (by convention) and hence such transformations are not ordinarily considered. In general relativity, the same convention holds at spatial infinity, where space is flat; there, ordinary t clocks are used. One requires, therefore, that all co-ordinates reduce to the conventional ones at infinity, leaving the freedom of making some $\bar{t}$-type transformations in the interior. More precisely, the requirement is that clocks run like conventional ones at infinity, that is, that [3] $\partial t / \partial \bar{x}^\mu \to \delta^0_\mu$ there. This permits $\bar{t}$ to differ from t by terms $\sim x^\mu / r$, for example. Similarly, for rods, $\bar{r}$ may differ from r by $\sim x^\mu / r$. The frames themselves, which are specified by the metric, will then differ from each other, and from the Lorentz metric $\eta_{\mu\nu}$, by terms that go to zero at spatial infinity.

A generator that parallels eq. (2.3) for the gravitational field is (see III)

$$G = \int \mathrm{d}^3 r [\pi^{ijTT}\, \delta g_{ij}{}^{TT} - (-\nabla^2 g^T)\, \delta(-\tfrac{1}{2}\nabla^{-2}\pi^T) + (-2\pi^{ij}{}_{,j})\, \delta g_i] \,, \tag{2.8}$$

where spatial divergences have been discarded (see III-a). In eq. (2.8), the notation is as in III. The quantities, $-\nabla^2 g^T$ and $-2\pi^{ij}{}_{,j}$ may be solved for in the constraint equations in terms of the remaining variables and are thus the counterpart of p_t. The coefficients of these four quantities are analogous to δq_t and may be chosen to be δx^μ, this co-ordinate condition being satisfactory at spatial infinity. The π^{ijTT} and $g_{ij}{}^{TT}$ are then two pairs of canonical variables analogous to p and q. In the examples of G.C. transformations exhibited in III,

---

[2] However, such co-ordinate transformations which depend upon the dynamics could create difficulties in quantum theory (see II).

[3] Latin indices run from 1 to 3, Greek from 0 to 3, and $x^0 = t$. We use units such that $c = 1 = 16\pi\gamma C^{-4}$, where γ is the Newtonian gravitation constant. Partial differentiation is denoted by a comma.

eq. (3.23), and in V, eq. (2.17), the new co-ordinates also obey the required boundary conditions. An example of a physically unallowed co-ordinate system is furnished by

$$\bar{t} = t + \int \mathrm{d}^3 r' \, \pi^{ijTT}(r', t) \, g_{ij}{}^{TT}(r', t) \, .$$

On the other hand, $\bar{t} = t + (1/\nabla^2)\pi^{ij\,TT}(t) g_{ij}{}^{TT}(t)$ is allowed. The latter type furnishes an example of « co-ordinate waves », that is, frames in which $\bar{g}_{\mu\nu,\alpha}$ vanishes like $\bar{g}_{\mu\nu} - \eta_{\mu\nu}$, namely like $1/r$ rather than $1/r^2$. Such frames are discussed further in IV*b* and IV*c*. These papers show in detail how one may distinguish between co-ordinate waves and the asymptotic physically significant parts of the metric (*i.e.* the radiation field and the Newtonian-like parts of the metric) for the case where $g_{\mu\nu} - \eta_{\mu\nu}$ is $\mathcal{O}(1/r)$ asymptotically.

3. – Physically preferred canonical forms.

The various canonical formulations of general relativity obtainable by imposing different co-ordinate conditions (and hence differing from each other by G.C. transformations) are all mathematically equivalent. In this section, we shall distinguish, by means of physical criteria, a preferred subclass of canonical formalisms which possess properties inherent in the Heisenberg representation used in the rest of physics. In the next section it will be proved that the Hamiltonian and the generator of spatial translations take on the same numerical value (for the same physical state) in all these preferred formalisms. Consequently, these quantities may be identified as the energy and momentum of the gravitational field.

The first condition we impose is that the co-ordinate frame be chosen such that the Hamiltonian density do not depend explicitly on the co-ordinate x^μ. This eliminates frames in which space-time isotropy and homogeneity is lost, and consequently insures conservation of the energy-momentum [4] vector. (We are, of course, assuming that our frames are asymptotically Lorentz.)

Second, we shall demand that the canonical variables in the acceptable frames be « Heisenberg variables ». We use the latter term in just the sense of quantum mechanics. The time motion of these quantities is to be generated by the full Hamiltonian. For ordinary particle mechanics, the fundamental Heisenberg variables which may be measured with rods and clocks are the position and velocity variables $\boldsymbol{r}(t)$ and $\mathrm{d}\boldsymbol{r}(t)/\mathrm{d}t$. The state of the system at a given time can be specified directly from these quantities at a given time. The physical interpretation of *any* set of canonical variables may be obtained

[4] A general discussion of co-ordinate independence and conservation is given in II.

by referring back to this fundamental pair. In general relativity, the fundamental Heisenberg variables measured by rods and clocks are $g_{\mu\nu}$ and $\partial_0 g_{\mu\nu}$. This is in agreement with the implicit assumption always made that the variables used in the original Lagrangian of a system are Heisenberg quantities. A set of canonical variables P, Q is a Heisenberg set, therefore, if the fundamental Heisenberg quantities are related to it in a fashion not involving time explicitly. In this way, Hamilton-Jacobi type transformations are eliminated. For a particle, this criterion reads

$$\boldsymbol{r}(t) = \boldsymbol{F}(P(t), Q(t)) \tag{3.1}$$

and hence $\partial \boldsymbol{F}/\partial t = 0$. Note that by differentiating and using the Hamilton equations of motion for $\dot{P}$ and $\dot{Q}$, one obtains an expression for $\mathrm{d}\boldsymbol{r}(t)/\mathrm{d}t$ involving only P and Q (for the conservative Hamiltonians we are considering). In general relativity, the requirement that a set of canonical variables $g^c(\boldsymbol{r}, t)$, $\pi^c(\boldsymbol{r}, t)$ be Heisenberg variables is that

$$g_{\mu\nu}(t) = f_{\mu\nu}[g^c(t), \pi^c(t)]\,, \tag{3.2}$$

where $f_{\mu\nu}$ is a functional of $g^c(\boldsymbol{r}, t)$ and $\pi^c(\boldsymbol{r}, t)$, but not explicitly of t. It may therefore require knowledge of these canonical variables over the entire $t = \text{const}$ surface to evaluate $g_{\mu\nu}$ at a particular point on that surface. The first restriction on $f_{\mu\nu}$ is thus that the directly measurable quantity $g_{\mu\nu}$ is obtainable *at a given time* purely on terms of the canonical variables *at that same time*. In field theory, the Heisenberg requirement is extended to refer to the spatial co-ordinates as well as to the time. The second restriction is, then, that a space translation of the canonical variables must correspond to the same space translation of the fundamental quantities $g_{\mu\nu}$. Dependence on the space co-ordinates of the type brought in by $1/\nabla^2$ is permitted in the functional $f_{\mu\nu}$, then, since it does not violate this criterion. To summarize the above discussion, we require that $f_{\mu\nu}$ be a « Heisenberg functional » which is defined as follows (5): *a*) $f_{\mu\nu}$ does not depend upon time explicitly, and *b*) if T_a is a spatial translation operator, *i.e.* $(T_a f)(\boldsymbol{r}) \equiv f(\boldsymbol{r}+\boldsymbol{a})$, then

$$T_a f_{\mu\nu}[g^c(t), \pi^c(t)] = f_{\mu\nu}[T_a g^c(t), T_a \pi^c(t)]\,. \tag{3.3}$$

The restriction to a Heisenberg representation has been made in order that the Hamiltonian correctly represent the energy. While a canonical for-

(5) Note that there is actually no asymmetry in the treatment of the space and time co-ordinates since $f_{\mu\nu}$ may also be non-local in time in a translationally invariant fashion. For then one may use the (translation invariant) equations of motion to express $g^c(t')$, $\pi^c(t')$ in terms of $g^c(t)$, $\pi^c(t)$ and $t' - t$ (without loss of space translation invariance). The time translation invariance of $f_{\mu\nu}$ would then guarantee that no explicit t dependence appears when $f_{\mu\nu}$ is expressed in terms of $g^c(t)$, $\pi^c(t)$.

malism in a Hamilton-Jacobi (« Schrödinger ») or an interaction representation correctly describes the dynamics, one cannot identify the Hamiltonians of these representations with the energy of the system.

Finally, we might mention that the second condition (Heisenberg representation) is closely related to the first (conservation). Thus, consider the coupling of a particle to the gravitational field, and choose a canonical form of the gravitational variables that would *not* be a Heisenberg representation for the uncoupled theory (though perhaps without any explicit time-dependence in the gravitational Hamiltonian). One would then find that the matter part of the Hamiltonian would depend upon time explicitly, and conservation of the total Hamiltonian would be lost. This follows from the fact that there would be an explicit appearance of time in $g_{\mu\nu}$ when expressed in terms of the gravitational canonical variables and that $g_{\mu\nu}$ appears in the matter part of the Lagrangian (6). Thus, one can replace the second condition by the first, together with the knowledge of what represents the Heisenberg representation in some non-gravitational system.

4. – Uniqueness of energy and momentum.

In any canonical formalism, one has a generator

$$G = \int \mathrm{d}^3 r \{\pi^c \, \delta g^c + \mathfrak{T}^0{}_\mu [g^c, \pi^c] \, \delta x^\mu\} , \tag{4.1}$$

so that the generators of space-time translations are

$$P_\mu = \int \mathfrak{T}^0{}_\mu \, \mathrm{d}^3 r . \tag{4.2}$$

[One obtains all such canonical forms by inserting co-ordinate conditions and solutions of the constraint equations into eq. (2.8). See III for a detailed discussion.] In this section we shall prove that, for all the physically preferred canonical forms defined in Section 3, (the Heisenberg forms), the numerical values of P_μ agree (for a fixed state of the gravitational field). Since we are in the Heisenberg representation, the numerical value of P_μ is correctly the total energy-momentum vector of the system.

One has a complete description of a Heisenberg canonical formalism when one is given the generator (4.1) *and* the construction of $g_{\mu\nu}(\boldsymbol{r}, t)$ by a relation of type (3.2). These equations contain implicitly a statement of the co-ordinate conditions specifying the frame in which $g_{\mu\nu}$ is given by eq. (3.2) are the metric

(6) See, for example, eq. (3.8) of IV for the simplest case of coupling to a point particle.

components. Thus, the co-ordinate conditions specify that four functionals, F^μ, of the metric vanish (7):

$$F^\mu[g_{\sigma\varrho}] = 0 \,. \tag{4.3}$$

From the respective co-ordinate conditions of two canonical formalisms, one can obtain a relation between the co-ordinate frames which most generally has the form

$$\bar{x}^\mu = x^\mu + f^\mu[g^c(x), \pi^c(x); x^\mu] \,. \tag{4.4}$$

The essential step in our proof is to recognize that, for two Heisenberg canonical formalisms, one actually has the relation

$$\bar{x}^\mu = x^\mu + f^\mu[g^c(t), \pi^c(t)] \,, \tag{4.5}$$

where f^μ is a Heisenberg functional (*i.e.*, f^μ has no explicit dependence on time and is translationally invariant in its dependence on x^c).

We will return later to the proof of eq. (4.5), but show first that it does indeed lead to the uniqueness of P_μ. We wish to compare the P_μ of two different Heisenberg formalisms. Let g^c, π^c be the variables of one, and x^μ the corresponding co-ordinates. Prior to the imposition of co-ordinate conditions, the (parametrized) generator may be written in the form

$$G = \int \mathrm{d}^3\tau[\pi^c(\tau)\delta g^c(\tau) + \mathfrak{T}^0{}_\mu \delta q^\mu(\tau)] \,. \tag{4.6}$$

Here q^μ are four gravitational variables which, when chosen as co-ordinates x^μ, yield the desired Heisenberg frame. [We have written the arguments of all functions as τ to emphasize that this is the generator in an (already) parametrized theory. To obtain the generator of the Heisenberg canonical formalism, we must insert the co-ordinate conditions $q^\mu = \tau^\mu$ (and then, of course, we may change notation $\tau^\mu \to x^\mu$).] The energy-momentum vector P^μ in the frame $q^\mu = x^\mu$ is

$$P_\mu(x^0) = \int \mathrm{d}^3x \, \mathfrak{T}^0{}_\mu[\pi^c(x^0), g^c(x^0)] \,, \tag{4.7}$$

(7) For example, the co-ordinate conditions defining the frame corresponding to the generator (2.8) [after the replacement $q_i = x^i$ and $(-\frac{1}{2}\nabla^2)\pi^T = t$ have been made] can be obtained directly from the relations of type (3.2) as follows. Since $q_i = x^i$, one has $g_{ij} = \delta_{ij} + g_{ij}{}^{TT} + g_{ij}{}^T[g_{mn}{}^{TT}, \pi^{rsTT}]$ and hence the condition $g_{ij,j} = 0$ is immediate from the transversality of $g_{ij}{}^{TT}$ and $g_{ij}{}^T$. To discover the condition $\pi^T = 0$, one must first differentiate the relations (3.2) (since π^{ij} is closely related to $g_{ij,0}$ and use the canonical equations of motion to eliminate $\pi^{ijTT}{}_{,0}$ and $g_{ij}{}^{TT}{}_{,0}$.

where $\mathfrak{T}^0{}_\mu$ is not explicitly dependent on x^μ (and consequently $\mathrm{d}P_\mu/\mathrm{d}x^0 = 0$) The canonical variables are g^c, π^c. [An example is provided by the frame (2.8).] To obtain the generator of a second Heisenberg formalism, we rewrite eq. (4.6) as

$$G = \int \mathrm{d}^3\tau \left\{ \pi^c \delta g^c + \mathfrak{T}^0{}_\mu \delta \{ q^\mu + f^\mu[\pi^c, g^c] \} - \mathfrak{T}^0{}_\mu \delta f^\mu[\pi^c, g^c] \right\}, \tag{4.8}$$

where f^μ is the functional which appears in the relation (4.5) between the two Heisenberg frames. The second frame is then specified by the co-ordinate conditions $Q^\mu = q^\mu + f^\mu = \bar{x}^\mu$. Before imposing this co-ordinate condition, we note that in

$$G = \int \mathrm{d}^3\tau [(\pi^c \delta g^c - \mathfrak{T}^0{}_\mu \delta f^\mu) + \mathfrak{T}^0{}_\mu \delta Q^\mu] . \tag{4.9}$$

The terms in the parentheses involve *only* π^c and g^c, but not Q^μ, since f^μ is a Heisenberg functional (8). Thus, by a simple canonical transformation,

$$\pi^c(\tau^0) = \pi^c[\bar{\pi}^c(\tau^0), \bar{g}^c(\tau^0)] , \tag{4.10a}$$

$$g^c(\tau^0) = g^c[\bar{\pi}^c(\tau^0), \bar{g}^c(\tau^0)] . \tag{4.10b}$$

They may be written as $\bar{\pi}^c \delta \bar{g}^c + \delta W[\bar{\pi}^c, \bar{g}^c]$, giving

$$G = \int \mathrm{d}^3\tau [\bar{\pi}^c \delta \bar{g}^c + \bar{\mathfrak{T}}^0{}_\mu \delta Q^\mu] . \tag{4.11}$$

In eq. (4.11) we have dropped the total variation $\delta \int \mathrm{d}^3\tau W$, and have defined $\bar{\mathfrak{T}}^0{}_\mu$ by

$$\bar{\mathfrak{T}}^0{}_\mu[\bar{\pi}^c(\tau^0), \bar{g}^c(\tau^0)] \equiv \mathfrak{T}^0{}_\mu[\pi^c[\bar{\pi}^c(\tau^0), \bar{g}^c(\tau^0)], g^c[\bar{\pi}^c(\tau^0), \bar{g}^c(\tau^0)]] . \tag{4.12}$$

In the new frame obtained by setting $Q_\mu = \tau_\mu$ in (4.11), the energy-momen-

---

(8) More precisely, $\mathfrak{T}^0_\mu$ may be a functional of not only π^c and g^c but also of q in such a way that for $q=\tau$, $\mathfrak{T}^0{}_\mu$ is τ-independent. Alternately, it is a functional of Q since $q=Q-f$. To obtain an expression which can be reduced to $\bar{\pi}^c \delta \bar{g}^c$ by a simple canonical transformation (4.10), we write

$$\mathfrak{T}^0{}_\mu = \mathfrak{T}^0{}_\mu|_{Q=\tau} + (\delta \mathfrak{T}^0{}_\mu / \delta Q)_{Q=\tau}(Q - \tau) + \ldots$$

and note that all terms but the first vanish when the new co-ordinate conditions $Q=\tau$ are imposed. Thus we need only « recanonize » the expression $\pi^c \delta g^c - \mathfrak{T}^0{}_\mu|_{Q=\tau} \delta f_\mu$, which can be accomplished by a simple canonical transformation since $\mathfrak{T}^0{}_\mu|_{Q=\tau}$ is independent of τ. The τ-independence of $\mathfrak{T}^0{}_\mu|_{Q=\tau}$ means that $\mathfrak{T}^0{}_\mu$ is a functional only of the derivatives of q, *e.g.* $\partial q/\partial\tau$, and therefore of $\partial(Q - f)/\partial\tau$ which is τ-independent at $Q=\tau$.

tum vector is

$$\bar{P}_\mu(\bar{x}^0) = \int \mathrm{d}^3\bar{x}\, \bar{\mathfrak{T}}^0{}_\mu[\bar{\pi}^c(\bar{x}^0), \bar{g}^c(\bar{x}^0)] \,, \tag{4.13}$$

(where, as in obtaining eq. (4.7), we changed notation $\tau^\mu \to \bar{x}^\mu$). To compare $\bar{P}_\mu$ with P_μ, we may use τ^μ to denote the co-ordinates in both eq. (4.7) and (4.13). Then, using (4.12), we find from (4.13) that

$$\bar{P}_\mu|_{\bar{x}^0=\tau^0} = \int \mathrm{d}^3\tau\, \mathfrak{T}^0{}_\mu[\pi^c(\tau^0), g^c(\tau^0)] = P_\mu|_{x^0=\tau^0} \,. \tag{4.14}$$

Since $\bar{P}_\mu$ and P_μ are conserved in their respective frames, we have simply $\bar{P}_\mu = P_\mu$.

We return now to the proof that the co-ordinate systems of any two Heisenberg canonical formalisms can be related in the fashion of (4.5). As noted earlier, the statement of a Heisenberg canonical formalism consists only of the relation (3.2) between $g_{\mu\nu}$ and g^c, π^c, and of the Hamiltonian in terms of g^c, π^c. Neither of these two basic elements gives a preferred status to any particular values of the co-ordinates x^μ, since there is no explicit x^μ dependence in $\mathfrak{T}^0_0$ or eq. (3.2). In order to construct the relation (4.5) we need from the second, $\bar{x}^\mu$, frame only the co-ordinate conditions (along with the full statement of the first formalism). [Recall that the co-ordinate conditions are implicit in (3.2).] For these co-ordinate conditions, by assumption, allow one to construct the co-ordinate $\bar{x}^\mu$, given any particular metric in any co-ordinate system. On the other hand, the relation (3.2) and the Hamiltonian of the first, x^μ, formalism allow one to construct the full space-time metric $g^{\mu\nu}$ given only g^c and π^c at one time x^0. Thus, one obtains $\bar{x}^\mu(x^\nu)$ as a functional of the g^c, π^c at the time x^0, which may, most generally, be written

$$\bar{x}^\mu = x^\mu + f^\mu[g^c(x^0), \pi^c(x^0), x^\mu] \,. \tag{4.16}$$

However, none of the relations used in constructing (4.16) gave a preferred status to any particular point, hence (4.16) itself cannot. This excludes the possibility of an explicit x^μ dependence in the f^μ of (4.16).

A more explicit proof of eq. (4.4) may be given by tracing the description of a particular state in two Heisenberg frames. We begin by considering the state of a system in the x^μ frame obtained by specifying the canonical variables, on the space-like surface $t = \text{const}$: g^c, $\pi^c - a$. Since the x^μ frame is assumed to be a Heisenberg one, the equations of motion for g^c, π^c do not involve x^μ explicitly ($\mathfrak{T}^0{}_0$ does not depend explicitly on x^μ). Thus g^c, π^c at any time are obtainable uniquely from the initial Cauchy-data, a, at time T and depend only on the time difference $t - T$:

$$g^c(t, \boldsymbol{r}) \,, \pi^c(t, \boldsymbol{r}) = G(t - T, a] \,. \tag{4.17}$$

In eq. (4.17) G depends upon the spatial co-ordinates vector $\boldsymbol{r}$ through the Cauchy-data $a(\boldsymbol{r})$. It will, in general, have explicit $\boldsymbol{r}$ dependence due to the appearance of such operators as $1/\nabla^2$. However, the Heisenberg requirements imply that the $\boldsymbol{r}$ dependence preserves translational invariance (as in the $1/\nabla^2$ example). Since the relationship between $g_{\mu\nu}$ and g^c, π^c has no explicit time dependence, one has

$$g_{\mu\nu}(t, \boldsymbol{r}) = g_{\mu\nu}[t - T, a] , \tag{4.18}$$

where the $\boldsymbol{r}$ dependence again preserves translational invariance. In the $\bar{x}^\mu$ frame, the co-ordinate conditions of the type (4.3) read

$$\bar{F}^\mu[\bar{g}_{\sigma\varrho}(\bar{x}); \bar{\boldsymbol{r}}] = 0 . \tag{4.19}$$

Due to the assumption that the $\bar{x}^\mu$ frame is a Heisenberg one, F^μ cannot depend explicitly on time and must depend on the space co-ordinates $\bar{\boldsymbol{r}}$ in a translationally invariant fashion. This explicit spatial dependence has been indicated in eq. (4.19). Inserting the tensor transformation relation to the x^μ frame, eq. (4.8) becomes

$$\bar{F}^\mu\left[\frac{\partial x^\lambda}{\partial \bar{x}^\varrho}\frac{\partial x^\mu}{\partial \bar{x}^\sigma} g_{\lambda\mu}(x)\right] = 0 . \tag{4.20}$$

This represents an equation which determines the relation between x^μ and $\bar{x}^\mu$. We assume that the co-ordinate conditions of both frames have been sufficiently specified so that they are unique to within at most a Lorentz rotation and space-time translation. Thus a solution of eq. (4.20) is assumed to exist in the form

$$\partial \bar{x}^\mu / \partial x^\nu = H^\mu{}_\nu[g_{\alpha\beta}] . \tag{4.21}$$

When the co-ordinate conditions are ambiguous to within Lorentz transformations, $H^\mu{}_\nu$ takes the form $H^\mu{}_\nu = \bar{L}^\mu{}_\lambda L^\beta{}_\nu H'^\lambda{}_\beta$ where $\bar{L}^\mu{}_\lambda$, $L^\beta{}_\nu$ are two arbitrary sets of homogeneous Lorentz transformation coefficients, and $H'^\alpha{}_\beta$ approaches $\delta^\alpha{}_\beta$ asymptotically. By making Lorentz transformations on $\bar{x}^\mu$, x^ν, one may eliminate $\bar{L}^\alpha{}_\beta$ and $\bar{L}^\alpha{}_\beta$. This corresponds to choosing the same Lorentz frame at spatial infinity for $\bar{x}^\mu$ and x^μ. By the Heisenberg condition, one may write

$$\partial \bar{x}^\mu / \partial x^\nu = H'^\mu{}_\nu[t - T, a] \tag{4.22}$$

which, upon integration, yields

$$\bar{x}^\mu = x^\mu + K^\mu[t - T, a] + c^\mu . \tag{4.23}$$

In eq. (4.23), the spatial dependence of K^μ must again be translationally invariant while c^μ are the four constants of integration. If K^μ approaches zero at spatial infinity, the c^μ may be determined to be zero by imposing the boundary condition that both the x^μ and $\bar{x}^\mu$ frame tie onto the same Lorentz frame at spatial infinity, which can be achieved by making an inhomogeneous Lorentz transformation. More generally, we have seen in Section 2 that it is possible that $\bar{x}^\mu - x^\mu$ do not approach zero at spatial infinity (*e.g.* $\bar{x}^\mu - x^\mu \sim \sim x^\mu/r$). In this case, K^μ will not approach zero asymptotically, though one must have $K^\mu{}_{,\nu} \to 0$. In this case, one can still make an inhomogeneous Lorentz transformation which sets c^μ to zero. Consequently, by a choice of Lorentz frame at spatial infinity, one may always eliminate c^μ. Returning to eq. (4.23) (with $c^\mu = 0$), we note that the reference time T is arbitrary. Choosing $t = T$, one has

$$\bar{x}^0 = x^0 + K^0[0, a] , \tag{4.24a}$$

$$\bar{x}^i = x^i + K^i[0, a] , \tag{4.24b}$$

with $a = g^c(x^0)$, $\pi^c(x^0)$, (where $x^0 = T$, an arbitrary time) and the spatial dependence in K^μ is translationally invariant as previously noted. Equations (4.24) are just the desired result (4.5).

5. – Conclusions.

In this paper, we have examined the class of canonical formalisms in general relativity for which the energy is the Hamiltonian. This class, the Heisenberg representation of the theory, was defined in a fashion completely analogous to that used in other branches of physics. Since within every co-ordinate frame one can set up a canonical formalism, it is clear that not all co-ordinate systems will lead to Heisenberg representations; indeed, two Heisenberg frames can only be connected by co-ordinate transformations $\bar{x}^\mu - x^\mu$ which do not single out particular space-time points (*i.e.*, $\bar{x}^\mu - x^\mu$ should be be a function only of the canonical variables, and only of x implicitly through them (9)). We saw that all Heisenberg canonical formalisms give the same

(9) It may be noted that *locally*-defined co-ordinate frames, *e.g.* those defined in terms of local scalars using the curvature (P. G. BERGMANN and A. KOMAR: *Phys. Rev. Lett.*, 4, 432 (1960)) are not, in general, of the Heisenberg type. Here one has $\bar{x}^\mu = h^\mu(R_{\alpha\beta\sigma\varrho})$ which means that the scalar h^μ depends only on the metric of some original Heisenberg frame, *i.e.* $h^\mu = h^\mu(R[g_{\alpha\beta}(x)])$. Since the x^μ frame is a Heisenberg one, there is no explicit x^μ dependence in the relation between $g_{\alpha\beta}(x)$ and the canonical variables g^c, π^c. One has, then, $\bar{x}^\mu = x^\mu + \{h^\mu(g^c, \pi^c) - x^\mu\}$ and hence $f^\mu \equiv h^\mu - x^\mu$ has explicit x^μ dependence.

numerical value of their Hamiltonians for a given physical situation. Thus, although the relation between any two such frames is of a more complicated nature than in Lorentz-covariant physics (the former involving both co-ordinate and simple canonical transformations), the physical results concerning energy-momentum are frame-invariant within the Heisenberg class. Of course, one would not expect this invariance to hold for all frames since the physical meaning of $\int \mathfrak{T}^0_{\ \mu}\, d^3r$ as the energy-momentum vector is valid only in a Heisenberg formalism. This is not to say that the energy cannot be correctly calculated in a non-Heisenberg representation, but only that it is *not* the Hamiltonian there. In IV*c*, an invariant prescription for calculating the energy in any frame where $g_{\mu\nu}-\eta_{\mu\nu}$ is asymptotically $\mathcal{C}(1/r)$ is given. It is also shown there that the energy so defined is satisfactory both from the inertial and gravitational viewpoint. Thus, it correctly describes energy transfer in the interaction of an (initially and finally) non-gravitational system with a gravitational system, on the gravitational mass that a test body at infinity would see when Newtonian conditions prevail asymptotically.

RIASSUNTO (*)

L'energia del campo gravitazionale (come di ogni altro sistema) non è sempre data dal valore numerico dell'hamiltoniano (per esempio, non lo è nella formulazione di Hamilton-Jacobi). Noi definiamo una classica « rappresentazione di Heisenberg » che esclude trasformazioni canoniche del tipo di quelle di Hamilton-Jacobi. Ordinariamente, entro la rappresentazione di Heisenberg, fra le variabili dinamiche rimane solo la possibilità di trasformazioni canoniche indipendenti dal tempo. Comunque, la libertà delle trasformazioni di coordinate nella relatività generale permette molte trasformazioni extracanoniche che non si trovano nella teoria covariante di Lorentz convenzionale. Questa più ampia classe di formalismi canonici possiede tutte le proprietà solitamente associate alla rappresentazione di Heisenberg in quanto in ogni formalismo le quantità misurabili $g_{\mu\nu}(t)$ sono ottenute dalla conoscenza delle variabili canoniche nello stesso tempo senza alcuna esplicita dipendenza dalle coordinate. Inoltre l'Hamiltoniano è una costante del moto. Solo negli schemi di Heisenberg l'Hamiltoniano deve essere associato all'energia del sistema. Malgrado la libertà addizionale delle trasformazioni canoniche (dovuta alla suddetta libertà nel cambiamento delle coordinate), si dimostra che per un determinato stato del campo gravitazionale l'Hamiltoniano è numericamente uguale in qualsiasi rappresentazione di Heisenberg. L'energia è quindi una quantità univocamente definibile nella teoria. Nel processo si stabilisce che due schemi di Heisenberg possono differire per trasformazioni di coordinate che dipendono solo dalle variabili canoniche e non dipendono esplicitamente dalle coordinate. Queste trasformazioni debbono anche conservare la proprietà che all'infinito, nello spazio, la metrica diviene Lorentziana in modo che rimangano inalterate le condizioni fisiche ai limiti.

(*) *Traduzione a cura della Redazione.*

Recoilless Emission and Absorption of 26 keV γ-Ray of ^{161}Dy.

S. Jha, R. K. Gupta, H. G. Devare, G. C. Pramila
and R. Srinivasa Raghavan

Tata Institute of Fundamental Research - Bombay

(ricevuto il 10 Ottobre 1960)

Summary. — Recoilless emission and resonance absorption of the 26 keV γ-ray emitted in the β-decay of ^{161}Tb have been observed. The existence of the first excited state of ^{161}Dy at 26 keV is thus confirmed. From the measurement of the transmission of this γ-ray through various thickness of the Dy_2O_3 absorber, the percentages of recoilless emission and recoilless absorption have been estimated to be $(10 \pm 2)\%$ and $(6.5 \pm 2)\%$ respectively. From the curve showing the change in the transmission as a function of the relative velocity of the source and the absorber, the width of the 26 keV state (for an absorber thickness of 19.65 mg/cm^2) was found to be about $1.04 \cdot 10^{-6}$ eV which is about 70 times what is expected from the measured half-life of this state.

Although very careful nuclear spectroscopic studies [1] of the radiations from 6-day ^{161}Tb seem to have resolved the earlier controversy [2-4] as to whether there was a level at 26 keV in ^{161}Dy, one would like to have an unambiguous proof of the existence of such a level, and the γ transition from it to the ground state of ^{161}Dy. Such a proof can be provided if one can observe resonance absorption or scattering of the 26 keV γ-ray in dysprosium. Such an experiment has been made very practicable by an effect, discovered by

[1] P. Gregors Hansen, O. Nathan, O. B. Nielsen and R. K. Sheline: *Nuclear Physics*, **6**, 630 (1958).

[2] J. M. Cork, M. K. Brice, C. L. Schmid and R. G. Helmer: *Phys. Rev.*, **104**, 482 (1956).

[3] W. G. Smith, J. H. Hamilton, R. L. Robinson and L. M. Langer: *Phys. Rev.*, **104**, 1020 (1956).

[4] C. W. McCutchen: *Phys. Rev.*, **109**, 1211 (1958).

MÖSSBAUER ([5]), which shows that when an isotope, emitting a low energy γ-ray, is imbedded in a strong crystal lattice, the recoil momentum is sometimes taken up by the lattice as a whole, and the γ-ray is emitted with its full energy. Also when the same isotope is situated in a similar crystal lattice, the nuclei of the isotopes can resonantly absorb the γ-rays, as the recoil momentum is again sometimes taken by the lattice as a whole. Such effects have been observed in a large number of cases. We have observed the resonant absorption of the 26 keV γ-ray of ^{161}Dy, emitted in the β-decay of ^{161}Tb, in dysprosium oxide.

The source of ^{161}Tb was made by ion-exchange separation of Tb from pile-irradiated samples of gadolinium oxide. The carrier-free ^{161}Tb source was mixed with one milligram of dysprosium oxide, the mixture was dissolved in nitric acid and converted into oxide form by intense heating. The dysprosium absorber was made up of spectroscopically pure dysprosium oxide in which the natural abundance of ^{161}Dy was 18.88%.

The source was mounted on a transducer, the collimated beam of γ-rays passing through the dysprosium oxide absorber was detected in a NaI(Tl) scintillation detector. Counts were observed for the 26 keV, 50 keV and the 75 keV γ-ray peaks, with the source stationary and the source vibrating with a 50 Hz sinusoidal wave, and an amplitude, which corresponded to a velocity of about 10 cm/s. Only in the case of the 26 keV γ-ray the counts were higher when the source was vibrating. This proved that there was a level in ^{161}Dy at 26 keV and that even at room temperature enough γ-rays of this energy were emitted and absorbed without recoil.

The transmission of the 26 keV γ-ray was measured using Dy_2O_3

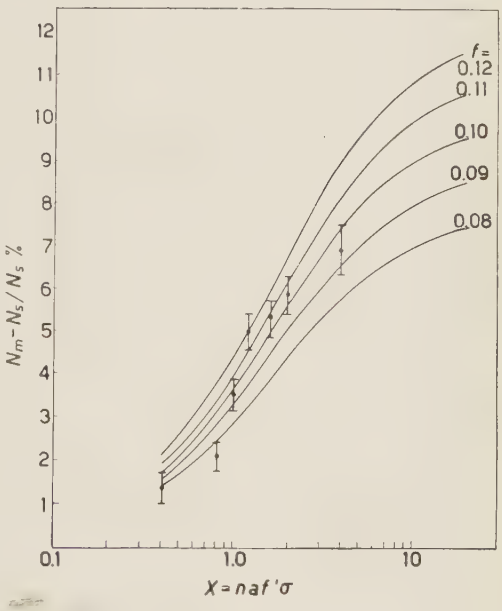

Fig. 1. – Percentage attenuation of the 26 keV γ-ray as a function of the Dy_2O_3 absorber thickness. $x = naf'\sigma$ is proportional to the absorber thickness ([6]).

([5]) R. L. MÖSSBAUER: *Zeits. f. Phys.*, **151**, 124 (1958).

([6]) P. P. CRAIG, J. G. DASH, A. D. MCGUIRE, D. NAGLE and R. R. REISWIG: *Phys. Rev. Lett.*, **3**, 221 (1959).

absorbers of thickness varying from 7.9 mg/cm² to 78.8 mg/cm². The counting rates N_s, with the source stationary, and N_m, with the source moving with the velocity of about 10 cm/s were recorded for each absorber. The results obtained are plotted in Fig. 1 where the ordinates represent the ratio $((N_m - N_s)/N_s) \times 100$ corrected for the background and the escape peak of the K X-ray and 50 keV γ-ray and for the Compton pulses of the higher energy γ-rays. The abscissa is proportional to the absorber thickness. The continuous curves are calculated from the theoretical relation used by the Los Alamos group and others ([6,7]). The experimental points seem to fit the curves for $f = 0.1 + 0.02$ from which f' is deduced to be 0.065 ± 0.02, where f and f' are the fraction of γ-rays emitted and absorbed without energy loss. These values of f and f' give the Debye's temperatures for the source and absorber material to be θ_D (source) = = 218 °K and θ_D (absorber) = 205 °K.

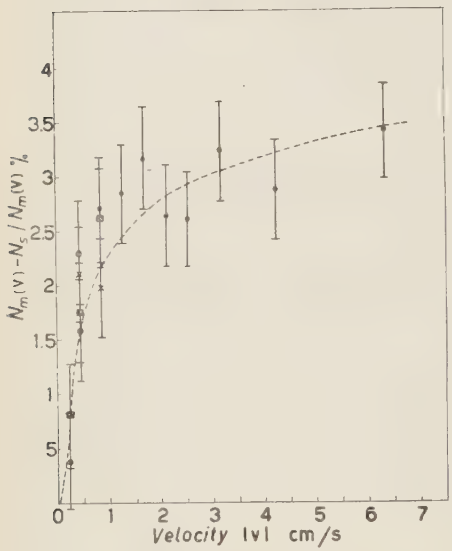

Fig. 2. – Curve representing the change in the transmission as a function of the source velocity taken with the 19.65 mg/cm² thick Dy_2O_3 absorber. The crosses, full circles, and full squares represent data for different sets of measurements.

Experiments were performed at room temperature using absorbers of known thickness to find the transmission of the 26 keV γ-ray as a function of the source velocity with respect to the absorber. This was accomplished by varying the amplitude of the sinusoidal voltage applied to the transducer. The amplitude of the mechanical vibration of the source as a function of the applied voltage was measured with a microscope. The results obtained are shown in Fig. 2 and Fig. 3. No correction has been made for the source thickness, the absorber thickness, and for the motion of the source which is sinusoidal. Dynamic experiments with Gd_2O_3 gave negative results.

From these experiments, the width of the curve showing the change in the transmission as a function of the source velocity is seen to be 1.2 cm/s for the absorber I (thickness 19.65 mg/cm²) and 2 cm/s for the absorber II

(7) G. DEPASQUALI, H. FRAUENFELDER, S. MARGULIES and R. N. PEACOCK: *Phys. Rev. Lett.*, **4**, 71 (1960).

(thickness 31.55 mg/cm^2). The width for the thinner absorber corresponds to $1.04 \cdot 10^{-6}$ eV, while the natural width of the level from the measured half-life ([1,8]) ($\tau = 2.7 \cdot 10^{-8}$ s) is $7.9 \cdot 10^{-9}$ eV. If one allows for the overlap of the emission and the absorption spectra, the observed width ought to be $1.58 \cdot 10^{-8}$ eV. There is thus a broadening of the width, in our experimental set-up, by a factor of about 70. This broadening may be due to the causes now familiar in experiments with ^{57}Co → ^{57}Fe ([7,9]) *viz.* hyperfine effects due to the electric and the magnetic fields at the nucleus. The velocity resolution in the set-up at our disposal is very poor. For this reason, no significance is being attached to the fluctuations in the curves of Fig. 2 and Fig. 3.

After this work was completed, we came across the report of the conference on Mössbauer effect at the University of Illinois (June 1960). Workers at the Hebrew University of Jerusalem, Israel, are reported to have observed the Mössbauer effect with the 26 keV γ-ray of ^{161}Dy.

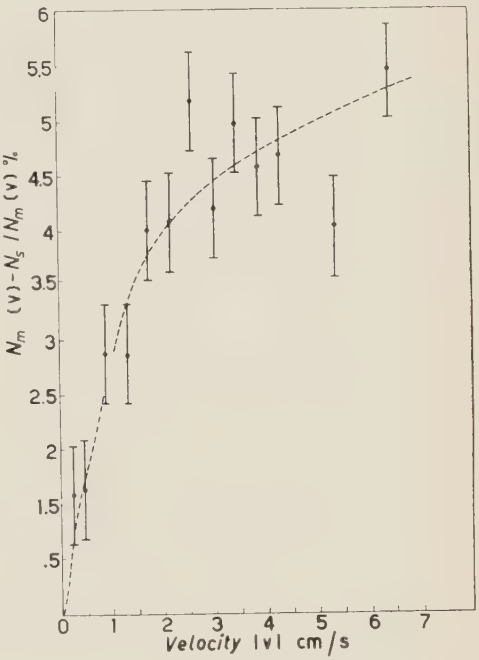

Fig. 3. – Curve representing the change in the transmission as a function of the source velocity taken with 31.55 mg/cm^2 thick Dy_2O_3 absorber.

* * *

We acknowledge gratefully the assistance of Mr. K. S. Bhatki and Mr. K. P. Gopinathan, who performed the separation of ^{161}Tb from the pile irradiated sample of gadolinium. Our thanks are due to Dr. A. Mukerji, discussions with whom have been of great value to us.

([8]) H. Vergnes: *Journ. de Phys. Rad.*, **18**, 579 (1957).

([9]) M. Cordey-Hayes, N. A. Dyson and P. B. Moon: *Proc. Phys. Soc.*, **75**, 810 (1960).

RIASSUNTO (*)

Sono stati osservati emissione ed assorbimento di risonanza senza rinculo dei raggi γ di 26 keV nel decadimento β del ^{161}Tb. Viene così confermata l'esistenza del primo stato eccitato del ^{161}Dy a 26 keV. Dalla misura della trasmissione di questo raggio γ attraverso vari spessori di assorbente di Dy_2O_3, si è valutata la percentuale di emissione ed assorbimento senza rinculo in $(10 \pm 2)\%$ e $(6.6 \pm 2)\%$ rispettivamente. Dalla curva che rappresenta la variazione della trasmissività in funzione della velocità relativa della sorgente e dell'assorbente, si è trovato che la larghezza dello stato di 26 keV (per una lunghezza di 19.65 mg/cm^2) è di circa $1.04 \cdot 10^{-6}$ eV, che è circa 70 volte quello che ci si sarebbe aspettato dalle misure della vita media di questo stato.

(*) *Traduzione a cura della Redazione.*

IL NUOVO CIMENTO Vol. XIX, N. 4 16 Febbraio 1961

Unitarity of the S-Matrix and Analyticity - I.

R. Ascoli

Istituto di Fisica dell'Università - Torino
Istituto Nazionale di Fisica Nucleare - Sezione di Torino

A. Bottino and A. Molinari

Istituto Nazionale di Fisica Nucleare - Sezione di Torino

(ricevuto l'11 Ottobre 1960)

Summary. — Here we have solved the problem of finding which analyticity properties of the production amplitudes are required to deduce, by means of the S-matrix unitarity relations, analyticity properties of scattering amplitudes as functions of the momentum transfer. The fundamental feature of the results is that analyticity properties of the production amplitudes are required as functions of two and only two dynamical variables, whichever be the number of produced particles. The general method given here does not require the actual calculation of any integral. In particular we give for the production amplitudes a condition sufficient for the analyticity within an ellipse of the imaginary part of the scattering amplitude as function of the momentum transfer.

1. – Introduction.

In this work we have solved the problem of finding which analytic properties of production amplitudes are required to deduce, by means of unitarity relations of the S-matrix, analytic properties of scattering amplitudes as functions of the momentum transfer.

Apparently this problem has become peculiarly important after the work by S. Mandelstam [1], in view of the possibility of extending analytic properties of scattering amplitudes beyond the threshold of the production processes.

(1) S. Mandelstam: *Nuovo Cimento*, **15**, 658 (1960).

2. – Definitions and preliminary considerations.

Scattering: Let us call W the total energy, ϑ the scattering angle in the center of mass system, write $z = \cos\vartheta$ and call $T(W, \vartheta)$ or $T(W, z)$ the scattering amplitude (we disregard spins).

Production: Let p_1, p_2 be the momenta of the initial particles, p_3, $p_4 \dots p_n$ the momenta of the final ones. Let us introduce $3n - 12$ dynamical variables w_1, w_2, ..., w_r, which fix completely the relative position and length of the momenta p_3, p_4, ..., p_n. Let us choose $w_1 = W$, where W is the total energy. The variables w_1, w_2, ..., w_r are otherwise arbitrary.

Let us further introduce in the center of mass system a unit vector $\boldsymbol{u}$ with the direction of the momenta $\boldsymbol{p}_1$, $\boldsymbol{p}_2$ of the initial particles. Then we define in some way in the center of mass system a reference frame by means of the vectors $\boldsymbol{p}_3$, $\boldsymbol{p}_4$, ..., $\boldsymbol{p}_n$ only and we call A, B two parameters which determine the direction $\boldsymbol{u}$ with reference to the frame.

The production amplitude depends on the $3n - 10$ dynamical variables w_1, w_2, ..., w_r, A, B: we call it $T_n(w_1, w_2, \dots, w_r, A, B)$.

In particular we may choose for A and B two polar co-ordinates Θ and Φ or the components X and Y with respect to two orthogonal axes (in this latter case for any set of values of X and Y there are in general two vectors $\boldsymbol{u}$, which are different by a reflection on the plane π of the axes X and Y).

L-ellipse of major halfaxis R $(L(R))$: Ellipse in the plane of one complex variable z with foci at the points $z = \pm 1$, and major halfaxis R.

Fundamental property of the L-ellipses: Let us consider the z variable as the component of a unit vector $\boldsymbol{u}$ of a plane on a direction: then the L-ellipses are the only lines invariant against (real) rotations of the direction in the plane of the unit vector.

Proof: We are looking for the lines that, in the complex z-plane, have the above mentioned invariance property. Let R be the intersection of one of such lines with the real z-axis. R is then the projection of the unit vector $\boldsymbol{u}$ on some direction forming with $\boldsymbol{u}$ an angle ϑ_0 such that $\cos\vartheta_0 = R$. We are interested to the case $R > 1$ (if $R \leqslant 1$ the line we are looking for is the real segment between $z = -1$ and $z = +1$: all the quantities concerned are real). The other points of the line are obtained by rotating the direction: if this direction is rotated by an angle φ, the component of $\boldsymbol{u}$ on such a new direction becomes:

$$(1) \qquad z = \cos(\vartheta_0 - \varphi) = \cos\vartheta_0 \cos\varphi + \sin\vartheta_0 \sin\varphi = R\cos\varphi + i\sqrt{R^2 - 1}\sin\varphi\,.$$

Therefore the result is that, by varying φ, z draws an L-ellipse (2).

I-hypersurface of radius R $(I(R))$. Let us consider in the (four-dimensional) space of two complex variables $X = X_r + iX_i$; $Y = Y_r + iY_i$ the hypersurface of equation:

$$\frac{X_r^2 + Y_r^2}{R^2} + \frac{X_i^2 + Y_i^2}{R^2 - 1} - \frac{(X_r Y_i - X_i Y_r)^2}{R^2(R^2 - 1)} = 1 , \tag{2}$$

where $R > 1$ is the positive real value of X for $Y = 0$.

We call hypersurface $I(R)$ in the space of two complex variables A and B connected with X and Y the image of the hypersurface (2) in the mapping of X, Y into A, B. (The hypersurface $I(R)$ is simply given by (2) when A and B coincide with X and Y). Furthermore whenever there may be ambiguity, we call interior of $I(R)$ in the space of A and B the image of the interior of $I(R)$ in the mapping of X, Y into A, B.

Fundamental property of the I-hypersurfaces. Let us consider X and Y as the components of a unit vector $\boldsymbol{u}$ of a three-dimensional space on two orthogonal axes. So A and B are two parameters which determine the direction of $\boldsymbol{u}$ with respect to a reference frame fixed to the X, Y axes.

Then the I-hypersurfaces in the space of A and B are the only hypersurfaces which are invariant against (real) rotations of the reference frame in the three-dimensional space of the unit vector $\boldsymbol{u}$.

Proof: It is analogous to the one that has been given for the L-ellipses. It may be found in a previous work (3).

(2) This is the easiest and most elegant way to introduce the Lehmann-ellipse. Really let us call $\boldsymbol{u}$ a unit vector with the direction of the momenta of the initial particles in the c.m. system; then if we choose a frame of reference defined by the momenta of the final particles, the Dyson representation gives finally a formula of the kind:

$$T(W, \boldsymbol{u}) = \int_{x_0}^{\infty} \mathrm{d}x \int \mathrm{d}\boldsymbol{u}' \frac{\varphi(x, \boldsymbol{u}', W)}{x - \boldsymbol{u} \cdot \boldsymbol{u}'} ,$$

where the unit vector $\boldsymbol{u}'$ rotates in the scattering plane. The domain of analyticity is then clearly invariant against rotations of the reference system in the scattering plane, for the denominator and the domain of integration are such. Therefore the domain of analyticity is an L-ellipse and we have immediately that $R = x_0$.

(3) R. Ascoli: *Analytic properties of production amplitudes as functions of two momentum transfers*, in *Nuovo Cimento* **18**, 754 (1960).

3. – The fundamental theorem.

Theorem: Let for a given energy W the real and the imaginary parts of the production amplitudes $T_n(w_1, w_2, ..., w_r, \Theta, \Phi)$ be analytic functions of Θ and Φ [4] inside the hypersurface $I(R)$, for all the n's for which the correspondent process is physically possible: then, in the scattering, the production contribution to $\mathrm{Im}\, T(W, z)$ is an analytic function of z inside the ellipse $L(2R^2 - 1)$.

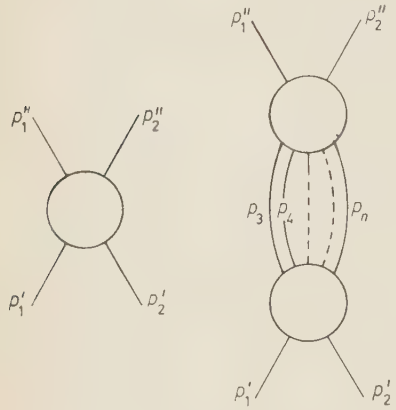

Fig. 1. – By means of the S-matrix unitarity relations the imaginary part of the amplitude for the scattering process indicated at left is expressed in terms of the amplitudes of the production processes indicated at right.

Proof: Let us write first the S-matrix unitarity relation that is of interest. To this purpose let us work in the center of mass system. We call $\boldsymbol{u}'$ a unit vector with the direction of the momenta $\boldsymbol{p}_1'$, $\boldsymbol{p}_2'$ of the initial particles of the scattering, $\boldsymbol{u}''$ a unit vector with the direction of the momenta $\boldsymbol{p}_1''$, $\boldsymbol{p}_2''$ of the final particles, and X_0, Y_0, Z_0, a frame of reference which is defined for each value of z by means of $\boldsymbol{u}'$ and $\boldsymbol{u}''$. Let us further define for each n a frame of reference X, Y, Z by means of the momenta $\boldsymbol{p}_3$, $\boldsymbol{p}_4$, ..., $\boldsymbol{p}_n$ of the final particles of the production process considered in the unitarity relation. Let us call φ, ζ, ψ the Euler angles of X, Y, Z relative to X_0, Y_0, Z_0 and $\boldsymbol{k}$ the unit vector of Z: ψ is then the angle of rotation about $\boldsymbol{k}$ (see Fig. 1, 2).

Then we have for the production contribution $\mathrm{Im}(T(W, z))_P$ to $\mathrm{Im}\, T(W, z)$:

$$(3) \qquad (\mathrm{Im}\, T(W, z))_P = \sum_n \int \mathrm{d}w_2\, \mathrm{d}w_3 \ldots \mathrm{d}w_r F(w_1, w_2, \ldots w_r)\, \mathrm{d}\Omega_k\, \mathrm{d}\psi \cdot$$

$$\cdot T_n^*(w_1, w_2, \ldots w_r, \Theta'(\boldsymbol{k}, \psi, z), \Phi'(\boldsymbol{k}, \psi, z))\, T_n(w_1, w_2, \ldots w_r, \Theta''(\boldsymbol{k}, \psi, z)\Theta'', (\boldsymbol{k}, \psi, z)),$$

where $\mathrm{d}\Omega_k$ is the element of solid angle in the space of the unit vector $\boldsymbol{k}$ and Θ', Φ' and Θ'', Φ'' are respectively the polar co-ordinates of $\boldsymbol{u}'$ and $\boldsymbol{u}''$ with respect to the polar axis Z, the azimuths being counted starting from the Z, X plane. $F(w_1, w_2, ..., w_r)$ is a function of the written variables which can be determined according to the choice of the variables: but such a choice is here unnecessary.

[4] The convenience of this assumption is clear from reference [3] or from perturbative examples, see also the last remark in the Appendix.

To justify (3) one needs only to notice that the sum is taken over all the n-particle states consistent with the energy W and that the weight function depends only on w_1, w_2, ..., w_r. Which can be easily seen: for every set of values of w_1, w_2, ..., w_r the *relative* configuration of the vectors $\boldsymbol{p}_3$, $\boldsymbol{p}_4$, ..., $\boldsymbol{p}_n$ is defined. By integrating over the direction of $\boldsymbol{k}$ and the angle ψ, one integrates over all the configurations arising from the previous one by means of *rigid* rotations of the set of the vectors $\boldsymbol{p}_3$, $\boldsymbol{p}_4$, ..., $\boldsymbol{p}_n$. Since there is no preferred direction in space, the weight function does depend neither on the direction $\boldsymbol{k}$, nor on the angle ψ of rotation about $\boldsymbol{k}$. Then we integrate over w_2, w_3, ..., w_r, *i.e.* over all the relative configurations of the vectors $\boldsymbol{p}_3$, $\boldsymbol{p}_4$, ..., $\boldsymbol{p}_n$. So it is proved that in (3), the sum is taken over all the configurations of the vectors $\boldsymbol{p}_3$, $\boldsymbol{p}_4$, ... $\boldsymbol{p}_n$ and that the weight function depends only on w_1, w_2, ..., w_r.

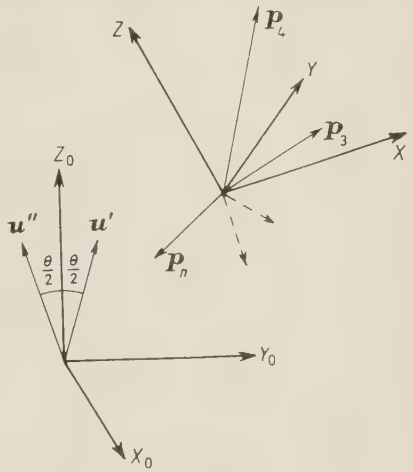

Fig. 2. – In the c.m. system $\boldsymbol{u}'$ and $\boldsymbol{u}''$ are unit vectors with the directions of the momenta of the initial and final particles respectively in the scattering process under consideration. $X_0Y_0Z_0$ is a reference frame defined by means of $\boldsymbol{u}'$ and $\boldsymbol{u}''$ in such a way that Y_0Z_0 lie in the scattering plane, Z_0 being the bisectrix of the angle between $\boldsymbol{u}'$ and $\boldsymbol{u}''$. XYZ is a reference frame defined by means of the momenta $\boldsymbol{p}_3, \boldsymbol{p}_4, \ldots \boldsymbol{p}_n$ of the intermediate particles, for any relative configuration of them. Then we have called φ, ζ, ψ, the Euler angles of XYZ relative to $X_0Y_0Z_0$.

By writing the unitarity relations with such variables, a fundamental favourable circumstance appears at once: *the variable z (in respect of which analyticity interests) appears only in two of the dynamical variables, on which the production amplitudes depend.*

By introducing the Eulerian angles φ, ζ, ψ, (3) can be written:

$$(4) \qquad (\mathrm{Im}\, T(w,z))_P = \sum_n \int \mathrm{d}w_2\, \mathrm{d}w_3 \ldots \mathrm{d}w_r F(w_1, w_2, \ldots w_r) \sin\zeta\, \mathrm{d}\zeta\, \mathrm{d}\varphi\, \mathrm{d}\psi \cdot$$

$$\cdot T_n^*(w_1, w_2, \ldots, w_r, \Theta'(\varphi,\zeta,\psi,z), \Phi'(\varphi,\zeta,\psi,z)) \cdot$$

$$\cdot T_n(w_1, w_2, \ldots, w_r, \Theta''(\varphi,\zeta,\psi,z), \Phi''(\varphi,\zeta,\psi,z)) .$$

For the purposes of the present work, let us choose now the Z_0-axis along the bisectrix of the unit vectors $\boldsymbol{u}'$ and $\boldsymbol{u}''$, the Y_0-axis lying also in the plane of the unit vectors $\boldsymbol{u}'$ and $\boldsymbol{u}''$ (see Fig. 2).

Now let us search which analytic properties of the T_n's are required in order to guarantee the analyticity of $\mathrm{Im}\, T(W, z)$ relative to z inside an ellipse $L(2R^2-1)$.

To this purpose *the fundamental problem is to examine the region covered by* Θ', Φ' *(and* Θ'', Φ''*) in the space of the two complex variables* Θ, Φ, *when* φ, ζ, ψ *take all their values and* z *varies inside the ellipse* $L(2R^2-1)$.

Owing to the particular choice of the system X_0, Y_0, Z_0, the problem is clearly identical for Θ', Φ', and for Θ'', Φ''. Let us examine the behaviour of Θ', Φ'.

Let φ, ζ, ψ vary. Then the system X, Y, Z rotates in all the possible ways with respect to $\boldsymbol{u}'$ (and $\boldsymbol{u}''$), $\boldsymbol{u}'$ (and $\boldsymbol{u}''$) being fixed to X_0, Y_0, Z_0. Then owing to the fundamental property of the I-hypersurfaces, Θ' and Φ', as polar co-ordinates of the unit vector $\boldsymbol{u}'$, describe one of such surfaces.

Now we let $z = \cos\vartheta$ vary on the boundary of the ellipse $L(2R^2-1)$. z is the projection of one of the unit vectors $\boldsymbol{u}'$, $\boldsymbol{u}''$ on the other; so, owing to the fundamental property of the L-ellipses, during such a variation of z, the unit vectors $\boldsymbol{u}'$ and $\boldsymbol{u}''$ rotate the one relative to the other by *real* angles. Now Z_0 is the bisectrix of the angle between $\boldsymbol{u}'$ and $\boldsymbol{u}''$, so $\boldsymbol{u}'$ and $\boldsymbol{u}''$ rotate by *real* angles even with respect to Z_0. Moreover, in this part of the reasoning, φ, ζ, ψ are constant, so the system X, Y, Z is fixed with the system X_0, Y_0, Z_0; therefore $\boldsymbol{u}'$ and $\boldsymbol{u}''$ rotate by real angles even with respect to the system X, Y, Z.

Then the polar co-ordinates Θ', Φ', of $\boldsymbol{u}'$ describe an I-hypersurface even by letting z vary on the boundary of the ellipse $L(2R^2-1)$.

What only remains to be determined is the radius of this I-hypersurface. This is immediately done by considering any particular case: for instance, $X \equiv Z_0$, $Y \perp \boldsymbol{u}'$, $z = \cos\vartheta = 2R^2-1$. Then we have $Y'=0$, $X'=\cos\vartheta/2$. By using $\cos\vartheta = 2\cos^2(\vartheta/2)-1$, we have $X' = \pm R$. The radius of an I-hypersurface is the real positive value of X at $Y=0$, so we conclude that the radius is R.

Since the interior of the I-hypersurface decreases with R and R decreases with $2R^2-1$, it follows finally that the region drawn by Θ', Φ' (or Θ'', Φ'') in the space of the two complex variables Θ, Φ, when φ, ζ, ψ take all their values and z varies inside the ellipse $L(2R^2-1)$, is the interior of the hypersurface $I(R)$.

It is now easy to complete the proof of the theorem: from the assumed analyticity of the amplitude T_n as function of Θ and Φ we deduce easily that T_n may be put into the form of a regular analytic function of the three components X, Y, Z of the unit vector $\boldsymbol{u}$, within $I(R)$ (see Lemma 3 of the Appendix).

Then we look to the explicit expressions of X', Y', Z' (and X'', Y'', Z'') as functions of ζ, φ, ψ, ϑ and we see that they are regular analytic functions

of ϑ:

$$(6)\qquad \begin{cases} X' = (\sin\varphi\cos\psi + \cos\zeta\cos\varphi\sin\psi)\sin\dfrac{\vartheta}{2} + \sin\zeta\sin\psi\cos\dfrac{\vartheta}{2}, \\ Y' = (-\sin\varphi\sin\psi + \cos\zeta\cos\varphi\cos\psi)\sin\dfrac{\vartheta}{2} + \sin\zeta\cos\psi\cos\dfrac{\vartheta}{2}, \\ Z' = \sin\zeta\cos\psi\sin\dfrac{\vartheta}{2} + \cos\zeta\cos\dfrac{\vartheta}{2}, \end{cases}$$

(the expressions for X'', Y'', Z'' are the same except for a change of the sign in front of $\sin\vartheta/2$).

Then the integrand of (4) is a regular analytic function of ϑ for the values of ϑ for which Θ', Φ' and Θ'', Φ'' are inside $I(R)$.

We have already shown that this happens for all the values of the variables of integration ζ, φ, ψ provided $z = \cos\vartheta$ lies within the ellipse $L(2R^2 - 1)$. So we conclude that the integral (4) is a regular analytic function of ϑ when $\cos\vartheta$ lies within the ellipse $L(2R^2 - 1)$.

The analyticity of $(\mathrm{Im}\, T)_p$ with respect to $z = \cos\vartheta$ within the ellipse $L(2R^2 - 1)$ follows immediately from the proved analyticity with respect to ϑ and from the fact that $(\mathrm{Im}\, T)_p$ is an even function of ϑ (because we know from rotation invariance that it depends on ϑ only through $\cos\vartheta$) (see Lemma 1 of the Appendix).

4. – Conclusions.

The fundamental feature of the here obtained results is clear from the beginning by writing the S-matrix unitarity relation in the form (3) or (4) (this may be done provided the production amplitudes are expressed as functions of dynamical variables of the type introduced at the beginning of this work or in [3]).

In fact it turns out that, to deduce analyticity properties of the imaginary part of the scattering amplitude as function of the momentum transfer, analyticity properties of the production amplitudes are required as functions of two and only two dynamical variables, whichever be the number of produced particles. So the complication of the problem does not increase with the number of particles: we believe that this fact will be useful in the development of quantum field theory.

Appendix

Lemma 1. – Let $\boldsymbol{u}'$ and $\boldsymbol{u}''$ be two unit vectors, let ϑ be their relative angle and let f be an invariant function of them; let further $f(\vartheta)$ be a regular analytic function of ϑ for $\cos\vartheta$ within some domain D of the complex $\cos\vartheta$ plane in-

cluding the real range $-1 < \cos\vartheta < 1$. Then for $\cos\vartheta$ within $Df(\vartheta)$ may be put into the form $f(\vartheta) = F(\cos\vartheta)$ where F is a regular analytic function of $\cos\vartheta$ within D.

In fact we may define for complex values of $\cos\vartheta$ within D the function $F(\cos\vartheta) = f(\arccos\cos\vartheta)$. Owing to the assumed analyticity $F(\cos\vartheta)$ is an analytic finite function of $\cos\vartheta$ within D except eventually for branch points at $\cos\vartheta = \pm 1$. Now, owing to rotation invariance, for real values of ϑ, $f(\vartheta)$ depends only on $\cos\vartheta$ so that $f(\pm\vartheta + 2n\pi) = f(\vartheta)$ for any integer n and real ϑ. Then from the assumed analyticity we have that $f(\pm\vartheta + 2n\pi) = f(\vartheta)$ must even hold for any complex $\cos\vartheta$ within D, so $F(\cos\vartheta)$ is a one-valued function of $\cos\vartheta$. Therefore $F(\cos\vartheta)$ is analytic and regular for $\cos\vartheta$ within D.

Let now $\boldsymbol{u}$ be a unit vector in three-dimensional space, let Θ and Φ be polar co-ordinates of $\boldsymbol{u}$ and let $X = \sin\Theta\cos\Phi$, $Y = \sin\Theta\sin\Phi$, $Z = \cos\Theta$ be carthesian components of $\boldsymbol{u}$.

Let f be a function of the unit vector $\boldsymbol{u}$. Then f may be put into the form of a function $f(\Theta, \Phi)$ of the polar angles Θ and Φ, such that $f(\Theta + 2m\pi, \Phi + 2n\pi) = f(\Theta, \Phi)$ for any integers m and n and $f(-\Theta, \Phi + \pi) = f(\Theta, \Phi)$.

On the contrary to any set of values of X and Y correspond in general two vectors $\boldsymbol{u}$, the one being obtained from the other by means of a reflection on the X, Y plane (plane π). If one of the vectors has polar angles Θ, Φ, the other one has polar angles $\pi - \Theta$, Φ. We call $F(X, Y) = f(\Theta, \Phi)$ and $F_\pi(X, Y) = f(\pi - \Theta, \Phi)$ the corresponding values of the function f.

Then we have the following trivial lemmas.

Lemma 2. – Let $f(\Theta, \Phi)$ be a function of the polar angles Θ and Φ such that $f(\pi - \Theta, \Phi) = f(\Theta, \Phi)$; let further $f(\Theta, \Phi)$ be an analytic regular function of Θ, Φ when $X = \sin\Theta\cos\Phi$, $Y = \sin\Theta\sin\Phi$ lie within some domain D of the X, Y space including the real circle $X^2 + Y^2 \leqslant 1$: then $f(\Theta, \Phi)$ may be put into the form $f(\Theta, \Phi) = F(X, Y)$ where F is a regular analytic function of X and Y within D.

In fact we may define for complex values of X and Y within D the function:

$$F(X, Y) = f(\arcsin\sqrt{X^2 + Y^2}, \operatorname{arctg}(Y/X)) .$$

Owing to the assumed analyticity $F(X, Y)$ is an analytic finite function of X and Y within D except eventually for branchings at $X^2 + Y^2 = \pm 1$ (due to the function arcsin) and at $X^2 + Y^2 = 0$ (due to the square root and to the function arctg). Now, owing to the assumptions, we have, for Θ and Φ real, $f(\Theta + 2m\pi, \Phi + 2n\pi) = f(\Theta, \Phi)$, for any integers m and n, $f(-\Theta, \Phi + \pi) = f(\Theta, \Phi)$ and $f(\pi - \Theta, \Phi) = f(\Theta, \Phi)$.

Then from the assumed analyticity we have that these relations must even hold for X and Y complex within D, so that $F(X, Y)$ is a one-valued function of X and Y. Therefore $F(X, Y)$ is analytic and regular within D.

Lemma 3. – Let $f(\Theta, \Phi)$ be a function of the polar angles Θ and Φ; let $F(X, Y)$ and $F_\pi(X, Y)$ be the two different values of $f(\Theta, \Phi)$ that correspond in general to given values of $X = \sin\Theta\cos\Phi$, $Y = \sin\Theta\sin\Phi$; let further

$f(\Theta, \Phi)$ be a regular analytic function of Θ and Φ when X, Y lie within some domain D including the real circle $X^2 + Y^2 \leqslant 1$: then the functions $G(X, Y) = F(X, Y) + F_\pi(X, Y)$ and $H(X, Y) = (F(X, Y) - F_\pi(X, Y))/\sqrt{1 - X^2 - Y^2}$ are regular analytic functions of X and Y within D and viceversa. The function $f(\Theta, \Phi)$ may be put into the form

$$f(\Theta, \Phi) = G(X, Y) + ZH(X, Y)\,, \tag{A.1}$$

where $Z = \cos\Theta$.

In fact

$$G(X, Y) = f(\Theta, \Phi) + f(\pi - \Theta, \Phi) \text{ and } H(X, Y) = (f(\Theta, \Phi) - f(\pi - \Theta, \Phi))/\cos\Theta\,,$$

satisfy the conditions of Lemma 2, so they are regular analytic functions of X and Y within S. The viceversa and the last statement of the Lemma are even more trivial.

As a consequence of this lemma the assumption of the theorem that the real and the imaginary parts of $T_n(w_1, w_2 \ldots w_r, \Theta, \Phi)$ are analytic functions of Θ and Φ within $I(R)$ is equivalent to the assumption that the real and the imaginary parts of the combinations $T_n(w_1 \ldots w_r, X, Y) + T_{n\pi}(w_1, w_2 \ldots w_r, X, Y)$ and $(T_n(w_1, \ldots w_r, X, Y) - T_{n\pi}(w_1, \ldots w_r, X, Y))/\sqrt{1 - X^2 - Y^2}$ are analytic functions of X and Y within $I(R)$. These combinations had been introduced in the previous work [3].

RIASSUNTO

In questo lavoro è risolto il problema di trovare quali proprietà analitiche delle ampiezze di produzione si richiedono per dedurre, attraverso le relazioni di unitarietà della matrice S, proprietà analitiche delle ampiezze di scattering in funzione dell'impulso trasferito. L'aspetto fondamentale dei risultati ottenuti in questo lavoro è che, per lo studio delle ampiezze di scattering, si richiedono per le ampiezze di produzione proprietà di analiticità rispetto a due e due sole variabili dinamiche, qualunque sia il numero di particelle prodotte. Il metodo generale qui presentato non richiede il calcolo esplicito di alcun integrale. In particolare viene data per le ampiezze di produzione una condizione sufficiente per l'analiticità entro un'ellisse della parte immaginaria dell'ampiezza di scattering, come funzione del momento trasferito.

IL NUOVO CIMENTO Vol. XIX, N. 4 16 Febbraio 1961

On the Calculation of Radial Wave Functions Corresponding to Energies in the Continuum Part of the Helium Spectrum.

C. C. Grosjean (*) and R. T. Van de Walle (**)

Interuniversitair Instituut voor Kernwetenschappen
Centrum van de Rijksuniversiteit te Gent - Gent

(ricevuto l'11 Ottobre 1960)

Summary. — For the purpose of recalculating the helium primary specific ionization values in an attempt to bridge the gap existing between theory and experiment in this field, this paper deals with the derivation of new wave functions corresponding to energies from the continuum part of the He spectrum, which are more accurate than those resulting from the commonly adopted approximations. Sect. **1** is devoted to an appropriate series expansion of the wave function for the two helium planetary electrons and to the corresponding transformation of the Schrödinger equation into an infinite system of simultaneous differential equations which the expansion entails. Further, it is shown how a suitable truncation leads to the basic, one-electron, Schrödinger-type differential equation for the approximate wave function describing the positive energy electron in the electric field of the helium nucleus and the bound electron. The physical reasons underlying the truncation procedure are discussed in detail. In Sect. **2**, it is shown that the correction due to the motion of the nucleus vanishes identically to within the present lowest-order approximation scheme. Sect. **3** deals with the radial part of the desired wave function, its reduction to atomic units, the ordinary second order differential equation which it satisfies, its Maclaurin series expansion and its general characteristics, especially its asymptotic behavior. Sect. **4** describes the numerical integration of the mentioned radial wave equation for 27 pairs of energy and orbital angular momentum quantum number values, using an IBM 650 ordinator. All wave functions have been obtained in an interval of at least 8 atomic units. Finally, the normalization of the resulting curves to unit amplitude at infinity is examined in Sect. **5**. Two very elegant methods are developed and studied in detail.

(*) *Address:* Natuurkundig Laboratorium, Universiteit te Gent, Rozier 6, Gent.
(**) On leave of absence to the Lawrence Radiation Laboratory, Berkeley Cal.

In the first procedure, the amplitude at infinity and the phase angle are rigorously given by certain integrals which are directly calculable. In the second and actually adopted method, the basic idea consists in introducing the Madelung transformation, leading to a non-linear differential equation for the local amplitude of the radial wave function. Calculating an asymptotic series expansion for this local amplitude, it becomes possible, in principle, to compute the normalized wave function starting at infinity down to a certain minimum abscissa dictated by the desired limit of precision. The corresponding curve to be normalized could then be fitted to the normalized one. However, it is shown that the entire procedure is enormously simplified by carrying out the matching operation at a zero of the oscillating radial wave function.

Introduction.

In recent years, results of measurements on the primary specific ionization of electrons in gaseous media have been published by some authors and by one of us ([1-3]). It has been found, that for several gases, there appear appreciable discrepancies with the Bethe-Moller-Williams theoretical values. Among these cases, the one of helium is particularly pronounced and therefore interesting to investigate. Although it is practically certain that theoretical imperfections alone cannot be held responsible for the observed differences ([2]), we have considered it worth-while to recalculate the He primary specific ionization values and some useful related quantities with wave functions corresponding to energies from the continuum part of the helium spectrum, which are more accurate than the commonly used hydrogenic wave functions.

The physical process under study concerns the passage of a charged particle through a helium atom initially in its ground state. Under the influence of the impinging particle, one of the planetary electrons is transferred to the continuum part of the energy spectrum whereas the other electron remains bound to the nucleus. To calculate the cross section for such an ionization, it is evident that one has to dispose of accurate wave functions describing the initial and final electron states of the bombarded atom. For the initial state, one customarily uses the well-known Hylleraas wave function, which is certainly more than satisfactory for the present purpose. However, for what the final state is concerned, all earlier calculations have been carried out using hydrogenic wave functions with some plausible choice for the effective nuclear

([1]) J. Allewaert, R. Van de Walle and J. Verhaeghe: *Compt. Rend. Acad. Sci. Paris.*, **245**, 1611 (1957).

([2]) R. Van de Walle and J. Verhaeghe: *Compt. Rend. Acad. Sci. Paris*, **245**, 1721 (1957).

([3]) R. Van de Walle and J. Verhaeghe: *Compt. Rend. Acad. Sci. Paris*, **248**, 3292 (1959).

charge, this under the assumption that the ionized helium atom could be regarded as some sort of superposition of two hydrogen-like atoms. This approach offers the advantage that the entire calculation can be carried out analytically, but as will appear further, the final electron state is not adequately described in this manner, especially in the case of low values of the orbital angular momentum quantum number l of the ejected electron.

It is the purpose of the present paper to investigate in sufficient detail the problem of obtaining better approximations for the mentioned final state He wave functions needed in the more refined calculations of the primary specific ionization which we want to carry out. There will be outlined a rigorous method to treat the appropriate Schrödinger equation, which ultimately leads to a complicated infinite system of coupled differential equations that can be truncated in various ways depending upon the degree of precision desired. The lowest order truncation which, from the point of view of numerical computation, has interested us most until now, gives rise to a one-particle Schrödinger equation with a so-called Hartree potential. After separation of the variables, the resulting differential equation for the radial part of the wave function is solved numerically by machine methods for various values of the parameters. Finally, the article deals with proper normalization methods which can be applied to the resulting continuum energy wave functions.

The proper way to use the final results of this study in actual calculations of primary specific ionization and certain distribution curves related to the subject, will be outlined and discussed in a subsequent paper.

It should be noted that some calculations of the type presented here have appeared as an intermediate step in earlier numerical work which has been carried out by ERSKINE [1] for a different purpose. However, at that occasion, only the case of $l=1$ was taken into consideration and the resulting wave functions were not explicitly published.

Theoretical Development.

1. – Derivation of the basic differential equation.

Neglecting spin (*), relativistic effects and a small perturbing term due to the motion of the nucleus (**), the fundamental Schrödinger equation for the

[1] G. A. ERSKINE: *Proc. Roy. Soc.*, A **224**, 362 (1954).

(*) That this is permitted here, will appear from the discussion (in our next article) on the ultimate form in which the wave function describing the final electron state of the ionized helium atom has to be brought for practical application.

(**) The importance of this term within the framework of the present study will be investigated in Sect. 2.

helium atom can be written in the following time-independent form:

$$\left(-\frac{\hbar^2}{2\mu}\nabla_1^2-\frac{\hbar^2}{2\mu}\nabla_2^2-\frac{2e^2}{r_1}-\frac{2e^2}{r_2}+\frac{e^2}{r_{12}}\right)\Psi(\boldsymbol{r}_1,\boldsymbol{r}_2)=\mathscr{E}\Psi(\boldsymbol{r}_1,\boldsymbol{r}_2)\,, \tag{1.1}$$

in which $\boldsymbol{r}_1$ and $\boldsymbol{r}_2$ represent the position vectors of the two electrons with respect to the nucleus as origin;

$\mu \equiv m_e M_{\mathrm{He}}/(M_{\mathrm{He}}+m_e)$ is the usual expression for the reduced mass of an electron, but calculated with the helium nuclear mass;

$r_{12} \equiv |\boldsymbol{r}_1-\boldsymbol{r}_2|$ symbolizes the distance between the two planetary electrons, and

$\mathscr{E}$ expresses their total energy.

The probability amplitude $\Psi(\boldsymbol{r}_1,\boldsymbol{r}_2)$, regarded as a function of $\boldsymbol{r}_1$, can always be developed in terms of any complete set of orthonormal functions of this position vector. For the present purpose, it is very convenient to choose the collection of all independent eigenfunctions of the hydrogen-like problem with $Z=2$ (nuclear charge $+2e$) and nuclear mass M_{He}, whose Schrödinger equation contains part of the terms of eq. (1.1), namely:

$$\left(-\frac{\hbar^2}{2\mu}\nabla_1^2-\frac{2e^2}{r_1}\right)\Psi(\boldsymbol{r}_1)=E\Psi(\boldsymbol{r}_1)\,. \tag{1.2}$$

As is well-known, the eigenfunctions corresponding to the discrete part of the energy spectrum can be written as

$$u_{nlm}(\boldsymbol{r}_1)=R_{nl}(r_1)\,Y_{lm}(\theta_1,\varphi_1) \qquad \begin{cases} (m=-l,-l+1,\ldots,l-1,l; \\ l=0,1,2,\ldots,n-1; \\ n=1,2,3,\ldots)\,. \end{cases} \tag{1.3}$$

where Y is the usual symbol for a spherical harmonic, R_{nl} is, apart from a suitable normalization factor, the product of a certain power of r_1, an exponential function and an associated Laguerre polynomial (with argument $4r_1/na_0$, where a_0 represents the Bohr radius calculated with the reduced electron mass μ: $a_0=\hbar^2/\mu e^2$).

The energy eigenvalues corresponding to the functions (1.3) are given by

$$E_n=-\frac{2e^2}{n^2a_0}\,. \tag{1.4}$$

To complete the orthonormal set (1.3), one should also add all independent eigenfunctions corresponding to the levels forming the continuum part of the energy spectrum. However, there will be no need to write these functions down explicitly.

Consequently, we put:

$$\Psi(\boldsymbol{r}_1, \boldsymbol{r}_2) = u_{100}(\boldsymbol{r}_1)\psi_{100}(\boldsymbol{r}_2) + u_{200}(\boldsymbol{r}_1)\psi_{200}(\boldsymbol{r}_2) + u_{210}(\boldsymbol{r}_1)\psi_{210}(\boldsymbol{r}_2) + \\ + u_{211}(\boldsymbol{r}_1)\psi_{211}(\boldsymbol{r}_2) + u_{21,-1}(\boldsymbol{r}_1)\psi_{21,-1}(\boldsymbol{r}_2) + \dots , \tag{1.5}$$

in which the three indices characterizing each unknown ψ-function only specify which u-function it is associated with. They should therefore not be interpreted as quantum numbers specifying possible states of the second electron.

Introducing this series expansion into eq. (1.1) and keeping in mind that the u-functions satisfy (1.2) for appropriate values of E contained in (1.4), we obtain the following equation:

$$-\frac{\hbar^2}{2\mu}[u_{100}(\boldsymbol{r}_1)\nabla_2^2\psi_{100}(\boldsymbol{r}_2) + u_{200}(\boldsymbol{r}_1)\nabla_2^2\psi_{200}(\boldsymbol{r}_2) + u_{210}(\boldsymbol{r}_1)\nabla_2^2\psi_{210}(\boldsymbol{r}_2) + \dots] - \\ - \left(\frac{2e^2}{r_2} - \frac{e^2}{r_{12}}\right)[u_{100}(\boldsymbol{r}_1)\psi_{100}(\boldsymbol{r}_2) + \dots] = \\ = \left(\mathscr{E} + \frac{2e^2}{a_0}\right)u_{100}(\boldsymbol{r}_1)\psi_{100}(\boldsymbol{r}_2) + \left(\mathscr{E} + \frac{e^2}{2a_0}\right)[u_{200}(\boldsymbol{r}_1)\psi_{200}(\boldsymbol{r}_2) + \\ + u_{210}(\boldsymbol{r}_1)\psi_{210}(\boldsymbol{r}_2) + u_{211}(\boldsymbol{r}_1)\psi_{211}(\boldsymbol{r}_2) + u_{21,-1}(\boldsymbol{r}_1)\psi_{21,-1}(\boldsymbol{r}_2)] + \dots . \tag{1.6}$$

Now, suppose we multiply both sides of the preceding equation by $u^*_{100}(\boldsymbol{r}_1)$, where the asterisk symbolizes complex conjugation. Integrating with respect to $\boldsymbol{r}_1$, the orthonormality properties of the u-functions introduce considerable simplifications and we are led to the following result:

$$-\frac{\hbar^2}{2\mu}\nabla_2^2\psi_{100}(\boldsymbol{r}_2) - \frac{2e^2}{r_2}\psi_{100}(\boldsymbol{r}_2) + e^2\psi_{100}(\boldsymbol{r}_2)\int\frac{u^*_{100}(\boldsymbol{r}_1)u_{100}(\boldsymbol{r}_1)}{|\boldsymbol{r}_1 - \boldsymbol{r}_2|}\,\mathrm{d}\boldsymbol{r}_1 + \\ + e^2\psi_{200}(\boldsymbol{r}_2)\int\frac{u^*_{100}(\boldsymbol{r}_1)u_{200}(\boldsymbol{r}_1)}{|\boldsymbol{r}_1 - \boldsymbol{r}_2|}\,\mathrm{d}\boldsymbol{r}_1 + e^2\psi_{210}(\boldsymbol{r}_2)\int\frac{u^*_{100}(\boldsymbol{r}_1)u_{210}(\boldsymbol{r}_1)}{|\boldsymbol{r}_1 - \boldsymbol{r}_2|}\,\mathrm{d}\boldsymbol{r}_1 + \dots = \\ = \left(\mathscr{E} + \frac{2e^2}{a_0}\right)\psi_{100}(\boldsymbol{r}_2) . \tag{1.7}$$

Similarly, multiplying (1.6) successively by $u^*_{200}(\boldsymbol{r}_1)$, $u^*_{210}(\boldsymbol{r}_1)$, etc., and integrating each time, we arrive at an infinity of analogous differential equations forming a coupled set. Introducing the abbreviation

$$T^{n'l'm'}_{nlm}(\boldsymbol{r}_2) \equiv \int\frac{u^*_{nlm}(\boldsymbol{r}_1)u_{n'l'm'}(\boldsymbol{r}_1)}{|\boldsymbol{r}_1 - \boldsymbol{r}_2|}\,\mathrm{d}\boldsymbol{r}_1 , \tag{1.8}$$

this set can be written as:

$$
(1.9)\qquad
\begin{cases}
-\dfrac{\hbar^2}{2\mu}\nabla_2^2\psi_{100}(\boldsymbol{r}_2)-\dfrac{2e^2}{r_2}\psi_{100}(\boldsymbol{r}_2)+e^2[T_{100}^{100}(\boldsymbol{r}_2)\psi_{100}(\boldsymbol{r}_2)+ \\
\qquad +T_{100}^{200}(\boldsymbol{r}_2)\psi_{200}(\boldsymbol{r}_2)+T_{100}^{210}(\boldsymbol{r}_2)\psi_{210}(\boldsymbol{r}_2)+\ldots]=\left(\mathscr{E}+\dfrac{2e^2}{a_0}\right)\psi_{100}(\boldsymbol{r}_2)\,, \\
-\dfrac{\hbar^2}{2\mu}\nabla_2^2\psi_{200}(\boldsymbol{r}_2)-\dfrac{2e^2}{r_2}\psi_{200}(\boldsymbol{r}_2)+e^2[T_{200}^{100}(\boldsymbol{r}_2)\psi_{100}(\boldsymbol{r}_2)+ \\
\qquad +T_{200}^{200}(\boldsymbol{r}_2)\psi_{200}(\boldsymbol{r}_2)+T_{200}^{210}(\boldsymbol{r}_2)\psi_{210}(\boldsymbol{r}_2)+\ldots]=\left(\mathscr{E}+\dfrac{e^2}{2a_0}\right)\psi_{200}(\boldsymbol{r}_2)\,, \\
-\dfrac{\hbar^2}{2\mu}\nabla_2^2\psi_{200}(\boldsymbol{r}_2)-\dfrac{2e^2}{r_2}\psi_{210}(\boldsymbol{r}_{21})+e^2[T_{210}^{100}(\boldsymbol{r}_2)\psi_{100}(\boldsymbol{r}_2)+ \\
\qquad +T_{210}^{200}(\boldsymbol{r}_2)\psi_{200}(\boldsymbol{r}_2)+T_{210}^{210}(\boldsymbol{r}_2)\psi_{210}(\boldsymbol{r}_2)+\ldots]=\left(\mathscr{E}+\dfrac{e^2}{2a_0}\right)\psi_{210}(\boldsymbol{r}_2)\,, \\
\ldots\ldots\ldots\ldots\ldots\ldots\ldots
\end{cases}
$$

Here, one needs to know the explicit expressions for the T-coefficients. These expressions can be obtained by direct integration in form. (1.8) using polar co-ordinates to describe the position of the two electrons with respect to the nucleus. Writing $|\boldsymbol{r}_1-\boldsymbol{r}_2|^{-1}$ explicitly in terms of these co-ordinates, making the appropriate expansion in Legendre series and applying the addition theorem for Legendre polynomials, the integration with respect to φ_1 becomes entirely straightforward and one finds:

$$
(1.10)\qquad \int_0^{2\pi}\frac{\mathrm{d}\varphi_1}{|\boldsymbol{r}_1-\boldsymbol{r}_2|}=
\begin{cases}
\dfrac{2\pi}{r_1}\displaystyle\sum_{l=0}^{\infty}\left(\frac{r_2}{r_1}\right)^l P_l(\cos\theta_1)P_l(\cos\theta_2)\,, & (r_2\leqslant r_1), \\
\dfrac{2\pi}{r_2}\displaystyle\sum_{l=0}^{\infty}\left(\frac{r_1}{r_2}\right)^l P_l(\cos\theta_1)P_l(\cos\theta_2)\,, & (r_2\geqslant r_1),
\end{cases}
$$

and more generally:

$$
(1.10')\qquad \int_0^{2\pi}\frac{\exp[\pm ip\varphi_1]}{|\boldsymbol{r}_1-\boldsymbol{r}_2|}\,\mathrm{d}\varphi_1=
$$

$$
=\begin{cases}
\dfrac{2\pi}{r_1}\displaystyle\sum_{l=p}^{\infty}\frac{(l-p)!}{(l+p)!}\left(\frac{r_2}{r_1}\right)^l P_l^p(\cos\theta_1)P_l^p(\cos\theta_2)\exp[\pm ip\varphi_2]\,, & (r_2\leqslant r_1), \\
\dfrac{2\pi}{r_2}\displaystyle\sum_{l=p}^{\infty}\frac{(l-p)!}{(l+p)!}\left(\frac{r_1}{r_2}\right)^l P_l^p(\cos\theta_1)P_l^p(\cos\theta_2)\exp[\pm ip\varphi_2]\,, & (r_2\geqslant r_1),
\end{cases}
$$

where p represents a positive integer. Indeed, the product $u^*_{n'l'm'}(\boldsymbol{r}_1)u_{nlm}(\boldsymbol{r}_1)$ depends on φ_1 solely through the term $\exp[i(m-m')\varphi_1]$ in which the integer $m-m'$ can be zero, positive or negative. Further integrations with respect

to θ_1 and r_1 become generally more tedious, but they can always be carried out by elementary means. As an example, let us write down the expressions for the four simplest T-functions, namely:

$$
\left\{
\begin{aligned}
T^{100}_{100}(\boldsymbol{r}_2) &= \frac{1}{r_2}\left[1-\left(1+2\,\frac{r_2}{a_0}\right)\exp\left[-4\,\frac{r_2}{a_0}\right]\right],\\
T^{200}_{200}(\boldsymbol{r}_2) &= \frac{1}{r_2}\left\{1-\left[1+\frac{3}{2}\,\frac{r_2}{a_0}+\left(\frac{r_2}{a_0}\right)^2+\left(\frac{r_2}{a_0}\right)^3\right]\exp\left[-2\,\frac{r_2}{a_0}\right]\right\},\\
T^{100}_{200}(\boldsymbol{r}_2) &= T^{200}_{100}(\boldsymbol{r}_2) = \frac{8\sqrt{2}}{27}\,\frac{1}{r_2}\left(1+3\,\frac{r_2}{a_0}\right)\frac{r_2}{a_0}\exp\left[-3\,\frac{r_2}{a_0}\right].
\end{aligned}
\right. \tag{1.11}
$$

The equality in the last formula results from the general property of $T^{n'l'm'}_{nlm}$ namely:

$$T^{nlm}_{n'l'm'}(\boldsymbol{r}_2) = \left(T^{n'l'm'}_{nlm}(\boldsymbol{r}_2)\right)^*,$$

and the fact that in the case under consideration, the T's are real.

Finally, in order to deduce from the set (1.9) the practical equation on which all further calculations in this paper will be based, let us clearly specify which kind of solution $\Psi(\boldsymbol{r}_1, \boldsymbol{r}_2)$ of eq. (1.1) we wish to obtain.

First, let us point out that, at present, we shall disregard the question of possible symmetry or antisymmetry with which the wave function Ψ should be endowed. Temporarily, our aim is to find a sufficiently accurate solution of the Schrödinger equation (1.1) from which we can construct the suitably symmetrized space part of a desired spin-dependent helium wave function. This permits us to treat the two helium electrons as distinguishable particles. Further, what we need is the description of a state in which the first electron is as strongly bound to the helium nucleus as quantum mechanics permits, whereas the second electron has an energy belonging to the continuum part of the spectrum. Let us suppose for a moment that the Coulomb interaction between the two electrons were « turned off ». Then, the first electron would be exactly described by the ground state wave function of (1.2), namely $u_{100}(\boldsymbol{r}_1)$, whereas the second electron would be characterized by a continuum energy Coulomb wave function (corresponding to a nuclear charge $Z = 2$). Switching on the interaction will cause a mutual perturbation of these states. For the second electron, this perturbation can be expected to be appreciable. Indeed, the bound electron is rather well localized around the nucleus and therefore produces a perturbing potential with a rather strong gradient, superimposing itself on the pure $1/r$-potential due to the nuclear charge, thus producing the expected screening. On the contrary, the perturbation exerted by the positive energy electron on the bound electron will be much less pronounced due to the fact that the charge cloud associated with the former is spread out over a much larger region of space. Thus, the second electron creates a much

smaller potential with a much weaker gradient. In conclusion, we can therefore say that it is chiefly the modification of the spatial configuration of the charge cloud associated with the positive energy electron which deserves our attention.

Now, returning to the preceding mathematical formalism, we see that it is perfectly well adapted to the physical ideas just expounded. Indeed, if there were no interaction between the two electrons, the series expansion (1.5) would break off right after the first product term. Switching on the interaction will cause essentially two effects:

1) influence rather strongly the function $\psi_{100}(\boldsymbol{r}_2)$;

2) introduce a weak perturbation of the bound electron state, so that it is no longer rigorously described by $u_{100}(\boldsymbol{r}_1)$. This perturbation of the wave function can be adequately accounted for by an admixture of some other hydrogenic states to $u_{100}(\boldsymbol{r}_1)$, as if it were expanded in a series of such states. This is precisely what is expressed by form (1.5). But on the ground of the above reasoning, it can be expected that the overall modification of $\Psi(\boldsymbol{r}_1, \boldsymbol{r}_2)$ will be largely due to the change of $\psi_{100}(\boldsymbol{r}_2)$ and much less to the sum of all terms containing excited hydrogenic states.

Consequently, the preceding discussion leads us to the assertion that the lowest order approximation for $\Psi(\boldsymbol{r}_1, \boldsymbol{r}_2)$ which consists in keeping only the first term on the right hand side of (1.5), *i.e.*:

$$\Psi(\boldsymbol{r}_1, \boldsymbol{r}_2) \simeq u_{100}(\boldsymbol{r}_1)\,\psi_{100}(\boldsymbol{r}_2) \tag{1.12}$$

is a sensible one to make provided we are able to deduce ψ_{100} as accurately as possible. To be consistent with (1.12), the equation permitting to find this function should be found by suitable truncation of the infinite set of coupled eqs. (1.9) in the way it is customarily done in such cases. Isolating the first differential equation of the set and neglecting all terms depending on ψ's other than ψ_{100}, we arrive at the following approximate equation for this function:

$$-\frac{\hbar^2}{2\mu}\nabla_2^2\psi_{100}(\boldsymbol{r}_2) - \frac{e^2}{r_2}\left[1 + \left(1 + 2\,\frac{r_2}{a_0}\right)\exp\left[-4\,\frac{r_2}{a_0}\right]\right]\psi_{100}(\boldsymbol{r}_2) = E\psi_{100}(\boldsymbol{r}_2)\,, \tag{1.13}$$

where

$$E = \mathcal{E} - \frac{2e^2}{a_0}$$

clearly represents the energy of the second electron in the electric field due to the nucleus and the charge cloud associated with the first electron.

Eq. (1.13) has the form of a Schrödinger equation, in which the total po-

tential appears to be the superposition of a Coulombic and a short range potential. As r_2 starts from zero and increases indefinitely, the factor within the square brackets starts from the value 2, decreases continuously and tends asymptotically to 1. In this way, the effective potential in the proposed equation for $\psi_{100}(\boldsymbol{r}_2)$ can be regarded as being due to the given helium nucleus screened by the charge cloud of the bound electron. More precisely, the perturbing potential superimposed on that produced by the helium nucleus charge, can be obtained from the charge distribution corresponding to an electron in the (unperturbed) hydrogenic ground state $u_{100}(\boldsymbol{r}_1)$. This potential has been used before in Hartree wave function calculations.

Actually, (1.13) could have been reached more directly if we had decided at once to make the first step of a Hartree calculation. But it is a merit of the procedure outlined above, that it provides a deeper insight on the simplifying assumptions initially made in such calculations, namely, in our case:

1) that $\Psi(\boldsymbol{r}_1, \boldsymbol{r}_2)$ can be sufficiently well represented by a product of two one-electron wave functions;

2) that the bound electron can be described by means of the hydrogenic ground state wave function corresponding to the nuclear charge $Z = 2$;

3) that the positive energy electron can be characterized by a wave function which satisfies a one-electron Schrödinger equation with a screened Coulombic potential.

However, a more important consequence of our method resides in the fact that it enables one to obtain higher order improvements of (1.13) in a straightforward manner, evidently by keeping more than one term on the right hand side of (1.5) and keeping a convenient number of coupled equations in (1.9). For example, if we wished to know to what degree the states corresponding to $n = 2$ play a role in the perturbation of the state $u_{100}(\boldsymbol{r}_1)$ of the first electron, we would have to consider a $\Psi(\boldsymbol{r}_1, \boldsymbol{r}_2)$-function of the form:

$$\Psi(\boldsymbol{r}_1, \boldsymbol{r}_2) \simeq \sum_{n=1}^{2} \sum_{l=0}^{n-1} \sum_{m=-l}^{l} u_{nlm}(\boldsymbol{r}_1)\, \psi_{nlm}(\boldsymbol{r}_2)\,, \tag{1.14}$$

in which the five unknown ψ-functions would have to satisfy the following set of simultaneous differential equations:

$$-\frac{\hbar^2}{2\mu} \nabla_2^2 \psi_{nlm}(\boldsymbol{r}_2) - \frac{2e^2}{r_2} \psi_{nlm}(\boldsymbol{r}_2) + \\ + e^2 \sum_{n'=1}^{2} \sum_{l'=0}^{n'-1} \sum_{m'=-l'}^{l'} T_{nlm}^{n'l'm'}(\boldsymbol{r}_2)\, \psi_{n'l'm'}(\boldsymbol{r}_2) = \left(\mathscr{E} + \frac{2e^2}{n^2 a_0}\right) \psi_{nlm}(\boldsymbol{r}_2)\,, \tag{1.15}$$

where the indices n, l, m are respectively put equal to 1, 0, 0; 2, 0, 0; 2, 1, 0; 2, 1, 1 and 2, 1, −1.

But, since for the moment at least, we shall be satisfied with an approximation of the type (1.12) for $\Psi(\boldsymbol{r}_1, \boldsymbol{r}_2)$, we only need to study eq. (1.13) and to deduce some of its solutions of particular interest for practical applications.

2. – Influence of the motion of the nucleus.

In establishing eq. (1.1) as a starting point in the previous section, we mentioned the omission of a perturbing term due to the motion of the nucleus. It is the purpose of this section to examine briefly the effect of the presence of this term on our preceding calculations.

It is well-known that after going over to relative co-ordinates and separating off the kinetic energy term due to the motion of the c.m., one arrives at eq. (1.1) corrected by one additional term, namely:

$$(2.1)\qquad \left[-\frac{\hbar^2}{2\mu}(\nabla_1^2+\nabla_2^2)-\frac{\hbar^2}{M_{\mathrm{He}}}\left(\frac{\partial^2}{\partial x_1\,\partial x_2}+\frac{\partial^2}{\partial y_1\,\partial y_2}+\frac{\partial^2}{\partial z_1\,\partial z_2}\right)-\right.$$
$$\left.-\frac{2e^2}{r_1}-\frac{2e^2}{r_2}+\frac{e^2}{r_{12}}\right]\Psi(\boldsymbol{r}_1,\boldsymbol{r}_2)=\mathscr{E}\Psi(\boldsymbol{r}_1,\boldsymbol{r}_2).$$

Still applying our method of Sect. **1**, *i.e.*, postulating the series expansion (1.5) for $\Psi(\boldsymbol{r}_1, \boldsymbol{r}_2)$, introducing it into the equation and integrating all terms after having multiplied both sides respectively by $u^*_{100}(\boldsymbol{r}_1)$, $u^*_{200}(\boldsymbol{r}_1)$, etc., we finally obtain a system of coupled differential equations similar to (1.9), but containing supplementary terms. If, however, we are again primarily interested in a differential equation for $\psi_{100}(\boldsymbol{r}_2)$ which must result from the appropriate truncation of the mentioned modified system of equations, we can easily show that the effect due to the presence of the additional term in (2.1) vanishes identically. Indeed, the term that tends to add itself to eq. (1.13) has the form

$$(2.2)\qquad -\frac{\hbar^2}{M_{\mathrm{He}}}\int u^*_{100}(\boldsymbol{r}_1)\left(\frac{\partial^2}{\partial x_1\,\partial x_2}+\frac{\partial^2}{\partial y_1\,\partial y_2}+\frac{\partial^2}{\partial z_1\,\partial z_2}\right)u_{100}(\boldsymbol{r}_1)\,\psi_{100}(\boldsymbol{r}_2)\,\mathrm{d}\boldsymbol{r}_1\,.$$

Considering that

$$(2.3)\qquad \left(\frac{\partial^2}{\partial x_1\,\partial x_2}+\frac{\partial^2}{\partial y_1\,\partial y_2}+\frac{\partial^2}{\partial z_1\,\partial z_2}\right)u_{100}(\boldsymbol{r}_1)\,\psi_{100}(\boldsymbol{r}_2)=$$
$$=\left(\sin\theta_1\cos\varphi_1\,\frac{\partial\psi_{100}(\boldsymbol{r}_2)}{\partial x_2}+\sin\theta_1\sin\varphi_1\,\frac{\partial\psi_{100}(\boldsymbol{r}_2)}{\partial y_2}+\cos\theta_1\,\frac{\partial\psi_{100}(\boldsymbol{r}_2)}{\partial z_2}\right)\frac{\mathrm{d}u_{100}}{\mathrm{d}r_1}\,,$$

and that $u^*_{100}(\boldsymbol{r}_1)$ is also a purely radial wave function, the integrations with respect to the angular variables implied in (2.2) will vanish identically due to the orthogonality properties of the first order spherical harmonics appearing on the right hand side of (2.3). Thus, for our present purposes, eq. (1.13) remains unchanged, justifying the omission originally introduced. If, however, we were interested in more refined calculations of $\Psi(\boldsymbol{r}_1, \boldsymbol{r}_2)$, for instance, representing this function by (1.14), the system of coupled equations for the unknown ψ-functions would certainly contain non-vanishing contributions from the term under consideration, but the correction terms caused by these contributions can be expected to be of an order μ/M_{Fe} (=1/7 295) smaller than *e.g.* the terms due to the presence of e^2/r_{12} which can also be regarded as a perturbation. In conclusion, the corrections due to the motion of the nucleus are practically negligible.

3. – Derivation of the ordinary differential equation for the radial part of $\psi_{100}(\boldsymbol{r}_2)$ and discussion of its regular solutions.

Our basic eq. (1.13), written in polar co-ordinates, lends itself to the well-known technique of separation of variables, since the potential is spherically symmetric. As we are primarily interested in states of the second electron characterized by definite angular quantum numbers l and m, let us generally propose:

$$\psi_{100}(\boldsymbol{r}_2) = R(r_2)\, Y_{lm}(\theta_2, \varphi_2)\,. \tag{3.1}$$

Substituting this into (1.13), we easily arrive at the following ordinary differential equation for the radial part:

$$-\frac{\hbar^2}{2\mu r_2^2}\frac{\mathrm{d}}{\mathrm{d}r_2}\left(r_2^2\frac{\mathrm{d}R(r_2)}{\mathrm{d}r_2}\right) + \frac{l(l+1)\hbar^2}{2\mu r_2^2}\,R(r_2) - \\ - \frac{e^2}{r_2}\left[1 + \left(1 + 2\,\frac{r_2}{a_0}\right)\exp\left[-\,4\,\frac{r_2}{a_0}\right]\right] R(r_2) = E\,R(r_2)\,. \tag{3.2}$$

In this equation, the « potential term » appears to be too complicated to permit a direct analytical solution of $R(r_2)$ in terms of a finite expression of known functions. Therefore, a numerical treatment imposes itself here.

To reduce this equation to its simplest mathematical form, ready for machine computations, let us introduce the so-called atomic (Hartree) units,

so that

$$r_2 = \varrho a_0 , \qquad \frac{2\mu E}{\hbar^2} a_0^2 = k^2 a_0^2 = \varkappa^2 .$$

With the energy scale thus becoming dimensionless, $|\psi_{100}(\boldsymbol{r}_2)|^2$, which is actually a probability density, has the dimension L^{-3} where L symbolizes a length. Hence, $\psi_{100}(\boldsymbol{r}_2)$ and consequently also $R(r_2)$, has the dimension $L^{-\frac{3}{2}}$ and this leads us to the substitution

$$R(r_2) \equiv R(\varrho a_0) = \frac{1}{a_0^{\frac{3}{2}}} \frac{f(\varrho)}{\varrho} . \tag{3.3}$$

In this manner, the new unknown probability amplitude $f(\varrho)$ is a dimensionless function of the dimensionless distance variable ϱ. As usual, the factor $1/\varrho$ in (3.3) serves to simplify the differential operator in eq. (3.2), so that finally, the latter is transformed into the following basic radial equation:

$$\frac{\mathrm{d}^2 f(\varrho)}{\mathrm{d}\varrho^2} + \left\{ \varkappa^2 - \frac{l(l+1)}{\varrho^2} + \frac{2}{\varrho}\left[1 + (1 + 2\varrho) \exp\left[-4\varrho\right]\right] \right\} f(\varrho) = 0 . \tag{3.4}$$

$$(l = 0, 1, 2, \ldots), \quad (\varrho \neq 0).$$

Before going over to actual machine calculations, it is necessary to examine the general features of this linear and homogeneous differential equation and its solutions. It has two singular points: one regular point at the origin and one irregular point at infinity. For each value of l, it is satisfied by two linearly independent solutions, called the regular and the irregular solution, determined apart from an arbitrary proportionality factor and behaving at the origin as ϱ^{l+1} and ϱ^{-l}, respectively. Since we are only interested in such solutions $f(\varrho)$ which are physically acceptable as radial parts of wave functions, we only need to consider the family of regular solutions, characterized by the well-known boundary conditions:

$$f(0) = 0 \qquad \text{and} \qquad \left(\frac{\mathrm{d}f}{\mathrm{d}\varrho}\right)_{\varrho=0} = \begin{cases} \text{a finite constant}, & (l = 0), \\ 0 & (l > 0). \end{cases} \tag{3.5}$$

In order to avoid the singularity of eq. (3.4) at the origin when starting the computations, it is important to dispose of a few initial terms in the Maclaurin series expansion of $f(\varrho)$. Introducing

$$f(\varrho) = \varrho^{l+1}(c_0 + c_1 \varrho + c_2 \varrho^2 + \ldots) ,$$

into (3.4) and solving the resulting recurrence relations connecting the c-coefficients, we easily find:

$$f(\varrho) = c_0 \varrho^{l+1} \left\{ 1 - 2\frac{2\varrho}{2l+2} + \left[2(l+3) - \frac{(l+1)}{2}\varkappa^2 \right] \frac{(2\varrho)^2}{2!(2l+2)(2l+3)} - \right.$$

$$- \left[12(l+2) - (3l+4)\varkappa^2 \right] \frac{(2\varrho)^3}{3!(2l+2)(2l+3)(2l+4)} +$$

$$\left. + \left[-4(l+2)(8l^2+17l-3) - (6l^2+30l+32)\varkappa^2 + \frac{3(l+1)(l+2)}{4}\varkappa^4 \right] \cdot \right.$$

$$\left. \cdot \frac{(2\varrho)^4}{4!(2l+2)(2l+3)(2l+4)(2l+5)} - \ldots \right\}, \tag{3.6}$$

where c_0 is the previously mentioned proportionality factor. It can be determined (apart from an arbitrary phase factor) as soon as one imposes the normalization condition which $f(\varrho)$ has to satisfy on account of the fact that it is a wave function. This question will be examined in detail in a subsequent section.

Further, it is important to note that (3.4) is in fact an equation corresponding to a perturbed Coulomb problem. Indeed,

$$\frac{\mathrm{d}^2 f(\varrho)}{\mathrm{d}\varrho^2} + \left(\varkappa^2 - \frac{l(l+1)}{\varrho^2} + \frac{2}{\varrho} \right) f(\varrho) = 0 \tag{3.7}$$

would have been the resulting equation if we had neglected the finite extension of the charge cloud due to the bound electron and no particular difficulty would have arisen since the set of regular solutions of this equation (the so-called radial Coulomb wave functions) is well-known and expressible in terms of a confluent hypergeometric series. But our basic eq. (3.4) differs from (3.7) by the presence of the short-range potential

$$\frac{2}{\varrho}(1+2\varrho)\exp[-4\varrho], \tag{3.8}$$

resulting from a more accurate description of the screening effect of the bound electron. This potential can be regarded as a perturbation modifying the radial Coulomb wave functions and necessitating a numerical treatment of (3.4). In this regard, it is instructive to subdivide the interval $0 < \varrho < +\infty$ into two regions separated by a value which we can choose in the vicinity of $\varrho = 2$, say. The first region containing the origin, is the domain in which the potential (3.8) is truly active and most strongly perturbs all solutions of eq. (3.7). In the second region ($\varrho > 2$), (3.8) can be regarded as negligible and (3.4) practically reduces to (3.7). This has as consequence that in this region, each

regular solution $f(\varrho)$ of eq. (3.4) approaches more and more closely a certain linear combination of the corresponding regular and irregular solutions of eq. (3.7), which are well-known. Let us represent respectively by $F_{\varkappa l}(\varrho)$ and $G_{\varkappa l}(\varrho)$, those regular and irregular solutions of (3.7) which have the following asymptotic form:

$$F_{\varkappa l}(\varrho) \xrightarrow[\varrho\to\infty]{} \sin\left(\varkappa\varrho + \frac{1}{\varkappa}\ln 2\varkappa\varrho - \frac{l\pi}{2} - \sigma_l\right), \tag{3.9}$$

$$G_{\varkappa l}(\varrho) \xrightarrow[\varrho\to\infty]{} \cos\left(\varkappa\varrho + \frac{1}{\varkappa}\ln 2\varkappa\varrho - \frac{l\pi}{2} - \sigma_l\right), \tag{3.10}$$

in which $\sigma_l = \arg\Gamma[l+1+(i/\varkappa)]$. Then, we can write for $\varrho > 2$:

$$f(\varrho) \simeq AF_{\varkappa l}(\varrho) + BG_{\varkappa l}(\varrho)\,. \tag{3.11}$$

The measure in which the irregular Coulomb solution is admixed to the regular Coulomb solution is entirely governed by the importance of the perturbation (3.8). Eq. (3.11) also permits us to find the asymptotic behavior of $f(\varrho)$ at great distances:

$$f(\varrho) \xrightarrow[\varrho\to\infty]{} C\sin\left[\varkappa\varrho + \frac{1}{\varkappa}\ln 2\varkappa\varrho - \frac{l\pi}{2} - \sigma_l + \eta_l(\varkappa)\right], \tag{3.12}$$

where C is a certain amplitude and $\eta_l(\varkappa)$, a certain phase angle, connected to A and B by the relationships:

$$A = C\cos\eta_l(\varkappa)\,, \qquad B = C\sin\eta_l(\varkappa)\,. \tag{3.13}$$

The amplitude C plays the same role of proportionality factor as c_0 does in (3.6). Its value also depends upon the kind of normalization proposed. On the contrary, $\eta_l(\varkappa)$ is entirely determined by the perturbing effect of (3.8) on the set of regular solutions of (3.7). It is a well-defined function of l and $\varkappa$.

4. – Solution of the differential equation (3.4) by numerical methods.

The radial eq. (3.4) has been integrated numerically on an IBM 650 Ordinator for $\varkappa = 0.3,\ 0.5,\ 0.7,\ 0.8,\ 1.0,\ 1.5,\ 2.0,\ 3.0$ and 4.0. In each of these cases, the radial wave functions were determined for $l = 0,\ 1$ and 2. The choice of the mentioned parameter values was dictated by the specific applications in which these functions will be used later on. In fact, let us also mention that from the physical point of view, these low-l wave functions are just the most interesting ones since they differ most considerably from the corresponding

Coulomb wave functions with nuclear charge $Z = 1$. It is indeed for the lowest l-values that the Coulomb wave functions exhibit the most rapid growth as ϱ increases from the origin on, and that the short-range potential (3.8) will exert the strongest perturbation on the initial part of these functions, thus producing the largest phase shifts. The practical applications have also determined that the interval of ϱ, in which the radial wave functions are needed extends from 0 to about 8 atomic units.

In addition, the solutions $f(\varrho)$ had to be suitably normalized in one way or another. Theoretically, if $f_{\varkappa l}(\varrho)$ and $f_{\varkappa' l}(\varrho)$ are two radial functions, the normalization condition in the $\varkappa$-scale can be brought in the form

$$\int_0^\infty f_{\varkappa l}(\varrho) f_{\varkappa' l}(\varrho)\, \mathrm{d}\varrho = \delta(\varkappa - \varkappa') .$$

Using the well-known method of coupling the differential equations satisfied by $f_{\varkappa l}(\varrho)$ and $f_{\varkappa' l}(\varrho)$, one can easily prove that this condition is equivalent to assigning the value $\sqrt{2/\pi}$ to the constant C in (3.12). In practice, however, we found it much more convenient to normalize each $f_{\varkappa l}(\varrho)$-function to unit amplitude at infinity, thereby keeping in mind that in actual applications, the results calculated numerically should be provided with the appropriate factor. How we succeeded in normalizing the $f_{\varkappa l}(\varrho)$-functions according to our chosen convention, will be discussed with the necessary detail in Sect. 5. But let us mention here, that the adopted method sometimes necessitated a numerical integration up to a $\varrho_{\max}$-value lying considerably higher than the previously mentioned 8 atomic units limit. It turned out that $\varrho_{\max}$ tends to become larger as $\varkappa$ diminishes and l increases.

To obtain all unnormalized curves, a machine time of about 20 h was needed. The results, involving not only the tabulation of the various $f_{\varkappa l}(\varrho)$-functions, but also that of the first and second derivatives, became available on punched cards and were listed in an unpublished report. In integrating the differential eq. (3.4), we had the opportunity to make use of an existing subroutine written in FLEX, so that we only needed to enter into the machine such specifications as the particular form of the coefficient of $f(\varrho)$ in (3.4), the order of the equation, the initial step and the desired precision. The method contained in the program and used in the step-by-step integration, was based on the well-known Milne formulas, in which the results in one point are calculated using the information obtained in the four preceding points. The initial step was conveniently chosen equal to $2.5 \cdot 10^{-3}$ atomic units, but as computations progressed, the step was not necessarily kept constant.

Indeed, the programming involved a mechanism by which the value of the step was at any moment governed by the degree of precision reached. The

idea is the following: if the error affecting the ordinate calculated by the machine at a certain point exceeded some fixed upper limit, the calculation proceeded with a twice smaller step value; if, on the contrary, the error became systematically smaller than a prescribed lower limit, then the machine automatically adopted a double step value. In choosing $2.5 \cdot 10^{-3}$ a.u. as initial step value, it turned out that practically no step splitting could occur. This situation was favoured in order to make sure that all functions were evaluated exclusively at points whose abscissas were multiples of the adopted initial step. The absolute error on each calculated $f(\varrho)$-value was lying between 10^{-6} and 10^{-5}. A desired over-all relative precision has been obtained by suitable choice of the coefficient c_0, when calculating the starting points by means of the series expansion (3.6). Let us also mention here that c_0 was always given the positive sign, in analogy to what one usually does in the case of regular Coulomb wave functions.

5. – Normalization of the radial functions $f_{\varkappa l}(\varrho)$.

As mentioned above, a normalization to unit amplitude at infinity was preferred for practical reasons. In principle, the most straightforward way to achieve this, would simply consist in calculating each $f_{\varkappa l}(\varrho)$-curve up to such large values of ϱ that the local amplitude can be considered as « stabilized », *i.e.*, sufficiently close to its limit value at infinity. Afterwards, the latter could always be reduced to unity by means of a linear ordinate-scale transformation. However, during the computations, it became clear that the slow convergence of the tabulated functions towards their asymptotic behavior made this direct method prohibitive from the point of view of machine time and costs. In what follows, we wish to outline two other normalization procedures, both interesting from the pratical viewpoint. One of them has actually been adopted.

5·1. – The first normalization method makes use of two formulas yielding direct integral representations of $C \cos \eta_l(\varkappa)$ and $C \sin \eta_l(\varkappa)$, where C and $\eta_l(\varkappa)$ are resp. the amplitude and the phase angle already appearing in (3.12). In what follows, we shall represent by

— $f_{\varkappa l}(\varrho)$: any regular solution of our basic eq. (3.4). All $f_{\varkappa l}(\varrho)$-functions differ from one another only by the value of a proportionality factor;

— $F_{\varkappa l}(\varrho)$ and $G_{\varkappa l}(\varrho)$: the same functions as in Sect. **3**, namely, the regular solution and the irregular solution of eq. (3.7) whose asymptotic forms are given by (3.9) and (3.10) respectively.

For all $\varrho \geqslant 0$, $F_{\varkappa l}(\varrho)$ can be rigorously expressed in terms of a confluent hypergeometric function ${}_1F_1$ (in Barnes' notation), *viz.*:

$$F_{\varkappa l}(\varrho) = \frac{2^l(\varkappa\varrho)^{l+1}\,|\Gamma[l+1+(i/\varkappa)]|\exp[\pi/2\varkappa]\exp[-i\varkappa\varrho]}{(2l+1)!} \cdot {}_1F_1\left(l+1+\frac{i}{\varkappa};\ 2l+2;\ 2i\varkappa\varrho\right).$$

The derivation of the formulas for $C\cos\eta_l(\varkappa)$ and $C\sin\eta_l(\varkappa)$ is based upon a transformation of (3.4) into an integral equation for $f_{\varkappa l}(\varrho)$, making use of the « unperturbed » Coulombic eq. (3.7). Multiplying (3.4) by $F_{\varkappa l}(\varrho)$ and (3.7) by $f_{\varkappa l}(\varrho)$, and subtracting, we obtain:

$$\frac{\mathrm{d}}{\mathrm{d}\varrho}\left[F_{\varkappa l}(\varrho)\frac{\mathrm{d}f_{\varkappa l}(\varrho)}{\mathrm{d}\varrho} - f_{\varkappa l}(\varrho)\frac{\mathrm{d}F_{\varkappa l}(\varrho)}{\mathrm{d}\varrho}\right] + 2\frac{1+2\varrho}{\varrho}\exp[-4\varrho]f_{\varkappa l}(\varrho)F_{\varkappa l}(\varrho) = 0\,. \tag{5.1}$$

After integration with respect to ϱ, the result is

$$F_{\varkappa l}(\varrho)\frac{\mathrm{d}f_{\varkappa l}(\varrho)}{\mathrm{d}\varrho} - f_{\varkappa l}(\varrho)\frac{\mathrm{d}F_{\varkappa l}(\varrho)}{\mathrm{d}\varrho} = -2\int_0^{\varrho}\frac{1+2\varrho'}{\varrho'}\exp[-4\varrho']f_{\varkappa l}(\varrho')F_{\varkappa l}(\varrho')\mathrm{d}\varrho'. \tag{5.2}$$

Dividing on both sides by $F^2_{\varkappa l}(\varrho)$ and performing a second integration from 0 to ϱ, we find, after changing the order of integration on the right hand side:

$$\frac{f_{\varkappa l}(\varrho)}{F_{\varkappa l}(\varrho)} - \left(\frac{f_{\varkappa l}(\varrho)}{F_{\varkappa l}(\varrho)}\right)_{\varrho=0} = -2\int_0^{\varrho}\frac{1+2\varrho'}{\varrho'}\exp[-4\varrho']f_{\varkappa l}(\varrho')F_{\varkappa l}(\varrho')\,\mathrm{d}\varrho'\int_{\varrho'}^{\varrho}\frac{\mathrm{d}\varrho''}{F^2_{\varkappa l}(\varrho'')}\,. \tag{5.3}$$

The integral with respect to ϱ'' can be worked out taking into account the well-known relationship between $F_{\varkappa l}(\varrho)$ and $G_{\varkappa l}(\varrho)$, namely:

$$G_{\varkappa l}(\varrho)\frac{\mathrm{d}F_{\varkappa l}(\varrho)}{\mathrm{d}\varrho} - F_{\varkappa l}(\varrho)\frac{\mathrm{d}G_{\varkappa l}(\varrho)}{\mathrm{d}\varrho} = \varkappa\,, \tag{5.4}$$

so that

$$\int_{\varrho'}^{\varrho}\frac{\mathrm{d}\varrho''}{F^2_{\varkappa l}(\varrho'')} = \frac{1}{\varkappa}\left(\frac{G_{\varkappa l}(\varrho')}{F_{\varkappa l}(\varrho')} - \frac{G_{\varkappa l}(\varrho)}{F_{\varkappa l}(\varrho)}\right).$$

After a few elementary operations, we arrive at the desired integral equation:

$$(5.5)\quad f_{\varkappa l}(\varrho) = \left(\frac{f_{\varkappa l}(\varrho)}{F_{\varkappa l}(\varrho)}\right)_{\varrho=0} \cdot F_{\varkappa l}(\varrho) - \frac{2}{\varkappa} F_{\varkappa l}(\varrho) \int_0^{\varrho} \frac{1+2\varrho'}{\varrho'} \exp\left[-4\varrho'\right] f_{\varkappa l}(\varrho') G_{\varkappa l}(\varrho')) \mathrm{d}\varrho' +$$

$$+ \frac{2}{\varkappa} G_{\varkappa l}(\varrho) \int_0^{\varrho} \frac{1+2\varrho'}{\varrho'} \exp\left[-4\varrho'\right] f_{\varkappa l}(\varrho') F_{\varkappa l}(\varrho') \mathrm{d}\varrho'.$$

Besides its intrinsic value for calculating approximations for $f_{\varkappa l}(\varrho)$ by the successive iteration method, this equation has the property, customarily found in integral equations which are deduced from homogeneous differential equations, that the asymptotic behavior of its solution appears to be built in. Here, indeed, letting ϱ tend to infinity, and taking (3.9) and (3.10) into account, we find:

$$(5.6)\quad f_{\varkappa l}(\varrho) \xrightarrow[\varrho\to\infty]{} \left[\left(\frac{f_{\varkappa l}(\varrho)}{F_{\varkappa l}(\varrho)}\right)_{\varrho=0} - \frac{2}{\varkappa} \int_0^{\infty} \frac{1+2\varrho'}{\varrho'} \exp\left[-4\varrho'\right] f_{\varkappa l}(\varrho') G_{\varkappa l}(\varrho') \mathrm{d}\varrho'\right] \cdot$$

$$\cdot \sin\left(\varkappa\varrho + \frac{1}{\varkappa} \ln 2\varkappa\varrho - \frac{l\pi}{2} - \sigma_l\right) +$$

$$+ \frac{2}{\varkappa}\left(\int_0^{\infty} \frac{1+2\varrho'}{\varrho'} \exp\left[-4\varrho'\right] f_{\varkappa l}(\varrho') F_{\varkappa l}(\varrho') \mathrm{d}\varrho'\right) \cos\left(\varkappa\varrho + \frac{1}{\varkappa} \ln 2\varkappa\varrho - \frac{l\pi}{2} - \sigma_l\right),$$

which, after straightforward identification with (3.12), leads to the desired formulas mentioned above:

$$(5.7)\quad C \cos \eta_l(\varkappa) = \left(\frac{f_{\varkappa l}(\varrho)}{F_{\varkappa l}(\varrho)}\right)_{\varrho=0} - \frac{2}{\varkappa} \int_0^{\infty} \frac{1+2\varrho}{\varrho} \exp\left[-4\varrho\right] G_{\varkappa l}(\varrho) f_{l\varkappa}(\varrho) \mathrm{d}\varrho\,,$$

$$(5.8)\quad C \sin \eta_l(\varkappa) = \frac{2}{\varkappa} \int_0^{\infty} \frac{1+2\varrho}{\varrho} \exp\left[-4\varrho\right] F_{\varkappa l}(\varrho) f_{\varkappa l}(\varrho) \mathrm{d}\varrho\,.$$

Let us point out that the previous method is sufficiently general to be applicable to any Schrödinger equation whose potential can be separated into two parts, one which, if it were alone, would lead to a completely solvable Schrödinger equation, and another which could be regarded as a perturbation, making the original equation too complicated for analytical treatment. In any such case, formulas similar to (5.7) and (5.8) can be set up. In scattering problems, such formulas could be very important to evaluate the effect of an additional

perturbing potential on the amplitude and phase angle in the asymptotic form of a wave function.

For the purpose of normalization, the final results (5.7) and (5.8) obviously yield an unequivocal expression for the amplitude C (> 0) which, in practice, will reduce to the product of a certain numerical factor (depending on l and $\varkappa$) and c_0, the undetermined initial coefficient appearing in (3.6). As an example, let us indicate the analytic expression of the first part on the right hand side of (5.7):

$$(5.9) \qquad \left(\frac{f_{\varkappa l}(\varrho)}{F_{\varkappa l}(\varrho)}\right)_0 = \frac{(2l+1)!\exp[-\pi/2\varkappa]}{2^l\varkappa^{l+1}|\Gamma[l+1+(i/\varkappa)]|}c_0 = \frac{(2l+1)!\,(1-\exp[-2\pi/\varkappa])^{\frac{1}{2}}}{2^l\sqrt{2\pi\varkappa}\prod_{m=0}^{l}(1+m^2\varkappa^2)^{\frac{1}{2}}}c_0 .$$

Unfortunately, the two remaining integrals cannot be expressed directly in terms of closed mathematical forms as simple as (5.9). But, from the preceding remarks, the normalization procedure becomes obvious, at least in principle:

1) starting the numerical integration of eq. (3.4) using a few initial values of a particular $f_{\varkappa l}(\varrho)$-function calculated by means of the series expansion (3.6), one is actually free to assign any positive value to c_0 in order to specify that function completely. There is, however, one practical restriction to be taken into account, namely, that the choice of c_0 should be consistent with the earlier mentioned relative accuracy condition;

2) one computes $f_{\varkappa l}(\varrho)$ up to the desired maximum value of ϱ and one calculates the right hand sides of (5.7) and (5.8), using a numerical integration procedure to deal with the integrals involved;

3) one calculates the value of C and one divides all tabulated $f_{\varkappa l}(\varrho)$-ordinates by this value.

Evidently, the normalized function $f^{(n)}_{\varkappa l}(\varrho)$ does not depend upon the initial choice of c_0, since one actually calculates

$$\frac{f_{\varkappa l}(\varrho)}{\left\{\left[\left(\frac{f_{\varkappa l}(\varrho)}{F_{\varkappa l}(\varrho)}\right)_0 - \frac{2}{\varkappa}\int_0^\infty \frac{1+2\varrho}{\varrho}\exp[-4\varrho]G_{\varkappa l}(\varrho)f_{\varkappa l}(\varrho)\mathrm{d}\varrho\right]^2 + \frac{4}{\varkappa^2}\left[\int_0^\infty \frac{1+2\varrho}{\varrho}\exp[-4\varrho]F_{\varkappa l}(\varrho)f_{\varkappa l}(\varrho)\mathrm{d}\varrho\right]^2\right\}^{\frac{1}{2}}}$$

Now, concerning the numerical evaluation of the integrals appearing in (5.7) and (5.8), let us first point out that their infinite integration interval causes no difficulty at all, due to the fast convergence of the integrands. Indeed, it is a particularly advantageous characteristic of these integrals that they only contain the *short-range perturbing* potential explicitly. The slowly

converging Coulomb potential is only implicitly present through the wave functions $F_{\varkappa l}(\varrho)$, $G_{\varkappa l}(\varrho)$ and $f_{\varkappa l}(\varrho)$ themselves. Further, adding to this the consideration that these functions have an oscillatory behavior which entails supplementary cancellations in the large-ϱ contribution to the integrals, one easily sees that the integration intervals can be reduced to only a few units. Thus, for example, since the $f_{\varkappa l}(\varrho)$-functions are tabulated up to at least 8 atomic units, the accuracy that would be reached by adopting (0, 8) as integration interval would certainly be more than sufficient.

Notwithstanding its advantages, the present normalization method has not been adopted in our case, but the reason has been a purely technical one. Indeed, to evaluate the integrals in (5.7) and (5.8) numerically using for instance the Simpson parabolic interpolation formula, we would have needed tables of both the regular and the irregular normalized Coulomb wave functions, providing their values at precisely the same abscissas as those at which the $f_{\varkappa l}(\varrho)$-functions were calculated and for exactly the same set of $\varkappa$- and l-values as those mentioned in Sect. 4. Such tables were of course not readily available in the literature. Hence, the easiest way to overcome the difficulty would simply have been to carry out the numerical integration of eq. (3.7) under exactly the same circumstances as it was done with eq. (3.4), starting with appropriate initial conditions to find both the desired regular and irregular Coulomb wave functions. However, this would at least have tripled the needed IBM 650 machine time and we did not dispose of such a number of hours for our project.

To end this discussion, let us remark that, as we have stated before, the preceding method could also yield the physically interesting phaseshift $\eta_l(\varkappa)$, but only apart from an arbitrary multiple of 2π. However, we wish to stress that there exists a possibility to eliminate even this ambiguity and to determine $\eta_l(\varkappa)$ in an absolute way.

5·2. – The second and actually adopted normalization procedure is based upon a method for treating second order differential equations of the type (3.4), known as the Madelung transformation [5]. Applying this method, one tries to satisfy eq. (3.4) by means of an expression of the form

$$f(\varrho) = A(\varrho) \sin \int_{\varrho_0}^{\varrho} g(\varrho')\, \mathrm{d}\varrho', \tag{5.10}$$

on the ground that any solution of (3.4) is expected to oscillate for sufficiently large ϱ and to tend towards a purely sinusoidal function as $\varrho \to +\infty$. Here,

[5] E. Madelung: *Zeits. f. Phys.*, **67**, 516 (1931); D. R. Hartree: *Numerical Analysis* (Oxford, 1958), p. 154.

it is indeed the region of large ϱ-values which interests us most. More precisely, what we need is a representation of each considered $f_{\varkappa l}(\varrho)$-function which covers an interval starting at a certain ϱ-value (which we called $\varrho_{\max}$ in Sect. 4) up to infinity. In (5.10), $A(\varrho)$ and $g(\varrho)$ are supposed to be real functions, and ϱ_0 is some constant lower limit of integration which must be conveniently chosen. As we are only interested in obtaining a representation of the *regular* normalized solution $f^{(n)}_{\varkappa l}(\varrho)$ of our perturbed Coulomb wave eq. (3.4) for every considered set of $(\varkappa, l)$-values, ϱ_0 should be identified with one of the zeros of that solution. Indeed, one can easily prove that this is a sufficient condition to guarantee that (5.10) contains no admixture of the singular solution. Strictly speaking, however, there is an additional precaution to be taken in order to avoid the possibility that (5.10) is affected with the wrong sign. But, as the amplitude $A(\varrho)$ will always be positive in the region of interest, and since $g(\varrho)$ will appear to be essentially positive (see form. (5.14)), one can get round the difficulty by specifying that ϱ_0 should be a zero of $f_{\varkappa l}(\varrho)$ where the curve has a *positive* slope.

Substituting (5.10) into (3.4), one easily arrives at a system of two simultaneous differential equations, one of which can be directly integrated to yield:

$$A^2(\varrho)g(\varrho) = \text{const}\,.$$

From the asymptotic form for each regular solution of (3.4), namely (3.12), it appears that one should have

$$\lim_{\varrho\to+\infty} A(\varrho) = C \qquad \text{and} \qquad \lim_{\varrho\to+\infty} g(\varrho) = \varkappa\,,$$

so that

$$A^2(\varrho)g(\varrho) = \varkappa C^2\,.$$

Normalization is achieved by putting $C = 1$, which leads to

$$A^2(\varrho)g(\varrho) = \varkappa\,. \tag{5.11}$$

Making use of this relationship to eliminate $g(\varrho)$ from the other differential equation, one arrives at the following non-linear second order equation for $A(\varrho)$:

$$\frac{\mathrm{d}^2A(\varrho)}{\mathrm{d}\varrho^2} - \frac{\varkappa^2}{A^3(\varrho)} + \left\{\varkappa^2 - \frac{l(l+1)}{\varrho^2} + \frac{2}{\varrho}\left[1 + (1+2\varrho)\exp\left[-4\varrho\right]\right]\right\} A(\varrho) = 0, \tag{5.12}$$

which should be solved from infinity inward with the following boundary conditions:

$$A(+\infty) = 1\,, \qquad A'(+\infty) = 0\,.$$

Let us remark that since $\varrho_{\max}$ will always be at least 8 atomic units, the term containing the factor $\exp\left[-4\varrho\right]$ turns out to be exceedingly small compared

to the other terms between the braces. It is therefore entirely negligible in the calculation of $A(\varrho)$ and eq. (5.12) can practically be reduced to

$$\frac{\mathrm{d}^2 A(\varrho)}{\mathrm{d}\varrho^2} - \frac{\varkappa^2}{A^3(\varrho)} + \left[\varkappa^2 - \frac{l(l+1)}{\varrho^2} + \frac{2}{\varrho}\right] A(\varrho) = 0\,, \tag{5.13}$$

which is still to be solved with the same boundary conditions. Afterwards, the phase function $g(\varrho)$ can directly be found by means of the formula

$$g(\varrho) = \frac{\varkappa}{A^2(\varrho)}\,, \tag{5.14}$$

which results from (5.11). In this way, it appears possible to meet each directly calculated and still unnormalized regular solution $f_{\varkappa l}(\varrho)$ of eq. (3.4) with the corresponding normalized solution provided by (5.10) in a certain point where appropriate equations of fit should enable us to carry out the desired normalization of $f_{\varkappa l}(\varrho)$.

To obtain the required solution of eq. (5.12), our first idea has been to rely once more on the IBM 650 ordinator to perform a numerical integration. Since the computer should calculate $A(\varrho)$ starting at $\varrho = +\infty$, it is clear that a transformation to the new variable $z = 1/\varrho$ was desirable in this case. This leads to a new non-linear differential equation for the function $B(z)$ $(\equiv A(1/z))$. To start the integration, we again needed a minimum of four initial points on the curve as it was the case in treating eq. (3.4). These points can be most readily obtained by series expansion of $B(z)$ around the origin $z = 0$, which is equivalent to postulate

$$A(\varrho) = 1 + \frac{a_1}{\varrho} + \frac{a_2}{\varrho^2} + \dots\,. \tag{5.15}$$

Substituting this into eq. (5.13), one easily finds:

$$\left\{\begin{aligned} &a_1 = -\frac{1}{2\varkappa^2}\,, && a_2 = \frac{1}{4\varkappa^2}\left[l(l+1) + \frac{5}{2\varkappa^2}\right], \\ &a_3 = -\frac{1}{4\varkappa^4}\left[\frac{5}{2}\,l(l+1) - 1 + \frac{15}{4\varkappa^2}\right], && a_4 = \frac{1}{16\varkappa^4}\left\{\left[\frac{5}{2}\,l(l+1) - 6\right] l(l+1) + \right. \\ &&& \left. + \left[\frac{45}{2}\,l(l+1) - 23\right]\frac{1}{\varkappa^2} + \frac{195}{8\varkappa^4}\right\}, \dots \end{aligned}\right. \tag{5.16}$$

coefficients, which have also been deduced by WHEELER (6) in a paper on a related subject.

(6) J. A. WHEELER: *Phys. Rev.*, **52**, 1123 (1937).

In contrast to what one logically would expect about the smoothness of the amplitude function $A(\varrho)$ or the corresponding $B(z)$, a few machine tests for various pairs of $(\varkappa, l)$-values have proved that long before the abscissa $\varrho = 8$ (or $z = \frac{1}{8}$) was reached, the amplitude after showing little variation for a while, suddenly started to oscillate tremendously. Each time, this caused overflow of capacity which forced the machine to stop. This disadvantage made us decide to give preference to the use of the series representation of $A(\varrho)$ in order to carry out the desired normalization. We must point out, however, that (5.15) in which we put the coefficients (5.16), is only a *semi-convergent* series. It is therefore endowed with all the properties, but also affected with all the drawbacks of asymptotic series. But, it will appear from what follows, that the properties of an expansion such as (5.15) make it sufficiently useful for our present purpose.

For every pair of values $\varkappa$, l, there exists an interval $(\varrho^*, +\infty)$ associated with (5.15), in which this series, suitably truncated, provides a representation of $A(\varrho)$ with a prescribed accuracy. In our case, the latter was chosen equal to 10^{-4} in order to keep ϱ^* within reasonable limits. Two typical examples are:

$$\varkappa = 0.5\,, \quad l = 2: \qquad \varrho^* = 28 \text{ (a.u.)}\,,$$

$$\varkappa = 4.0\,, \quad l = 0: \qquad \varrho^* < \text{the fixed 8 a.u. limit}\,,$$

illustrating the tendency of ϱ^* to increase as $\varkappa$ diminishes and l increases. With an asymptotic series as (5.15), the determination of ϱ^* is particularly easy because, as soon as the terms start to alternate in sign, an upper limit of the error due to truncation is furnished by the absolute value of the first neglected term. From this, it follows logically that a normalization based upon the previous considerations, will necessarily imply a machine computation of each regular solution $f_{\varkappa l}(\varrho)$ of eq. (3.4) up to an abscissa $\varrho_{\max}$ exceeding the ϱ^*-value associated with each particular $(\varkappa, l)$-pair. What remains to be done now is simply to derive a formula for the fitting of the unnormalized, numerically obtained curves to the corresponding normalized functions analytically defined by (5.10), (5.14), (5.15) and (5.16).

In principle, equations of fit could be established in any point between ϱ^* and $\varrho_{\max}$. It is, however, particularly convenient to perform this operation at a zero $\tilde{\varrho}$ of $f_{\varkappa l}(\varrho)$. In $\varrho = \tilde{\varrho}$, both curves become equal to zero, the numerical one due to the definition of $\tilde{\varrho}$, and the analytical one given by (5.10) in virtue of the imposed choice of ϱ_0. Indeed, $g(\varrho)$ integrated between two roots of $f_{\varkappa l}(\varrho)$ always leads to a multiple of π. In this way, the only remaining equation of fit must result from the matching of the slopes at $\varrho = \tilde{\varrho}$. For a normalized $f_{\varkappa l}(\varrho)$-function, the mathematical description of this condition gives

rise to the following relation:

$$\left(\frac{\mathrm{d}f_{\varkappa l}^{(n)}(\varrho)}{\mathrm{d}\varrho}\right)_{\varrho=\tilde{\varrho}} = \left\{\frac{\mathrm{d}}{\mathrm{d}\varrho}\left[A(\varrho)\sin\int_{\varrho_0}^{\varrho} g(\varrho')\,\mathrm{d}\varrho'\right]\right\}_{\varrho=\tilde{\varrho}} = \tag{5.17}$$

$$= A(\tilde{\varrho})g(\tilde{\varrho})\cos\int_{\varrho_0}^{\tilde{\varrho}} g(\varrho')\,\mathrm{d}\varrho' = (-1)^p\frac{\varkappa}{A(\tilde{\varrho})},$$

where p represents the number of « half oscillations » lying between ϱ_0 and $\tilde{\varrho}$. When the slope of $f_{\varkappa l}^{(n)}(\varrho)$ is positive at $\varrho=\tilde{\varrho}$, then p must be even since the slope at ϱ_0 should always be positive as we have seen. In this case, both sides of (5.17) are positive. When the slope of $f_{\varkappa l}^{(n)}(\varrho)$ is negative at $\varrho=\tilde{\varrho}$, then the number of half oscillations will be odd, so that both sides are negative. At any rate, we find in both cases:

$$\left|\left(\frac{\mathrm{d}f_{\varkappa l}^{(n)}(\varrho)}{\mathrm{d}\varrho}\right)_{\varrho=\tilde{\varrho}}\right| = \frac{\varkappa}{A(\tilde{\varrho})}. \tag{5.18}$$

Now, let the equation connecting a normalized and the corresponding unnormalized regular solution of (3.4) be

$$f_{\varkappa l}^{(n)}(\varrho) = N f_{\varkappa l}(\varrho), \tag{5.19}$$

where N represents the proportionality factor with which all ordinates of $f_{\varkappa l}(\varrho)$ furnished by the machine ought to be multiplied to make the curve correspond to unit amplitude at infinity. N is a positive factor, since both $f_{\varkappa l}(\varrho)$ and $f_{\varkappa l}^{(n)}(\varrho)$ are ascending in the neighborhood of $\varrho=0$. From (5.18) and (5.19), we obtain the following final result for the normalizing factor:

$$N = \frac{\varkappa}{A(\tilde{\varrho})\,\left|(\mathrm{d}f_{\varkappa l}(\varrho)/\mathrm{d}\varrho)_{\varrho=\tilde{\varrho}}\right|}. \tag{5.20}$$

To conclude, let us sum up the various steps of the actually adopted practical normalization method resulting from the preceding theoretical study:

1) for each pair of $(\varkappa, l)$-values, evaluation of an abscissa ϱ^* at which the amplitude function $A(\varrho)$ can be represented by the sum of a conveniently chosen finite number of terms in (5.15) to an accuracy better than a preassigned degree of precision. The nature of the series (5.15) implies that in representing $A(\varrho)$ by the mentioned sum for all $\varrho>\varrho^*$, the same degree of accuracy will certainly hold, since the error diminishes gradually with increasing ϱ. Demanding 10^{-4} as upper limit of inaccuracy, it turned out that keeping the

first five terms in (5.15) was sufficient to guarantee that ϱ^* did not become exceedingly large (in practice not larger than 30 a.u., say);

2) direct evaluation of a certain regular solution $f_{\varkappa l}(\varrho)$ by numerical integration of eq. (3.4) using the IBM 650 ordinator, up to an abscissa ϱ_{max} greater, by at least three elementary integration steps, than the first zero of $f_{\varkappa l}(\varrho)$, called $\tilde{\varrho}$, which has the property of exceeding the largest among the two quantities ϱ^* and 8 (a.u.);

3) precise determination of $\tilde{\varrho}$ by means of a five point Stirling interpolation formula;

4) precise evaluation of $\mathrm{d}f_{\varkappa l}(\varrho)/\mathrm{d}\varrho$ at $\varrho = \tilde{\varrho}$ by means of a sixth order Lagrange interpolation polynomial, using the values of this derivative provided by the machine in six neighboring points of $\tilde{\varrho}$;

5) calculation of $A(\tilde{\varrho})$ and N;

6) multiplication of all ordinates of $f_{\varkappa l}(\varrho)$ by N.

It is interesting to note that, remarkably enough, ϱ_0 does not appear explicitly in any of the practical steps described above. Its significance is purely theoretical and one never needs to assign a particular value to it. Another equally remarkable feature is the absence of the phase function $g(\varrho)$. Finally, for what $A(\varrho)$ is concerned, it appears to be unnecessary to compute its entire behavior from $\varrho = +\infty$ down to $\varrho = \varrho^*$. Only its value at $\varrho = \tilde{\varrho}$ enters the calculations.

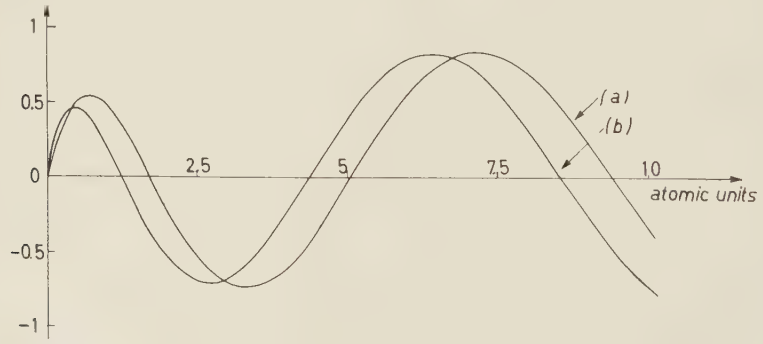

Fig. 1. – Example of comparison between two normalized radial wave functions in the case of $\varkappa = 0.5$ and $l = 0$: (a) corresponds to the pure Coulomb potential due to a hydrogen nucleus ($Z = 1$); (b) corresponds to the perturbed Coulomb potential appearing in (1.13).

As an illustration of the differences existing between regular Coulomb wave functions and the results of our calculations, we have plotted in Fig. 1,

two normalized radial wave functions for the case of $\varkappa = 0.5$ ($E = 3.40$ eV) and $l = 0$. The curve (a) corresponds to the pure $1/r$-potential due to the charge of a hydrogen nucleus ($Z = 1$); it pictures a regular normalized solution of eq. (3.7), *viz.*:

$$F_{\varkappa 0}(\varrho) = \frac{(2\pi\varkappa)^{\frac{1}{2}}}{(1 - \exp[-2\pi/\varkappa])^{\frac{1}{2}}}\,\varrho\,\exp[-i\varkappa\varrho]_1F_1\left(1 + \frac{i}{\varkappa};\,2;\,2i\varkappa\varrho\right)$$

$$= \frac{(2\pi\varkappa)^{\frac{1}{2}}}{(1 - \exp[-2\pi/\varkappa])^{\frac{1}{2}}}\,\varrho\left[1 - \varrho + \left(1 - \frac{\varkappa^2}{2}\right)\frac{\varrho^2}{3} - (1 - 2\varkappa^2)\frac{\varrho^3}{18} + \right.$$

$$\left. + (2 - 10\varkappa^2 + 3\varkappa^4)\frac{\varrho^4}{360} + \ldots\right].$$

In contrast, curve (b) depicts the corresponding solution $f_{\varkappa 0}^{(m)}(\varrho)$ of eq. (3.4) containing the Hartree potential. Since the latter differs from the pure $1/r$-potential by an additional attractive short-range potential, it could be expected that curve (b) would have the general tendency to be shifted to the left with respect to curve (a).

* * *

It is a particular pleasure to express our gratitude to the Fonds National de la Recherche Scientifique and to the Institut Interuniversitaire des Sciences Nucléaires for their financial support. We are also very much indebted to the IBM of Belgium (Brussels) and particularly to Mr. J. Francot, Jr., for having offered us computational facilities and effective collaboration. Finally, we wish to thank Prof. Dr. J. L. Verhaeghe for his interest in this work.

RIASSUNTO (*)

Allo scopo di ricordare i valori della ionizzazione specifica dell'elio nel tentativo di superare la distanza esistente in questo campo fra teoria ed esperimenti, questo lavoro tratta la derivazione di nuove funzioni d'onda corrispondenti ad energie della parte continua dello spettro dell'elio, che siano più precise di quelle risultanti dalle approssimazioni solitamente adottate. La Sezione **1** è dedicata ad un appropriato sviluppo in serie della funzione d'onda per i due elettroni planetari dell'elio ed alla corrispondente trasformazione dell'equazione di Schrödinger in un sistema infinito di equazioni

(*) *Traduzione a cura della Redazione.*

differenziali simultanee, rese necessarie dallo sviluppo in serie. Poi si mostra come un taglio opportuno porti alla fondamentale equazione differenziale, per un elettrone, del tipo di Schrödinger, per la funzione d'onda approssimata che descrive l'elettrone di energia positiva nel campo elettrico del nucleo di elio e l'elettrone legato. Si discutono in dettaglio le ragioni fisiche che sono alla base del procedimento di taglio. Nella Sezione 2 si mostra che la correzione dovuta al moto del nucleo si annulla identicamente entro il presente schema di approssimazione di minimo ordine. Nella Sezione 3 viene trattata la parte radiale delle funzioni d'onda desiderata, la sua riduzione in unità atomiche, l'equazione differenziale ordinaria di secondo ordine che essa soddisfa, il suo sviluppo in serie di McLaurin e le sue caratteristiche, specialmente il suo comportamento asintotico. Nella Sezione 4 si descrive l'integrazione numerica della detta equazione radiale d'onda per 27 coppie di valori dell'energia e del numero quantico del momento angolare orbitale, usando un ordinatore IBM 650. Tutte le funzioni d'onda si sono ottenute entro un intervallo di almeno 8 unità atomiche. Infine, nella Sezione 5 si esamina la rinormalizzazione delle curve risultanti dall'ampiezza unitaria all'infinito. Si sviluppano e si studiano dettagliatamente due metodi molto eleganti. Col primo procedimento, l'ampiezza all'infinito e l'angolo di fase sono dati in modo rigoroso da alcuni integrali che sono direttamente calcolabili. Nel secondo metodo, effettivamente adottato, l'idea fondamentale consiste nell'introdurre la trasformazione di Madelung che porta ad una equazione differenziale non lineare per l'ampiezza locale della funzione d'onda radiale. Calcolando uno sviluppo in serie asintotico di questa ampiezza locale diviene possibile, in linea di principio, di calcolare la funzione d'onda normalizzata partendo dall'infinito giù sino ad una certa ascissa minima indicata dal limite di precisione desiderato. Poi la curva corrispondente da normalizzare può essere accordata con quella rinormalizzata. Si mostra tuttavia come l'intera procedura sia enormemente semplificata eseguendo le operazioni di raccordo ad uno zero della funzione d'onda radiale oscillatoria.

IL NUOVO CIMENTO Vol. XIX, N. 4 16 Febbraio 1961

Flow Properties of Superfluid Systems of Fermions (*).

A. E. Glassgold

Lawrence Radiation Laboratory, University of California - Berkeley, Cal.

A. M. Sessler (**)

The Ohio State University - Columbus, Ohio

(ricevuto il 14 Ottobre 1960)

Summary. — The nonspherically symmetric solutions to the Bardeen-Cooper-Schrieffer theory are given a physical interpretation in terms of an anisotropic fluid model. These solution have been used previously to predict a phase transition in liquid ^{3}He by Emery and Sessler and by Brueckner, Soda, Anderson and Morel. An investigation of the flow properties of such systems is made that involves the calculation of the effective mass for flow in a straight channel and the moment of inertia of a cylindrical container of the liquid. The angular dependent energy gap characteristic of this type of theory leads to an effective mass for flow that depends on the angle between the axis of symmetry of the fluid and the direction of flow. The effective mass for flow vanishes as the absolute temperature tends to zero, although not as rapidly as for a spherically symmetric gap. The moment of inertia, when the symmetry direction for the fluid and the rotation axis are the same, is simply related to the mass for flow.

1. – Introduction.

The work of Bardeen, Cooper and Schrieffer (BCS) provides a remarkably successful solution to the problem of superconductivity (1). The basic feature in their approach is the strong correlation between conduction electrons

(*) Supported in part by the U.S. Atomic Energy Commission, and in part by the National Science Foundation.

(**) Work performed while a visitor at the Lawrence Radiation Laboratory.

(1) J. Bardeen, L. N. Cooper and J. R. Schrieffer: *Phys. Rev.*, **108**, 1175 (1957).

with equal and opposite momentum and spin. This type of correlation probably plays an essential role in other many-fermion systems. For example, VAN HOVE and EMERY have shown how the usual perturbation theory for an imperfect Fermi gas breaks down under just those conditions when the BCS approach is valid [2].

Direct extensions of the BCS theory have already been made to finite nuclei [3], infinite nuclear matter, and liquid ^{3}He [4,5]. Of special interest is the prediction that liquid ^{3}He undergoes a phase transition at very low temperatures to a highly correlated phase related to the phase change observed for superconductors [6,7]. The predicted transition temperature is of the order of 0.08 °K, but so far no anomalous effects have been observed in this temperature range [8].

The theoretical description of this phase transition differs from that for the electrons in a superconductor in the following important respect. If the Fermi surface in a metal is considered to be spherically symmetric, then the correlation function in the original BCS theory is spherically symmetric. For liquid ^{3}He, on the other hand, the correlation function is not thought to be spherically symmetric. (This is a direct consequence of the fact that the interaction at the Fermi surface for two helium atoms in a relative S state is repulsive.) The possible existence of such solutions in the BCS theory was first noted by ANDERSON [9]. The anisotropic correlations contained in these solutions raise interesting questions of interpretation, particularly for liquid ^{3}He, where there is no long-range order.

It is the purpose of this paper to discuss qualitatively the physical significance of these anisotropic solutions in the BCS theory. We often consider liquid ^{3}He as a specific example, although much of the discussion is more general. The interpretation is mainly given in terms of two quantities, the *effective mass for flow* through a straight channel, and the *moment of inertia*

[2] L. VAN HOVE: *Physica*, **25**, 849 (1959); V. J. EMERY: *Reaction matrix singularities and the energy gap in an infinite system of fermions*, Lawrence Radiation Laboratory Report UCRL-9076, (February 8, 1960) (Submitted for publication to Nuclea Physics).

[3] S. T. BELYAEV: *Kgl. Danske Videnskab. Selskab, Mat.-fys. Medd.*, **31**, No. 11 (1959).

[4] L. N. COOPER, R. L. MILLS and A. M. SESSLER: *Phys. Rev.*, **114**, 1377 (1959).

[5] N. N. BOGOLJUBOV, V. V. TOLMACHEV and D. V. SHIRKOV: *A New Method in the Theory of Superconductivity* (New York, 1959),

[6] V. J. EMERY and A. M. SESSLER: *Phys. Rev.*, **119**, 43 (1960).

[7] K. A. BRUECKNER, T. SODA, P. W. ANDERSON and P. MOREL: *Phys. Rev.*, **118**, 1442 (1960).

[8] D. F. BREWER, J. G. DAUNT and A. K. SREEDHAR: *Phys. Rev.*, **115**, 836 (1959). A. C. ANDERSON, H. R. HART Jr. and J. C. WHEATLEY: *Phys. Rev. Lett.*, **5**, 133 (1960).

[9] P. W. ANDERSON: *Phys. Rev.*, **112**, 1900 (1958).

for the rotation of a cylindrical container of the fluid. These quantities determine the ability of the fluid to transport linear and angular momentum.

The outline of the remainder of this communication is as follows: Bogoljubov's « quasi-particle » form of the BCS theory is first reviewed in Section 2. The physical interpretation of the theory in terms of an anisotropic fluid is also given in this section. In Section 3 the general formulae for the inertial parameters are reviewed, and in Sections 4 and 5 the effective masses for flow and rotation are evaluated.

2. – Quasi-particle theory of superfluid fermion systems.

BOGOLJUBOV has emphasized the quasi-particle nature of the BCS theory ([5]). By a quasi-particle approximation, we mean that the actual Hamiltonian for this problem is truncated and transformed into the form

$$H_0 = E_0 + \sum_{\boldsymbol{k}} E(\boldsymbol{k})(\alpha_{\boldsymbol{k}}^{\dagger}\alpha_{\boldsymbol{k}} + \beta_{\boldsymbol{k}}^{\dagger}\beta_{\boldsymbol{k}}) \,. \tag{2.1}$$

The operators $\alpha_{\boldsymbol{k}}^{\dagger}$ and $\beta_{\boldsymbol{k}}^{\dagger}$ ($\alpha_{\boldsymbol{k}}$ and $\beta_{\boldsymbol{k}}$) create (destroy) the excitations of the many-particle system. These excitations have definite energy $E(\boldsymbol{k})$ and momentum $\boldsymbol{k}$. The quasi-particle operators obey the same anti-commutation rules as the corresponding operators for the actual particles making up the system. (In order to avoid introducing a spin label, we use two sets of quasi-particle operators.) The linear transformation between particle operators and quasi-particle operators is

$$\begin{cases} \alpha_{\boldsymbol{k}} = u(\boldsymbol{k})a_{\boldsymbol{k}_+} - v(\boldsymbol{k})a_{-\boldsymbol{k}_-}^{\dagger} \\ \alpha_{\boldsymbol{k}} = u(\boldsymbol{k})a_{-\boldsymbol{k}_-} + v(\boldsymbol{k})a_{\boldsymbol{k}_+}^{\dagger} \end{cases} \tag{2.2}$$

or

$$\begin{cases} a_{\boldsymbol{k}_+} = u(\boldsymbol{k})^*\alpha_{\boldsymbol{k}} + v(\boldsymbol{k})\beta_{\boldsymbol{k}}^{\dagger} \,, \\ a_{\boldsymbol{k}_-} = u(\boldsymbol{k})^*\beta_{-\boldsymbol{k}} - v(\boldsymbol{k})\alpha_{-\boldsymbol{k}}^{\dagger} \,. \end{cases} \tag{2.2a}$$

The operators $a_{\boldsymbol{k}\sigma}^{\dagger}$ ($a_{\boldsymbol{k}\sigma}$) create free-particle states of momentum $\boldsymbol{k}$ and « spin » projection $\sigma = \pm 1$ ([10]). The anticommutation relations are preserved for

$$|u(\boldsymbol{k})|^2 + |v(\boldsymbol{k})|^2 = 1 \,. \tag{2.3}$$

It has also been assumed that we have $u(-\boldsymbol{k}) = u(\boldsymbol{k})$ and $v(-\boldsymbol{k}) = v(\boldsymbol{k})$.

([10]) The asterisks in eq. (2.2), as well as elsewhere in this paper, stand for « complex conjugation ».

According to eq. (2.3) we may write the two complex functions as

$$\begin{cases} u(\boldsymbol{k}) = \cos\chi(\boldsymbol{k}) \exp[i\eta(\boldsymbol{k})], \\ v(\boldsymbol{k}) = \sin\chi(\boldsymbol{k}) \exp[i\zeta(\boldsymbol{k})]. \end{cases} \tag{2.4}$$

It can be shown that all physical observables depend only on the difference in phase,

$$\varphi(\boldsymbol{k}) = \zeta(\boldsymbol{k}) - \eta(\boldsymbol{k}). \tag{2.5}$$

Hence the two real functions, $\chi(\boldsymbol{k})$ and $\varphi(\boldsymbol{k})$, characterize the quasi-particle transformation. At absolute zero, BOGOLJUBOV determined the transformation in the following way. The Hamiltonian of the system is written in the new representation with all creation operators to the left. No quadrilinear terms are retained and the resulting *truncated* Hamiltonian is diagonalized, *i.e.* forced to have the form of eq. (2.1.) This procedure is equivalent to the BCS variational calculation of the ground-state energy. At finite temperatures, the thermodynamic potential is minimized instead (as discussed, for example, in ref. [6]). As a result, the theory is essentially determined by the following coupled equations:

$$C(\boldsymbol{k}) = -\tfrac{1}{2}\sum_{\boldsymbol{k}'} (\boldsymbol{k}, -\boldsymbol{k}|v|\boldsymbol{k}', -\boldsymbol{k}') \frac{C(\boldsymbol{k}')}{E(\boldsymbol{k}')} \operatorname{tgh}\tfrac{1}{2}\beta E(\boldsymbol{k}'), \tag{2.6}$$

$$\xi(\boldsymbol{k}) = [\varepsilon(\boldsymbol{k}) - \mu] + \sum_{\boldsymbol{k}'} (\boldsymbol{k}, \boldsymbol{k}'|\bar{v}|\boldsymbol{k}, \boldsymbol{k}')\{f(\boldsymbol{k}') + [1 - 2f(\boldsymbol{k}')]|v(\boldsymbol{k}')|^2\}. \tag{2.7}$$

The function C is defined as

$$C(\boldsymbol{k}) = \sum_{\boldsymbol{k}'} (\boldsymbol{k}, -\boldsymbol{k}|v|\boldsymbol{k}', -\boldsymbol{k}') u^*(\boldsymbol{k}') v(\boldsymbol{k}')[1 - 2f(\boldsymbol{k}')], \tag{2.8}$$

where

$$E(\boldsymbol{k}) = [\xi^2(\boldsymbol{k}) + |C(\boldsymbol{k})|^2]^{\frac{1}{2}} \tag{2.9}$$

and

$$f(\boldsymbol{k}) = \frac{1}{\exp[\beta E(\boldsymbol{k})] + 1}. \tag{2.10}$$

The symbol μ stands for the chemical potential and $\varepsilon(k)$ for the unperturbed single-particle energy. For a spherically symmetric Fermi surface ε depends only on the magnitude $k = |\boldsymbol{k}|$. The matrix elements of the two-body potential are $(\boldsymbol{k}_1\boldsymbol{k}_2|v|\boldsymbol{k}_1'\boldsymbol{k}_2')$; the forward scattering of the quasiparticles, which

appears in the expression for their energy in eq. (2.7), is

$$(2.11)\quad (\boldsymbol{k}, \boldsymbol{k}'|\bar{v}|\boldsymbol{k}, \boldsymbol{k}') = (\boldsymbol{k}, \boldsymbol{k}'|v|\boldsymbol{k}, \boldsymbol{k}') - (\boldsymbol{k}, \boldsymbol{k}'|v|\boldsymbol{k}', \boldsymbol{k}) + (\boldsymbol{k}, -\boldsymbol{k}'|v|\boldsymbol{k}, -\boldsymbol{k}') .$$

We also note

$$(2.12)\quad C(\boldsymbol{k}) = |C(\boldsymbol{k})| \exp[i\varphi(\boldsymbol{k})] ,$$

where $\varphi(\boldsymbol{k})$ was defined in eq. (2.5), and

$$(2.13)\quad \operatorname{tg} 2\chi(\boldsymbol{k}) = -\frac{|C(\boldsymbol{k})}{\xi(\boldsymbol{k})} .$$

In this brief résumé of the theory, we have indicated explicitly the possible dependence of the properties of an excitation on its *vector* momentum, in particular on its direction measured with respect to an arbitrary axis $\hat{\boldsymbol{n}}$ henceforth called the « quantization » axis. The original BCS theory of superconductivity for a spherically-symmetric Fermi surface corresponds to the special case of isotropic properties. The possibility of this anisotropy stems directly from the lack of invariance of the *truncated* Hamiltonian under an arbitrary rotation, which in turn arises from the direction dependence of the excitation energies in eq. (2.1). This absence of rotational symmetry is associated with the truncation process, since the original many-particle Hamiltonian describing the liquid is certainly invariant under arbitrary rotations. (It should be noted that the quasi-particle transformation of the original Hamiltonian leads to a new Hamiltonian that is still rotation-invariant. This is true even for the angular-dependent solutions, since eq. (2.3), the requirement that the transformation be canonical, is satisfied.)

Despite the fact that the model Hamiltonian is not invariant under arbitrary rotations, there are physical situations to which the solutions correspond. For example, at absolute zero, the ground state corresponds to a fluid with a preferred direction common to the whole sample and determined by the walls of the container. In this case, the arbitrarily small interactions with the walls (which are not usually included in the original rotationally invariant Hamiltonian) play a crucial role just as in the formation of a crystal. Other cases in which the walls serve to establish preferred directions are quasi-equilibrium situations corresponding to macroscopic fluid flow, discussed more fully in the next sections.

To arrive at a better understanding of the quasi-particle model with angular-dependent solutions, we recall that the quantity $C(\boldsymbol{k})$ determines the pair-correlation function. The pair-correlation function in this type of theory describes *short-range* order, with a correlation length of order $\beta_c \hbar v_F$ (where v_F is the Fermi velocity and β_c^{-1} is the transition temperature). In addition, the

particle density is uniform and isotropic, whereas the correlation function is angular dependent. In other words, we are describing here an *anisotropic liquid*, as defined by LANDAU and LIFSHITZ [11].

The correlation length in the BCS theory is rather large compared with atomic spacings. For example, for ^{3}He, for which the transition temperature is predicted to be of the order of 0.08 °K, the correlation length is about 200 Å. For equilibrium at a non-zero temperature, this implies the formation of a loose domain structure with a domain size no smaller than the correlation length. The existence of a domain structure for this system was suggested by BRUECKNER *et al.* [7]. When the pair-correlation function is anisotropic, each domain has a preferred axis and, in first approximation, these domains are randomly oriented.

The existence of domains is inferred from the following energetic considerations. Particles in the liquid interact strongly only if they are within a correlation length of one another. Therefore the division of a domain in two has associated with it an increase in the total energy of the system which is proportional to the correlation length times the surface area in contact between the new domains. Thus a *negligible* change in the total energy of the sample is required for the sample to break up into a large number of domains. At a non-zero temperature the number of domains into which the fluid is subdivided is determined by the condition that the formation energy of a domain is of the order of kT. As a consequence, at absolute zero, there is just a single domain, as was previously remarked. On the other hand, as the transition temperature is approached from below, the number of domains increases rapidly, since the correlation energy approaches zero. For quasi-equilibrium situations corresponding to fluid flow, these energetic considerations must be extended; this is done in the following sections.

3. – General formulae for the inertial properties of a superfluid.

We now discuss the superfluid properties of the system in a quantitative way, using the effective masses for uniform translation and rotation. Our discussion is clearly motivated by Landau's discussion of the superfluidity of liquid He II [12]. For the special case of spherically symmetric solutions,

[11] L. D. LANDAU and E. M. LIFSHITZ: *Statistical Physics* (London, 1958), paragraph 126, p. 412 et seq. Professor W. D. KNIGHT has kindly informed us of some recent observations on anisotropic-fluid behavior in the melting of metals: *Ann. Phys.*, 8, 173 (1959). These authors find that the short-range order in metals is often preserved in the transition to the liquid phase.

[12] L. D. LANDAU: *Journ. Phys.* (*USSR*), **5**, 71 (1941).

BARDEEN ([13]) and KHALATNIKOV and ABRIKOSOV ([14]) have already discussed the relation between the BCS theory and the two-fluid model. These authors have calculated the density of normal electrons, which is simply proportional to our effective mass for flow. In this section we review the general statistical formulae for the inertial parameters. The explicit calculation of the effective mass for flow and the moment of inertia is discussed separately in succeeding sections.

3·1. *Effective mass for flow.* – We consider the uniform flow of the fluid down an infinite channel. If $\boldsymbol{v}$ is the mean drift velocity of the excitations and if $\boldsymbol{P}$ is the mean total momentum per unit volume, then the effective mass for flow is defined by the equation

$$\langle \boldsymbol{P} \rangle = M_f(\boldsymbol{v})\boldsymbol{v} \,. \tag{3.1}$$

The velocity $\boldsymbol{v}$ is, by definition, the velocity (with respect to the laboratory system) of the reference frame in which the quasi-particle distribution function is that for a fluid at rest, *i.e.* eq. (2.10) for this problem. Unless stated otherwise, the effective mass for flow is that obtained in the limit of zero velocity.

$$M_f(0) = \left. \frac{\partial \boldsymbol{P}(\boldsymbol{v})}{\partial \boldsymbol{v}} \right|_{\boldsymbol{v}=0} . \tag{3.2}$$

We conveniently define a superfluid as a system with $M_f(0) < nm$, where n is the density and m the particle mass. This characterization of a superfluid emphasizes the contrast with a classical fluid with respect to a liquid's ability to transfer momentum. We note that Landau's normal density is just $\varrho_n = M_f(0)/m$.

According to the general principles of statistical mechanics, the mean momentum per unit volume is

$$\langle \boldsymbol{P} \rangle = \frac{\mathrm{Tr}\left[\boldsymbol{P} \exp\left[-\beta(H - \mu N - \boldsymbol{P}\cdot\boldsymbol{v})\right]\right]}{\mathrm{Tr}\left[\exp\left[-\beta(H - \mu N - \boldsymbol{P}\cdot\boldsymbol{v})\right]\right]} . \tag{3.3}$$

The symbol Tr[...] indicates the trace operation appropriate to the grand canonical ensemble, and H, N, and $\boldsymbol{P}$ are the operators for the Hamiltonian, the number of particles, and momentum density, respectively. Carrying out the differentiation indicated in eq. (3.2), using the fact that $\boldsymbol{P}$ commutes with $H - \mu N$, and that $\langle \boldsymbol{P} \rangle = 0$ for $\boldsymbol{v} = 0$, we obtain the formula for

([13]) J. BARDEEN: *Phys. Rev. Lett.*, **1**, 399 (1958).
([14]) I. M. KHALATNIKOV and A. A. ABRIKOSOV: *Adv. Phys.*, **8**, 45 (1959).

the effective mass for flow:

$$M_f(0) = \beta\langle(\boldsymbol{P}\cdot\hat{\boldsymbol{v}})^2\rangle \,, \tag{3.4}$$

where $\hat{\boldsymbol{v}} = \boldsymbol{v}/v$. The statistical average is carried out in the rest frame ($\boldsymbol{v} = 0$). We emphasize once more that this is just Landau's definition of the normal density.

3·2. *Momenta of inertia.* – We now consider a cylindrical container of the fluid rotating with angular velocity ω about uts axis of symmetry $\hat{\boldsymbol{\omega}}$. If $\boldsymbol{J}$ is the operator for the total angular momentum of the system, then the moment of inertia is defined by the relation

$$\langle\boldsymbol{J}\cdot\hat{\boldsymbol{\omega}}\rangle = I(\omega)\omega \,. \tag{3.5}$$

We discuss only the limiting value

$$I(0) = \frac{\partial}{\partial\omega}\langle\boldsymbol{J}\cdot\hat{\boldsymbol{\omega}}\rangle\Big|_{\omega=0} \,. \tag{3.6}$$

By applying the same statistical equilibrium discussion used above for M_f, the formula for the moment of inertia is found to be

$$I(0) = \beta\langle(\boldsymbol{J}\cdot\hat{\boldsymbol{\omega}})^2\rangle \,. \tag{3.7}$$

Again, the statistical average is carried out. This result is due to BLATT, BUTLER, and SCHAFROTH ([15]). We note that this derivation takes for granted that $\langle\boldsymbol{J}\rangle = 0$ for $\omega = 0$. ANDERSON and MOREL have recently raised questions about this particular point which we shall comment on in our discussion of the moment of inertia in Section **5** ([16]).

4. – Effective mass for flow.

The above formulae, eq. (3.2) and (3.7), show how $M_f(0)$ and $I(0)$ are related to the statistical average of $(\boldsymbol{P}\cdot\hat{\boldsymbol{v}})^2$ and $(\boldsymbol{J}\cdot\hat{\boldsymbol{\omega}})^2$. The evaluation of these averages is carried out in the quasi-particle representation. This is precisely the procedure followed in a recent discussion of the moment of inertia for the low-density theory of liquid ^{4}He ([17]).

([15]) J. B. BLATT, S. T. BUTLER and M. S. SCHAFROTH: *Phys. Rev.*, **100**, 481 (1955)
([16]) P. W. ANDERSON and P. MOREL: *Phys. Rev. Lett.*, **5**, 136 (1960).
([17]) A. E. GLASSGOLD, A. N. KAUFMAN and K. M. WATSON: *Phys. Rev.* **120**, 660. (1960).

In order to evaluate eq. (3.4) for $M_f(0)$, we need the expression for the momentum operator in the quasi-particle representation

$$\boldsymbol{P} = \sum_{\boldsymbol{k}} \boldsymbol{k}(\alpha_{\boldsymbol{k}}^{\dagger}\alpha_{\boldsymbol{k}} - \beta_{\boldsymbol{k}}^{\dagger}\beta_{\boldsymbol{k}}) \,. \tag{4.1}$$

We next write the average of $(\boldsymbol{P}\cdot\hat{\boldsymbol{v}})^2$ as

$$\begin{aligned}\langle(\boldsymbol{P}\cdot\hat{\boldsymbol{v}})^2\rangle = \sum_{\boldsymbol{k}\neq\boldsymbol{k}'} (\boldsymbol{k}\cdot\hat{\boldsymbol{v}})(\boldsymbol{k}'\cdot\hat{\boldsymbol{v}})[\langle\alpha_{\boldsymbol{k}}^{\dagger}\alpha_{\boldsymbol{k}}\rangle - \langle\beta_{\boldsymbol{k}}^{\dagger}\beta_{\boldsymbol{k}}\rangle][\langle\alpha_{\boldsymbol{k}'}^{\dagger}\alpha_{\boldsymbol{k}'}\rangle - \langle\beta_{\boldsymbol{k}'}^{\dagger}\beta_{\boldsymbol{k}'}\rangle] + \\ + \sum_{\boldsymbol{k}} (\boldsymbol{k}\cdot\hat{\boldsymbol{v}})^2[\langle\alpha_{\boldsymbol{k}}^{\dagger}\alpha_{\boldsymbol{k}}\alpha_{\boldsymbol{k}}^{\dagger}\alpha_{\boldsymbol{k}}\rangle + \langle\beta_{\boldsymbol{k}}^{\dagger}\beta_{\boldsymbol{k}}\beta_{\boldsymbol{k}}^{\dagger}\beta_{\boldsymbol{k}}\rangle - 2\langle\alpha_{\boldsymbol{k}}^{\dagger}\alpha_{\boldsymbol{k}}\rangle\langle\beta_{\boldsymbol{k}}^{\dagger}\beta_{\boldsymbol{k}}\rangle] \,.\end{aligned} \tag{4.2}$$

Since the statistical averages of $\alpha_{\boldsymbol{k}}^{\dagger}\alpha_{\boldsymbol{k}}$, $\beta_{\boldsymbol{k}}^{\dagger}\beta_{\boldsymbol{k}}$, and their squares are *all* just $f(\boldsymbol{k})$, the first line of eq. (4.2) is zero and the second line leads to the following equation for $M_f(0)$:

$$M_f(0) = 2\beta \sum_{\boldsymbol{k}} (\boldsymbol{k}\cdot\hat{\boldsymbol{v}})^2 f(\boldsymbol{k})[1 - f(\boldsymbol{k})] \,. \tag{4.3}$$

As remarked previously, this is essentially Landau's expression for the normal density ([12]). This formula shows explicitly how the excitation spectrum, through the statistical factor $f(k)$ determines the effective mass for flow.

As a first simple example, we consider the spherically symmetric energy gap $C(\boldsymbol{k}) = \Delta$, corresponding to the « excitation spectrum »

$$E(k) = \left[\left(\frac{k^2 - k_F^2}{2m}\right)^2 + \Delta^2\right]^{\frac{1}{2}}. \tag{4.4}$$

Eq. (4.3) becomes

$$\frac{M_f(0)}{nm} = 2\beta \int_{\Delta}^{\infty} \mathrm{d}E \, \frac{E \exp[\beta E]}{[E^2 - \Delta^2]^{\frac{1}{2}}(\exp[\beta E] + 1)^2} \,. \tag{4.5}$$

The most important contributions of the integrand come from the neighborhood of the Fermi surface where $E = \Delta$. It is convenient to rewrite this equation as

$$\frac{M_f(0)}{nm} = 2\int_0^{\infty} \mathrm{d}x \, \frac{x + \lambda}{[x^2 + 2\lambda x]^{\frac{1}{2}}} \, \frac{\exp[x + \lambda]}{(\exp[x + \lambda] + 1)^2} \,, \tag{4.6}$$

where $\lambda = \beta\Delta(\beta)$. It is now easy to establish the following asymptotic limits of this integral, corresponding to the limits $T \to 0$ $(\Delta \to \Delta_0)$ and $T \to T_c$

$(\Delta \to 0)$:

$$\frac{M_f}{nm} = \begin{cases} (2\pi\lambda)^{\frac{1}{2}} \exp[-\lambda], & \lambda \to \infty (T \to 0,\ \Delta \to \Delta_0)\,, \quad (4.7) \\ 1, & \lambda \to 0 (T \to T_c,\ \Delta \to 0)\,. \quad (4.8) \end{cases}$$

A more detailed discussion of M_f at intermediate temperature is given by KHALATNIKOV and ABRIKOSOV [14]. As T decreases from T_c, M_f decreases (linearly at first) to zero, vanishing exponentially as absolute zero is approached. If the energy gap is set equal to zero for all temperatures, the case of the ideal gas is recovered. From eq. (4.8) we see that the effective mass for the flow of an ideal gas is the true mass.

For asymmetric solutions, the angular-dependent factor $(\boldsymbol{k}\cdot\hat{\boldsymbol{v}})^2$ in eq. (4.3) is now important. We introduce the spherical polar co-ordinates (k, θ, φ) for the quasi-particle momentum $\boldsymbol{k}$, with the preferred direction $\hat{\boldsymbol{n}}$ of the domain under consideration as quantization axis, and the angle τ betwen $\hat{\boldsymbol{n}}$ and $\hat{\boldsymbol{v}}$. We assume here that the excitation spectrum has cylindrical symmetry about $\hat{\boldsymbol{n}}$. $E = E(k, \theta)$; and, for simplicity, that $C = C(\theta)$. In this case, eq. (4.5) must be replaced by

$$\frac{M_f(0)}{nm} = 2\beta \int_{-1}^{1} \mathrm{d}(\cos\theta)\, \tfrac{3}{2}(\cos^2\tau\cos^2\theta + \tfrac{1}{2}\sin^2\tau\sin^2\theta) \cdot \int_{|C(\theta)|}^{\infty} \mathrm{d}E\, \frac{E\exp[\beta E]}{[E^2 - |C(\theta)|^2]^{\frac{1}{2}}(\exp[\beta E]+1)^2}\,. \quad (4.9)$$

Current applications to liquid ^{3}He make use of the form

$$C(\boldsymbol{k}) = \Delta_{lm}(\theta)\, Y_{ml}(\theta, \varphi)\,, \quad (4.10)$$

and thus

$$|C(\boldsymbol{k})|^2 = \Delta^2_{ml}(\theta)\, P^2_{lm}(\theta)\,.$$

This function vanishes at several points, and the contributions to the integrand of eq. (4.9) from the neighborhood of these points are the most important ones. As a result, M_f does not vanish as rapidly as $T \to 0$, as it does for a spherically symmetric gap.

We now turn our attention to the question of the orientation of the preferred axis $\hat{\boldsymbol{n}}$ with respect to the flow direction $\hat{\boldsymbol{v}}$ in an actual experiment. Eq. (4.9) may be rewritten

$$\frac{M_f(0)}{nm} = \cos^2\tau\, K_1 + \sin^2\tau\, K_2\,, \quad (4.11)$$

where $(x = \cos\theta)$

$$K_1 = \int_{-1}^{1} \mathrm{d}x\, x^2 F(x)\,, \tag{4.12a}$$

$$K_2 = \frac{1}{2}\int_{-1}^{1} \mathrm{d}x\,(1 - x^2) F(x)\,, \tag{4.12b}$$

and

$$F(x) = 3\beta \int_{|C(x)|}^{\infty} \mathrm{d}E\, \frac{E}{[E^2 - |C(x)|^2]^{\frac{1}{2}}} \frac{\exp[\beta E]}{(\exp[\beta E] + 1)^2}\,. \tag{4.12c}$$

The mass for flow, and therefore the total energy, is a minimum for $\tau = 0$ and π for $\tau = \pi/2$, depending on whether $K_2 > K_1$ or $K_1 > K_2$ holds.

In the special case, $K_1 = K_2$, the effective mass is independent of τ and all directions of the preferred axes are equally probable, energetically. In this improbable case $(K_1 = K_2)$, the fluid would maintain its domain structure although the orientation of the various domain axes would be essentially uncorrelated. In the more likely situation, with $K_1 \neq K_2$, the preferred axes and the flow direction are, on the average, either perpendicular $(K_2 < K_1)$ or parallel $(K_1 < K_2)$. (There is no difference between $\tau = 0$ and $\tau = \pi$.) There is, of course, a statistical distribution of the directions about these average values. Which of the two directions is most probable depends on the relative magnitude of K_1 and K_2. A general conclusion on this point depends on obtaining more complete solutions to the basic equation (eq. (2.6) and (2.7)).

This question can, of course, be discussed in the approximation of equation (4.10) ([6,7]). As $T \to 0$, the different energy gaps Δ_{lm} for the various m values are generally distinct, and the lowest energy is obtained with the largest energy gap. The integrals K_1 and K_2 can then be evaluated for this value of m and the parallel and perpendicular directions distinguished. For example, the solution that gives the lowest energy for $l = 1$ is $C = \Delta_{11} Y_{11}$, and a simple calculations gives $K_1 > K_2$. This means that the preferred direction in the fluid is perpendicular to the flow direction in this case. As the temperature is increased, the fluid breaks up into domains, and there are Boltzmann distributions both for the domain directions and for the various solutions characterized by the different m values.

5. – Moment of inertia.

Before evaluating eq. (3.7) for the moment of inertia, we recall that, in the derivation of this equation, it is assumed that $(H - \mu N)$ and $\boldsymbol{J}\cdot\hat{\boldsymbol{\omega}}$ commute. Since $\boldsymbol{J}\cdot\hat{\boldsymbol{\omega}}$ is the projection of the total angular momentum along

the axis of rotation, it follows that the operator $H - \mu N$ must be invariant under rotations about $\boldsymbol{\omega}$. This condition is fulfilled for quasi-particles whose excitation energy does not depend on φ, where k, θ and φ are the spherical co-ordinates of the quasi-particle momentum $\boldsymbol{k}$ with $\boldsymbol{\omega}$ as polar axis. This property is possessed by the approximate solutions to eq. (2.6) given in eq. (4.10), which are valid just below the transition temperature. There is a wider class of functions that vary as $\exp[im\varphi]$ and which, therefore, correspond to an axially symmetric model Hamiltonian. Since little is known about the general properties of the solutions to eq. (2.6) and (2.7), however, we cannot exclude even more general solutions. In any case, the calculation of the moment of inertia in this section is confined to axially symmetric solutions for which the general formulae, eq. (3.7), is valid. This corresponds to the physical situation in which there is a single preferred direction in the fluid parallel to the axis of rotation.

We now evaluate eq. (3.7) for the moment of inertia following the method recently used for the low-density theory of liquid ^{4}He ([17]). The operator for the projection of the total angular momentum along the rotation axis is, in the notation of second quantization,

$$\boldsymbol{J}\cdot\hat{\boldsymbol{\omega}} = \sum_{\boldsymbol{k}\boldsymbol{k}'}\sum_{\sigma} L_{\boldsymbol{k}\boldsymbol{k}'} a^{\dagger}_{\boldsymbol{k}\sigma} a_{\boldsymbol{k}'\sigma} \,. \tag{5.1}$$

We ignore the negligible contribution of the intrinsic spin of the particles and the effect recently discussed by ANDERSON and MOREL, which is similar to an intrinsic angular momentum of one particle about another. The symbol L stands for the projection of the orbital angular momentum of one particle along $\hat{\boldsymbol{n}} = \hat{\boldsymbol{\omega}}$. Its matrix elements in momentum space satisfy the relations

$$L_{\boldsymbol{k}\boldsymbol{k}} = L^{*}_{\boldsymbol{k}'\boldsymbol{k}} \,, \tag{5.2a}$$

$$L_{\boldsymbol{k}\boldsymbol{k}'} = L_{-\boldsymbol{k}-\boldsymbol{k}'} \,, \tag{5.2b}$$

$$L_{\boldsymbol{k}\boldsymbol{k}'} = -\,L^{*}_{\boldsymbol{k}\boldsymbol{k}'} \,, \tag{5.2c}$$

and

$$L_{\boldsymbol{k}\boldsymbol{k}'} = L_{\boldsymbol{k}\boldsymbol{k}'}\,\delta_{\boldsymbol{k}\boldsymbol{k}'}\,\delta_{\boldsymbol{k}\cdot\hat{\boldsymbol{n}},\boldsymbol{k}'\cdot\hat{\boldsymbol{n}}} \,, \tag{5.3a}$$

$$L_{\boldsymbol{k}\boldsymbol{k}} = 0 \,. \tag{5.3b}$$

Eq. (5.2a), (5.2b), and (5.2c) follow from the requirements of hermiticity, inversion invariance, and time-reversal invariance. The last relation, eq. (5.3), expresses the property of L as the generator of infinitesimal rotations about $\hat{\boldsymbol{n}}$. Upon transformation to the quasi-particle representation by direct substi-

tution of eq. (2.1), eq. (5.1) becomes

$$\boldsymbol{J}\cdot\hat{\boldsymbol{n}} = \sum_{\boldsymbol{k}\boldsymbol{k}'} L_{\boldsymbol{k}\boldsymbol{k}'}[u(\boldsymbol{k})u^*(\boldsymbol{k}') + v(\boldsymbol{k})v^*(\boldsymbol{k}')](\alpha^\dagger_{\boldsymbol{k}}\alpha_{\boldsymbol{k}'} + \beta^\dagger_{\boldsymbol{k}}\beta_{\boldsymbol{k}'}) \,. \tag{5.4}$$

We note that $\boldsymbol{J}\cdot\hat{\boldsymbol{n}}$ involves only « diagonal operators », *i.e.*, operators involving the same number of creation and destruction operators. That no other operators occur (such as products of two creation or two destruction operators) is a direct consequence of the axial symmetry of the quasi-particle transformation. Another consequence of this symmetry is

$$\boldsymbol{J}\cdot\hat{\boldsymbol{n}}\,|0\rangle = 0 \,,$$

where $|0\rangle$ is the ground-state or quasi-particle vacuum. Furthermore, the expectation value or the ensemble average of $\boldsymbol{J}\cdot\hat{\boldsymbol{n}}$ is *always* zero, since it involves the terms in eq. (5.4) for which $\boldsymbol{k} = \boldsymbol{k}'$ and $L_{\boldsymbol{k}\boldsymbol{k}'} = 0$.

The square of $\boldsymbol{J}\cdot\hat{\boldsymbol{n}}$ which appears in eq. (3.7) is

$$(\boldsymbol{J}\cdot\hat{\boldsymbol{n}})^2 = \sum_{\boldsymbol{k}_1\boldsymbol{k}_1'}\sum_{\boldsymbol{k}_2\boldsymbol{k}_2'} L_{\boldsymbol{k}_1\boldsymbol{k}_1'}L_{\boldsymbol{k}_2\boldsymbol{k}_2'}[u(\boldsymbol{k}_1)u^*(\boldsymbol{k}_1') + v(\boldsymbol{k}_1)v^*(\boldsymbol{k}_1')]\cdot$$

$$\cdot[u(\boldsymbol{k}_2)u^*(\boldsymbol{k}_2') + v(\boldsymbol{k}_2)v^*(\boldsymbol{k}_2')](\alpha^\dagger_{\boldsymbol{k}_1}\alpha_{\boldsymbol{k}_1'} + \beta^\dagger_{\boldsymbol{k}_1}\beta_{\boldsymbol{k}_1'})(\alpha^\dagger_{\boldsymbol{k}_2}\alpha_{\boldsymbol{k}_2'} + \beta^\dagger_{\boldsymbol{k}_2}\beta_{\boldsymbol{k}_2'}) \,.$$

In the averaging of this expression, the terms $\boldsymbol{k}_1 = \boldsymbol{k}_1'$ and $\boldsymbol{k}_2 = \boldsymbol{k}_2'$ do not occur because the corresponding matrix elements vanish. The only non-zero terms are those involving four α or four β operators.

$$\langle(\boldsymbol{J}\cdot\hat{\boldsymbol{n}})^2\rangle = \sum_{\boldsymbol{k}\boldsymbol{k}'} L_{\boldsymbol{k}\boldsymbol{k}'}L_{\boldsymbol{k}'\boldsymbol{k}}\,|u(\boldsymbol{k})u^*(\boldsymbol{k}') + v(\boldsymbol{k})v^*(\boldsymbol{k}')\,|^2\cdot \tag{5.5}$$

$$\cdot[\langle\alpha^\dagger_{\boldsymbol{k}}\alpha_{\boldsymbol{k}}\rangle(1 - \langle\alpha^\dagger_{\boldsymbol{k}'}\alpha_{\boldsymbol{k}'}\rangle) + \langle\beta^\dagger_{\boldsymbol{k}}\beta_{\boldsymbol{k}}\rangle(1 - \langle\beta^\dagger_{\boldsymbol{k}'}\beta_{\boldsymbol{k}'}\rangle)] \,.$$

According to eq. (5.3), the only non-zero terms in this equation are for $\boldsymbol{k}$ and $\boldsymbol{k}'$ differing only in their azimuthal angles φ and φ'. Since the quasi-particle transformation does not depend on the azimuthal angle, the u's and v's drop out completely (when eq. (2.3) is used) and all the statistical factors are the same:

$$\langle(\boldsymbol{J}\cdot\hat{\boldsymbol{n}})^2\rangle = 2\sum_{\boldsymbol{k}\boldsymbol{k}'} f(\boldsymbol{k})[1 - f(\boldsymbol{k})]L_{\boldsymbol{k}\boldsymbol{k}'}L_{\boldsymbol{k}'\boldsymbol{k}} \,,$$

or, using closure,

$$\langle(\boldsymbol{J}\cdot\hat{\boldsymbol{n}})^2\rangle = 2\sum_{\boldsymbol{k}} f(\boldsymbol{k})[1 - f(\boldsymbol{k})](L^2)_{\boldsymbol{k}\boldsymbol{k}} \,. \tag{5.6}$$

For the diagonal matrix element of L^2 appropriate to a cylindrical container,

we have

$$(L^2)_{kk} = \tfrac{1}{2}(\boldsymbol{k}\times\hat{\boldsymbol{n}})^2\langle x^2 + y^2\rangle ,$$

where

$$\langle x^2 + y^2\rangle = \frac{1}{V}\int \mathrm{d}^3 r(x^2 + y^2) .$$

The momenta of inertia is therefore

$$I(0) = \langle x^2 + y^2\rangle 2\beta \sum_{\boldsymbol{k}} \tfrac{1}{2}(\boldsymbol{k}\times\hat{\boldsymbol{n}})^2 f(\boldsymbol{k})[1 - f(\boldsymbol{k})] . \tag{5.7}$$

For a spherically symmetric gap the angular average of $\frac{1}{2}(\boldsymbol{k}\times\hat{\boldsymbol{n}})^2$ is equal to the angular average of $(\boldsymbol{k}\cdot\hat{\boldsymbol{v}})^2$, which means

$$\frac{I(0)}{I_0} = \frac{M_f(0)}{nm} , \tag{5.8}$$

where I_0 is the rigid-body moment of inertia. For an ideal gas, therefore, we have $I(0) = I_0$.

This result for the spherically symmetric case has been obtained previously by more tedious methods ([18,19]). The statistical approach employed here is more attractive because it emphasizes the role of the energy spectrum of the system. It is particularly easy to apply to quasi-particle models, which encompass a large class of approximations to the many-body problem.

For the asymmetric case $[E = E(k, \theta)]$, eq. (5.7) may be transformed to

$$\frac{I(0)}{I_0} = K_2 , \tag{5.9}$$

where K_2 was defined by eq. (4.12) and (4.13). This result is easily understood by recalling that, for the case considered in this section, the flow velocity is always perpendicular to the quantization axis. Hence we expect that eq. (5.8), originally written for the spherically symmetric case, should now be valid when we use eq. (4.11) for $M_f(0)/nm$ with $\tau = \pi/2$.

It must be emphasized that the results of this paper are based on the quasi-particle approximation and that the interaction between quasi-particles has been ignored. These interactions may be important for the calculation of the moment of inertia ([19]), but the investigation of their effect has not yet been completed. Similarly, the problem of viscosity has not been discussed. However, we do expect the viscosity to vanish at low temperatures in the limit of small flow velocities. This follows from the fact that in this limit only a very limited class of excitations are possible in view of the modified energy

---

([18]) R. D. Amado and K. A. Brueckner: *Phys. Rev.*, **115**, 1778 (1959).

([19]) R. M. Rockmore: *Phys. Rev.*, **116**, 469 (1959), and private communication.

spectrum in the superfluid state. In any case the viscosity should be drastically reduced below the viscosity in the normal fluid which, in the limit $T \to 0$, varies as T^{-2} ([20]).

According to ANDERSON and MOREL ([16]), the most remarkable property of the superfluid phase is its intrinsic angular momentum. They think of the anisotropic pair correlation in terms of small circulating currents which cancel everywhere in the interior of the fluid but lead to a non-vanishing current on the fluid surface. This current is proportional to the surface area, and hence implies a total angular momentum proportional to the volume. This angular momentum is, however, so small as to defy experimental observation. Even at extremely low temperatures, it is always very much less than the angular momentum calculated here. Nevertheless the discussion of ANDERSON and MOREL rasises an important question of principle. The work of this paper does not touch on this point because it is based on a method appropriate only to an infinite system, and hence does not incorporate any surface current phenomena. A rigorous treatment of boundary effects appears to be necessary for an understanding of these effects.

* * *

The authors have been helped by conversations wity numerous colleagues and owe special thanks to Dr. P. W. ANDERSON, Dr. V. J. EMERY and Professor R. L. MILLS for their comments.

([20]) A. A. ABRIKOSOV and I. M. KHALATNIKOV: *Sov. Phys. Uspekhi*, **1**, 68 (1958).

RIASSUNTO (*)

Si dà una interpretazione fisica in termini di un modello di fluido anisotropo alle soluzioni sfericamente asimmetriche della teoria di Bardeen-Cooper-Schrieffer. Queste soluzioni sono state precedentemente usate da EMERY e SESSLER e da BRUECKNER, SODA, ANDERSON e MOREL per predire una transizione di fase nel ^{3}He liquido. Si esegue una ricerca delle caratteristiche di flusso di tali sistemi, che comporta il calcolo della massa effettiva per il flusso in un canale diritto e del momento d'inerzia di un cilindro contenente il liquido. Il gap di energia dipendente dall'angolo caratteristico di questo tipo di teoria porta ad una massa effettiva per il flusso che dipende dall'angolo fra l'asse di simmetria del fluido e la direzione del flusso. La massa effettiva per il flusso si annulla al tendere a zero della temperatura assoluta, anche se non altrettanto rapidamente che per un gap a simmetria sferica. Quando la direzione di simmetria del fluido coincide con l'asse di rotazione, il momento d'inerzia sta in un rapporto semplice con la massa per il flusso.

(*) *Traduzione a cura della Redazione.*

IL NUOVO CIMENTO Vol. XIX, N. 4 16 Febbraio 1961

$\overline{\mathrm{K}}$ Capture Frequency in Hydrogen.

A. A. Kamal

Osmania University - Hyderabad

(ricevuto il 21 Ottobre 1960)

Summary. — From the study of $\overline{\mathrm{K}}$ capture stars in photographic emulsions, the $\overline{\mathrm{K}}$ capture frequency in the hydrogen atom is estimated and the result is compared with the Fermi-Teller theory of the capture of negative mesons in matter. A strong disagreement is found from the expected value. This discrepancy has been attributed to the transfer of the meson to an atom of the CNO group.

1. – Introduction.

The general results of 3 480 $\overline{\mathrm{K}}$-interactions at rest have already been reported ([1,2]). The selection criteria, experimental details and the scanning biases have been thoroughly discussed in these papers and will be omitted in the present one.

2. – The capture of $\overline{\mathrm{K}}$-mesons in matter.

According to the Fermi-Teller theory ([3]), if negative mesons are sufficiently slowed down in a homogeneous chemical mixture, then the probability of capture in an element of atomic number Z is, to a good approximation, proportional to Z itself. This Z dependence is invalidated in emulsions, because the silver bromide crystals have dimensions of the order of thousands of atomic

([1]) K-Collaboration: *Nuovo Cimento*, **13**, 690 (1959).
([2]) K-Collaboration: *Nuovo Cimento*, **14**, 315 (1959).
([3]) E. Fermi and E. Teller: *Phys. Rev.*, **72**, 399 (1947).

diameters and the medium is essentially heterogeneous. But it is possible to estimate capture frequency in the hydrogen of the gelatin. The proportion of captures in gelatin may be estimated from the separation of light and heavy elements. This may be carried out on the basis of the potential barrier effects for particles emerging from the nuclei, and the recoil of the residual nuclei resulting from K nuclear reactions. No distinction is, however, made between protons and α-particles. This, we shall see immediately, has no serious bearing on the experimental results. The separation between light and heavy nuclei is made as follows:

i) Stars with recoils $\leqslant 3$ μm were attributed to heavy elements. It is very improbable that such events will represent light nuclei, because they either break up with very little excitation energy or suffer large recoils.

ii) Stars with a stable prong of length $3\ \mu\text{m} < R < 40\ \mu\text{m}$ have been attributed to the recoils of light nuclei. For heavy nucleus recoils it can be shown, from the conservation of momentum and energy, that the maximum energy carried by the fragment is 1 to 2 MeV, which cannot correspond to a track > 3 μm. The result being true for both single and two nucleon $\overline{\text{K}}$ capture.

iii) Stars with a stable prong of length $40\ \mu\text{m} < R < 180\ \mu\text{m}$ have been attributed to light nuclei. The upper limit of R is imposed by the expected ranges of evaporated α-particles crossing Coulomb's barrier in heavy elements. The evaporation process would result, if some excitation energy had been given away to the nucleons, when the product particles of the reaction leave the nucleus. For the same reason the evaporated protons arising from heavy nuclei are expected to have ranges much larger than 180 μm. Alphas and protons which arise from light nuclei as a result of « break up » processes will fall in this range interval, considering the Coulomb field acting between these particles and the residual nucleus. The contamination due to evaporated protons, which have tunneled through the potential barrier, is expected to be small.

iv) Stars with stable prongs of length $180\ \mu\text{m} < R < 300\ \mu\text{m}$ have been attributed to heavy elements. In this group one should find some contamination of light elements, since the ejected particles from the light nuclei can be given some kinetic energy in the « knock-on » process.

If the star consists of more than one stable prong, then only the shorter prong has been considered. The stars of the type π only, Σ only, $\Sigma+\pi$ only and $\overline{\text{K}}_0$ without recoils, which all represent heavy elements and have not been included in Fig. 1, must also be considered. This number is 672. Allowing for this, the proportion of captures in gelatin is about 43 % of the

total number of captures. In spite of this crude analysis, the results ought to give at least the order of magnitude. It is well known that the analysis of π^- captures in emulsion also suggests the same results.

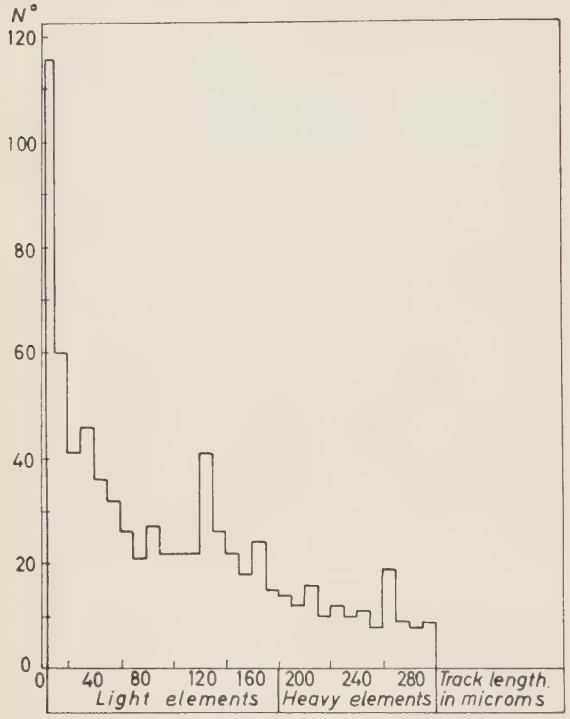

Fig. 1. – Heavy elements.

The captures in hydrogen are readily detected, from the collinearity of tracks of $\Sigma^{\pm}+\pi^{\mp}$. The number of such events is 20 in a total of 3480. Allowing for the neutral particles ($\Sigma^0+\pi^0$ or $\Lambda^0+\pi^0$) observed in $\overline{K}$ captures in hydrogen bubble chambers [4] the proportion is 0.8% of all the stars or 1.8% of captures in gelatin.

The expected capture probability in an element of gelatin is given by $Z_i N_i$ where Z_i = charge of the element, N_i = number of atoms/cm^3

From the known constitution of G-5 emulsions, the expected relative probabilities of captures in gelatin are shown below:

H	C	N	O
0.15	0.43	0.11	0.31

It follows that 15% of the captures in gelatin are expected to happen in hydrogen. We thus conclude that this discrepancy by a factor of 8 is certainly outside the limits of statistical and experimental errors. However, we do not dispute the validity of the Fermi-Teller theory which has been conclusively verified with electronic counters [5]. We are inclined to attribute this discrepancy

[4] Alvares, Bradner, Falk-Variant, Gow, Rosenfeld, Solmitz and Tripp: *Rochester Conference*, 1957.

[5] Stearns: *Rochester Conference*, 1956.

to the diffusion of the hydrogen mesic atom and the subsequent transfer of the $\overline{\text{K}}$-meson to an atom of the CNO group. Thus when the $\overline{\text{K}}$-meson is once captured in a hydrogen atom, it cascades down to the lower orbits. But it can reach the low lying orbits only via optical transitions, the probability of which in the hydrogen mesic atom is relatively small. Meanwhile, the neutral mesic atom will diffuse and collide with atoms of the CNO group, and in such collisions, the transfer of $\overline{\text{K}}$ to an atom of the CNO group, in the presence of a large Coulomb field, is conceivable. This has the obvious effect of lowering the actual proportion of captures in the nuclei of hydrogen.

It may be added that the study of X-rays [6] arising from the meson cascade has shown that while the Fermi-Teller rule of Z dependence is substantiated in chemical compounds such as Al_2O_3 and CaS, very few mesons are captured in lithium in the compounds LiCl or LiF; indicating that the meson may be easily lost from Li to the more highly charged nuclei.

* * *

The author is deeply grateful to Prof. C. F. Powell, F.R.S., for his hospitality at the H. H. Wills Physics Laboratory, University of Bristol.

---

[6] Stearns: *Spectroscopy of mesic atoms* in *Progress in Nuclear Physics*, Vol. 6.

RIASSUNTO (*)

Dallo studio delle stelle di cattura dei $\overline{\text{K}}$ nelle emulsioni fotografiche, si è valutata la frequenza di cattura dei $\overline{\text{K}}$ nell'atomo di idrogeno ed il risultato si è confrontato con la teoria di Fermi-Teller per la cattura di mesoni negativi nella materia. Si trova un forte disaccordo col valore previsto. La discrepanza si è attribuita al trasferimento del mesone ad un atomo del gruppo CNO.

(*) *Traduzione a cura della Redazione.*

IL NUOVO CIMENTO Vol. XIX, N. 4 16 Febbraio 1961

The Population Ratio of the 4.433 MeV and 7.656 MeV States in ^{12}C in the Reaction $^{9}Be(\alpha, n)^{12}C$, and the Parameters of the 7.656 MeV Level.

N. H. Gale and J. B. Garg

The Physical Laboratories - The University, Manchester

(ricevuto il 24 Ottobre 1960)

Summary. — A pulsed beam neutron time-of-flight spectrometer has been used to study the reaction $^{9}Be(\alpha, n)^{12}C^*$ at bombarding energies of 5.53, 5.76 and 5.97 MeV. Angular distributions of neutron groups leading to the ground state and first two excited states of ^{12}C were measured, and the population ratio of the 4.433 and 7.656 MeV levels has been established as 10.7 ± 0.8 at ~ 5.5 MeV. In conjunction with other evidence the measured value of population ratio establishes the alpha particle decay width of the 7.656 MeV level as approximately the Wigner limit, the spin and parity as $0+$, and allows estimates to be made of the probabilities of pair and γ decay of this state.

1. – Introduction.

The recent measurement by Alburger (1) of the intensity ratio of the 7.656 MeV pair line to the 4.433 MeV pair line from the first and second excited states of ^{12}C in the reaction $^{9}Be(\alpha, n)^{12}C$ has made it of some importance to establish exactly the ratio of neutron populations of the two levels in the same reaction. The unusual significance attached to the modes of decay and the level parameters of the 7.656 MeV level in ^{12}C is well known to arise from its importance in the helium fusion process $3\,^{4}He \rightarrow {}^{12}C$, proposed by Öpik (2) as the mechanism of energy generation and element synthesis in red

(1) D. E. Alburger: *Phys. Rev.*, **118**, 235 (1960).
(2) E. J. Öpik: *Proc. Roy. Irish Acad.*, A **54**, 49 (1951).

giant stars. Indeed, the very existence of the 7.656 MeV level was predicted by HOYLE (3) as the result of the assumption that the helium fusion process takes place in the two stages:

$$2\ ^4He \rightarrow\ ^8Be$$

$$^8Be + ^4He \rightarrow\ ^{12}C^* .$$

In an attempt to explain the isotopic abundances and reaction rates in red giant stars, HOYLE was led to postulate that the reaction $^8Be + ^4He \rightarrow\ ^{12}C^*$ takes place as a resonance reaction at an energy of ≈ 0.33 MeV, via a level in ^{12}C at ≈ 7.7 MeV. The existence of this level in ^{12}C is now well established from a variety of evidence (4). The fact that the 7.656 MeV level can indeed be formed by the reaction $^8Be + ^4He$ was shown indirectly, by invoking the principle of the reversibility of nuclear reactions, by COOK *et al.* (5), who observed the α-particle break-up of this level. They were able to establish that the state breaks up chiefly into three α-particles, with the process $^8Be + ^4He$ as an intermediate stage. COOK *et al.* also presented arguments based on the then available experimental evidence in favour of a $0+$ assignment to the 7.656 MeV level. However, the arguments were not conclusive, and notwithstanding the probability of a $0+$ assignment the evidence presented established only that the state has either even-even or odd-odd parameters.

From the astrophysical aspect, the most important question remaining to be answered after the work of COOK *et al.* had established the possibility of the process $^8Be + ^4He \rightarrow\ ^{12}C^*$, was the question of the possible modes of decay of the 7.656 MeV level of ^{12}C. It is clear that if the state never decays to the ground state of ^{12}C, but always breaks up into α-particles, the helium fusion process is of no importance as a mechanism for element synthesis. If the high probability of a $0+$ level assignment is accepted, then there exist two possible modes of decay to the ground state of ^{12}C. The direct transition to the $0+$ ground state would be an $E0$ positon-negaton pair emission process, whilst the other possibility is a γ-ray cascade proceeding via the 4.433 MeV first excited state.

There is at present conflicting evidence on the existence of the γ-ray cascade process; possibly the most reliable measurements are those of KAVANAGH (6) and ECCLES and BODANSKY (7), who both place an upper limit on its frequency of occurrence of 0.1% of all decays of the 7.656 MeV level.

(3) F. HOYLE: *Suppl. Astrophys. Journ.*, **1**, 121 (1954).

(4) F. AJZENBERG-SELOVE and T. LAURITSEN: *Nucl. Phys.*, **11**, 1 (1959).

(5) C. W. COOK, W. A. FOWLER, C. C. LAURITSEN and T. LAURITSEN: *Phys. Rev.*, **107**, 508 (1957).

(6) R. W. KAVANAGH: *Bull. Am. Phys. Soc.*, **3**, 316 (1958).

(7) S. F. ECCLES and D. BODANSKY: *Phys. Rev.*, **113**, 608 (1959).

The nuclear pair decay has now been observed in the $^{9}Be(\alpha, n)^{12}C^{*}$ reaction by ALBURGER [1], who summarizes the results of previous attempts to observe both the γ-ray cascade and the nuclear pair transition. He found that the thick target intensity ratio of the 7.656 pair line to the 4.433 MeV pair line (from the first excited state of ^{12}C) was $(5 \pm 1.5) \cdot 10^{-4}$ at a mean bombarding energy in the target of 5.46 MeV.

The result of Alburger's work coupled with a knowledge of the relative population, R, of the 7.656 MeV and 4.433 MeV states in the reaction $^{9}Be(\alpha, n)^{12}C^{*}$ makes possible a direct calculation of the ratio of the width of the 7.656 MeV level for pair emission, $\Gamma'_{e^{\pm}}$, to the total width, Γ, of the state by means of the relation:

$$\frac{\Gamma_{e^{\mp}}}{\Gamma} = (5 \pm 1.5) \cdot 10^{-4} \cdot \varepsilon \cdot \alpha \cdot R \, .$$

In this formula, $\varepsilon = 1.26$ is the relative efficiency of the spectrometer used by Alburger for the detection of pairs from the 4.433 MeV $E2$ transition compared with the $E0$ pairs from the 7.656 MeV transition; $\alpha = 1.3 \cdot 10^{-3}$ is the internal pair conversion coefficient of the 4.433 MeV transition [8], and $R = N_{4.433}/N_{7.656}$ is the ratio of neutron population of the two levels at the mean bombarding energy used by ALBURGER in measuring the pair line ratio of $(5 \pm 1.5) \cdot 10^{-4}$. Therefore

$$\frac{\Gamma_{e^{\pm}}}{\Gamma} = (8.2 \pm 2.5) \cdot 10^{-7} \cdot R \, .$$

It was mentioned by ALBURGER that at the time of his experiment there existed no precise measurement of the neutron population ratio R. The only published measurement was of the ratio of the neutron group intensities at 0° (obtained by bombarding a thin beryllium foil with α-particles from a Po source) by GUIER *et al.* [9], who obtained a ratio of ≈ 8. It is important to note that this does not constitute a measurement of R, for which it is necessary to integrate the differential cross-sections over all angles in order to obtain the ratio of the total cross-sections for formation of the two levels. The danger of relying on the 0° yield ratio appeared to be particularly great in view of the large anisotropy known to be present in the neutron angular distributions previously measured in this reaction [10,11]. In view of this, and because of

[8] M. E. ROSE: *Phys. Rev.*, **76**, 678 (1949).
[9] W. H. GUIER, H. W. BERTINI and J. H. ROBERTS: *Phys. Rev.*, **85**, 426 (1952).
[10] J. R. RISSER, J. E. PRICE and C. M. CLASS: *Phys. Rev.*, **105**, 1288 (1957).
[11] J. B. GARG, J. M. CALVERT and N. H. GALE: *Nucl. Phys.*, **19**, 264 (1960).

the fact, mentioned by ALBURGER, that an accurate measurement of R might lead to a definite 0+ assignment to the 7.656 MeV level of ^{12}C, it was decided to make such a precise measurement at three bombarding energies spanning that used by ALBURGER in his work on the nuclear pair ratio.

2. – Experimental procedure.

Singly charged ^4He ions were accelerated by the University of Manchester 6 MV Van de Graaff accelerator, and were analyzed by a 90° deflecting magnet. The energy calibration was obtained in terms of the threshold energies of the $^7Li(p, n)$ and $^{19}F(p, n)$ reactions.

The ^4He particles were used to bombard a beryllium target (a Bradner foil) $\approx 330\ \mu g \cdot cm^{-2}$ thick; the mean energy loss in the target at the bombarding energies employed was ≈ 260 keV.

The neutron spectra were obtained with a pulsed-beam time-of-flight neutron spectrometer; its chief features have been described in a previous article ([12]). A peak beam deflecting field strength of about 7 kV/cm and a chopping frequency of 4 MHz was employed in these measurements, resulting in a pulse duration of about 1 nanosecond at the target. A reasonable compromise between energy resolution and the ratio of true to chance counts for the ground state and second excited state neutron groups was secured by using a flight path of 75 cm throughout. In order to avoid the double spectrum display typical of such a spectrometer ([13]), and in order to reduce the random background by a factor of two, a « negative time elimination » system was used, similar in principle to those described by GREEN and BELL ([14]) and by NEILSON *et al.* ([15]).

The neutron detector was an NE 211 (*) liquid fluor contained in a cylindrical glass cell $5\frac{1}{2}$ cm long by 7.8 cm diameter, bonded by a short truncated conical light guide to an RCA 6810A photomultiplier tube. The calibration of the neutron detection efficiency as a function of neutron energy, and the arrangement of the ancillary electronic apparatus, were both described in a previous paper ([12]).

([12]) N. H. GALE, J. B. GARG, J. M. CALVERT and K. RAMAVATARAM: *Nucl. Phys.*, **20**, 302 (1960).

([13]) L. CRANBERG and J. S. LEVIN: *Phys. Rev.*, **100**, 434 (1955).

([14]) R. F. GREEN and R. E. BELL: *Nucl. Instr.*, **3**, 127 (1958).

([15]) G. C. NEILSON, W. K. DAWSON and F. A. JOHNSON: *Rev. Sci. Instr.*, **30**, 963 (1960).

(*) Supplied by Nuclear Enterprises Ltd., Edinburgh.

3. – Experimental results.

A typical neutron time-of-flight spectrum is presented in Fig. 1. As will be seen, the energy resolution is not as good as would be attainable by the use of the photographic plate technique, but on the other hand the detection efficiency, and hence the attainable statistical accuracy for reasonable exposures, is many times greater. The use of the neutron-γ discrimination technique ([15]) and longer flight paths would have resulted in better resolution, but for the present experiment the resolution was thought to be sufficient.

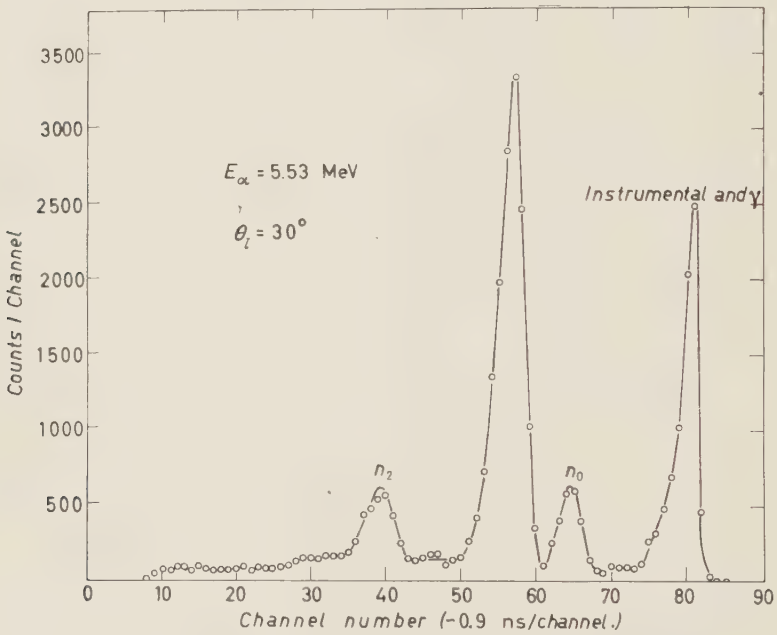

Fig. 1. – Time-of-flight neutron spectrum for the reaction ^{9}Be(α, n)^{12}C.

Angular distributions of the neutron groups leading to the ground state and first two excited states of ^{12}C were measured at incident α-particle energies of 5.53 MeV, 5.76 MeV and 5.97 MeV. The mean beam energy in the target was 5.40, 5.63 and 5.84 MeV respectively. Measurements were made at about fourteen angles at each bombarding energy.

It was observed that in all the spectra taken at forward angles up to $\theta_{lab} = 30°$ there was a rather flat contribution due to neutrons of energies less than those leading to the 7.656 MeV level of ^{12}C. The contribution appeared to be negligible after $\theta_{lab} = 30°$, indicating a fairly sharp angular distribution.

It is possible that these neutrons may have arisen from the $^{9}Be(\alpha, n)^{12}C^{*}$ reaction leading to the 9.63 MeV and 10.1 MeV levels, or from spontaneous three particle break-up reactions such as $^{9}Be(\alpha, n\alpha)^{8}Be$, $^{9}Be(\alpha, n) \rightarrow 3\ ^{4}He$. The effect of the merging of the flat background with the group leading to the 7.656 MeV state led to an uncertainty in estimating the background level at forward angles for this group.

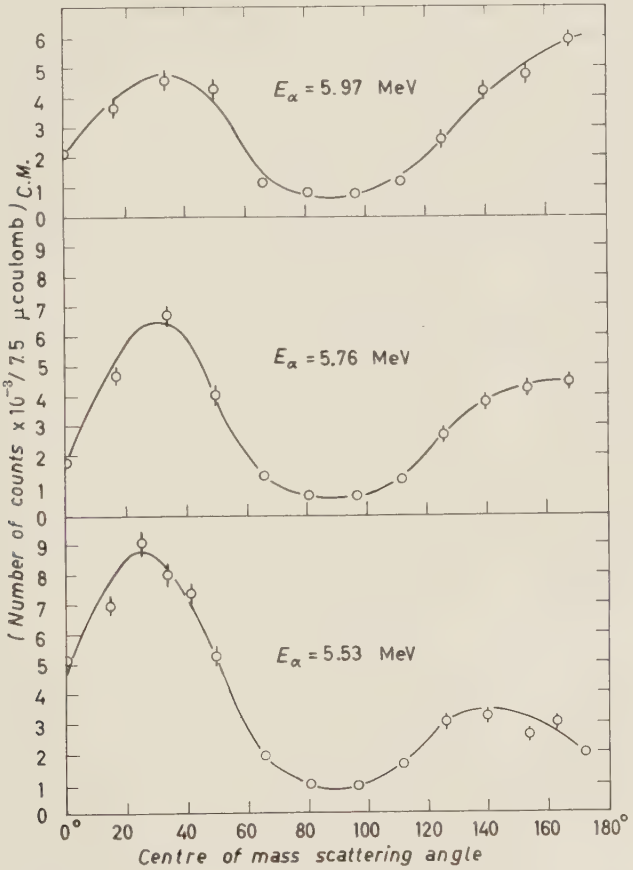

Fig. 2. – Ground state (n_0) neutron group angular distributions. Errors are shown except when smaller than the experimental points. Energy values specified are the incident α-particle energies.

There appeared to be no neutron groups in any spectra due to target contaminants. The most likely target impurities were thought to be carbon, oxygen and nitrogen. There could be no contribution from the reactions $^{12}C(\alpha, n)^{15}O$, $^{16}O(\alpha, n)^{19}Ne$ whose Q-values are respectively -8.45 MeV and

— 12.16 MeV. The reaction kinetics for the reaction $^{13}C(\alpha, n)^{16}O$ were computed, and there was no observed yield of ground state neutrons at the calculated positions in any of the neutron spectra. Neutrons leading to the 6 MeV levels of ^{16}O would have too small an energy to be accepted by the spectrometer save at the highest bombarding energy at angles up to about 30°. Even here, they would have been well separated from the neutron group leading to the 7.656 MeV level in ^{12}C.

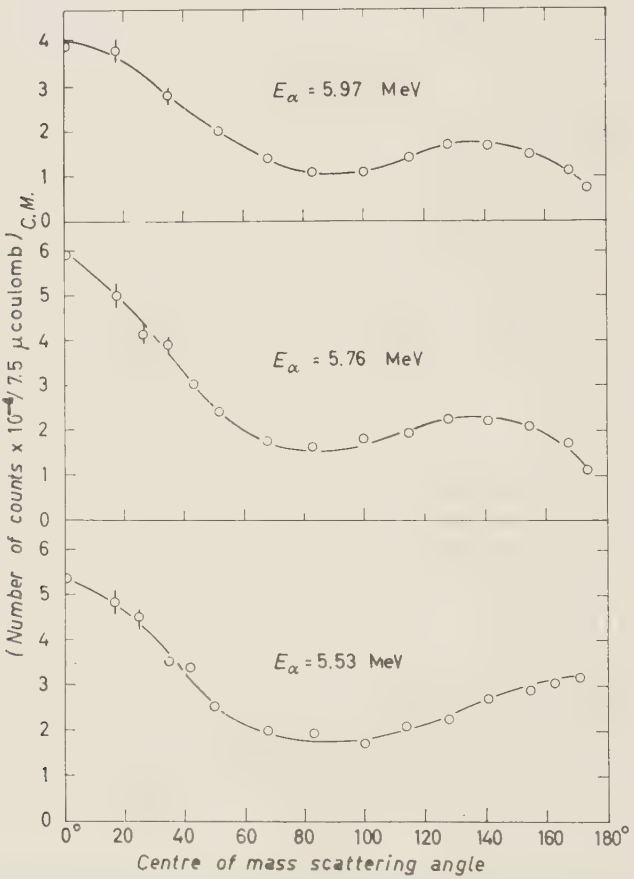

Fig. 3. – First excited state (n_1) neutron group angular distributions. Errors are shown except when smaller than the experimental points.

The angular distributions obtained are presented in Fig. 2, 3 and 4. The ground state and first excited state angular distributions are similar to those obtained previously by RISSER *et al.* [10] and GARG *et al.* [11] at 5.1 MeV.

The total cross-sections (on an arbitrary scale) were obtained for each state at each bombarding energy by multiplying each point on the relevant angular distribution in the centre-of-mass system by $\sin(\theta_{c.m.})$, and numerically integrating the resulting curve. The ratios of the populations of the ground

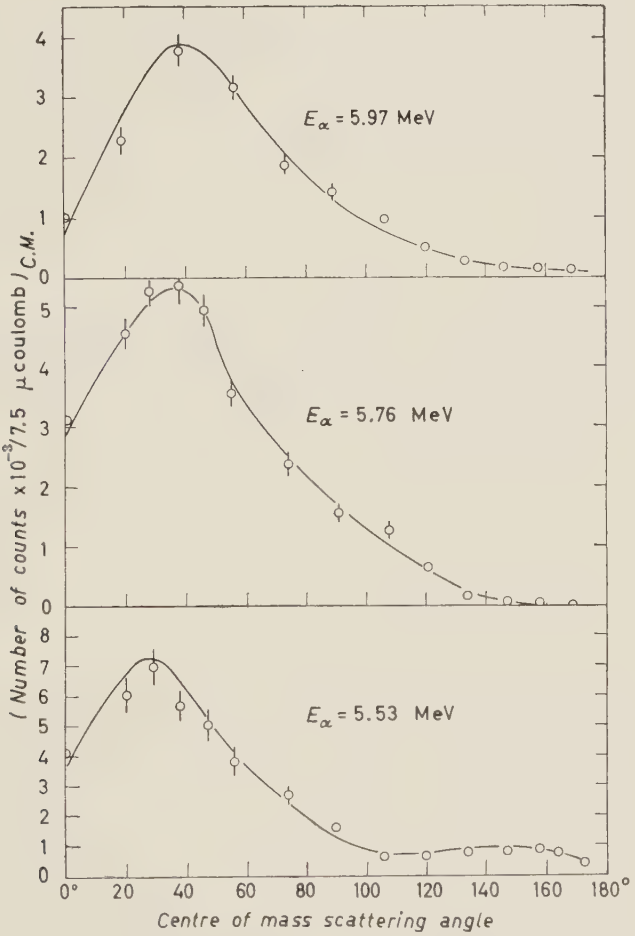

Fig. 4. – Second excited state (n_2) neutron group angular distributions. Errors are shown except when smaller than the experimental points.

state, first excited and second excited states are presented in Table I. The quoted errors include the statistical errors, the errors in the estimation of the variation of neutron detection efficiency with energy, and the estimated errors due to background uncertainties in the case of the second excited state group. The errors are standard deviations taking into account all these factors.

TABLE I. – *The neutron population ratios of the first three states of* ^{12}C *in the reaction* $^{9}Be(\alpha, n)^{12}C$.

Bombarding energy (MeV)	Average energy in target (MeV)	$\frac{n_1}{n_0}$	$\frac{n_0}{n_2}$	$\frac{n_1}{n_2}$
5.53	5.40	8.1 ± 0.5	1.3 ± 0.1	10.2 ± 0.8
5.76	5.63	8.1 ± 0.5	1.4 ± 0.1	11.3 ± 0.8
5.97	5.84	6.9 ± 0.5	1.6 ± 0.1	10.7 ± 0.8

4. – Discussion.

It appears that the value of R at the three bombarding energies used does not alter appreciably, since all three experimental values are the same within the errors. It therefore appears to be justified to take R as the mean of the three measured values, namely $R = 10.7 \pm 0.8$.
Hence

$$\frac{\Gamma_{e^\pm}}{\Gamma} = (8.2 \pm 2.5) \cdot 10^{-7} \cdot (10.7 \pm 0.8) ,$$

$$\frac{\Gamma_{e^\pm}}{\Gamma} = (8.2 \pm 2.7) \cdot 10^{-6} .$$

The pair width $\Gamma_{e^\pm}$ has been estimated to be $5 \cdot 10^{-5}$ eV by COOK *et al.* [5] from the cross-section for inelastic scattering of electrons by ^{12}C [16]. Hence:

$$\Gamma \approx \frac{5 \cdot 10^{-5}}{(8.8 \pm 2.7) \cdot 10^{-6}} \approx 5.7 \text{ eV} .$$

This estimate for the total width is fairly close to the estimated value of ≈ 7 eV calculated for the Wigner limit on the basis of a $0+$ assignment, and is about 30 times larger than the Wigner limit of ≈ 0.2 eV for a $2+$ assignment; it therefore constitutes strong evidence for the $0+$ assignment. Taken together with Alburger's measurement of the intensity ratio of the 7.656 MeV pair line to the 4.433 MeV pair line, which is a factor of about three greater than that calculated on the basis of a $2+$ assignment, it seems clear that the 7.656 MeV state of ^{12}C is indeed a $0+$ state.

---

[16] J. H. FREGAU: *Phys. Rev.*, **104**, 225 (1956).

If the estimated width $\Gamma_\gamma \approx 0.0014$ eV for the 7.656 MeV $\rightarrow$ 4.433 MeV transition, quoted by COOK *et al.*, is correct, then

$$\frac{\Gamma_\gamma}{\Gamma} \approx \frac{0.0014}{5.7} \approx 0.025\,\% .$$

It is clear, therefore, that if these estimates are correct it will be a task of some difficulty to observe the 3.2 MeV γ-ray transition. However, it is of considerable importance from the astrophysical aspect to make the attempt, since the stellar reaction rates depend on the dominant mode of decay to the ground state of ^{12}C, and it is not altogether clear how much reliance can be placed on the present estimate for Γ_γ.

* * *

We would like to thank Dr. K. RAMAVATARAM for his assistance in performing the experiment, and JEAN HEWITT for her help in analysing the results.

RIASSUNTO (*)

Uno spettrometro a fascio pulsante per il tempo di volo dei neutroni è stato usato per studiare la reazione $^9Be(\alpha, n)^{12}C^*$ per energie di bombardamento di 5.53, 5.76 e 5.97 MeV. Si sono misurate le distribuzioni angolari dei gruppi di neutroni che conducono allo stato fondamentale ed ai primi due stati eccitati del ^{12}C, e si è determinato che il rapporto fra le popolazioni dei livelli 4.433 e 7.656 MeV è 10.7 ± 0.5 a 5.5 MeV. In congiunzione ad altri argomenti, dal valore misurato del rapporto fra le popolazioni si determina che l'ampiezza di decadimento delle particelle α del livello a 7.656 MeV è approssimativamente al limite di Wigner, lo spin e la parità $0+$, e si possono fare valutazioni delle probabilità di decadimento di questo stato in coppie e γ.

(*) *Traduzione a cura della Redazione.*

IL NUOVO CIMENTO Vol. XIX, N. 4 16 Febbraio 1961

Theory of the Low-Energy Pion-Pion Interaction - II (*).

G. F. Chew and S. Mandelstam (**)

Lawrence Radiation Laboratory and Department of Physics
University of California - Berkeley, Cal.

(ricevuto il 31 Ottobre 1960)

Summary. — It is shown that when P-wave pion-pion scattering is large at low energies, the integral equations previously formulated by the authors require a cut-off. Because of the cut-off and the unstable nature of the solution, the numerical integration procedure becomes much more involved. The original equations are therefore replaced by a series of conditions at the symmetry point, and the unphysical cuts of the partial-wave amplitudes are replaced by a corresponding series of poles. Within this framework one need not speak of a cut-off, but one new parameter appears. Self-consistent solutions can be found in which a P-wave resonance is sustained by a « bootstrap » mechanism; that is, a strong attractive force in the $I=1$ state results from the exchange of a resonating pair of P-wave pions. The symmetry-point conditions used would be modified by the cut-off and quantitative accuracy is not attempted; however, this and other corrections are not expected to change the qualitative nature of our solutions. Rough estimates of the corrections are made.

1. – Introduction.

In an earlier paper (1), hereafter to be referred to as CM-I, a single-parameter set of integral equations for the low-energy pion-pion scattering amplitudes has been derived. These equations satisfy the requirements of analyticity and crossing symmetry but are based on the assumption that the imag-

(*) This work was supported in part by the U.S. Atomic Energy Commission and in part by the U.S. Air Force under contract No. AF 638-327 monitored by the AFOSR of the Air Research and Development Command.

(**) Present address: Departement of Matematical Physics, University of Birmingham, Birmingham.

(1) G. F. Chew and S. Mandelstam: *Phys. Rev.*, **119**, 467 (1960).

inary part of the amplitude is adequately represented by keeping elastic S- and P-waves only. It has been shown by explicit calculation ([2]) that there exists a class of solutions of these equations consistent with this assumption. These solutions, however, have very small P phase-shifts, whereas the only information available so far about the π-π interaction suggests that there is a low-energy P-resonance ([3]). In this paper we examine the problem further and show that if the P phase-shift is large at low energies, the original assumption about the imaginary part is inconsistent; the CM equations require modification and a new parameter appears.

It is possible to make the necessary modification through a cut-off of the partial-wave imaginary parts on the left-hand (unphysical) cut. Actually three cut-offs would be needed, for the $I=0$ and $I=2$ S-states as well as for the P-state, but crossing symmetry may be used to correlate the three in terms of a single real parameter. It will be made plausible that in a correct calculation, where inelastic processes and the imaginary parts of higher partial waves are included, unitarity will make any new parameters unnecessary.

At the present level of approximation it will be argued that the cut-offs of the imaginary parts on the left-hand cut probably occur for values of $\omega = -q^2$ substantially greater than 9, the mathematical limit of convergence of the polynomial expansion. It will be shown that in such a case a strong intermediate-range attractive force capable of producing a P-wave resonance occurs in the $I=1$ state. The force is due to the exchange of a pair of P-wave pions resonanting in transit (or in other words to the left-cut contribution obtained by crossing relations from the P-wave absorptive part on the right), so we have a « bootstrap » mechanism. The corresponding strong intermediate range force in the $I=0$ state is repulsive and in the $I=2$ case attractive.

We assume that the short-range contributions from D- and higher waves, except for their role in producing the cut-off, may be absorbed into the parameter λ already introduced in CM-I. That is, we replace them, together with all other exchange mechanisms of high energy, by a phenomenological zero-range force. The consistency of such an approach can be investigated *a posteriori* by calculating the higher angular-momentum contributions to the force once the S and P phase-shifts have been determined. Rough estimates of this kind are reported below.

In Section **2**, the necessity for the cut-off, when the P-wave is « bootstrapping » itself, will be demonstrated and the relation of the cut-off to our

([2]) G. F. Chew, S. Mandelstam and H. P. Noyes: *Phys. Rev.*, **119,** 478 (1960).

([3]) W. R. Frazer and J. R. Fulco: *Effect of a Pion-Pion Scattering Resonance on Nucleon Structure*, UCRL-8880, August 1959; *Phys. Rev.*, to be published (1960).

approximations is discussed. Section 3 treats certain exact and almost exact crossing conditions that put powerful restrictions on the scattering amplitudes. In Section 4 further conditions at the symmetry point, corresponding to the basic approximation of CM-I, are developed and used in the replacement of left-hand discontinuities by a small number of δ-functions. The straightforward iteration procedure previously employed does not converge when the P-amplitude is large because the « bootstrap » character of the mechanism makes the solution very unstable. Section 5 tests the new method on the « known » S-dominant problem, while Section 6 deals with the P-dominant situation. It is shown that a reasonable choice of the new parameter leads to a P-resonance with a position and width roughly that required by the electromagnetic structure of the nucleon. Our results are not quantitatively accurate, because the crossing conditions at the symmetry point should be modified by the cut-off, and also because we neglect the S-waves in the crossing relations. Corrections to the results obtained are discussed in Section 7, and future calculations are outlined.

2. – Properties of the integral equations when there is strong P-wave scattering.

To derive the integral equations in CM-I, the partial-wave amplitudes were written in the form

$$\frac{1}{\nu^l} A^{(I)I}(\nu) = \frac{N_l^I(\nu)}{D_l^I(\nu)}, \tag{2.1}$$

where N has a cut along the negative real axis and D along the positive real axis only. The index l denotes the angular momentum and I the isotopic spin. On defining $\omega = -\nu$, $E_l^I(\omega) = D_l^I(\nu)$, we found the following integral equations [CM-I, eq. (V.14) and (V.26)]:

$$E_0^I(\omega) = 1 + (\omega + \nu_0) K(\omega, -\nu_0) a_I + \frac{\omega + \nu_0}{\pi} \int_1^\infty \mathrm{d}\omega' \, \frac{K(\omega, \omega') f_0^I(\omega') E_0^I(\omega')}{\omega' + \nu_0}, \tag{2.2}$$

and

$$E_1^1(\omega) = 1 + \frac{\omega}{\pi} \int_1^\infty \mathrm{d}\omega' \, \frac{K(\omega, \omega') f_1^1(\omega') E_1(\omega')}{\omega'}, \tag{2.3}$$

where

$$K(\omega, \omega') = \frac{2}{\pi(\omega - \omega')} \left\{ \frac{\omega}{\omega - 1} \ln \left[\sqrt{\omega} + \sqrt{\omega - 1} \right] - \right.$$

$$\left. - \frac{\omega'}{\omega' - 1} \ln \left[\sqrt{\omega'} + \sqrt{\omega' - 1} \right] \right. . \tag{2.4}$$

In these equations, a_I is the S-wave amplitude for isotopic spin I at $\nu = \nu_0$ and f_l^I the discontinuity across the cut of $A^{(l)I}(\nu)$ for $-\omega = \nu < 0$.

The f's are not known explicitly, but must be calculated by crossing symmetry from the absorptive parts for positive energies. In CM-I, we denoted the absorptive parts of the complete amplitude by $A_s^I(\nu, \cos\theta)$ and wrote the necessary equations in the form

$$f_l^I(\omega) = -\frac{1}{\omega}\int_0^{\omega-1} d\nu' \, P_l\left(1 - 2\,\frac{\nu'+1}{\omega}\right) \sum_{I'=0,1,2} \alpha_{II'} A_s^{I'}\left(\nu', 1 - 2\,\frac{\omega-1}{\nu'}\right), \quad (\omega > 1), \tag{2.5}$$

where the crossing matrix $\alpha_{II'}$ is

$$\alpha_{II'} = \begin{pmatrix} 2/3 & 2 & 10/3 \\ 2/3 & 1 & -5/3 \\ 2/3 & -1 & 1/3 \end{pmatrix}. \tag{2.6}$$

If $A_s^{I'}$ in eq. (2.5) is resolved into partial waves and the expansion cut-off after the P-wave, the formula becomes

$$f_l^I(\omega) = -\frac{1}{\omega}\int_0^{\omega-1} d\nu' \, P_l\left(1 - 2\,\frac{\nu'+1}{\omega}\right)\Big\{\alpha_{I0}\,\mathrm{Im}\,A^{(0)0}(\nu') + \alpha_{I2}\,\mathrm{Im}\,A^{(0)2}(\nu') + 3\left(1 - 2\,\frac{\omega-1}{\nu'}\right)\alpha_{I1}\,\mathrm{Im}\,A^{(1)1}(\nu')\Big\}. \tag{2.7}$$

The right-hand side of eq. (2.7) involves the imaginary parts of the partial-wave amplitudes for positive energies, which are given by the simple formula

$$\mathrm{Im}\,A^{(l)I}(\nu) = \sqrt{\frac{\nu+1}{\nu}}\,\sin^2\delta_l^I. \tag{2.8}$$

The phase-shifts, δ_l^I, can be calculated from the functions E by the formulae CM-I (V.20) and (V.26), so we have a self-consistency problem; the functions E are determined in terms of the f's by eq. (2.2) and (2.3), while the f's are determined in terms of the E's from crossing by eq. (2.6) to (2.8).

In our previous calculations an iteration procedure was used to obtain self-consistency. The convergence was rapid, and the solutions had the property that the P-wave amplitude was extremely small. The reason was that the terms $\mathrm{Im}\,A^{(0)0}(\nu')$ and $\mathrm{Im}\,A^{(0)2}(\nu')$ in eq. (2.7) are bounded by unitarity and, further, have opposite signs for $I = 1$ so that $f_l^1(\omega)$ cannot become large. According to CM-I (V.26), the P-wave amplitude then remains small, and its smallness in turn means that the third term on the right of eq. (2.7) is small.

The question now arises whether there are any other solutions of our equations. An immediate possibility is a solution dominated by the P-wave, in which $f_1^1(\omega)$ is large and receives its main contribution from the third term of eq. (2.7), *i.e.*, from the imaginary part of the P-wave itself. Owing to the large numerical factor multiplying the third term, the unitarity limitation no longer makes $f_1^1(\omega)$ small. To determine the sign of the P-wave phase-shift in such a solution, we notice that $f_1^1(\omega)$ according to eq. (2.7) is negative for small ω and positive for large ω, and that, as may easily be verified, the positive part always predominates in the sense that the dispersion integral

$$\frac{1}{\pi}\int_1^\infty d\omega' \frac{f_1(\omega')}{\omega'(\omega'+\nu)},$$

is positive. According to our equations, it then follows that the phase shift is positive. We are led to the possibility of a P-wave resonance, which FRAZER and FULCO [3] require in order to bring the calculations on nucleon electromagnetic structure into agreement with experiment. Rough examination indicates that we can achieve self-consistency in our equations with such a resonance.

The type of solutions suggested here would exist even without any coupling to the S-waves, though of course it becomes modified by such coupling. For each value of the constant λ, there are two solutions—one of the type discussed previously with small P-waves, and one of the type under consideration here with large P-waves. One might raise the objection that, if λ is interpreted as a coupling constant, it would be expectd to define uniquely the solution. However, it must be borne in mind that we are dealing with a renormailzed coupling constant whose definition is largely a matter of convenience. There seems to be no reason why such a quantity cannot be the same for two different solutions of our equations. To put it another way, it would be quite possible that two different values of the unrenormalized coupling constant—if such a quantity had a meaning—could give the same value of the renormalized coupling constant. The question as to which of the two solutions is actually realized in nature is on the same level as the question of the value of the coupling constant, and at present must be determined by experiment.

The qualitative nature of the solution with large P-wave phase-shifts is encouraging from the point of view of the nucleon electromagnetic structure. The fact that $f_1^1(\omega)$ is not positive over its entire range but is negative if ω is sufficiently small has the effect of considerably narrowing the resonance. This property follows from eq. (2.3), or it may be seen by expressing the problem in more conventional language. The potential corresponding to an $f_1^1(\omega)$ of our form has a repulsive outer part and an attractive inner part, and it is hardly necessary to remark that such a potential favors a narrow resonance. Now

FRAZER and FULCO have shown that a resonance sufficiently narrow to explain the electromagnetic structure cannot be obtained with a purely positive $f_1(\omega)$, corresponding to a purely attractive force, without making the predominant values of ω unreasonably high—at least 150 and, for a good fit, nearer 600 [3]. If f_1 changes sign in the manner described, a narrow resonance can be obtained without going to such high values of ω. This class of solutions to the pion-pion problem seems therefore to be qualitatively just what is required to fit the electromagnetic structure data.

There are unfortunately two difficulties that must be overcome before we can obtain a solution of the type described in the foregoing paragraphs. The first is purely practical in nature; the iteration procedure used previously does not converge now, as mentioned in the introduction. We shall have to use some trial-and-error procedure to obtain a consistent solution, and the numerical work is therefore considerably increased. The second difficulty is one of principle. We have pointed out in CM-I that the integral eq. (2.2) and (2.3) above become singular if f_0^I of f_1^1 approach a constant value with infinite ω. It follows from eq. (2.7) that the contribution to f_l^I from the third term does approach a constant, even if only a finite range of values of ν' is taken. The behavior of f_l^I at infinity is therefore just bad enough to make our integral equations singular, and in such a case the integral equation usually has a unique solution if and only if the coefficient of the singular term is sufficiently small.

By replacing our integral equation by one with the same asymptotic behavior but which is exactly soluble, we can show that a unique solution exists provided that the limit of $f_1(\omega)$ as ω becomes infinite is less than unity. (A negative limit never gives trouble.) If the function $\mathrm{Im}\,A^{(1)1}(\nu')$ on the right of eq. (2.7) is obtained from a solution that has approximately the characteristics required by FRAZER and FULCO [3], the limit of $f_1(\omega)$ is found to be considerably greater than unity—of the order of magnitude of six. We are therefore well within the range where the equation does not have a unique solution.

The situation here is precisely analogous to that occurring in th relativistic scattering by a potential with a $1/r$ behavior at the origin. Again we find a unique solution in the attractive case only if the coefficient of the singularity is sufficiently small (less than $\hbar c$). In the repulsive case, which corresponds to a negative $f_1^1(\omega)$, there is of course no trouble.

One may easily see the reason for the limit 1 of $f_1^1(\omega)$ at infinity by considering the dispersion relation for $A^{(1)1}(\nu)$:

$$\frac{1}{\nu}A^{(1)1}(\nu)=\frac{1}{\pi}\int_1^\infty \mathrm{d}\omega'\,\frac{f_1^1(\omega')}{\omega'(\omega'+\nu)}+\frac{1}{\pi}\int_0^\infty \mathrm{d}\nu'\,\frac{\mathrm{Im}\,A_1^{(1)1}(\nu')}{\nu'(\nu'-\nu)}\,. \tag{2.9}$$

If $f_1(\omega')$ approaches the constant c without oscillation as ω' tends to infinity, the first term will behave like $(1/\pi)(c/\nu)\log\nu$ as ν tends to infinity. Since $|A^{(1)1}(\nu)|$ is bounded by unitarity and cannot be greater than $\sqrt{(\nu+1)/\nu}$ in the physical region, this logarithmic behavior must be cancelled by an opposite logarithmic behavior of the second term. The function $\mathrm{Im}\, A^{(1)1}(\nu)$ must therefore approach c as ν tends to infinity. However, $|\mathrm{Im}\, A^{(1)1}(\nu)|$ is of course also less than $\sqrt{(\nu+1)/\nu}$, so that c cannot be greater than unity. This argument seems to apply to the repulsive as well as the attractive case, but the presence of « ghosts » in the former complicates the situation and the singularity at infinity does not have any further adverse effect.

The source of the singularity in the integral equation appears to be the use of the Legendre expansion for A_s^I in eq. (2.5) at all values of ω, whereas we know it to be justified only if ω is less than 9. If we could use the full expression (2.5) and calculate $f_1(\omega)$ correctly at high values of ω, a uniquely soluble equation would result. Our procedure for calculating $f_1(\omega)$ is, however, not accurate for high ω. At this stage, therefore, there appears to be no alternative to cutting off $f_1(\omega)$ at some point. This cut-off is meant to replace the excluded contributions, which should remove the difficulty in the integral equation. The cut-off is a second parameter (in addition to λ), which seems unavoidable at present. If the calculation could be taken to higher approximations, it should be possible to see the natural cut-off (or high-energy oscillations) appearing, so that the extra parameter would be unnecessary. It represents our lack of knowledge at present of processes at high energies.

An important physical consideration is whether the cut-off may occur at such a low value of ω as to remove the attractive part of the interaction in the $I=1$ state. To investigate this point, let us caculate $f_1^1(\omega)$ from eq. (2.7) keeping only the third term on the right and assuming a sharp resonance at $\nu=\nu_R$. The functional form of $f_1^1(\omega)$ is then roughly

$$f_1^1(\omega)\sim\frac{1}{\omega}\left(1-2\,\frac{\nu_R+1}{\omega}\right)\left(2\,\frac{\omega-1}{\nu_R}-1\right), \qquad \omega>\nu_R+1, \tag{2.10}$$

$$\sim 0\,, \qquad \omega<\nu_R+1,$$

which changes sign at $\omega=2(\nu_R+1)$, being attractive for larger values of ω and repulsive for smaller values. According to Frazer and Fulco [3], the position of the resonance should correspond to $\nu_R\leqslant 2$, so the attractive region on the left cut begins at $\omega\leqslant 6$. Therefore, if the cut-off occurs at $\omega\geqslant 12$ there will be a substantial region of attraction.

Now, the polynomial expansion of A_s^I in eq. (2.5) formally breaks down at $\omega=9$, but if there is in fact a P-resonance and the higher partial waves are not of abnormal size, one expects the S- and P-waves to give a reasonable

approximation to the full absorptive part up to somewhat higher values of ω. One may easily, in fact, estimate the D phase-shifts produced by the exchange of a resonating P-wave pair and investigate how large ω must be before the D-wave contributions to $A_s^{I'}$ become important. The result suggests that the cut-off will not occur until $\omega \gtrsim 20$.

Another consideration is the influence of inelastic processes, which have been neglected but which certainly will be important at high energies. In CM-I it was estimated that on the right cut the elastic approximation should be adequate for $\nu \lesssim 10$. The crossing relation (2.5) tells us that a value ω on the left corresponds to an « average » value of ν on the right equal to $\frac{1}{2}(\omega - 1)$. Thus a breakdown of the elastic approximation at $\nu \sim 10$ corresponds to a failure of our formulas on the unphysical cut at $\omega \sim 20$. On this score as well, therefore, there is reason for confidence in the intermediate-range attractive force, which is the crucial element in the problem.

3. – Exact and almost-exact crossing conditions at the symmetry point.

With no cut-off, the equations of CM-I satisfy crossing symmetry exactly. We shall lose this feature if cut-offs are introduced in an arbitrary fashion into the different partial wave amplitudes, so it is desirable to establish in advance certain important consequences of crossing symmetry that can be used as a guide.

The general crossing conditions are given by eq. (II.5) to (II.7) of CM-I. It was also pointed out there that a singularity-free point of maximum symmetry in the $\pi\pi$ problem occurs at $s = t = u = 4/3$ or at

$$\cos\theta = 0\,, \qquad \nu = \nu_0 = -2/3\,.$$

Advantage was taken of the first crossing condition at this point, namely that $A - B = C$, in order to define the $\pi\pi$ coupling constant through CM-I (III.4). An infinite number of further conditions on the derivatives of the amplitudes are also derivable, as we now show.

Consider the condition

$$A(s, t, u) = B(t, s, u)\,. \tag{3.1}$$

This may also be written in terms of the variables ν and $\cos\theta$ which are connected to s, t, and u through CM-I (II.2). The result is

$$A(\nu, \cos\theta) = B(\nu', \cos\theta')\,, \tag{3.2}$$

where

$$\nu' = \frac{\nu}{2}(1 + \cos\theta) - (\nu + 1)\,, \tag{3.3}$$

and

$$\cos\theta' = \frac{(\nu/2)(1 + \cos\theta) + (\nu + 1)}{(\nu/2)(1 + \cos\theta) - (\nu + 1)}\,. \tag{3.4}$$

Evidently, at the symmetry point, $\nu = \nu' = -2/3$ and $\cos 0 = \cos\theta' = 0$, so we have immediately

$$A(-\tfrac{2}{3}, 0) = B(-\tfrac{2}{3}, 0)\,, \tag{3.5}$$

or, in view of CM-I (II.8), remembering that

$$C(\nu, \cos\theta) = B(\nu, -\cos\theta)\,, \tag{3.6}$$

we have

$$\tfrac{1}{5}A^0(-\tfrac{2}{3}, 0) = \tfrac{1}{2}A^2(-\tfrac{2}{3}, 0) = -\lambda\,, \tag{3.7}$$

the result already stated in CM-I (III.5).

Next let us differentiate eq. (3.2) above with respect to ν and evaluate at the symmetry point. We find

$$\left[\frac{\partial A}{\partial \nu} = -\frac{1}{2}\frac{\partial B}{\partial \nu} - \frac{9}{4}\frac{\partial B}{\partial \cos\theta}\right]_{\cos\theta = 0}^{\nu = -\frac{2}{3}}. \tag{3.8}$$

Similarly, by differentiating with respect to $\cos\theta$ we find

$$\left[-\frac{1}{3}\frac{\partial B}{\partial \nu} + \frac{1}{2}\frac{\partial B}{\partial \cos\theta}\right]_{\cos\theta = 0}^{\nu = -\frac{2}{3}} = 0\,. \tag{3.9}$$

Replacing A and B by A_1, A_2, and A_3 through CM-I (II.8), one may then deduce the two symmetry-point conditions,

$$\frac{\partial A^0}{\partial \nu} = 2\frac{\partial}{\partial \cos\theta}\left(\frac{A^1}{\nu}\right), \tag{3.10}$$

and

$$\frac{\partial A^2}{\partial \nu} = -\frac{\partial}{\partial \cos\theta}\left(\frac{A^1}{\nu}\right). \tag{3.11}$$

There are three second-derivative conditions, corresponding to the operations, $\partial^2/\partial\nu^2$, $\partial^2/\partial \cos^2\theta$, and $\partial^2/\partial \cos\theta\,\partial\nu$ on eq. (3.1). Remembering that all

odd derivatives of A_0 and A_2 with respect to $\cos\theta$ vanish at $\cos\theta = 0$, at do all even derivatives of A_1, we can write these three new symmetry-poins conditions as

$$\frac{\partial^2 A^0}{\partial \nu^2} - \frac{5}{2}\frac{\partial^2 A^2}{\partial \nu^2} = -\frac{9}{2}\frac{\partial^2}{\partial \cos\theta\, \partial \nu}\left(\frac{A^1}{\nu}\right), \tag{3.12}$$

$$\frac{\partial^2}{\partial \cos^2\theta}\left(\frac{A^0}{\nu^2}\right) - \frac{5}{2}\frac{\partial^2}{\partial \cos^2\theta}\left(\frac{A^2}{\nu^2}\right) = \frac{3}{2}\frac{\partial^2}{\partial \cos\theta\, \partial \nu}\left(\frac{A^1}{\nu}\right), \tag{3.13}$$

and

$$\frac{\partial^2}{\partial \cos^2\theta}\left(\frac{A^0}{\nu^2}\right) - 7\frac{\partial^2}{\partial \cos^2\theta}\left(\frac{A^2}{\nu^2}\right) = -\frac{\partial^2 A^0}{\partial \nu^2} + \frac{\partial^2 A^2}{\partial \nu^2}. \tag{3.14}$$

Evidently such a procedure can be extended indefinitely, giving an infinite number of conditions on the derivatives of the scattering amplitudes. The conditions written above, however, seem the most interesting for the time being because we shall be concerned principally with S- and P-waves; higher derivatives give conditions that mainly involve higher l values.

It was pointed out in CM-I that eq. (3.7) above implies at $\nu = -\frac{2}{3}$ a simple relation between the two S-amplitudes that holds to a high degree of accuracy even though it is not exact. So long as D- and higher waves are not of abnormal size, the relation is

$$\tfrac{1}{5}a_0 \approx \tfrac{1}{2}a_2 \approx -\lambda\,. \tag{3.15}$$

Similarly, if we define

$$\lambda_1 = \left[\frac{\partial}{\partial \cos\theta}\left(\frac{A^1}{\nu}\right)\right]_{\substack{\nu=-\frac{2}{3} \\ \cos\theta = 0}}, \tag{3.16}$$

then the conditions (2.10) and (2.11), to a good approximation, become

$$\tfrac{1}{2}a_0' \approx -a_2' \approx \lambda_1\,, \tag{3.17}$$

where a_0' and a_2' are the derivatives of the S-amplitudes at $\nu = -\frac{2}{3}$.

The very simple conditions (3.15) and (3.17), while not exact, have a higher order of reliability than the other approximations to be made. Because of them, the low-energy S phase-shifts are fairly well determined once the two constants λ and λ_1 are known.

The new constant, λ_1, is closely related to the P-amplitude at the symmetry point. Neglecting F- and higher waves, we have

$$a_1 = \left(\frac{A^{(1)1}}{\nu}\right)_{\nu=-\frac{2}{3}} \approx \frac{1}{3}\lambda_1\,. \tag{3.18}$$

The task of the following sections might be described as that of developing a procedure for calculating a_1', the derivative of the P-amplitude at the symmetry point, in terms of λ and λ_1. We shall strive, in other words, for a two-parameter theory, but the symmetry conditions of this section are already sufficient to allow the construction of reasonable S and P effective-range formulas with a *total* of no more than *three* arbitrary parameters.

The second-derivative condition (3.12) is more sensitive to the D-wave than our first three conditions, but a correction can be made using condition (3.13). We then find

$$a_0'' - \tfrac{5}{2} a_2'' \approx -12 a_1' . \tag{3.19}$$

Estimates of the D-amplitudes, themselves, are given by conditions (3.13) and (3.14) in terms of a_1', a_0'', and a_2''. It does not seem possible, however, to get conditions on a_0'' and a_2'' separately in terms of a_1'. This circumstance illustrates again the incompleteness of the exact crossing relations if we confine ourself to the symmetry point. Some of the physics certainly lies elsewhere.

4. – Approximate conditions at the symmetry point.

A straightforward approach to the large P-wave problem is to set the left-hand partial-wave imaginary parts equal to zero beyond a certain value of ω and to use eq. (2.7) for smaller values. The integral equations of CM-I are then non-singular and can be solved without difficulty. Furthermore, as explained in Section 2 above, we know that the consequence of the higher partial waves is to produce such a cut-off. A complication arises, however, in the necessity for correlating the cut-offs in the three states ($I = 0$, 1, and 2) so as to satisfy the exact crossing conditions (3.10) and (3.11). These conditions mean that only one new arbitrary parameter occurs, not three. (Higher derivative conditions are relatively intensitive to the cut-offs.) A further difficulty is the instability of the large P-wave problem because of its « bootstrap » aspect. It seems impossible to construct a convergent iteration procedure by the straightforward approach used in the S-dominant problem.

Eventually we hope to solve the cut-off equations by a modified numerical iteration scheme, and progress in this direction is described below. However, an understanding of the essential elements of the problem may be achieved by an analytical approach making maximum use of crossing symmetry at the expense of an accurate handling of certain cut-off effects.

If the functions $f_l^I(\omega)$ are approximated by a finite number of δ-functions—a procedure that corresponds to replacing the left-hand branch cuts by a series of poles—then the integral equations (2.2) and (2.3) become algebraic and trivially soluble in terms of the residues of the poles. It will be verified below that

the S-dominant solutions obtained by numerical integration of the original CM-I equations ([2]), can be well approximated in this way and there seems to be no reason why such an approach should be less accurate when the P-wave is large. The essential question, then, is how to determine the residues and positions of the poles, or in other words the strength and range of the various contributing interactions.

Since the poles are inserted as an approximation to the left-hand branch cuts, the equations used to determine them will be relations between the left and right cuts. From these relations it is possible to obtain sufficient equations to determine the positions and residues of the poles in terms of the parameters λ and λ_1. These equations contain more information than the exact crossing relations at the symmetry point, which we showed in the last section to be insufficient.

To achieve our object, let us first consider not quite the S- and P-amplitudes but $A^{0,2}$ and $(\partial/\partial\cos\theta)A^1$ evaluated at $\cos\theta = 0$. From eq. (IV.10) and (IV.11) of CM-I, keeping only S and P imaginary parts, we may derive the following formulas, which show the relative contributions to these functions from the right-hand and left-hand cuts ([4]):

$$(4.1)\qquad \mathscr{F}_{0,2}(\nu) = A^{0,2}(\nu, 0) = \begin{pmatrix} -5 \\ -2 \end{pmatrix}\lambda + \frac{\nu-\nu_0}{\pi}\int_0^\infty \frac{d\nu'}{\nu'-\nu}\,\frac{\operatorname{Im} A^{(0)1}(\nu')}{\nu'-\nu_0} -$$

$$-\frac{1}{2}\,\frac{\nu-\nu_0}{\pi}\int_0^\infty \frac{d\nu'}{\nu'-\nu_0+\frac{1}{2}(\nu-\nu_0)}\left\{\begin{pmatrix} 2/3 \\ 2/3 \end{pmatrix}\frac{\operatorname{Im} A^{(0)0}(\nu')}{\nu'-\nu_0} -\right.$$

$$\left. -\begin{pmatrix} 10/3 \\ 1/3 \end{pmatrix}\frac{\operatorname{Im} A^{(0)2}(\nu')}{\nu'-\nu_0} + \begin{pmatrix} -2 \\ 1 \end{pmatrix} 9\,\frac{\operatorname{Im} A^{(1)1}(\nu')}{\nu'}\right\};$$

$$(4.2)\qquad \mathscr{F}_1(\nu) = \frac{1}{3}\left[\frac{\partial}{\partial\cos\theta}\,\frac{A^1(\nu,\cos\theta)}{\nu}\right]_{\cos\theta=0} = \frac{1}{\pi}\int_0^\infty d\nu'\,\frac{\operatorname{Im} A^{(1)1}(\nu')}{\nu'(\nu'-\nu)} +$$

$$+\frac{1}{2\pi}\int_0^\infty \frac{d\nu'}{[\nu'-\nu_0+\frac{1}{2}(\nu-\nu_0)]^2}\left\{\frac{2}{9}\operatorname{Im} A^{(0)0}(\nu') -\right.$$

$$\left. -\frac{5}{9}\operatorname{Im} A^{(0)2}(\nu') + \frac{\nu'-\nu_0+2(\nu-\nu_0)}{\nu'}\operatorname{Im} A^{(1)1}(\nu')\right\}.$$

([4]) In deriving these formulas, we use the fact that the contribution to the first term of eq. (IV.10) and (IV.11) of CM-I from the left-hand cut just cancels the integral over the logarithm in these equations.

Evidently, the first integral in each case is the contribution from the right cut and the second integral that from the left.

The importance of these formulas lies in the fact that at the symmetry point the contributions from the left are simply related to those from the right. Defining

$$A_R^{(0)I}(\nu) = \frac{\nu - \nu_0}{\pi} \int_0^\infty \frac{d\nu'}{\nu' - \nu} \frac{\operatorname{Im} A^{(0)I}}{\nu' - \nu_0}, \tag{4.3}$$

and

$$\frac{A_R^{(1)1}(\nu)}{\nu} = \frac{1}{\pi} \int_0^\infty \frac{d\nu'}{\nu' - \nu} \frac{\operatorname{Im} A^{(1)1}(\nu')}{\nu'}, \tag{4.4}$$

where the meaning of the notation is obvious, we see by inspection of eq. (4.1) and (4.2) that at $\nu = \nu_0$, we have

$$\frac{d}{d\nu}\mathcal{F}_{0,2} = \begin{pmatrix} 2/3 \\ -1/3 \end{pmatrix} \frac{d}{d\nu} A_R^{(0)0} + \begin{pmatrix} -5/3 \\ 5/6 \end{pmatrix} \frac{d}{d\nu} A_R^{(0)2} + 9 \begin{pmatrix} 1 \\ -1/2 \end{pmatrix} \begin{pmatrix} A_R^{(1)1} \\ \nu \end{pmatrix}, \tag{4.5}$$

$$\frac{d^2\mathcal{F}_{0,2}}{d\nu^2} = \begin{pmatrix} 7/6 \\ 1/6 \end{pmatrix} \frac{d^2}{d\nu^2} A_R^{(0)0} + \begin{pmatrix} 5/6 \\ 13/12 \end{pmatrix} \frac{d^2}{d\nu^2} A_R^{(0)2} - 9 \begin{pmatrix} 1 \\ -1/2 \end{pmatrix} \frac{d}{d\nu} \begin{pmatrix} A_R^{(1)1} \\ \nu \end{pmatrix}, \tag{4.6}$$

$$\mathcal{F}_1 = \frac{1}{9} \frac{d}{d\nu} A_R^{(0)0} - \frac{5}{18} \frac{d}{d\nu} A_R^{(0)2} + \frac{3}{2} \frac{A_R^{(1)1}}{\nu}, \tag{4.7}$$

$$\frac{d}{d\nu}\mathcal{F}_1 = -\frac{1}{18} \frac{d^2}{d\nu^2} A_R^{(0)0} + \frac{5}{36} \frac{d^2}{d\nu^2} A_R^{(0)2} + \frac{3}{2} \frac{d}{d\nu} \left(\frac{A_R^{(1)1}}{\nu} \right). \tag{4.8}$$

There are, in fact, relations of this kind for all derivatives at the symmetry point, but these four will suffice for our purposes. It may easily be verified that they satisfy the exact conditions (3.10) to (3.12) of the preceding section. Of course the above conditions have more content and correspondingly are not exact; the imaginary parts of amplitudes for $l > 1$ have been dropped in their derivation. The chief error is associated with the cut-off effect. That is to say, in (4.1) and (4.2) we should reduce the contribution from the left branch cuts by an amount that varies inversely with the cut-off. An estimate made below shows that this error is non-negligible for the expected position of the cut-off; however, the qualitative features of the problem are not changed by disregarding the effect of a cut-off in these formulas.

Accepting the derivative relations (4.5) to (4.8), we can calculate the positions and residues of the poles which are to replace the unphysical cuts of the partial-wave amplitudes. It is easy to establish that at the symmetry

point the values of $\mathscr{F}_{0,1,2}(\nu)$, as well as the first two derivatives, are well approximated by the S- and P-wave parts of these functions. One may make the correction in a self-consistent calculation through formulas of the type (V.18) of CM-I, but here we ignore such refinements. If we remember that

$$A^{(0)I}(\nu) = a_I + A_R^{(0)I}(\nu) + A_L^{(0)I}(\nu) \tag{4.9}$$

and

$$\frac{A^{(1)1}(\nu)}{\nu} = \frac{A_R^{(1)1}}{\nu} + \frac{A_L^{(1)1}}{\nu}, \tag{4.10}$$

the symmetry-point conditions (4.5) to (4.8) become approximately

$$\frac{\mathrm{d}}{\mathrm{d}\nu} A_L^{(0)I} = \begin{pmatrix} -1/3 \\ -1/3 \end{pmatrix} \frac{\mathrm{d}}{\mathrm{d}\nu} A_R^{(0)0} + \begin{pmatrix} -5/3 \\ -1/6 \end{pmatrix} \frac{\mathrm{d}}{\mathrm{d}\nu} A_R^{(0)2} + 9 \begin{pmatrix} 1 \\ -1/2 \end{pmatrix} \begin{pmatrix} A_R^{(1)1} \\ \nu \end{pmatrix}, \tag{4.11}$$

$$\frac{\mathrm{d}^2}{\mathrm{d}\nu^2} A_L^{(0)I} = \begin{pmatrix} 1/6 \\ 1/6 \end{pmatrix} \frac{\mathrm{d}^2}{\mathrm{d}\nu^2} A_R^{(0)0} + \begin{pmatrix} 5/6 \\ 1/12 \end{pmatrix} \frac{\mathrm{d}^2}{\mathrm{d}\nu^2} A_R^{(0)2} + 9 \begin{pmatrix} -1 \\ 1/2 \end{pmatrix} \frac{\mathrm{d}}{\mathrm{d}\nu} \begin{pmatrix} A_R^{(1)1} \\ \nu \end{pmatrix}, \tag{4.12}$$

$$\frac{A_L^{(1)1}}{\nu} = \frac{1}{9} \frac{\mathrm{d}}{\mathrm{d}\nu} A_R^{(0)0} - \frac{5}{18} \frac{\mathrm{d}}{\mathrm{d}\nu} A_R^{(0)2} + \frac{1}{2} \frac{A_R^{(1)1}}{\nu}, \tag{4.13}$$

and

$$\frac{\mathrm{d}}{\mathrm{d}\nu} \left(\frac{A_L^{(1)1}}{\nu} \right) = -\frac{1}{18} \frac{\mathrm{d}^2}{\mathrm{d}\nu^2} A_R^{(0)0} + \frac{5}{36} \frac{\mathrm{d}^2}{\mathrm{d}\nu^2} A_R^{(0)2} + \frac{1}{2} \frac{\mathrm{d}}{\mathrm{d}\nu} \left(\frac{A_R^{(1)1}}{\nu} \right). \tag{4.14}$$

The relations (4.11) to (4.14) could also have been derived from the fundamental crossing formula (V.8) of CM-I (or (2.7) above). Had we done so, the effect of a cut-off clearly would have been to reduce the coefficient of $A_R^{(1)1}/\nu$ on the right-hand side of relations (4.11) and (4.13). (At the same time the change in the higher derivative relations is much less important.) If the sharp resonance form (2.10) for $f_1^1(\omega)$ is cut-off at $\omega = \omega_c$, a simple calculation shows that the coefficient of $A_R^{(1)1}/\nu$ in (4.13) is reduced roughly by a factor $1 - 12(\nu_R/\omega_c)$. We shall have to consider such a reduction factor when evaluating the validity of results based on the above formulas.

5. – The S-wave problem by the pole approximation.

These formulas, (4.11) to (4.14), for the contribution from the left cuts of the partial-wave amplitudes tell us what we need to know about the equivalent poles. Consider first the S-waves, where we attempt to represent the left cuts in each case by a single pole:

$$A_L^{(0)I}(\nu) = b_I(\nu - \nu_0) \frac{\omega_{SI} + \nu_0}{\omega_{SI} + \nu}. \tag{5.1}$$

By the use of eq. (4.11) and (4.12), the values of b_I and ω_{sI} may be determined, since at the symmetry point we have

$$b_I = \frac{\mathrm{d}}{\mathrm{d}\nu} A_L^{(0)I}, \tag{5.2}$$

and

$$\frac{b_I}{\omega_{sI} + \nu_0} = -\frac{1}{2}\frac{\mathrm{d}^2}{\mathrm{d}\nu^2} A_L^{(0)I}. \tag{5.3}$$

It may be seen from eq. (4.11) [5] that b_2 is always negative, corresponding to attractive forces in the $I = 2$ state, but the sign of b_0 depends on the relative magnitudes of S- and P-wave scattering. The force in the $I = 0$ state due to S-pair exchange is attractive, but that due to P-pairs is repulsive.

Using the N/D technique of CM-I, we may immediately write down the S-wave amplitudes corresponding to eq. (5.1). Equations (V.11) and (V.14) of CM-I then become

$$N_0^I(\nu)) = a_I + (\nu - \nu_0)\frac{\omega_{sI} + \nu_0}{\omega_{sI} + \nu} B_I, \tag{5.4}$$

and

$$E_0^I(\omega) = 1 + (\omega + \nu_0)\{K(\omega, -\nu_0)a_I + (\omega_{sI} + \nu_0)K(\omega_{sI}, \omega)B_I\}, \tag{5.5}$$

where

$$B_I = b_I E_0^I(\omega_{sI}). \tag{5.6}$$

To implement the conditions (5.2) and (5.3), we first remember eq. (4.9) which allows us to write

$$\frac{\mathrm{d}^n A^{(0)I}}{\mathrm{d}\nu^n} = \frac{\mathrm{d}^n}{\mathrm{d}\nu^n} A_R^{(0)I} + \frac{\mathrm{d}^n}{\mathrm{d}\nu^n} A_L^{(0)I}. \tag{5.7}$$

---

[5] Note that from eq. (4.4), at the symmetry point, we have

$$\frac{\mathrm{d}^n}{\mathrm{d}\nu^n} A_R^{(0)I} = \frac{n!}{\pi}\int_0^\infty \mathrm{d}\nu' \sqrt{\frac{\nu'+1}{\nu'}}\,\frac{\sin^2\delta_0^I}{(\nu' + \frac{2}{3})^{n+1}} \qquad \text{for } n \geqslant 1$$

and

$$\frac{\mathrm{d}^n}{\mathrm{d}\nu^n}(A_R^{(1)1}/\nu) = \frac{n!}{\pi}\int_0^\infty \mathrm{d}\nu' \sqrt{\frac{\nu'+1}{\nu'^3}}\,\frac{\sin^2\delta_1'}{(\nu' + \frac{2}{3})^{n+1}} \qquad \text{for } n \geqslant 0,$$

so all «right-hand» functions and derivatives are positive.

In particular, at the symmetry point we have

$$\frac{\mathrm{d}A^{(0)I}}{\mathrm{d}\nu} = \frac{\mathrm{d}A_R^{(0)I}}{\mathrm{d}\nu} + b_I \,, \tag{5.8}$$

so that from eq. (4.11),

$$\frac{\mathrm{d}}{\mathrm{d}\nu} A^{(0)0} = -2\,\frac{\mathrm{d}}{\mathrm{d}\nu} A^{(0)2} = \frac{4}{3}\, b_0 - \frac{10}{3}\, b_2 - 18 \left(\frac{A_R^{(1)1}}{\nu}\right). \tag{5.9}$$

From eq. (5.4) and (5.5) we can calculate the derivative of the S-amplitudes at the symmetry point:

$$\frac{\mathrm{d}}{\mathrm{d}\nu} A^{(0)I} = B_I + a_I\{K(-\nu_0, -\nu_0)\, a_I + (\omega_{SI} + \nu_0)\, K(\omega_{SI}, -\nu_0)\, B_I\} \,. \tag{5.10}$$

Eq. (5.9) and (5.10), together with (5.6), determine b_0 and b_2 once ω_{SI} and $A_R^{1(1)}/\nu$ are given.

To establish the positions of the poles, we must consider the second derivative of the amplitudes. Again at the symmetry point, from eq. (5.7), we have

$$\frac{\mathrm{d}^2 A^{(0)I}}{\mathrm{d}\nu^2} = \frac{\mathrm{d}^2 A_R^{(0)I}}{\mathrm{d}\nu^2} - \frac{2b_I}{\omega_{SI} + \nu_0} \,, \tag{5.11}$$

so that from eq. (5.3), we can write

$$\frac{\mathrm{d}^2 A^{(0)I}}{\mathrm{d}\nu^2} = -\begin{pmatrix} 2/3 \\ 8/3 \end{pmatrix} \frac{b_0}{\omega_{S0} + \nu_0} + \begin{pmatrix} -40/3 \\ 2/3 \end{pmatrix} \frac{b_2}{\omega_{S2} + \nu_0} - \begin{pmatrix} 1 \\ -1/2 \end{pmatrix} 54\, \frac{\mathrm{d}}{\mathrm{d}\nu} \left(\frac{A_R^{(1)1}}{\nu}\right). \tag{5.12}$$

The second derivative of the S amplitudes may be calculated from eq. (5.4) and (5.5), so we have enough conditions to determine ω_{S0} and ω_{S2} if $A_R^{(1)1}/\nu$ and its derivative are given.

In general the problem is one of self-consistency, involving the P-wave. Let us consider first, however, the situation when the low-energy P phase-shift is so small that $A_R^{(1)1}$ and its derivatives may be set equal to zero. Such is the case for the solutions determined in reference [2] by numerical integration and iteration of the CM-I equations. One possible procedure for determining b_0, b_2, ω_{S0} and ω_{S2} in this simple case will now be described.

The first leg of eq. (5.9), together with eq. (5.10), gives a linear relation between B_0 and B_2,

$$\varrho_0 B_0 + \xi_0 + 2(\varrho_2 B_2 + \xi_2) = 0 \,, \tag{5.13}$$

where

$$\xi_I = a_I^2 K(\tfrac{2}{3}, \tfrac{2}{3}) \,, \tag{5.14}$$

and

$$\varrho_I = 1 + a_I(\omega_{sI} - \tfrac{2}{3})\, K(\omega_{sI}, \tfrac{2}{3}) \,. \tag{5.15}$$

The second leg of eq. (5.9), together with eq. (5.6), yields a quadratic relation,

$$\varrho_0 B_0 + \xi_0 = \frac{4}{3}\frac{B_0}{\varrho_0 + l_0 B_0} - \frac{10}{3}\frac{B_2}{\varrho_2 + l_2 B_2} \,, \tag{5.16}$$

where

$$l_I = (\omega_{sI} - \tfrac{2}{3})^2 K(\omega_{sI}, \omega_{sI}) \,. \tag{5.17}$$

Taken together, eq. (5.16) and (5.13) correspond to a cubic equation for either B_0 or B_2 separately, which can easily be solved once a_I and ω_{sI} are given. It turns out that there is only one real root of the equation.

The relations (5.12) are transcendental, so our procedure is to guess ω_{s0} and ω_{s2}, solve eq. (5.13) and (5.16) for B_0 and B_2, and then check to see how badly eq. (5.12) is violated. The two pole positions are then adjusted until eq. (5.12) is finally satisfied. For small values of λ, it can easily be shown that

$$\omega_{s0} - \frac{2}{3} = \omega_{s2} - \frac{2}{3} = 2\,\frac{[-(\mathrm{d}/\mathrm{d}\omega)\, K(\frac{2}{3}, \omega)]_{\omega=\frac{2}{3}}}{K(\frac{2}{3}, \frac{2}{3})} = 3.43 \,,$$

or

$$\omega_{s0} = \omega_{s2} = 4.1 \,.$$

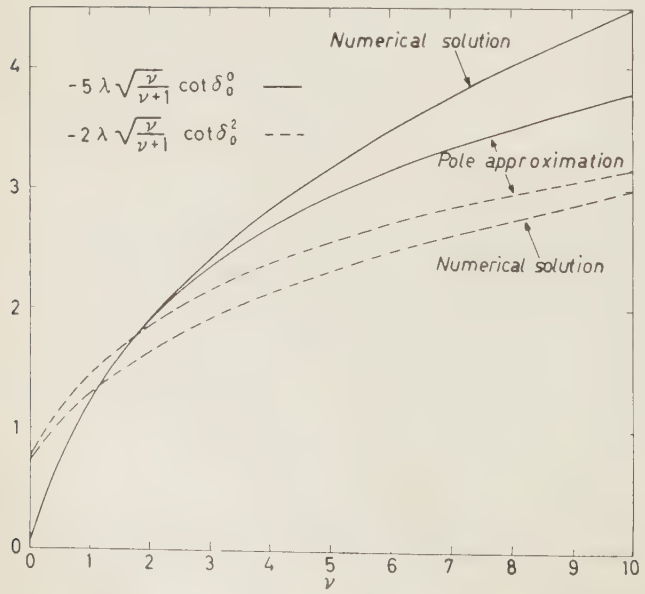

As λ increases in the negative (attractive) direction, both ω_{s0} and ω_{s2} decrease, the latter slightly faster than the former. However, at the time the $I = 0$ bound state is reached ($\lambda = -0.46$), the two

Fig. 1. – The single-pole approximation to the S-dominant solution for $\lambda = 0.433$, compared to the numerical solution of reference [2].

poles are still quite close together. For example, at $\lambda = -0.433$ we find $\omega_{S0} = 2.5$ and $\omega_{S2} = 2.7$. At the same time, we have $b_0 = 0.42$ and $b_2 = 0.27$. In Fig. 1 is shown, for this value of λ, a comparison between the pole approximation and the numerical solution obtained in reference ([2]). One observes that there are no important differences.

The value of λ we have chosen for our example, -0.433, is barely small enough not to give a bound state, and the error in the pole approximation is consequently a maximum. This circumstance occurs not only because the relative importance of the left-hand cut is greater for greater magnitudes of λ, but also because the dominant part of the right-hand cut is now at the lowest possible energy. It follows by crossing symmetry that the « average position » of the left-hand cut will be close to the low-energy physical region and the error in replacing it by a pole will be relatively large.

6. – The P-dominant problem in the pole approximation.

Our task now is to repeat the approach of the preceding section when the low-energy P-wave phase shift is allowed to become large. The coupled S-P problem is quite complicated, so we begin by assuming that the contribution of S-pair exchange to the left cut of the P-wave is small and that the main force in the P-state comes from the exchange of a P-wave pair. In other words, we neglect the contribution to eq. (4.13) from the S-wave terms on the right. Such an approximation is not quantitatively reliable, but it serves to show certain essential features of the large P-wave situation. In any case, an accurate calculation must include a cut-off correction as well as the S-wave.

The symmetry-point conditions (4.13) and (4.14) become, in this approximation,

$$\frac{A_L^{(1)1}}{\nu} = \frac{1}{2}\frac{A_R^{(1)1}}{\nu}, \tag{6.1}$$

and

$$\frac{\mathrm{d}}{\mathrm{d}\nu}\left(\frac{A_L^{(1)1}}{\nu}\right) = \frac{1}{2}\frac{\mathrm{d}}{\mathrm{d}\nu}\left(\frac{A_R^{(1)1}}{\nu}\right), \tag{6.2}$$

and we may add the corresponding second-derivative condition,

$$\frac{\mathrm{d}^2}{\mathrm{d}\nu^2}\left(\frac{A_L^{(1)1}}{\nu}\right) = -\frac{5}{8}\frac{\mathrm{d}^2}{\mathrm{d}\nu^2}\left(\frac{A_R^{(1)1}}{\nu}\right), \tag{6.3}$$

which is easily obtained from eq. (4.2). Now, the fact that both $A_L^{(1)1}/\nu$ and

its first derivative at the symmetry point are positive means that a single pole cannot represent the left cut ([5]), since a function of the type

$$\frac{c}{\omega_p + \nu},$$

has the opposite sign to its first derivative so long as $\omega_p + \nu$ is positive. We shall therefore need two poles, the outer one attractive and the inner one repulsive in order to satisfy conditions (6.1) and (6.2). This circumstance could have been anticipated from formula (2.10).

We write, then,

$$\frac{A_L^{(1)1}}{\nu} = c_A \frac{\omega_A + \nu_0}{\omega_A + \nu} - c_R \frac{\omega_R + \nu_0}{\omega_R + \nu}, \tag{6.4}$$

where the subscripts A and R stand for « attractive » and « repulsive », respectively. Here c_A and c_R are defined so as to be both positive, and the normalization is such that at $\nu = \nu_0$, we have

$$\frac{A_L^{(1)1}}{\nu} = c_A - c_R, \tag{6.5}$$

$$\frac{\mathrm{d}}{\mathrm{d}\nu}\left(\frac{A_L^{(1)1}}{\nu}\right) = \frac{c_R}{\omega_R + \nu_0} - \frac{c_A}{\omega_A + \nu_0}, \tag{6.6}$$

and

$$-\frac{1}{2}\frac{\mathrm{d}^2}{\mathrm{d}\nu^2}\left(\frac{A_L^{(1)1}}{\nu}\right) = \frac{c_R}{(\omega_R + \nu_0)^2} - \frac{c_A}{(\omega_A + \nu_0)^2}. \tag{6.7}$$

Observe now that the repulsive pole will dominate both in eq. (6.6) and (6.7) if ω_R is substantially smaller than ω_A, so there is effectively only the one condition (6.5) restricting the attractive-pole position and residue, and one parameter remains arbitrary ([6]).

This free parameter corresponds to the cut-off that would have to be introduced in (2.7) if we were to attempt to solve the equations of CM-I. In our pole approach here we do not speak of a cut-off, but the position of the outer (attractive) pole is a closely related concept. Actually it is more convenient to introduce the free parameter as the value of λ_1, defined by eq. (3.16), a procedure that through eq. (3.18) amounts to specifying $C_A - C_R$. It should be

([6]) If higher-derivative conditions were invoked, these would serve only to determine the parameters of new poles that are closer to the physical region than ω_R.

noted that λ_1 will not have an unlimited range of possible values. For example, in the approximation (6.1), we have

$$\frac{1}{3}\lambda_1 = \frac{3}{2}\frac{A_R^{(1)1}}{\nu},$$

so λ_1 is necessarily positive. (When S-waves and the cut-off correction are included, small negative values for λ_1 may become possible.)

Corresponding to eq. (6.4) we find, from eq. (V.24) and (V.26) of CM-I,

$$N_1(\nu) = C_A \frac{\omega_A + \nu_0}{\omega_A + \nu} - C_R \frac{\omega_R + \nu_0}{\omega_R + \nu}, \tag{6.8}$$

and

$$E_1(\omega) = 1 + (\omega + \nu_0)\{C_A[\omega_A K(\omega_A, \omega) + \nu_0 K(\omega_A, -\nu_0)] - C_R[\omega_R K_R(\omega_R, \omega) + \nu_0 K(\omega_R, -\nu_0)]\}, \tag{6.9}$$

where

$$\left\{\begin{array}{l} C_A = c_A E_1(\omega_A), \\ \text{and} \\ C_R = c_R E_1(\omega_R). \end{array}\right. \tag{6.10}$$

By using eq. (4.10) at the symmetry point, it is then a straightforward if tedious calculation to find values of C_A, C_R, ω_A, and ω_R that satisfy conditions (4.1) to (4.3) for various choices of λ_1.

Carrying out this program, we found that as λ_1 varies from zero to unity, the position ω_R of the repulsive pole moves only slightly—from 5 to about 3.5—while the attractive pole moves from infinity down to about 8. It was decided then, for simplicity, to fix the position of the repulsive pole at 4.0 and to ignore the second-derivative condition (6.3). The maximum violation of the second derivative condition is never worse than about 20% under these circumstances and in Fig. 2 the insensitivity of the solution to the position of the repulsive pole is demonstrated. The two functions shown correspond to the same value of λ_1 (0.81) and both satisfy the conditions (5.1) and (6.2). In one case, however, the pole positions are $\omega_A = 10$, $\omega_R = 4$, while in the other they are $\omega_A = 7$, $\omega_R = 6$. In the first instance the violation of the second-derivative condition (6.3) is 18%, while in the second it is 40%; nevertheless, the difference in the physical region is negligible. This insensitivity shows that the detailed form of the left-hand discontinuity is unimportant so long as the symmetry-point conditions on the function and its first derivative are satisfied.

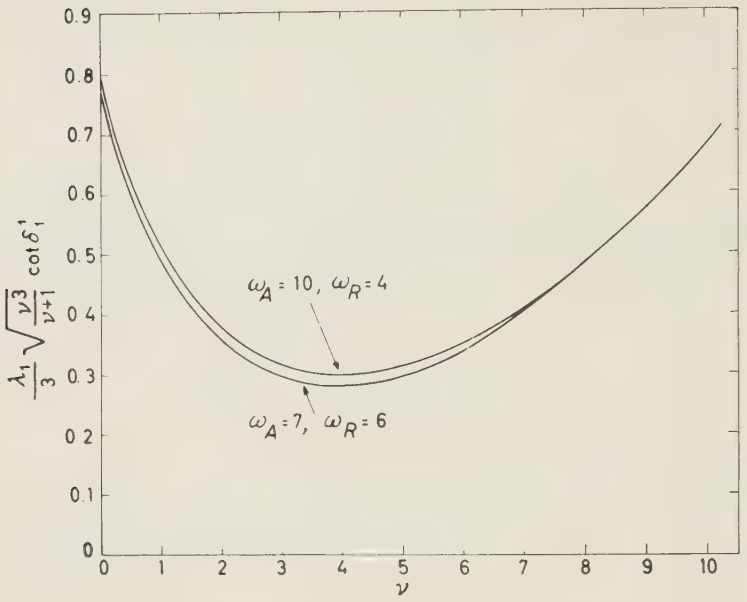

Fig. 2. – Two double-pole, P-wave solutions for $\lambda_1 = 0.84$. Both solutions satisfy conditions (4.1) and (5.2) but violate (5.3) by widely varying amounts.

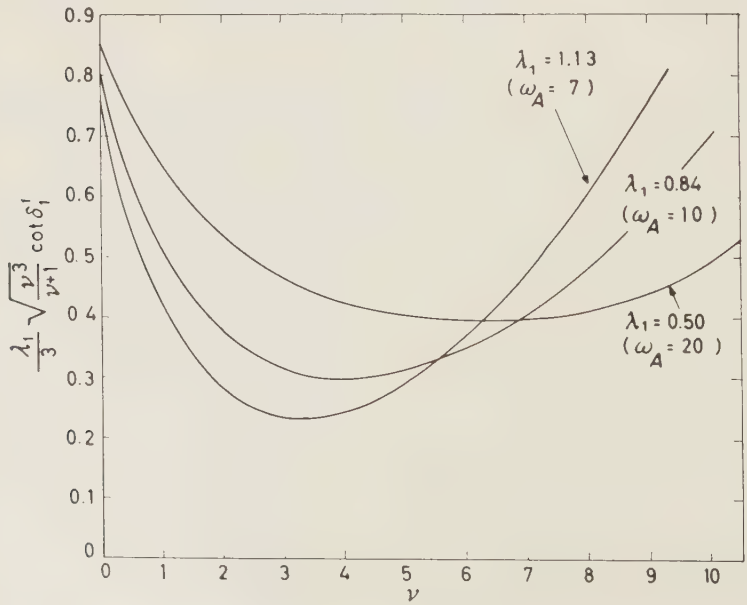

Fig. 3. – Double-pole solutions based on conditions (6.1) and (6.2) for three different values of λ_1, with the repulsive-pole position fixed at $\omega_R = 4$.

Thus the replacement of the left-cut by poles seems justified. Unfortunately, the main error in our approach stems from a cut-off modification of the symmetry-point condition (6.1).

In Fig. 3 are shown P-wave solutions with $\omega_R = 4$, satisfying (6.1) and (6.2) for three different values of λ_1. One sees that with ω_A in the anticipated range, these are of a resonance character, although the phase shift never actually passes through 90°. The resonance position is satisfactory for $\lambda_1 \sim 1$, but the width is about twice that implied by nucleon electromagnetic structure, according to the calculations of FRAZER and FULCO [3]. However, the presence of the repulsive pole has been tremendously effective in narrowing the resonance. Without it, we would not even approach the required width, and when the repulsion is augmented by S-wave contributions and the cut-off correction included, it may be possible to achieve the desired additional narrowing through reduction of λ_1.

The cut-off correction to eq. (6.1) produces a substantial narrowing of the resonance. For example, the uncoupled P-wave equations of CM-I with a cut-off have been solved numerically for $\lambda_1 = 0.53$, with the result shown in Fig. 4.

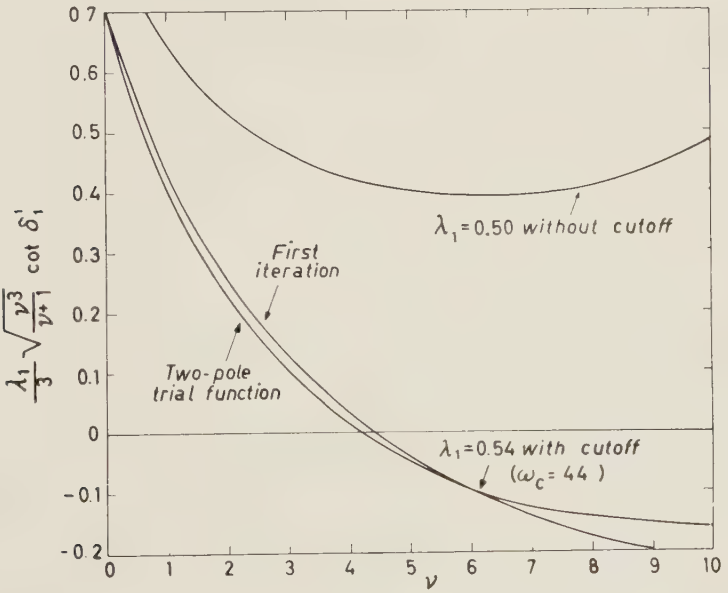

Fig. 4. – Numerical solution of the uncoupled and cut-off P-wave equations for $\lambda_1 = 0.54$. A double-pole solution based on conditions (6.1) and (6.2) for $\lambda_1 = 0.50$ is shown for comparison.

Here the phase shift actually passes through 90° and the resonance is about 40% narrower than in the family of solutions shown in Fig. 3. The method

of solution was to use as a trial function a two-pole P-amplitude of the form (6.8) and (6.9), but with C_A, C_R, ω_A, and ω_R completely arbitrary. These four parameters were then varied until one complete cycle of the CM-I equations (with a cut-off and no S-wave) approximately reproduced the trial function in the physical region. No attempt was made to get the best possible reproduction. Fig. 4 shows the pole function for $C_A = 0.38$, $C_R = 0.20$, $\omega_A = 25$, and $\omega_R = 4$ compared to the first iteration of the uncoupled P equations, with the cut-off at $\omega_c = 44$. Also shown is a solution satisfying conditions (4.1) and (6.2) for a comparable value of λ_1.

One may ask how badly our solution of the cut-off equations violates the condition (6.1). The answer is in rough agreement with the estimate of Section **4** that a cut-off correction factor of $\sim (1 - 12(v_R/\omega_c))$ should be applied to the right-hand side of condition (6.1). In the example of Fig. 4, we have $\omega_c = 44$ and $v_R \sim 3$. It is not surprising then to find that for our solution we have $A_L^{(1)1} \approx 0$; in other words, the contributions from the attractive and repulsive interactions now just about cancel each other at the symmetry point. One can show from conditions (6.1), (6.2), and (6.3) that, before the cut-off correction, the contribution from the attractive pole is generally about twice that of the repulsive. Thus, the cut-off reduces the attraction by about a factor of two (and of course left the repulsion alone).

If one takes literally the results of FRAZER and FULCO [3], some further narrowing of the P-resonance is desirable. This might be accomplished through an increase of our long-range repulsion as a result of S-pair exchange. Our experience with S-dominant solutions showed that the force due to S-pair exchange cannot by itself produce a P-resonance [2], but if exchange in the $I = 2$ S-state is more important than that for $I = 0$, there will be a net long-range *repulsion* in the $I = 1$ state that can narrow the P-resonance, provided the basic intermediate-range *attraction* is supplied by some other source. We have shown above that P-pair exchange can provide the necessary intermediate-range attraction as well as *some* long-range repulsion. It will require further calculation to establish whether values for λ and λ_1 actually can be found that make the $I = 2$ S-pair exchange sufficiently important to give the desired additional repulsion. Such calculations are being undertaken and will be described in a later paper. Qualitatively it seems likely that if P-resonance narrowing requires a preponderance of $I = 2$ over $I = 0$ S-pairs, the value of λ will be positive (repulsive). One sees from formula (4.11) that in this case a strong P-exchange force alters the 2 : 5 symmetry-point ratio of the $I = 2$ and $I = 0$ amplitudes so as to favor the former in the physical region.

7. – Conclusion.

The reader may well find confusing the question as to how many independent parameters there are in the $\pi\pi$ problem. On a completely fundamental level, when all other particles and interactions are considered, there may be none; even the pion mass may someday be related to other masses. However, one does not see at present even the outline of a procedure for calculating m_π, and the same statement may be made for the constant λ. This constant is not supposed to be calculable in conventional field theory, and in the S-matrix dispersion-theory approach one correspondingly finds that the combined requirements of Lorentz invariance, analyticity, and unitarity permit *one* independent real parameter in the π-π interaction. Further independent parameters are *not* allowed, but as explained in Section 2, our definition of λ is somewhat arbitrary, so it is possible that more than one solution exists fo a given λ.

In this paper we have introduced a second parameter, λ_1, which has been treated as independent of λ for the large P-wave type of solution. However, we believe that λ_1 represents parts of the interaction that are at present difficult to calculate, and that eventually it will be possible to determine λ_1 once λ is given. For the S-dominant type of solution, the procedure for calculating λ_1 has already been established.

The question still remains, assuming that λ_1 is a function of λ, as to whether the large P-wave solutions can be reached by a continuous variation of λ, starting with S-dominant solutions. We do not know the answer to this question, and it appears that the answer will not be known until enough of the high-energy contributions can be included to produce a natural cut-off.

On the practical level, a further possible source of confusion arises from the circumstance that, for the large P-wave solution, we have here discussed a crude approximation in which the P phase-shift is controlled entirely by λ_1, without any specification of λ. Needless to say, such is not the case in general. It is also worth emphasizing that in this second type of solution, the S phase-shifts will depend as much on λ_1 as on λ. In a later paper this dependence will be investigated, together with the P phase-shift dependence on λ.

In conclusion we remind the reader that if an as yet undiscovered « elementary » particle exists, with the quantum numbers of a two-pion system and a mass greater than $2m_\pi$ (so that it is unstable), then the $\pi\pi$ scattering amplitude must include further independent parameters associated with this particle. Our approach could be generalized to accommodate such a situation, but for the moment we may hope that there are no « hidden » elementary particles.

RIASSUNTO (*)

Si mostra che quando lo scattering pione-pione in onda P è grande a basse energie, le equazioni integrali formulate in precedenza dagli autori richiedono un cut-off. Per il cut-off e per la natura instabile della soluzione, il procedimento di integrazione numerica diviene molto più complicato. Le equazioni originarie vengono perciò sostituite da una serie di condizioni al centro di simmetria, ed i tagli non fisici delle ampiezze delle onde parziali sono sostituiti da una corrispondente serie di poli. Entro questo schema non occorre parlare di un cut-off, ma compare un nuovo parametro. Si possono trovare soluzioni autocongruenti in cui una risonanza dell'onda P è sostenuta da un meccanismo a «stringa»; cioè una intensa forza di attrazione nello stato $I=1$ nasce dallo scambio di una coppia in risonanza di pioni dell'onda P. Le condizioni nel centro di simmetria adottate sarebbero modificate dal cut-off e non si tenta, pertanto, di raggiungere la esattezza quantitativa; tuttavia non ci si attende che questa ed altre correzioni modifichino la natura qualitativa delle nostre soluzioni. Si fanno alcune grossolane valutazioni delle correzioni.

(*) *Traduzione a cura della Redazione.*

IL NUOVO CIMENTO Vol. XIX, N. 4 16 Febbraio 1961

Some Remarks on the Phase-Shift Analysis with D-waves for Track-Chamber Histograms.

I. Derado and R. Van de Walle (*)

CERN - Geneva

(ricevuto il 17 Novembre 1960)

Summary. — A possible new method of phase-shift analysis of track-chamber histograms is discussed. Methods available for correcting the angular distribution for Coulomb scattering and for calculating the phase-shift errors are considered. As an example of application a re-analysis is given of the π^+-scattering experiment at 310 MeV of Foote *et al.* (1)

1. – Introduction.

The measurement of D-waves in π-p scattering could give among other things, evidence of an eventual π-π interaction. The energy region situated between 250 and 400 MeV is particularly favourable for such a D-wave analysis, as at a lower energy they are too small to be observed and at higher energy the imaginary part of phase-shifts can no longer be neglected and thus the interpretation is no longer unique.

As the D-wave contributions are most explicitly present in the small angle data, visual techniques are particularly suitable for measuring. However, when a π-p elastic-scattering angular distribution is obtained in the form of a histogram, the methods to be applied to obtain the phase-shifts are somewhat different from those normally used in analysing counter distribution results.

There are two steps in the calculation (**). Firstly, a polynomial in $\cos\theta$

(*) On leave of absence from the « Inter-University Institute for Nuclear Sciences », Belgium.

(1) J. Foote, O. Chamberlain, E. H. Rogers, H. M. Steiner, C. Wiegand and T. Ypsilantis: *Phys. Rev. Lett.*, **4**, 30 (1960).

(**) For all details the reader is referred to ref. (2).

(2) I. Derado and R. Van de Walle: CERN 60-21.

or $P_i(\cos\theta)$ (θ: CM-scattering-angle) must be fitted to the angular distribution, *i.e.* the angular distribution is forced into the known form it must have according to the formalism of partial wave-analysis.

Using either a least-squares or a maximum likelihood method according to the « richness » of each individual $\cos\theta$-interval of the histogram under consideration a set of polynomial coefficients C_i and an error-matrix G^{-1} associated with these quantities is obtained.

The fact whether a certain partial wave component is present or not can be statistically establisted by comparing χ^2-values for different order fits, or more quantitatively by calculating the F-test-variate and using tables of Fisher-distributions.

The second step consists of looking for a set of phase shifts $\underline{\alpha}$ representing with a sufficient accuracy the C_i-coefficients previously mentioned.

Let us define

$$M = \sum_i \sum_j [C_i - F_i(\underline{\alpha})] \cdot G_{ij} \cdot [C_j - F_j(\underline{\alpha})] ,$$

$F_i(\underline{\alpha})$ being the theoretical expression for the C_i-quantities as a function of the involved phase-shifts as predicted by the isospin-formalism and the charge-independence hypothesis, and G_{ij} the ith-jth element of the inverse matrix of the previously mentioned C_i-error-matrix. Then a general and convenient procedure to obtain the desired set or sets of phase-shifts consists of searching for minima of M as a function of α_i.

There are several methods which can be used to find the minima of the M-surface.

As sufficiently approximate starting values for each of the type of solutions wanted can be obtained either by using inter or extrapolations of existing experimental data or by having recourse to graphical methods, the use of very strong convergence procedures based on the *a priori* knowledge of such starting values are permissible.

A very convenient method in this respect has been described by NIERENBERG [3] and consists of an iteration procedure using the second order derivatives of the M-surface. It is geometrically equivalent to a fitting of a second order surface to the M-surface at the trial point and taking the minimum of the fitted surface as a next trial point.

This method can be considered as an extension of the more familiar method « steepest descent » in which the information « borrowed » from the hypersurface at the trial point is limited to the values of the first-order derivatives, or in other words, to the *direction* in which an eventual minimum will lie.

---

[3] W. NIERENBERG: UCRL - 3816 - Rev.

To perform the operations implied by the methods described, a set of Mercury computer programmes was written, specifying the second-step part in the special case of π^+-p scattering and only SPD-wave contribution. As an example of application of this method and in order to test the programmes a re-analysis was made of the π^+-p angular distribution obtained by J. FOOTE *et al.* [1] using counter techniques.

Using the method normally adopted in analysing counter-results, these authors obtain the Fermi-solution shown in Table I-(*a*).

TABLE I. – *Fermi-Solutions.*

	α_3	α_{31}	α_{33}	δ_{33}	δ_{35}	
a	$-17.7^0 \pm 1.2^0$	$-3.5^0 \pm 0.8^0$	$131.2^0 \pm 1.7^0$	$2.4^0 \pm 0.5^0$	$-5.0^0 \pm 0.6^0$	FOOTE *et al.* [1]
b	-19.8^0	-5.1^0	132.8^0	0.8^0	-4.2^0	Fermi I
c	-21.7^0	-6.2^0	133.2^0	-0.8^0	-2.4^0	Fermi II
d	-18.1^0	-4.1^0	132.9^0	2.4^0	-4^0	Fermi I (incomplete distribution)
e	$-18.2^0 \pm 1.8^0$	$-4.0^0 \pm 0.9^0$	$133.1^0 \pm 0.2^0$	$2.1^0 \pm 1.5^0$	$-5.1^0 \pm 1.4^0$	Fermi I (corrected)

It should be pointed out that the authors quoted have taken polarization data directly into account. This is a procedure we will not follow as it is not likely that such polarization results will be present in track-chamber measurements. Furthermore we will also treat the published results as though they were absolute measurements neglecting overall uncertainties coming from normalization (*).

The coefficients C_i, their errors, and the associated χ^2-value resulting from a first SP and SPD-least-squares fit on the complete angular distribution, are shown in Tables II and III.

Taking into account the fact that the number of degrees of freedom for both fit is given by 13 and 11 respectively, the two corresponding χ^2-values

(*) In actual applications and in those cases where sufficiently rich histograms will be available, it might be necessary to modify the first step least-squares fits in order not to be restricted by the precision of the total cross-section used for normalization. Among other things this would imply the use of non-linear least-squares methods.

TABLE II. – *SP-fit* (*complete distribution*).

C_i	ΔC_i	$\lambda^2 C_i$ (mb)	
0.542	0.019	2.286	
1.124	0.037	4.745	$\chi^2 \simeq 38$
1.933	0.064	8.156	$(\nu = 13)$

TABLE III. – *SPD-fit* (*complete distribution*).

C_i	ΔC_i	$\lambda^2 C_i$ (mb)	
0.510	0.009	2.151	
0.949	0.024	4.005	
2.108	0.075	8.894	
0.445	0.056	1.880	$\chi^2 \simeq 4$
0.04	0.104	0.059	$(\nu = 11)$

clearly indicate that D-waves have to be taken into account in order to obtain a satisfactory fit to the measurements (*).

Performing a phase-shift analysis on these rough uncorrected C_i-values in the manner described, with the adopted restriction of Fermi-type solutions, the solutions shown in Table I (*b* and *c*) are obtained. Some other solutions were also found, not shown in Table I, which were rejected as they were associated with large M-values.

By comparing the recoil-proton polarization predicted by both Fermi I and II-solutions with the experimental values obtained by FOOTE *et al.*, it was clearly demonstrated that the Fermi I-solution was to be preferred.

In order to correct the angular distribution for Coulomb-effects a method has been adopted which is a straightforward relativistic extension of the procedures used at lower energies for S and P-waves by ASHKIN and collaborators (4).

It involves the calculation of a correction-curve with the help of a set of phase-shifts derived from the original distribution after omission of the forward scattering information (see Appendix A).

(*) The *SPD*-χ^2 value is somewhat low. As in the case of too large χ^2-value this means an improbable hypothesis, but unlike that case, it implies a good fit. It is a general experience, however, that χ^2-values which are too small should not be given the same weight as the reverse. They are very often the consequence of a too pessimistic assumption of the errors or a not quite normal distribution of the initial measurements.

(4) J. ASHKIN, J. P. BLASER, F. FEINER and M. D. STERN: *Phys. Rev.*, **101**, 1149 (1956).

After correction of the angular distribution for Coulomb scattering a re-determination of the C_i-quantities becomes necessary. In Table V the new coefficients are shown while in Table VI the full correlation-matrix is given, both for the case of the Fermi I-solution.

TABLE IV. – *SPD-fit (incomplete distribution).*

C_i	ΔC_i	$\lambda^2 C_i$ (mb)	
0.510	0.009	2.151	
0.965	0.027	4.072	
2.128	0.075	8.974	
0.370	0.080	1.561	$\chi^2 \simeq 3$
— 0.073	0.121	— 0.309	($\nu = 9$)

TABLE V. – *SPD-fit (corrected distribution - Fermi I).*

C_i	ΔC_i	$\lambda^2 C_i$ (mb)	
0.510	0.008	2.152	
0.946	0.024	3.992	
2.087	0.074	8.806	
0.362	0.055	1.529	$\chi^2 \simeq 4$
— 0.054	0.102	— 0.226	($\nu = 11$)

TABLE VI. – *Correlation-matrix (corrected distribution - Fermi I).*

$-0.77 \cdot 10^{-4}$	$-0.04 \cdot 10^{-4}$	$-4.83 \cdot 10^{-4}$	$-0.37 \cdot 10^{-4}$	$5.15 \cdot 10^{-4}$
	$5.68 \cdot 10^{-4}$	$6.12 \cdot 10^{-4}$	$-11.17 \cdot 10^{-4}$	$-11.68 \cdot 10^{-4}$
		$55.48 \cdot 10^{-4}$	$-15.87 \cdot 10^{-4}$	$-69.96 \cdot 10^{-4}$
			$30.14 \cdot 10^{-4}$	$34.98 \cdot 10^{-4}$
				$103.97 \cdot 10^{-4}$

Final phase-shift calculations were then made and the results can be found in Table I-*e*).

For the final solution the errors were calculated using both methods described in Appendix B. The results can also be found in Table I-*e*). In this discussion and in parallel with the authors quoted, the effects on the phase-shift treatment coming from a noticeable inelastic cross-section at 310 MeV have been neglected. The same authors performed, however, some calculation about possible influences of some inelastic contribution on the phase-shifts with the conclusion that these changes would probably lie within the limits set by the errors of Table I-*a*).

2. – Conclusions.

1) Comparison of lines (*a*) and (*e*) of Table I leads to the conclusion that both methods give *essentially* the same results. Our results for Fermi I-solution are within the errors of FOOTE *et al.* and in agreement with their results and vice-versa.

The small differences between both phase-shift-results are due to the fact that the authors quoted took polarization-data directly into account.

2) The main distinction between the results lies in the errors obtained.

The *D*-errors we obtained are at least 2 times larger than the corresponding errors of Foote while our α_{33}-error is an order of magnitude smaller. The fact that the relative behaviour of our α_{33}-error as compared with the other error values is strikingly different from the one observed by FOOTE *et al.* is a consequence of the fact that we neglected the $\pm 6\%$ overall error on the differential cross-section scale (*). This neglect practically affects only α_{33}. The *D*-wave error differences can again be explained as a consequence of not taking polarization data directly into account. The polarization is such a very « steep » function of the *D*-wave contribution that even crude polarization data result in a very considerable reduction of the *D*-wave errors.

3) We would like to draw attention to some features of the analysis:

a) The resemblance between the final *D*-wave phase-shifts (Table I(*e*)) and those obtained with two points left out of the histogram (Table I-(*d*) is considerably closer than with those initially obtained using the complete angular distribution (Table I-(*b*)).

b) The Coulomb-correction, often considered as unimportant at energies such as 310 MeV, has a considerable influence on the *D*-phase-shifts because these phase-angles get their main contribution from the corrected zone.

* * *

The authors would like to express their appreciation to Mr. D. LAKE, Dr. R. BÖCK and Dr. J. REIGNIER for valuable help and discussions throughout the course of this work. Mr. W. KLEIN should be thanked for computational aid.

The interest of Dr. Y. GOLDSCHMIDT-CLERMONT and Professor G. BERNARDINI is gratefully acknowledged.

(*) J. H. FOOTE: private communication.

Appendix A

Coulomb correction.

For not too low primary energies, the differential cross-section for elastic scattering in CMS as measured in presence of both nuclear and Coulomb interaction can be approximated theoretically by:

$$\left(\frac{\mathrm{d}\sigma}{\mathrm{d}\Omega}\right)_{\mathrm{tot}} = \lambda^2[|f_\alpha + f_c^{nf}|^2 + |f_\beta + f_c^f|^2], \tag{1}$$

where f_α and f_β are the familiar «direct» and spin-flip nuclear scattering amplitudes and f_c^{nf} and f_c^f are respectively the relativistic Born-approximation non spin-flip and spin-flip Coulomb scattering amplitudes. It should be pointed out that expression (1) is obtained under the assumption that nuclear and Coulomb interaction are confined to different regions in space *i.e.* that the effect of the Coulomb-force inside the action-radius of the nuclear forces is considered as negligible.

Solmitz [5] gave approximate expressions for both Coulomb-scattering amplitudes in the form of a development of the first order in the interaction strength constant $e^2/\hbar c$ and up to the second order in the variable v_p/c (v_p: proton velocity in CMS).

In absence of f_c^{nf} and f_c^f the Coulomb-interaction evidently reduces to the expression

$$\left(\frac{\mathrm{d}\sigma}{\mathrm{d}\Omega}\right)_n = \lambda^2[|f_\alpha^2|^2 + |f_\beta|^2]. \tag{2}$$

If we now define the quantity

$$C(\theta, \underline{\alpha}) = \left(\frac{\mathrm{d}\sigma}{\mathrm{d}\Omega}\right)_{\mathrm{tot}} - \left(\frac{\mathrm{d}\sigma}{\mathrm{d}\Omega}\right)_n, \tag{3}$$

then the curve $C(\theta, \underline{\alpha})$ *versus* θ or $\cos\theta$ can be considered as a correction-curve of which the value in each point has to be *subtracted* from the measured curve in order to obtain the pure nuclear angular distribution (*). $C(\theta, \underline{\alpha})$

[5] F. Solmitz: *Phys. Rev.*, **94**, 1799 (1954).

(*) The correction as defined and calculated with (3) automatically comes out with the correct sign. This means, it comes out with a *negative* sign (indicating *destructive* Coulomb-interference) for phase-shift-sets corresponding with a *positive* value of the forward scattering amplitude whilst on the other hand, it comes with *positive* sign (indicating *constructive* Coulomb-interference) for phase-shift sets corresponding with a *negative* value of that same quantity.

should, in principle, be calculated with the real set of nuclear phase-shifts which at that stage of the calculations is still unknown.

After a few tests it became clear that the $C(\theta, \underline{\alpha})$-values obtained do not depend very critically on the set introduced in the programme, so that it is a rather good approximation to feed in a set derived with the foregoing procedures but by using the histogram without the measurements in the forward direction (neglecting, say, those lying below 45°).

Analysing the angular distribution of Foote with the SPD-least-squares fit, leaving out however the first two points (corresponding to a θ-value of resp. 34.5° and 36.3°) leads to the set of co-efficients displayed in Table IV.

Performing a new phase-shift analysis on these coefficients gives the results of Table I(d). On the basis of this solution the $C(\theta, \underline{\alpha})$-curve was calculated.

Appendix B

Phase-shift error calculation.

Methods for phase-shift error calculation described in the literature are mostly rather indirect and based on an examination in hyperspace of the sensitivity of the M-surface towards slight changes of the α_i-minimum values. In the neighbourhood of a minimum, M can always be approximated by the expression

$$M \simeq M_0 + \sum_i \sum_j H_{ij}(\alpha_i - \alpha_i^0)(\alpha_j - \alpha_j^0) \,, \tag{1}$$

in which $\boldsymbol{H}$ is a real symmetric matrix of which the elements can be considered as the « scale factors » associated with these α_i-variations. Using the known statistical meaning of the M-function it can further be shown that the inverse of the H-matrix is nothing else but the error-matrix of the α_i. The examination mentioned above consists of finding numerical values for these $\boldsymbol{H}$-elements.

It should be pointed out that in expression (1) M can be considered as defined either as a function of the C_i-quantities and their errors, as for the case of the « histogram »-method, or directly as function of the measured $(\mathrm{d}\sigma/\mathrm{d}\Omega)_i$-values and their corresponding errors, as required for the method adopted in analysing counter-results.

A method frequently used in order to get an approximate value for, say, H_{ij}, consists of giving a small increment to respectively the i-th and the j-th phase-shift angle leaving the others unaltered and equal to their values at the minimum. Having calculated with the appropriate M-expression the *new* M-value (say M^1) corresponding to the *new* phase-shift-set, it can be said that:

$$\frac{(M^1 - M)}{\Delta\alpha_i \, \Delta\alpha_j} \,,$$

is an approximation to the value of H_{ij} (*). The wanted errors are then obtained by means of a simple matrix-inversion.

In connection with the problem of the error-calculation it seemed worthwhile to look for other possibly more direct methods than the one given above. In the following a description of such a « direct » error-computation method will be given. The discussion is restricted to the special case of the « histogram »-method but the ideas behind it can also be extended to cases in which the method is appropriate to the analysis of counter results.

If the transformation leading from the C_i to the α_i was *analytic* and *linear* represented by say

$$\underline{C} = \boldsymbol{A} \cdot \underline{\alpha} \tag{2}$$

then the solution of the problem of obtaining the correlation-matrix associated with the α_i (say $\boldsymbol{K}$) would be straightforward.

It is indeed known that in the conditions implied by (2), $\boldsymbol{K}$ is given by

$$\boldsymbol{K} = [\boldsymbol{A}^T \cdot \boldsymbol{G} \cdot \boldsymbol{A}]^{-1} \tag{3}$$

which, for cases where $\underline{\alpha}$ is a vector of the same dimension as $\underline{C}$, can further be written as:

$$\boldsymbol{K} = \boldsymbol{A}^{-1} \cdot \boldsymbol{G}^{-1} \cdot (\boldsymbol{A}^{-1})^T . \tag{4}$$

In both previous expressions $\boldsymbol{G}^{-1}$ should be the error-matrix on the C_i-values mentioned. There are now two steps to be taken in order to arrive at the situation implied by (2):

1) the transformation $\underline{C} \to \underline{\alpha}$ has to be considered as equivalent to solving the system

$$C_i = F_i(\underline{\alpha}) .$$

2) The F_i-functions have to be approximated locally by a linear transformation.

For cases in which the minima found have the required low M-value there is no difficulty in supposing the first condition to be satisfied. The second condition is, on the other hand, easily satisfied by means of a Taylor expansion of F_i around $\underline{\alpha}^0$ limited to first order terms.

Writing

$$C_i \simeq F_i(\underline{\alpha}^0) + \sum_j \left(\frac{\partial F_i}{\partial \alpha_j} \right)_{\underline{\alpha}^0} \cdot (\alpha_j - \alpha_j^0) , \tag{5}$$

(*) In our case, however, and as a consequence of the fact that the convergence-system previously mentioned necessitates the analytic evaluation of the quantities $\partial^2 M / \partial \alpha_i \, \partial \alpha_j = H_{ij}$, we can obtain the required values directly (and even more accurately) by introducing the set of minimum-angles in those expressions.

and defining

$$A_{ij} = \left(\frac{\partial F_i}{\partial \alpha_j}\right)_{\underline{\alpha}^0}$$

it is easily seen that the wanted errors are again given by (3) and (4). Clearly this error calculation method gives a more *direct* relation between the original experimental errors on the angular distribution and those finally obtained on the phase-shifts than for the preceding method.

Two computer programmes were written to perform the error calculation using respectively the two methods discussed above.

Present experience shows that both methods give results which are consistent with each other.

RIASSUNTO (*)

Si discute la possibilità di usare un nuovo metodo nell'analisi dello spostamento di fase degli istogrammi ottenuti in camera a tracce. Si esaminano i metodi disponibili per correggere la distribuzione angolare nello scattering di Coulomb e per calcolare gli errori di spostamento di fase. Come esempio di applicazione si da una nuova analisi dell'esperimento di scattering di π^+ di 310 MeV di FOOTE *et al.*

(*) *Traduzione a cura della Redazione.*

IL NUOVO CIMENTO Vol. XIX, N. 4 16 Febbraio 1961

Über die Vollständigkeit lorentzinvarianter Felder in einer zeitartigen Röhre.

H. J. Borchers

Institut für Theoretische Physik der Universität - Hamburg

(ricevuto il 24 Novembre 1960)

Summary. — It will be shown that a complete field is already complete in a timelike tube. This is a consequence of invariance and spectrum condition alone.

1. – Ergebnisse.

R. Haag (1) hat neben den üblichen Axiomen der Feldtheorie noch das Zeitschichtaxiom eingeführt, welches besagt, daß ein vollständiges Feld schon in einer Zeitschicht $|x^0|<\varepsilon$ vollständig sein soll. Damit ist allgemein die Frage aufgeworfen, ob ein Teilsystem eines Feldes schon vollständig sein kann.

Es soll hier gezeigt werden, daß ein vollständiges Feld schon in einer Röhre $\boldsymbol{x}|<r$ vollständig ist. Dabei zeigt es sich, daß diese Eigenschaft allein eine Konsequenz der Lorentzinvarianz und Spektrumsbedingung ist.

Die Frage, ob das Zeitschichtaxiom ein unabhängiges Axiom ist, bleibt hier unbeantwortet. Es kann aber gezeigt werden, daß es sich nicht mit Hilfe der linearen Eigenschaften (Lorentzinvarianz, Spektrumsbedingung, Lokalität ohne Unitarität) beweisen läßt.

Um die Ergebnisse formulieren zu können, beginnen wir mit wohlbekannten Begriffsbildungen, die hier noch einmal kurz zusammengestellt werden sollen. Es sei S (2) der Raum der stark abfallenden Testfunktionen $f(x)$, G ein Gebiet

(1) R. Haag: Reports of the International Conference on Mathematical Problems of the Quantum Theory of Fields (Lille, 1957).

(2) L. Schwartz: *Théorie des distributions* (Paris, 1951).

im x-Raum, S_G die Menge aller Funktionen aus S mit einem Träger, der in G enthalten ist. Weiter sei $A(x)$ ein invariantes skalares Feld. Wir bezeichnen mit R_G den kleinsten schwach abgeschlossenen Ring, der alle Operatoren

$$A(f) = \int f(x) A(x) \, \mathrm{d}x \,, \qquad f(x) \in S_G \,, \tag{1}$$

enthält.

Nach v. NEUMANN [3] läßt sich der kleinste schwach abgeschlossene Ring eines Systems von Operatoren auch durch die Kommutatoralgebra kennzeichnen.

Sei $\mathscr{A} = \{A_1, A_2, \ldots\}$ ein System von Operatoren, so ist die Kommutatoralgebra $\mathscr{A}'$ definiert als die Menge der Operatoren, die mit allen Operatoren $A \in \mathscr{A}$ vertauschbar sind:

$$\mathscr{A}' = \{B \,|\, [B, A] = 0 \;\forall A \in \mathscr{A}\} \,. \tag{2}$$

Der Satz von J. v. NEUMANN besagt nun, daß der kleinste schwach abgeschlossene Ring $R_{\mathscr{A}}$, der das System $\mathscr{A}$ enthält, mit der Kommutatoralgebra der Kommutatoralgebra von $\mathscr{A}$ identisch ist:

$$R_{\mathscr{A}} = \mathscr{A}'' \,. \tag{3}$$

Mit diesen Bezeichnungen können wir die Ergebnisse wie folgt formulieren:

1) Sei Z der Zylinder

$$|\boldsymbol{x}| < \varepsilon \,, \qquad |x_0| < T \,, \tag{4}$$

D der Doppelkegelstumpf

$$\begin{cases} |x_0| + |\boldsymbol{x}| < T + \varepsilon \,, & \text{für } |\boldsymbol{x}| \geqslant \varepsilon, \\ |x_0| < T \,, & \text{für } |\boldsymbol{x}| < \varepsilon, \end{cases} \tag{5}$$

und $A(x)$ ein skalares Feld, so ist die Lorentzinvarianz und Positivität der Energie hinreichend für

$$R_D = R_Z \,.$$

Als eine Folgerung ergibt sich dann aus 1):

[3] J. v. NEUMANN: *Math. Ann.*, **102**, 370 (1929).

2) (Röhrensatz). Sei C eine stetige zeitartige Kurve, d.h. $x(s_1) - x(s_2)$ zeitartig für $s_1 \neq s_2$ mit den Eigenschaften

$$\lim_{s \to \pm \infty} x_0(s) = \pm \infty , \qquad |\boldsymbol{x}| \leqslant M < \infty ,$$

und U ein Gebiet mit der Eigenschaft

$$C \subset U ,$$

so ist

$$R_U = R_M .$$

Dabei ist mit M der gesamte x-Raum bezeichnet.

Schließlich zeigen wir durch Angabe eines Gegenbeispiels: Das Zeitschichtaxiom ist unabhängig von den linearen Eigenschaften der Feldtheorie. Dabei verstehen wir unter den linearen Eigenschaften alle Eigenschaften der Matrixelemente von Operatorprodukten, die aus Lorentzinvarianz, Spektrumsbedingung und lokaler Vertauschbarkeit folgen.

2. – Beweise.

Die Beweise gehen zurück auf eine Verallgemeinerung des Edge of the Wedge Theorems [4].

Hilfssatz: $F^{\pm}(x + iy)$ seien analytische Funktionen mit den Regularitätsgebieten $R^{\pm} : y \in L^{\pm}$, deren Randwerte

$$F^{\pm}(x) = \lim_{\substack{y \to 0 \\ y \in L^{\pm}}} F^{\pm}(x + iy)$$

als Distributionen existieren. Seien weiter Z bzw. D die in 1) gekennzeichneten Zylinder bzw. Doppelkegelstumpf und gilt

$$F^{+}(x) = F^{-}(x) \qquad \text{für } x \in Z ,$$

so folgt

$$F^{+}(x) = F^{-}(x) \qquad \text{für } x \in D .$$

Zum Beweise des Hilfssatzes stellen wir fest, daß nach dem Edge of the Wedge Theorem $F^{+}(\zeta)$ und $F^{-}(\zeta)$ verschiedene Funktionselemente einer einzigen analytischen Funktion $F(\zeta)$ sind und daß die Punkte aus dem Zylinder

[4] H. J. Bremermann, R. Oehme and J. G. Taylor: *Phys. Rev.*, **109**,2178 (1958).

nebst gewissen Umgebungen zum Regularitätsgebiet der Funktion $F(\zeta)$ gehören.

Wir betrachten nun

$$\varphi(x, \lambda, u) = F\{x_0 \sinh u,\ \boldsymbol{x}(1 - \lambda \cosh u) = F(\zeta)\} \tag{6}$$

als eine analytische Funktion der reellen Variablen x, λ und der komplexen Variablen $u = u_1 + iu_2$.

Nun ist

$$\operatorname{Im} \zeta = \sin\ u_2 \{x_0 \cosh u_1,\ \boldsymbol{x}\lambda \sinh u_1\},$$

somit ist $\varphi(x, \lambda, u)$ regulär in

$$\left\{\begin{array}{l} 0 < |u_2| < \dfrac{\pi}{2}, \qquad |x_0| \cosh u_1 > |\lambda|\,|\boldsymbol{x}|\,|\sinh u_1|, \\ \text{sowie} \\ 0 = u_2, \qquad |x_0 \sinh u_1| < T, \qquad |\boldsymbol{x}(1 - \lambda \cosh u_2)| < \varepsilon. \end{array}\right. \tag{7}$$

Betrachten wir jetzt das Gebiet

$$G\colon\ 1 > \lambda > 0, \qquad |\lambda \boldsymbol{x}| < |x_0|, \qquad \sqrt{1 + \left(\frac{T}{x_0}\right)^2} > \frac{|\boldsymbol{x}| - \varepsilon}{\lambda |\boldsymbol{x}|}, \tag{8}$$

so ist die erste Bedingung von (7) für alle u_1 automatisch erfüllt. Ist $u_2 = 0$, so sind auch

$$\operatorname{Min}\left\{\frac{|\boldsymbol{x}| + \varepsilon}{\lambda |\boldsymbol{x}|}, \quad \sqrt{1 + \left(\frac{T}{x^0}\right)^2}\right\} > \cosh u_1 > \operatorname{Max}\left\{1, \frac{|\boldsymbol{x}| - \varepsilon}{\lambda |\boldsymbol{x}|}\right\}.$$

Regularitätspunkte von $\varphi(x, \lambda, u)$. Somit existiert für alle $(x, \lambda) \in G$ ein geschlossener Weg in der u-Ebene, der den 0-Punkt umläuft, und der ganz im Regularitätsgebiet von $\varphi(x, \lambda, u)$ enthalten ist. Für $|\boldsymbol{x}(1 - \lambda)| < \varepsilon$ ist nach Voraussetzung auch das Innere des Weges ganz im Regularitätsgebiet enthalten. Somit ist nach bekannten Sätzen über analytische Fortsetzung [5] für alle Punkte aus G das Innere der betrachteten Kurve in einer Erweiterung des Regularitätsgebietes von $\varphi(x, \lambda, u)$ enthalten. Die reellen Punkte dieses Gebietes sind:

$$u_2 = 0, \qquad (x, \lambda) \in G, \qquad \cosh u_1 < \operatorname{Min}\left\{\frac{|\boldsymbol{x}| + \varepsilon}{\lambda |\boldsymbol{x}|}, \quad \sqrt{1 + \left(\frac{T}{x^0}\right)^2}\right\}. \tag{9}$$

[5] z. B., S. Bochner and W. T. Martin: *Several Complex Variables* (Princeton, 1948), Chapter IV, Theorem 1.

Da vor der analytischen Fortsetzung q nur eine Funktion der Variablen $\zeta = \{x_0 \sinh u,\ \boldsymbol{x}(1 - \cosh u)\}$ war, ist dieses auch nach der analytischen Fortsetzung der Fall. Durch die Abbildung $(x, \lambda, u) \to \zeta$ gehen die reellen Regularitätspunkte (9) in den Doppelkegelstumpf (5) über. Damit ist gezeigt, daß (5) Regularitätspunkte der Funktion $F(\zeta)$ sind. Somit gilt in (5) auch $F^+(x) = F^-(x)$, $q \cdot e \cdot d$. Die Punkte (5) liefern genau alle reellen Regularitätspunkte, welche man durch Hüllenbildung gewinnen kann, wie man durch Anwendung der JOST-LEHMANN-DYSON-Darstellung [6] auf den Doppelkegelstumpf (5) erkennt.

2·1. *Beweis von* 1). – Es sei C ein beschränkter Operator und es seien P, Q Eigenzustände zum Energie-Impulsoperator, sei Z der Zylinder (4) und es gelte

$$[A(x), C] = 0\,, \qquad \text{für } x \in Z\,. \tag{10}$$

Wir betrachten nun die Matrixelemente

$$\begin{cases} F^+(x) = \langle P \,|\, A(x)\, C \,|\, Q\rangle\,, \\ F^-(x) = \langle P \,|\, C\, A(x) \,|\, Q\rangle\,, \end{cases} \tag{11}$$

dabei sind $F^{\pm}(x)$ in x temperierte Distributionen und in P und Q aus $\mathscr{L}^2$. Aus der Translationsinvarianz und der Spektrumsbedingung folgt nun, daß die Fouriertransformierten folgende Trägereigenschaften haben:

$$\begin{cases} F^+(k) \neq 0 & \text{nur für } k + P \in L^+, \\ F^-(k) \neq 0 & \text{nur für } k - Q \in L^-. \end{cases} \tag{12}$$

Hieraus folgt, daß $F^+(x)$ und $F^-(x)$ Randwerte analytischer Funktionen sind, und zusammen mit (10) folgt, daß diese Funktionen die Voraussetzungen des Hilfssatzes erfüllen. Somit gilt

$$F^+(x) = F^-(x) \qquad \text{für } x \in D, \tag{13}$$

dabei ist D der Doppelkegelstumpf (5). (13) ist zunächst richtig für $|P_0|$, $|Q_0| < \infty$. Da nun $F^{\pm}(x)$ in P, Q aus $\mathscr{L}^2$ sind, gilt (13) allgemein. Somit erhalten wir

$$[A(x), C] = 0 \qquad \text{für } x \in D, \tag{14}$$

[6] R. JOST und H. LEHMANN: *Nuovo Cimento*, **5**, 1598 (1957); F. J. DYSON: *Phys. Rev.*, **110**, 1460 (1958).

oder

$$R'_D = R'_Z ,$$

und daraus

$$R_D = R_Z .$$

2·2. *Beweis von* 2). – C sei die in 2) gekennzeichnete Kurve und U ein Gebiet, welches diese Kurve enthält. Sei nun y ein beliebiger Punkt, so betrachten wir die Schicht

$$S\colon y_0 - (|\boldsymbol{y}| + M + 1) < x_0 < y_0 + (|\boldsymbol{y}| + M + 1) . \tag{15}$$

x_1 bzw. x_2 seien der Anfangs- bzw. Endpunkt von C in S. Man erhält durch Anwendung von 1) auf alle Geradenstücke in $U \cap S$ eine Erweiterung U_1 von U mit

$$R_{U_1} = R_U .$$

Durch sukzessive Wiederholung dieses Verfahrens erhält man schließlich eine Erweiterung U_N, die mindestens den Doppelkegel $(x - x_1) \in L^+$, $(x - x_2) \in L^-$ enthält, und es gilt

$$R_{U_N} = R_U .$$

In U_N ist der Punkt y enthalten. Da y beliebig war, ist 2) bewiesen.

Um schließlich zu zeigen, daß das Zeitschichtaxiom nicht aus den linearen Eigenschaften folgt, betrachten wir die Matrixelemente

$$F(x_{i_1}, \ldots, x_{i_k};\ x_{i_{k+1}}, \ldots, x_{i_n}) = \langle P \,|\, A(x_{i_1}), \ldots, A(x_{i_k}) C A(x_{i_{k+1}}), \ldots, A(x_{i_n}) \,|\, Q \rangle ,$$

$$F(z_{i_1}, \ldots, z_{i_k};\ z_{i_{k+1}}, \ldots, z_{i_n}) , \qquad (z = x + iy),$$

ist regulär in

$$\left.\begin{aligned} & y_{i_1} - y_{i_2}, \ldots, y_{i_{k-1}} - y_{i_k}, y_{i_k} \in L^+ \\ & -y_{i_{k+1}}, y_{i_{k+1}} - y_{i_{k+2}}, \ldots, y_{i_{n-1}} - y_{i_n} \in L^+ \end{aligned}\right\} R_{i_1}, \ldots, i_k; i_{k+1}, \ldots, i_n .$$

Dabei ist C ein beschränkter Operator. Die Analytizität folgt dabei wie üblich aus Translationsinvarianz und Spektrumsbedingung. Sei nun $[A(x), C] = 0$ für $|x_0| < a$ und $A(x)$ ein lokales Feld, so folgt aus dem Edge of the Wedge Theorem, daß alle $(n+1)!$ Funktionen F verschiedene Funktionselemente einer einzigen Funktion $q(z)$ sind. Diese Funktion ist regulär in dem Gebiet

$$R = \bigcup_{i_1, \ldots, i_n} R i_1, \ldots;\ \ldots, i_n \bigcup \{(x_i - x_k)^2 < 0;\ |x_j^0| < a\} .$$

Nun sind aber die Funktionen

$$\prod_{i \neq k} \frac{1}{(x_i - x_k)^2} \cdot \prod_j \frac{1}{(x_j - \boldsymbol{u}_j)^2 - a^2},$$

in dem Gebiet R regulär und haben Singularitäten an jedem beliebigen Randpunkt des Gebietes

$$\{(x_i - x_k)^2 < 0;\ |x_j^0| < a\}$$

Dieses zeigt, daß die Regularitätshülle keine weiteren reellen Punkte enthält.

RIASSUNTO (*)

Si intende dimostrare che un campo completo è già completo in un tubo temposimile. Ciò è una conseguenza solo dell'invarianza e della condizione di spettro.

(*) *Traduzione a cura della Redazione.*

IL NUOVO CIMENTO Vol. XIX, N. 4 16 Febbraio 1961

On the Pion-Hyperon Resonances and on the Possible Uses Thereof.

(Determination of the Σ-Λ Relative Parity and of the α_Λ/α_0 Ratio).

Ph. Meyer (*), J. Prentki and Y. Yamaguchi (**)

CERN - Geneva

(ricevuto il 24 Novembre 1960)

Summary. — The esistence of a resonance in the hyperon-pion system leads to a possibility of determining the Σ-Λ relative parity and the ratio α_Λ/α_0 of asymmetry coefficients α_Λ (in $\Lambda \to p+\pi^-$) and α_0 (in $\Sigma^+ \to p+\pi^0$). In this paper a proposal is made which allows the determination of these quantities by measuring only the up/down asymmetries of pions coming from Λ- and Σ-decays. Various aspects of this proposal are discussed. The possible existence of other resonances has also been emphasized. In particular it is shown that the existence of a resonance in the isotopic spin state $I = 1$ leads to some predictions concerning the existence of another resonance, probably in the $I = 2$ state.

Introduction.

Evidence for the existence of a resonance in the pion-hyperon system has been recently reported [1]. In the same way that the (33) resonance has played an essential role in the development of pion physics, it may happen (if the experimental results are confirmed) that the pion-hyperon resonance(s) will help us in understanding certain aspects of strange particle physics.

(*) On leave from the Faculté des Sciences, Orsay and Université de Bordeaux.

(**) On leave from Osaka City University, Osaka, Japan.

[1] Reported by M. L. Good at the Rochester Conference (August 1960), to be published.

One of the most immediate applications that has been proposed [2] is to use this resonance in order to determine the relative Σ-Λ parity and the ratio of the asymmetry coefficients α_Λ (in $\Lambda \to p + \pi^-$) to α_0 (in $\Sigma^+ \to p + \pi^0$).

The main content of this paper is to describe in some detail a series of experiments which might allow the determination of the above mentioned quantities by measuring only up/down asymmetries.

In order to fulfill the proposed program a number of conditions must be met which can be checked only through experiment. These conditions will be specified, and a set of possible reactions by which the resonance in question can be excited will be suggested.

Strictly speaking, the method which is proposed and the relations which are derived are rigorously valid only in the case where the resonance is so narrow and pronounced that the excited hyperon formed can be considered to have a « long » lifetime and that all channels except the resonating one can be neglected. The validity of such a model and the corrections to be expected will be briefly discussed.

Quite independently of the possible measurement of the Σ-Λ parity and of the ratio α_Λ/α_0 the properties of the resonance(s) of the pion-hyperon system should be studied both theoretically and experimentally. This is particularly true of the isotopic spin properties since a number of models which shall be discussed predict the existence of other resonances for which it would be interesting to have experimental evidence.

In Section **1** the experimental situation concerning the π-Λ resonance is briefly recalled. In Section **2** the method for the determination of the Σ-Λ relative parity from the existence of the H^* isobar is described in some detail. In Section **3** we show how to determine $\pi(\Sigma)/\pi(\Lambda)$ and α_Λ/α_0 from the measurement of up/down asymmetries only. Section **4** is devoted to isotopic spin properties of the isobars; it is shown, by studying various models, that a new isobar of $I = 2$ should very probably exist. The general discussion is given in Section **5**.

1. – The π-Λ resonance: production and decay of the hyperon isobar.

The study of the reaction

$$K^- + p \to \Lambda + \pi^+ + \pi^- \tag{1}$$

with a separated K^- beam of 1.15 GeV/c shows that there exists a peak around 400 MeV/c in the π^+ and π^- spectra. The most obvious interpretation [1] is

[2] PH. MEYER, J. PRENTKI and Y. YAMAGUCHI: *Phys. Rev. Lett.*, **5**, 442 (1960).

that reaction (1) proceeds in 2 steps; first an excited hyperon H^* is formed

$$K^- + p \to H^{*\pm} + \pi^{\mp} \tag{2}$$

followed by the immediate decay

$$H^{*\pm} \to \Lambda + \pi^{\pm} . \tag{3}$$

The position of the peak in the π-spectrum shows that H^* has a mass of 1370 MeV which gives a Q value of ~ 115 MeV in the decay (3). According to preliminary results, the width of the resonance seems to be about 25 MeV, approximately 75% of the π's in (1) going through the resonant channel.

The Q value in (3) shows that the decay

$$H^* \to \Sigma + \pi \tag{4}$$

must also exist with a Q value of ~ 40 MeV. Therefore the study of the reaction

$$K^- + p \to \Sigma + \pi + \pi \tag{5}$$

should also show a peak in the π-spectrum corresponding to the resonant channel (2), if the branching ratio Σ/Λ is not too small. In the case of an incident K^- beam the set of reactions involving H^* (with a « threshold » of 400 MeV/c) would be

$$K^- + p \to \begin{cases} H^{*+} + \pi^- & (6) \\ H^{*0} + \pi^0 & (7) \\ H^{*-} + \pi^+ & (8) \end{cases}$$

with subsequent decay (the lifetime of H^* being $\sim 10^{-23}$ s)

$$H^{*+} \to \begin{cases} \Sigma^+ + \pi^0 & (9) \\ \Sigma^0 + \pi^+ & (10) \\ \Lambda + \pi^+ & (11) \end{cases}$$

$$H^{*0} \to \begin{cases} \Sigma^+ + \pi^- & (12) \\ \Sigma^- + \pi^+ & (13) \\ \Lambda + \pi^0 & (14) \end{cases}$$

$$H^{*-} \to \begin{cases} \Sigma^- + \pi^0 & (15) \\ \Sigma^0 + \pi^- & (16) \\ \Lambda + \pi^- & (17) \end{cases}$$

The existence of the decay (3) demonstrates that H^* must be in a pure isotopic spin state $I=1$. This, of course, forbids the decay $K^- + p \to \Sigma^0 + \pi^0 + \pi^0$ going through the $I=1$ resonant channel.

Needless to say that other reactions than (2) can be used in principle to excite the H^* resonance. As examples we list here the following (*)

(18) $\pi + p \to H^* + K$ (1.24 GeV)

(19) $K^- + d \to H^* + \mathcal{N}$ (rest)

(20) $\overline{p} + p \to H^* + \overline{\Lambda}$ (1.41 GeV)

(20′) $\overline{p} + p \to H^* + \overline{H}^*$ (2.11 GeV)

(21) $\gamma + p \to H^* + K$ (1.39 GeV), etc.

The thresholds for these reactions are put in brackets.

It is, of course, difficult to say *a priori* which reaction is most favourable for the production of the resonating state and at what energy one should work. Furthermore, in the considerations to follow it will be essential for H^* to have a large polarization and again the most favourable situation can only be discovered through experiment.

2. – Determination of the Σ-Λ relative parity.

A method will now be proposed to measure the Σ-Λ parity taking advantage of the existence of the H^* resonance. This method will be successful provided the two following conditions are satisfied:

i) The isobar H^* must be a resonance which is sufficiently narrow and pronounced so that one can choose experimental conditions under which the resonant process dominates. This means that the reaction which excites the isobar H^*

$$\begin{array}{l} a + b \to H^* + c \\ \qquad\quad \lfloor\!\!\longrightarrow d + e \end{array}$$

can be considered as a quasi-two-body reaction. Knowing the « mass » of H^* one selects the events for which the energy of reaction product c is in a narrow

(*) The H^* resonance cannot be excited in K-$\mathcal{N}$ elastic scattering, the corresponding energy being in the unphysical region.

band around the resonance peak. If H* is a « good » resonance this choice of events will ensure that the observed reaction is passing through the formation of the isobar H* and that under these experimental conditions the background for the non-resonant channel $a+b \to c+d+e$ is minimised. We shall come back later to this point.

ii) The method proposed for determining the Σ-Λ relative parity and the ratio α_Λ/α_0 rests upon the measure of the polarization of the Σ's and Λ's in the decay of H^{*+} for instance. Therefore a second condition which must be met is that the branching ratio of reactions (9)/(11) = (10)/(11) be not too small, and that the polarization of H* be large. Large polarizations having been observed in strange particle creation it is expected that one can find an energy for which this will also be true of the isobar.

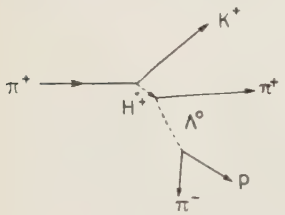

Fig. 1.

To discuss the method proposed let us take as an example the excitation of the isobar through the reaction

(22) $\qquad \pi^+ + p \to K^+ + \pi + \Lambda(\Sigma)\,.$

Knowing the position of the resonance H* for a given energy of the incident π^+ one select the K^+ associated with the resonant channel. *In what follows, the analysis will always refer to such processes.* If condition (i) is satisfied, then reaction (22) can be thought of (see Fig. 1) as a two step process:

(23) $\qquad \pi^+ + p \to H^{*+} + K^+$

followed by the immediate decay

(a) $\quad \Sigma^+ + \pi^0$
(a′) $\quad \Sigma^+ + \pi^0 \to p + \pi^0$
(b) $\quad \Sigma^0 + \pi^+$
(b′) $\quad H^{*+} \to \Sigma^0 + \pi^+ \to \Lambda + \gamma$
(b″) $\quad \Lambda + \gamma \to p + \pi^-$
(c) $\quad \Lambda + \pi^+$
(c′) $\quad \Lambda + \pi^+ \to p + \pi^-$

Furthermore, the direction of the outgoing K^+ together with that of the incident π^+ defines a plane which shall be referred to as the production plane S in what follows.

Now consider P_Λ and P_Σ defined as the « average » polarization of the Λ's and Σ's coming via the resonant reaction (23) through the decay (a), (b) and (c). By « average » we mean an average over all directions of hyperons keeping the energy and direction of the associated K^+ fixed. From conservation of parity it is clear that the polarization of H^* must be normal to S. In the decay of H^*, for a given direction of $\Lambda(\Sigma)$ the polarization of $\Lambda(\Sigma)$ will in general not be perpendicular to the plane S. But if an average is made over all directions of the hyperons this average polarization $\boldsymbol{P}_\Lambda$ and $\boldsymbol{P}_\Sigma$ will be necessarily normal to the plane S.

Let us call $\pi(\Lambda)$, $\pi(\Sigma)$ and $\pi(H^*)$ the parity of Λ, Σ, and H^* respectively (only relative parities are relevant) and J the spin of H^*. If M is the component of J along the normal to S which we shall take as the z axis, the polarization of H^* is given by

$$P_{H^*} = \frac{1}{J} \frac{\sum_M M \, |W_J^M|^2}{\sum_M |W_J^M|^2}, \tag{24}$$

where W_J^M is the amplitude for the production of H^* in the spin state (J, M).

The final state wave function of the π-Λ (π-Σ) system coming from the decay of H^* is given, in the rest system of H^*, by

$$\psi_J = \sum_M W_J^M a_J \left\{ \sqrt{\frac{J+M}{2J}} \cdot \alpha \cdot Y_J^{M-\frac{1}{2}}(\theta, \varphi) + \sqrt{\frac{J-M}{2J}} \cdot \beta \cdot Y_J^{M+\frac{1}{2}}(\theta, \varphi) \right\}, \tag{25}$$

for $l = J - \frac{1}{2}$, and

$$\psi_J = \sum_M W_J^M b_J \left\{ \sqrt{\frac{J-M+1}{2J+2}} \, \alpha Y_J^{M-\frac{1}{2}}(\theta, \varphi) - \sqrt{\frac{J+M+1}{2J+2}} \, \beta Y_J^{M+\frac{1}{2}}(\theta, \varphi) \right\}, \tag{26}$$

for $l = J + \frac{1}{2}$; where l is the orbital angular momentum of the decay products of H^*, the a_J, b_J are the decay amplitudes for the given l and given $\Lambda(\Sigma)$ channels and where α and β are the 2 component spin functions of the hyperon for spin up and down respectively. The final state wave function is given by either (25) or (26) depending on the value of l, *i.e.* on the relative parity of $\Lambda(\Sigma)$ and H^*.

After averaging over θ and φ it is easily seen that only the z component of $\boldsymbol{\sigma}$ has a non vanishing expectation value in the $\Lambda(\Sigma)$-π final state, and one obtains in the usual way

$$P_{\Lambda(\Sigma)} = \langle \sigma_z \rangle = \frac{\sum_M |a_J|^2 \, |W_J^M|^2 \left(\frac{J+M}{2J} - \frac{J-M}{2J} \right)}{\sum_M |a_J|^2 \, |W_J^M|^2} = \sum_M \frac{M}{J} \frac{|W_J^M|^2}{\sum_{M'} |W_J^{M'}|^2}, \tag{27}$$

for $l = J - \frac{1}{2}$,

$$(28) \qquad P_{\Lambda(\Sigma)} = \langle \sigma_z \rangle = \frac{\sum_M |b_J|^2 |W_J^M|^2 \left(\frac{J-M+1}{2J+2} - \frac{J+M+1}{2J+2} \right)}{\sum_M |b_J|^2 |W_J^M|^2} =$$

$$= \sum_M \left(- \frac{M}{J+1} \right) \frac{|W_J^M|^2}{\sum_{M'} |W_J^{M'}|^2} .$$

for $l = J + \frac{1}{2}$.

However, in the decay of H*, l is related to the parity by

$$(29) \qquad \pi(\mathrm{H}^*) = \pi(\Lambda \text{ or } \Sigma)(-1)^{l+1} .$$

Using equations (24) and (29), the relations (27) and (28) can be written in the compact form

$$(30) \qquad P_\Lambda [P_\Sigma] = \begin{Bmatrix} 1 \\ -\frac{J}{J+1} \end{Bmatrix} P_{\mathrm{H}^*} \text{ for } \pi(\Lambda)[\pi(\Sigma)] = \begin{Bmatrix} (-1)^{J+\frac{1}{2}} \\ (-1)^{J-\frac{1}{2}} \end{Bmatrix} \cdot \pi(\mathrm{H}^*) .$$

As a consequence one can specialize relation (30) to the cases of interest and make the following statements:

i) If $\pi(\Lambda) = \pi(\Sigma)$ then

$$(31) \qquad P_\Lambda / P_\Sigma = +1$$

for arbitrary spin J of H*.

ii) If $\pi(\Lambda) = -\pi(\Sigma)$ then

$$(32) \qquad P_\Lambda / P_\Sigma = \begin{cases} -\frac{1}{3}(-\frac{5}{3}) & \pi(\Lambda) = \pi(H^*) \\ \text{for } J = \frac{1}{2}(\frac{3}{2}) \text{ and} & \\ -3\,(-\frac{3}{5}) & \pi(\Lambda) = -\pi(H^*) \end{cases}$$

It is important to notice that for any J or $\pi(\mathrm{H}^*)$, the sign of P_Λ / P_Σ is either positive or negative according to whether the Σ-Λ relative parity is even or odd. A measure of the sign of P_Λ / P_Σ is therefore a measure of the Σ-Λ parity.

However, P_Λ and P_Σ are not easily accessible to experiment. What one can actually measure most simply is the up/down asymmetries with respect to the production plane S, of the pions coming from the hyperon decays (a')

and (c′) for instance. Both reactions are good analysers of polarization since α_Λ and α_0 are known to be large in magnitude. Such measurements will provide us with the ratio (*)

$$\frac{\alpha_\Lambda P_\Lambda}{\alpha_0 P_{\Sigma^+}} \equiv n \,. \tag{33}$$

Note that from our definition of $P_\Lambda(P_{\Sigma^+})$ the up/down asymmetry to be measured concerns the pions coming from the decay of *all* $\Lambda(\Sigma^+)$ in reactions (a) and (c′) whatever their direction as long as they are associated with the K^+'s which have been selected as explained above. The decay of the Λ's coming from (b) can be distinguished from those coming from (c′) by kinematics (**).

If α_Λ/α_0 is known from other experiments, (*e.g.* such as would be given by a measurement of the longitudinal polarization of the proton in the decay of unpolarized $\Lambda(\Sigma^+)$ ([3])). Then, by measuring n one obtains P_Λ/P_{Σ^+} and hence the Σ-Λ parity.

However, it is important to realize that the existence of the resonant channel H^{*+} makes it possible to obtain separately P_Λ/P_{Σ^+} and α_Λ/α_0 by considering the whole set of reactions (a), (b) and (c) and by measuring only up/down asymmetries in the subsequent decay of the hyperons. This we discuss in the next section.

3. – Determination of $\pi(\Lambda)/\pi(\Sigma)$ and α_Λ/α_0 from the measurement of up/down asymmetries.

3·1. *Determination of* $\pi(\Lambda)/\pi(\Sigma)$. – Consider the Λ's coming from reactions (b′) and (c). Let us recall first that in the decay $\Sigma^0 \to \Lambda + \gamma$ one has the well-known relation ([4])

$$P_\Lambda = -\tfrac{1}{3} P_{\Sigma^0} \tag{34}$$

if an average is made over all directions of Λ's. This statement is independent of the Σ-Λ relative parity.

Remembering the definition of P_{Σ^0} it can be shown (see Appendix II) that relation (34) will still hold to a very good approximation for the polarization

(*) The connection between the measured up/down asymmetries and the quantity (33) will be discussed in Appendix II.

(**) For this reason among many others, the use of a hydrogen bubble chamber seems more suitable.

([3]) T. D. Lee and C. N. Yang: *Phys. Rev.*, **108**, 1645 (1957).

([4]) R. Gatto: *Phys. Rev.*, **109**, 610 (1958); G. Feldman and T. Fulton: *Nucl. Phys.*, **8**, 106 (1958).

(normal to S) when an average is made over all directions of Σ^0 coming from (b'). Calling $P_{\Lambda\,\mathrm{ind}}$ the polarization of the Λ's produced from all Σ^0's, in the indirect reaction (b') one has

$$P_{\Lambda\,\mathrm{ind}} = -\tfrac{1}{3} P_{\Sigma^0} . \tag{35}$$

Now by measuring the up/down asymmetry with respect to S in the decay of all the Λ's coming from direct reaction (c) and indirect reaction (b') one can get the ratio

$$\frac{\alpha_\Lambda P_\Lambda}{\alpha_\Lambda P_{\Lambda\,\mathrm{ind}}} = \frac{\alpha_\Lambda P_\Lambda}{\alpha_\Lambda(-\frac{1}{3} P_{\Sigma^0})} = -3\,\frac{P_\Lambda}{P_{\Sigma_0}} . \tag{36}$$

Hence we can deduce the Σ-Λ relative parity as described in Section 2, without knowing the signs of the α's.

3·2. *Determination of the sign of* α_Λ/α_0. – The H* has an isotopic spin $I=1$; the π-Σ systems are therefore in a pure $I=1$ state, from which it follows that

$$P_{\Sigma^0} \text{ in (b)} = P_{\Sigma^+} \text{ in (a)} .$$

Consequently a measurement of (36) is also a measurement of P_Λ/P_{Σ^+}.

Furthermore if one mesures the ratio of the up/down asymmetries with respect to S in the decays (c') and (a') one gets

$$\frac{\alpha_\Lambda P_\Lambda}{\alpha_0 P_{\Sigma^+}} - \frac{\alpha_\Lambda P_\Lambda}{\alpha_0 P_{\Sigma^0}} = \frac{\alpha_\Lambda}{\alpha_0}\left(-\frac{P_\Lambda}{3P_{\Lambda\,\mathrm{ind}}}\right), \tag{37}$$

where eq. (35) has been used. $P_\Lambda/P_{\Lambda\,\mathrm{ind}}$ being known from the previous experiment in 3·1, one obtains in this way a direct measurement of α_Λ/α_0 (*).

We want to conclude this section with the following remarks.

(*) The following remark seems to be appropriate here. If H*+ isobar can be produced in a reaction then it is possible to measure both P_Λ/P_Σ and α_Λ/α_0 as it was explained above. That is not the case for reactions giving H*− and H*0. Indeed

i) $\mathrm{H}^{*-} \to \begin{cases} \Lambda + \pi^-; \\ \Sigma^0 + \pi^-; \\ \Sigma^- + \pi^0; \end{cases}$ ii) $\mathrm{H}^{*0} \to \begin{cases} \Lambda + \pi^0; \\ \Sigma^+ + \pi^-; \\ \Sigma^- + \pi^+ . \end{cases}$

As is well known Σ^- is not a « good analyser », *i.e.* $\alpha_-=0$. From i) we see that only $P_\Lambda/P_{\Lambda\,\mathrm{ind}} = -3P_\Lambda/P_{\Sigma^0}$ can be measured (which give Σ-Λ relative parity). From ii) only $\alpha_\Lambda P_\Lambda/\alpha_0 P_{\Sigma^+}$ can be obtained, because P_{Σ^+} in ii) and P_{Σ^0} in i) are in general not correlated.

All proposals discussed here are based on measurements of up/down asymmetries which are manifestly connected with polarization effects. Formula (30) shows that P_Λ and P_Σ are expressed in terms of P_{H^*}. It is necessary to choose such experimental conditions where P_{H^*} is as large as possible. Large P_{H^*} can be expected at least if the incident energy is not very far from the « H* production threshold » (cf. the high degree of polarization of hyperons produced at moderate energies). Obviously all steps which lead to a loss of polarization make our proposal more difficult to perform (see eq. (35) connected with $\Sigma^0 \to \Lambda - \gamma$, or also some cases of eq. (30) connected with different possible combinations of spins, parities of H*, Λ and Σ).

It is very important to stress that too much significance should not be attached to the actual numbers given in (31) and (32) nor to the numerical values of the α_Λ/α_0 ratio which can be deduced from the described proposal. Two reasons can be given for this: *a*) the interference effects caused by channels other than the resonating one. This will be discussed further in Section **5**. *b*) The fact that decaying hyperons are moving in the rest system of H* with, however, a small velocity. This leads to minor corrections described in Appendix II.

Nevertheless, it is very likely that the signs of P_Λ/P_Σ and α_Λ/α_0 still survive after all these corrections and the only information which is needed for the determination of the Σ-Λ relative parity is precisely the sign of P_Λ/P_Σ. Concerning the α_Λ/α_0 ratio, its absolute value is known experimentally to be close to 1 [5]. The sign of this ratio which can be trusted in these experiments, in spite of the above mentioned corrections, is particularly important to know because of its bearing on the proposed theories of weak interactions [6].

4. – Isotopic properties of the isobars and the probable existence of other resonances.

We have seen that the isotopic spin of H* must be equal to 1. The resonant mechanism that has been discussed leads then to relations between the different cross-sections. For instance, consider the reactions

$$\pi^+ + p \to \begin{cases} \Lambda + \pi^+ + K^+ & (38) \\ \Sigma^+ + \pi^0 + K^+ & (39) \\ \Sigma^0 + \pi^+ + K^+ & (40) \end{cases}$$

[5] *E.g.*, see: B. Cork, L. Kerth, W. A. Wenzel, Z. W. Cronin and R. L. Cool: *Phys. Rev. Lett.*, **5**, 128 (1960).

[6] B. d'Espagnat and J. Prentki: *Phys. Rev.*, **114**, 1366 (1959); *Nucl. Phys.*, **11**, 700 (1959); S. Treiman: *Nuovo Cimento*, **15**, 916 (1960); A. Pais: *Nuovo Cimento*, **18**, 1003 (1960), predicted $\alpha_\Lambda/\alpha_0 < 0$, while S. Bludman: *Phys. Rev.*, **115**, 468 (1960), predicted $\alpha_\Lambda/\alpha_0 > 0$.

The branching ratios are hardly predictable in general but if the K^+ events are chosen as explained in Section **2** in such a way that the reaction goes through the resonant channel (23) then one has the branching ratio (39)/(40)=1, which provide a valuable test of the isobar model.

In the resonant reactions (6)–(8) followed by the decay (9)–(17) the fact that H^* has $I=1$ implies again that one has the branching ratios (9)/(10) = = (12)/(13) = (15)/(16) = 1. But now only triangular relations can be established between reactions involving Σ's and π's passing through different charge states of H^* since $K^+ + p$ is not a pure isotopic spin state. Similar considerations can be applied to $\pi^- + p \to \Sigma + \pi + K$ if one of the π's is on the resonance.

It is clear that in general nothing can be said on the branching ratios Σ/Λ, unless specific models are introduced. A number of models for the strong interactions have been proposed. It will be seen that they lead to certain important predictions concerning the existence of other resonances in the pion-hyperon system for which it would be interesting to have experimental evidence. For this reason these problems will be briefly discussed.

4·1. *Global* (7) *and restricted* (8) *symmetry.* – When global or restricted symmetries are valid it is possible to describe the Λ- and Σ-hyperons which have ordinary isotopic spins of 0 and 1 respectively by the Y and Z doublets:

$$Y = \begin{pmatrix} - & \Sigma^+ \\ & Y^0 \end{pmatrix} \quad \text{and} \quad Z = \begin{pmatrix} Z^0 \\ \Sigma^- \end{pmatrix}, \tag{41}$$

where

$$Y^0 = \frac{\Lambda - \Sigma^0}{\sqrt{2}} \quad \text{and} \quad Z^0 = \frac{\Lambda - \Sigma^0}{\sqrt{2}}.$$

In the global symmetry description Y and Z have «isotopic spins of global symmetry» $i = \frac{1}{2}$. The $Y\pi$ and $Z\pi$ systems can be in states with $i = \frac{1}{2}$ and $\frac{3}{2}$. It is possible to express the wave functions of the $Y\pi$ and $Z\pi$ systems corresponding to $i = \frac{1}{2}$ and $\frac{3}{2}$ in terms of the wave functions of the $\pi\Lambda$ and $\pi\Sigma$ systems (9) of ordinary isotopic spin $I = 0, 1, 2$.

The relations are given in Appendix I (5.A). It is seen that the $I=0$ state is expressed in terms of the $i=\frac{1}{2}$ state only, $I=2$ in terms of the $i=\frac{3}{2}$ only, whereas for $I=1$ the following formulae are valid:

$$|\tfrac{1}{2};\ 1\ I_3\rangle = \sqrt{\tfrac{2}{3}}|1\ I_3\rangle_\Lambda + \sqrt{\tfrac{1}{3}}|1\ I_3\rangle_\Sigma \tag{42}$$

$$|\tfrac{3}{2};\ 1\ I_3\rangle = \sqrt{\tfrac{1}{3}}|1\ I_3\rangle_\Lambda - \sqrt{\tfrac{2}{3}}|1\ I_3\rangle_\Sigma \tag{43}$$

(7) M. Gell-Mann: *Phys. Rev.*, **106**, 1296 (1957).
(8) *E.g.*, see: B. d'Espagnat and J. Prentki: *Nucl. Phys.*, **9**, 326 (1958).
(9) D. Amati and B. Vitale: *Nuovo Cimento*, **9**, 895 (1958).

$|1\, I_3\rangle_\Lambda$ and $|1\, I_3\rangle_\Sigma$ are the normalized charge wave functions for $I=1$ and $\frac{1}{2}$; $1\, I_3\rangle$ and $|\frac{3}{2}$; $1\, I_3\rangle$ are the normalized wave functions for $i=\frac{1}{2}$ and $i=\frac{3}{2}$ respectively corresponding to $I=1$.

As a consequence when one discusses the resonating state which we have considered and which has $I=1$, in the frame of global or restricted symmetry, the appropriate description is in terms of the functions $|\frac{1}{2}; 1\, I_3\rangle$ and $|\frac{3}{2}; 1\, I_3\rangle$. In other words, the wave functions of π-Λ and π-Σ which correspond to the decay of the isobar H* must appear either in the combination $|\frac{1}{2}\, 1\, I_3\rangle$ or in the combination $|\frac{3}{2}\, 1\, I_3\rangle$ of the $|1\, I_3\rangle_\Lambda$ and $|1\, I_3\rangle_\Sigma$. Evidently this determines the branching ratios $(\Lambda+\pi)$ to $(\Sigma+\pi)$. Two cases must be distinguished.

i) Global symmetry. – In global symmetry (where all π interactions are identical $g_1=g_2=g_3=g_4$) (*) one knows that the resonant $(Y\pi)$ and $(Z\pi)$ systems must be in the state $i=\frac{3}{2}$, $J=\frac{3}{2}$ which is the analogue of the (3, 3) resonance of the π-$\mathcal{N}$ system. It is therefore the function $|\frac{3}{2}\, 1\, I_3\rangle$ which appears in our considerations. One then obtains for the Σ/Λ branching ratios for instance

$$\text{(44)} \qquad \mathrm{H}^{*+} \rightarrow \begin{cases} \Sigma^+ + \pi^0 : & 1 \\ \Sigma^0 + \pi^+ : & 1 \\ \Lambda \ + \pi^+ : & 4 \end{cases}$$

where kinematical corrections (**) due to the Σ-Λ mass difference have not been included.

In the case of global symmetry the fact that the resonating state has $i=\frac{3}{2}$ leads to an important prediction. Indeed from the formulae (A.6) in Appendix I, one sees that the state $I=2$ which corresponds to a $i=\frac{3}{2}$ state must also give rise to a resonance. If global symmetry were strictly valid these two resonance would coincide. However, the interactions which are responsible for the violation of global symmetry will tend to separate the position of the $I=1$ and $I=2$ resonances. Roughly speaking one would expect that this separation will be of the order of magnitude of the Σ-Λ mass difference. It seems therefore that if global symmetry has any validity one must find a second resonance with $I=2$ corresponding to an isobar H** of mass ~ 1500 MeV. It would be very interesting to detect it experimentally for instance in the reaction

$$\text{(45)} \qquad \pi + \mathrm{p} \rightarrow \Sigma + \mathrm{K} + \pi$$

through the appearance of a second resonance in the K spectrum. Obviously the H** isobar can decay in $\Sigma+\pi$ and not in $\Lambda+\pi$. The branching ratios cor-

(*) $g_1 \ldots g_4$ are the coupling constants for $\mathcal{N}\mathcal{N}\pi$, $\Sigma\Lambda\pi$, $\Sigma\Sigma\pi$ and $\Xi\Xi\pi$, respectively.
(**) This factor (~ 4) would predict a ratio $\Lambda/\Sigma^0 \simeq 16$.

responding to the decay of H** can be calculated in the standard manner. For instance the reaction

$$(46)\qquad \pi^+ + p \to \begin{cases} H^{***++} + K^0 \to \Sigma^+ + \pi^+ + K^0 \quad (8) \\ H^{***+} + K^+ \to \begin{cases} \Sigma^+ + \pi^0 + K^+ \quad (1) \\ \Sigma^0 + \pi^+ + K^+ \quad (1) \end{cases} \end{cases}$$

has the branching ratios indicated in the brackets.

ii) Restricted symmetry ($g_2 = g_3$). – The case of restricted symmetry is similar to the one just discussed. The only difference is that now the π-$\Sigma\Sigma$ and π-$\Sigma\Lambda$ coupling constants need not be equal to those of the π-$\mathcal{N}\mathcal{N}$. It is therefore impossible to assert that the resonance appears in the $i = \frac{3}{2}$ state. Two cases can occur:

a) The $I = 1$ resonance corresponds to $i = \frac{3}{2}$. One then gets the same conclusions as in the case of global symmetry, *i.e.* the branching ratio $\Lambda/\Sigma^{0(+)} = 4$ and a resonance with $I = 2$ must exist.

b) The $I = 1$ resonance corresponds to the state with $i = \frac{1}{2}$. In this case the appropriate wave functions are the $|\frac{1}{2}\ 1\ I_3\rangle$ given by (42). One gets for the branching ratio (ignoring again the Σ-Λ mass difference)

$$(47)\qquad H^{*+} \to \begin{cases} \Sigma^+ + \pi^0 : \ 1 \\ \Sigma^0 + \pi^+ : \ 1 \\ \Lambda + \pi^+ : \ 1 \end{cases}$$

If this were the case, the situation would be more favourable for the set of experiments proposed in Sections **2** and **3**.

Should the resonance occur in the $i = \frac{1}{2}$ state then one can predict the existence of another resonance in the isotopic state $I = 0$, as can be seen from expression (A.5) of Appendix I. As to the position of this resonance analogous remarks can be made in this case as in the one discussed in i). The $I = 0$ resonance H*** could be observed for instance in reactions $\pi^- + p \to H^{0***} + K^0$ or $K^- + p \to H^{0***} + \pi^0$ with the branching ratios (*)

$$(48)\qquad H^{0***} \to \begin{cases} \Sigma^- + \pi^+ : \ 1 \\ \Sigma^+ + \pi^- : \ 1 \\ \Sigma^0 + \pi^0 : \ 1 \end{cases}$$

(*) The isobars H** and H*** with $I = 2$ and $I = 0$ respectively cannot decay in $\Lambda + \pi$. However, they can give $\Lambda + \pi + \pi$ or $\Sigma + \pi + \pi$ if energetically possible. The isobar H*** could, in principle, be seen in the K^--p scattering if its mass is of the order, or heavier, than 1.4 GeV.

To summarize: if restricted symmetry holds the existence of a $I = 1$ resonance implies:

a) Either the existence of another resonance with $I = 2$ if the $I = 1$ resonance corresponds to $i = \frac{3}{2}$. In this case one has a branching ratio $\Sigma^0/\Lambda^0 = \frac{1}{4}$ (*).

b) Or the existence of an other resonance with $I = 0$ if the $I = 1$ resonance corresponds to $i = \frac{1}{2}$. The branching ratio Σ^0/Λ^0 is then equal to 1 (*).

Of course it might happen that there are resonances in all three isotopic spin states.

4·2. *A composite theory.* – We would like to add a remark on another possibility of a high symmetry property possessed by strong interactions, which is suggested from the Sakata model. Namely, a complete symmetry (valid of course only approximately) among (bare) proton, neutron and Λ-hyperon has been proposed ([10]). It is then possible to find a correspondence between the 33-resonance in π-$\mathcal{N}$ system and possible pion-hyperon resonance(s) in the $J = \frac{3}{2}$ state. Up to the « 3 body configurations » one finds three possibilities:

Pion-hyperon resonances.

case (1)	2 resonances with $I = 0$ and 1
case (2)	1 resonance with $I = 1$
case (3)	1 resonance with $I = 0$

Under this condition there are no isobars with $I = 2$ (**). It is clear that experimental studies of the isospin nature of pion-hyperon resonances are very important for eliminating some models of strong interactions. *E.g.* we know already that case (3) is excluded.

4·3. *Static model.* – It is well known that the static model in the one meson approximation describes quite well the π-$\mathcal{N}$ scattering. The same methods

(*) Ignoring the Σ-Λ mass difference.

([10]) S. Ogawa: *Prog. Theor. Phys.*, **21**, 209 (1959); Y. Yamaguchi: *Prog. Theor. Phys. Suppl.*, **11**, 1, 37 (1959); *Prog. Theor. Phys.*, **23**, 882 (1960); M. Ikeda, S. Ogawa and Y. Ohnuki: *Prog. Theor. Phys.*, **22**, 715 (1959); W. Thirring: *Nucl. Phys.*, **14**, 565 (1959-60); J. E. Wess: *Nuovo Cimento*: **15**, 52 (1960).

(**) The isobar with $S = -1$, $I = 2$ can be formed if one uses 5 (or more) body configurations.

can be applied in the case of π-hyperon scattering. This has been done by AMATI, STANGHELLINI and VITALE ([11]), and we shall discuss here certain of their results.

The position and shape of the resonances in the $\Lambda(\Sigma)$-π system depend on three parameters; a quantity related to the cut-off λ, the mass difference $m_\Sigma - m_\Lambda = \Delta$, and a parameter $\delta = (g_2^2 - g_3^2)/(g_2^2 - g_3^2)$, where g_2 and g_3 were defined above.

The position of the resonance $I = 1$, $J = \frac{3}{2}$ fixes the value of λ. If one uses the same λ as in the π-N scattering and coupling constants g_2 and g_3 of the same order of magnitude as g_1, the calculated position of H* agrees with experiment. Once λ is fixed to fit the $I = 1$ resonance one can calculate the position of the other resonances. If $g_2 \simeq g_3$ a resonance H** with $I = 2$ is predicted. The energy difference between the resonances H* and H** depends only on Δ, the contribution due to δ being negligible in this case, (only some percent of the contribution is due to δ). The difference in the position of the 2 resonances is given by $M_{\mathrm{H}^{**}} - M_{\mathrm{H}^{*}} \simeq 2\Delta$, where M_{H} is the « mass » of the corresponding isobar. With $g_2 \simeq g_3$ there is no resonance in the isotopic spin state $I = 0$. Also for reasonable coupling constants the resonances appear in the spin state $J = \frac{3}{2}$ and not $J = \frac{1}{2}$.

Of course by varying g_2 and g_3 in an arbitrary manner other situations could arise. These will not be discussed here ([12]). We wish only to point out that in the static model one expects the appearance of a resonance with $I = 2$. The predictions of the static model briefly summarised here are very similar to the ones of the global symmetry discussed in i). This is not surprising since the conditions on the cut-off and the coupling constants introduce in the static model assumptions which are in a certain way connected with a globally symmetric picture of strong interactions.

We have seen that different models predict the existence of other resonances in particular in the state $I = 2$. Experimental confirmation of these predictions would be of great interest. This could be most easily done for instance by observing the K* spectrum in the reaction

$$\pi^- + \mathrm{p} \rightarrow \begin{cases} \mathrm{H}^{*-} + \mathrm{K}^+ \rightarrow \Sigma(\Lambda) + \pi + \mathrm{K}^+ \\ \mathrm{H}^{**-} + \mathrm{K}^+ \rightarrow \Sigma + \pi + \mathrm{K}^+ \end{cases} \tag{49}$$

Such an experiment could be performed either with counters or by a time of flight measurement. One expects to find 2 peaks in the K^+ spectrum, a peak corresponding to $I = 1$ resonance and another to $I = 2$. Knowing the energy

([11]) D. AMATI, A. STANGHELLINI and B. VITALE: *Nuovo Cimento*, **13**, 1143 (1959).

([12]) For a more detailed analysis see: D. AMATI, A. STANGHELLINI and B. VITALE: *Phys. Rev. Lett.*, **5**, 524 (1960).

of the incident π and the masses M_{H^*} and $M_{H^{**}}$ to be expected, it is easy to calculate the position of the peaks in the K spectrum.

Furthermore, from the observed energies and isotopic spins of the resonances it will be possible to get some indication on the strength of the coupling constants g_2 and g_3.

In any case a counter experiment such as the one proposed here will give indications on the cross-sections for the resonant process. This information is necessary for the planning of the bubble chamber experiments proposed in Sections **2** and **3**, to measure the Σ-Λ parity and the ratio α_Λ/α_0.

To conclude, let us remark that all the considerations of Section **4** have been made under the assumption that the Σ-Λ parity is even. Calculations are in progress at CERN to study the predictions of the static model in the one meson approximation for the case of opposite Σ-Λ parity.

5. – Discussion and conclusions.

Our proposal for determining the Σ-Λ parity and the ratio α_Λ/α_0 rests upon the measure of up/down asymmetries with respect to the production plane S, in the decay (a′), (b″) and (c′) of all the Σ^+ and of all the direct and indirect Λ's respectively. By fixing the K^+ direction and energy, in the manner explained in Section **2**, one expects to minimize the background of non resonant channels (1) and (5) where the isobar H^* is not formed in the intermediate stage. If the lifetime of H^* were long, one would be in a more favourable situation for the neglect of interference effects due to non resonating channels. The fact that the H^* resonance has an observed width of ~ 25 MeV (which means a lifetime $\sim 10^{-23}$ s) implies that even with our choice of events around the resonance peak the total cross-section for the resonating process will be spread out thus reducing the ratio of resonating to non resonating cross-section in the K^+ energy band considered. In the present situation of the theory of strange particles it is extremely difficult to estimate this interference effect, and one will have to rely on future experimental investigation of the resonance to appraise the validity of the isobar model. Along this line several tests can be suggested. For instance in the resonating channel $I = 1$ one must have $\sigma(\pi^+ + p \to K^+ + \Sigma^0 + \pi^+) = \sigma(\pi^+ + p \to K^+ + \Sigma^+ + \pi^0)$. The deviation from this expected branching ratio would give an indication on the relative importance of the non resonating interference terms mentioned above. Furthermore, one can investigate by the usual methods (Adair test, etc.) the resonances and check if the angular distribution of the pions associated with the decay of the conjectured isobar is compatible with a π-Λ (π-Σ) system in a pure total angular momentum state, etc.

Another possible test of the validity of the isobar model will be to check whether the $|\alpha_\Lambda/\alpha_0|$ obtained from our proposed experiment is close to 1 or not.

An indication which is favourable to the isobar model is that $\sim \frac{3}{4}$ of the $K^- + p \to \Lambda + \pi^+ + \pi^-$ events in the experiment ([1]) mentioned in Section **1** seem to pass through the resonance H^*. This lends support to our assumption (1) of Section 2 that H^* is a « good » resonance.

Let us also remark that in the case where the isobar is excited through the $K^- + p$ reactions (6)–(8) there is an additional interference due to the presence of 2 pions in the final state. Even if one considers only resonating channels the transition amplitude for the process describing a π^- associated with the production of H^{*+} will interfere coherently with the corresponding one for the π coming from the decay of H^{*-} produced in association with π^+. This effect can be appreciable if H^* has a short lifetime. A similar situation arises in the pion production,

$$\pi + \mathcal{N} \to \mathcal{N} + \pi + \pi \,. \tag{50}$$

The influence of the short lifetime of the pion-nucleon isobar on the branching ratios and on the pion spectrum in reaction (50) has been previously considered ([13]). In analogy to the problems discussed here it would be also interesting to study the validity of the pion-nucleon isobar model by measuring the branching ratios in reaction (50) when the energy of one of the emitted pion is on the resonance (*).

For the reasons just mentioned it seems therefore that reactions (18) with production of a K and a π in the final state might have smaller interference effects at the resonance (than *e.g.* reactions (1) and (5)) and might be better suited for our purpose (**).

Apart from the condition that H^* be a good resonance we have mentioned in Section **2** that the proposed measurements of the Σ-Λ parity and of α_Λ/α_0 is feasible if the Σ/Λ branching ratio is not disastrous. As was discussed in Section **4**, the cases of the global symmetry and of the static model (with however some assumptions on the coupling constants g_2 and g_3) lead to a very unfavourable branching ratio Σ/Λ of the order of 1/20. There are, however, no strong reasons to believe such predictions. In particular, it was assumed that the Σ-Λ relative parity is even and this is just what we are looking for.

([13]) *E.g.*, see: B. D'Espagnat and J. Prentki: *Nuovo Cimento*, **1**, 486 (1955); S. Bergia, F. Bonsignori and A. Stanghelini: *Nuovo Cimento*, **16**, 1073 (1960).

(*) If, for example, the H^* isobar is the perfect analogue of the 3.3 isobar of the π-$\mathcal{N}$' system (see, *e.g.* the global symmetry case) then the experimental information observed by studying reaction (50) can be used for an estimation of the interference effects connected with $K^- + p \to \Lambda(\Sigma) + \pi + \pi$.

(**) A systematic study of reactions of the type (22) can give eventually also some indications on the existence (or non-existence) of a ΛK and a πK resonance. If a ΛK resonance would exist, some interesting conclusions could be deduced from it.

It should be remarked that if the resonance happens to be in a state of $i = \frac{1}{2}$ or $J = \frac{1}{2}$ (or both) the Σ/Λ branching ratio would be more favourable for our proposal. In all other cases it is difficult to predict the Σ/Λ branching ratio and an experimental study of it is urgently needed.

In any case, and this will be our conclusion, it seems that a systematic investigation of reactions like (18) leading to resonant processes of the systems $\pi\Lambda$ and $\pi\Sigma$ can be very rich in consequences. If the resonances are sufficiently pronounced and if the polarization are large enough, a quite ambitious program giving the Σ-Λ relative parity, α_0/α_Λ, etc., can be attempted. Even if some of these conditions are not satisfied, such an investigation would certainly provide a check of the theoretical predictions concerning other resonances. The properties of various resonances or even their non-existence will give a clearer idea on the fundamental nature of the interactions of strange particles.

* * *

We are grateful to Drs. D. Amati, V. Glaser and B. Vitale for interesting discussions.

Two of us (P.M. and Y.Y.) would like to thank CERN for its hospitality.

Appendix I

In the global (and restricted) symmetry, the « doublet » description for Λ and Σ is used. The « i » spin is introduced; $i = \frac{1}{2}$ for all baryons

$$\begin{pmatrix} p \\ n \end{pmatrix}, \qquad \begin{pmatrix} -\Sigma^+ \\ \Upsilon^0 \end{pmatrix}, \qquad \begin{pmatrix} Z_0 \\ \Sigma^- \end{pmatrix}, \qquad \begin{pmatrix} \Xi^0 \\ \Xi^- \end{pmatrix},$$

and $i = 1$ for pions. The i spin is the same as the ordinary isotopic spin I for pions, nucleons and cascade.

The systems $\pi\mathrm{Y}$ and $\pi\mathrm{Z}$ can be described in terms of charge wave functions

$$(\mathrm{A.1}) \qquad |\tfrac{1}{2} i_3\rangle_\mathrm{Y}, \quad |\tfrac{1}{2} i_3\rangle_\mathrm{Z} \quad \text{and} \quad |\tfrac{3}{2} i_3\rangle_\mathrm{Y}, \quad |\tfrac{3}{2} i_3\rangle_\mathrm{Z},$$

corresponding to the total $i = \frac{1}{2}$ and $i = \frac{3}{2}$ respectively. These functions are easily obtained. They are analogous to the wave functions of the $\pi\mathcal{N}$ system with $i = I = \frac{1}{2}$ or $\frac{3}{2}$.

Since the global (restricted) symmetry is a particular case of the charge independent theory the wave functions (A.1) can be expressed in terms of the (normalised) eigenfunctions

$$(\mathrm{A.2}) \qquad |I\, I_3\rangle_\Lambda, \qquad |I\, I_3\rangle_\Sigma, \qquad (I = 0, 1, 2),$$

of the usual total isotopic spin I of the $\pi\Lambda$ and $\pi\Sigma$ systems. For our purpose it is necessary to have wave functions

$$|i;\, I\, I_3\rangle\,, \tag{A.3}$$

which are simultaneously eigenfunctions of i and I. Such wave functions can be formed by linear combinations of wave functions (A.1). Some examples are given below

$$|\tfrac{1}{2};\,0\,0\rangle = \frac{1}{\sqrt{2}}\left(|\tfrac{1}{2},\tfrac{1}{2}\rangle_Y + |\tfrac{1}{2},\tfrac{1}{2}\rangle_Z\right),$$

$$|\tfrac{1}{2};\,1\,1\rangle = |\tfrac{1}{2}\,\tfrac{1}{2}\rangle_Y\,,$$

$$|\tfrac{3}{2};\,1\,1\rangle = \tfrac{1}{2}\left(|\tfrac{3}{2},\tfrac{1}{2}\rangle_Y + \sqrt{3}\,|\tfrac{3}{2},\tfrac{3}{2}\rangle_Z\right),$$

$$|\tfrac{3}{2};\,2\,2\rangle = |\tfrac{3}{2}\,\tfrac{3}{2}\rangle_Y\,.$$

It is not necessary to write explicitly all these combinations. We want to express functions $|i;\, I\, I_3\rangle$ in terms of functions $|I\, I_3\rangle_\Lambda$ and $|I\, I_3\rangle_\Sigma$. From the charge independence, these relations are obviously independent of I_3. They must be of the form

$$|i\, I\, I_3\rangle = \alpha_{Ii}|I\, I_3\rangle_\Sigma + \beta_{Ii}|I\, I_3\rangle_\Lambda\,. \tag{A.4}$$

For $I=0$ and $I=2$ the second term of right hand side of (A.4) is evidently zero. One has then

$$|\tfrac{1}{2};\,0\,0\rangle = |0\,0\rangle_\Sigma\,, \tag{A.5'}$$

and

$$|\tfrac{3}{2};\,2I_3\rangle = |2I_3\rangle_\Sigma\,, \tag{A.5''}$$

because $|\tfrac{3}{2}\,\tfrac{3}{2}\rangle_Y = |\pi^+\Sigma^+\rangle = |2\,2\rangle_\Sigma$ and it is sufficient to find such a relation for a particular value of I_3. For $I=1$ the situation is more complicated. Bot α_{1i} and β_{1i} are different from zero. An explicit calculations shows

$$\begin{cases} |\tfrac{1}{2};\,1\,I_3\rangle = \sqrt{\tfrac{1}{3}}\,|1\,I_3\rangle_\Sigma + \sqrt{\tfrac{2}{3}}\,|1\,I_3\rangle_\Lambda\,, \\ |\tfrac{3}{2};\,1\,I_3\rangle = -\sqrt{\tfrac{2}{3}}\,|1\,I_3\rangle_\Sigma + \sqrt{\tfrac{1}{3}}\,|1\,I_3\rangle_\Lambda\,. \end{cases} \tag{A.5'''}$$

From these formulae it is clear that wave functions with $i=\frac{1}{2}$ contain $I=1$ and $I=0$ only, whereas those with $i=\frac{3}{2}$ contain $I=1$ and $I=2$.

When the π-hyperon scattering is considered in the approximation of the global (or restricted) symmetry, one can express the S-matrix elements of the I description by those of the i description. This is easily done by the use of formulae (A.5). With obvious notations one has:

$$\begin{cases} \langle\pi\Sigma|S|\pi\Sigma\rangle_{I=2} = S_{\frac{3}{2}}\,, \\ \langle\pi\Sigma|S|\pi\Sigma\rangle_{I=1} = \tfrac{1}{3}S_{\frac{3}{2}} + \tfrac{2}{3}S_{\frac{1}{2}}\,, \\ \langle\pi\Sigma|S|\pi\Lambda\rangle_{I=1} = -\dfrac{\sqrt{2}}{3}S_{\frac{3}{2}} + \dfrac{\sqrt{2}}{3}S_{\frac{1}{2}}\,, \\ \langle\pi\Lambda|S|\pi\Lambda\rangle_{I=1} = \tfrac{2}{3}S_{\frac{3}{2}} + \tfrac{1}{3}S_{\frac{1}{2}}\,, \\ \langle\pi\Sigma|S|\pi\Sigma\rangle_{I=0} = S_{\frac{1}{2}}\,, \end{cases} \tag{A.6}$$

where

$$S_i = \langle i\, I\, I_3 | S | i II_3 \rangle = {}_{\mathrm{Y}}\langle i\, i_3 | S | i\, i_3 \rangle_{\mathrm{Y}},$$

do not depend on I_3 by charge independence and also not on I, because

$${}_{\mathrm{Y}}\langle i\, i_3 | S | i\, i_3 \rangle_{\mathrm{Y}} = {}_{\mathrm{Z}}\langle i\, i_3 | S | i\, i_3 \rangle_{\mathrm{Z}} \qquad \text{and} \qquad {}_{\mathrm{Z}}\langle i\, i_3 | S | i\, i_3 \rangle_{\mathrm{Y}} = 0\,.$$

If a resonance occurs in a given state of i, formulae (A.5) give various branching ratios. From (A.6) it is seen that if a resonance occurs in $i = \frac{3}{2}$ (or $\frac{1}{2}$) then there must exist two resonances with $I = 1$ and 2 (or $I = 1$ and 0).

Appendix II

We want to discuss briefly the effect of the motion of the Λ's (or Σ's) on the up/down asymmetries. Corrections connected with this problem enter when the average described in Sect. 3 is performed. Obviously, the discussion can be done in the rest system of H* (referred to as the H* system). It is possible to treat this problem exactly but for our purpose a simple, approximate treatment is quite sufficient because, as was said, we do not think that the actual numbers given in this paper have more than a 20% significance. A non-relativistic approximation for baryons may be sufficient for our purpose (pions are treated relativistically).

Let us introduce the following notations:

$\boldsymbol{v}_\Lambda$ velocity of Λ in H* system; $\quad v_\Lambda \equiv |\boldsymbol{v}_\Lambda| = \text{const} \simeq \frac{1}{4}c$

$\boldsymbol{v}_\pi = \dfrac{\boldsymbol{q}_\pi}{\omega}$ velocity of π^- coming from Λ decay in H* system,

$\boldsymbol{v}_\pi^* = \dfrac{\boldsymbol{q}^*}{\omega^*}$ velocity of π^- coming from Λ decay in the rest system of the Λ,

$$v_\pi^* = |\boldsymbol{v}_\pi^*| = \text{const} = 0.58c\,,$$

θ^* angle between Z axis (normal to the plane S which is the direction of $\boldsymbol{P}_{\mathrm{H}^*}$) and $\boldsymbol{v}_\pi^*$;

ξ angle between Z axis and $\boldsymbol{v}_\Lambda$.

Now $\boldsymbol{v}_\pi = \boldsymbol{v}_\pi^* + \boldsymbol{v}_\Lambda$, so for the z component

$$(\boldsymbol{v}_\pi^*)_z = v_\pi^* \cos\theta^* + v_\Lambda \cos\xi\,. \tag{B.1}$$

The π^- emitted upward (downward) with respect to the plane S have $(\boldsymbol{v}_\pi)_z > 0$ ($(\boldsymbol{v}_\pi)_z < 0$). From (B.1) it is seen that the division into « up » and « down » corresponds to a critical angle θ_c^* given by:

$$\cos\theta_c^* = -\frac{v_\Lambda}{v_\pi^*}\cos\xi\,. \tag{B.2}$$

Defining $\boldsymbol{P}_\Lambda(\boldsymbol{v}_\Lambda)$ as the polarization of the Λ's in the rest system of Λ emitted in the direction $\boldsymbol{v}_\Lambda$ (*) by a polarized Π^* the up-down asymmetry, can be found from

$$\text{(B.3)} \qquad \frac{(\text{up})}{(\text{down})} = \frac{\int_{-1}^{1} f(\xi)\,\mathrm{d}\cos\xi \int_{\cos\theta_c^*}^{1} \mathrm{d}\cos\theta^* \int_0^{2\pi} \mathrm{d}\varphi^* \left[1 + \alpha_\Lambda \boldsymbol{P}_\Lambda(\boldsymbol{v}_\Lambda)\cdot(\boldsymbol{q}^*/|\boldsymbol{q}^*|)\right]}{\int_{-1}^{1} f(\xi)\,\mathrm{d}\cos\xi \int_{\cos\theta_r^*}^{1} \mathrm{d}\cos\theta^* \int_0^{2\pi} \mathrm{d}\varphi^* \left[1 - \alpha_\Lambda \boldsymbol{P}_\Lambda(\boldsymbol{v}_\Lambda)\cdot(\boldsymbol{q}^*/|\boldsymbol{q}^*|)\right]},$$

where $f(\xi)$ is the angular distribution of Λ's in the Π^* system (an average over the azimuthal angle is already done).

Now

$$\text{(B.4)} \qquad \int_{-1}^{1} f(\xi)\,\mathrm{d}\cos\xi \int_{\cos\theta_c^*}^{1} \mathrm{d}\cos\theta^* \int_0^{2\pi} \mathrm{d}\varphi^* \left(1 + \alpha_\Lambda \boldsymbol{P}_\Lambda(\boldsymbol{v}_\Lambda)\cdot\frac{\boldsymbol{q}^*}{|\boldsymbol{q}^*|}\right) =$$

$$= 2\pi \int_{-1}^{1} f(\xi)\,\mathrm{d}\cos\xi \int_{\cos\theta_c^*}^{1} \mathrm{d}\cos\theta^* \left(1 + \alpha_\Lambda P_{\Pi^*} g(\xi)\cos\theta^*\right) =$$

$$= 2\pi \int_{-1}^{1} f(\xi)\,\mathrm{d}\cos\xi \left[1 + \frac{v_\Lambda}{v_\pi^*}\cos\xi + \frac{1}{2}\left\{\alpha_\Lambda P_{\Pi^*} g(\xi)\left(1 - \frac{v_\Lambda^2}{v_\pi^{*2}}\cos^2\xi\right)\right\}\right],$$

where (B.3) has been used. $g(\xi)$ is a known function of ξ since the explicit form of $\boldsymbol{P}_\Lambda(\boldsymbol{v}_\Lambda)$ can be found. The linear term in $\cos\xi$ in the last integrand does not contribute to the final result because $f(\xi)$ is an even function of $\cos\xi$ due to the parity conservation. This shows that the corrections due to the finite velocity of Λ's are quadratic in v_Λ/v_π^*.

Further we notice that

$$\text{(B.5)} \qquad \frac{\int_{-1}^{1} f(\xi) g(\xi)\, P_{\Pi^*}\,\mathrm{d}\cos\xi}{\int_{-1}^{1} f(\xi)\,\mathrm{d}\cos\xi} = P_\Lambda\,,$$

is precisely what we have called the « average polarization » of the Λ's in the text (see Sect. 2). From (B.3), (B.4) and (B.5) one has

$$\text{(B.6)} \qquad \frac{(\text{up})}{(\text{down})} = \frac{1 + \frac{1}{2}\alpha_\Lambda P_\Lambda\{1 - \varepsilon(v_\Lambda/v_\pi^*)^2\}}{1 - \frac{1}{2}\alpha_\Lambda P_\Lambda\{1 - \varepsilon(v_\Lambda/v_\pi^*)^2\}},$$

where

$$\text{(B.7)} \qquad \varepsilon = \frac{\int_{-1}^{1} f(\xi) g(\xi)\cos^2\xi\,\mathrm{d}\cos\xi}{\int_{-1}^{1} f(\xi) g(\xi)\,\mathrm{d}\cos\xi}.$$

(*) For given J and $\pi(\Pi^*)/\pi(\Lambda)$, $\boldsymbol{P}_\Lambda(\boldsymbol{v})$ can be explicitly written down in terms of P_{Π^*} and $\boldsymbol{v}_\Lambda$.

We have calculated ε for the very simple case $J = \frac{1}{2}$, $\pi(\mathrm{H}^*)/\pi(\Lambda) = -1$ with the results $\varepsilon = \frac{1}{3}$. In general $|\varepsilon|$ must be a small number. From this property of ε together with $(v_\Lambda/v_\pi^*)^2 \simeq \frac{1}{5}$ it is seen that the corrections on the up/down asymmetry induced by the motion of the Λ's are of the order of $(5 \div 10)\%$ at most, so they are of no importance for the considerations of Sects. 3 and 4. Similar estimations can be made for the case of decays of H^* via Σ. The corrections induced by the motion of Σ's are even smaller because $v_\Sigma < v_\Lambda$.

Furthermore, similar calculation applied to the chain decay process $\Sigma^0 \to \Lambda + \gamma$ shows that the effect of finite velocity of the Λ's to the $\searrow \mathrm{p} + \pi$ up/down asymmetry of π^- with respect to the plane perpendicular to the Σ^0-polarization is negligibly small ($< 1\%$).

RIASSUNTO (*)

L'esistenza di una risonanza nel sistema iperone-pione porta alla possibilità di determinare la parità relativa Σ-Λ ed il rapporto α_Λ/α_0 dei coefficienti di asimmetria α_Λ (in $\Lambda \to \mathrm{p} + \pi^-$) e α_0 (in $\Sigma^+ \to \mathrm{p} + \pi^0$). In questo scritto si fa una proposta che permette di determinare queste quantità misurando soltanto le asimmetrie alto/basso dei pioni provenienti dai decadimenti Λ e Σ. Si discutono vari aspetti di questa proposta. Si è anche messa in evidenza la possibile esistenza di altre risonanze. In particolare si mostra che l'esistenza di una risonanza nello stato di spin isotopico $I=1$ porta ad alcune predizioni relative all'esistenza di un altra risonanza, probabilmente nello stato $I=2$.

(*) *Traduzione a cura della Redazione.*

LETTERE ALLA REDAZIONE

(La responsabilità scientifica degli scritti inseriti in questa rubrica è completamente lasciata dalla Direzione del periodico ai singoli autori)

Dielectric Properties of SnO_2.

L. V. Deshpande and V. G. Bhide

Institute of Science - Bombay

(ricevuto il 13 Settembre 1960)

The discovery of the phenomenon currently known as ferroelectricity was made in 1921 by Valasek [1] during an investigation of the dielectric properties of Rochelle salt. Since this early discovery, large number of substances [2] have been identified as ferroelectrics and a search is still going on to find a few more mainly because of their great utility in electronics and electroacoustics. Recently, Bhide *et al.* [3] and Das [4] have established that naturally occurring ores of pyrolusite (MnO_2) exhibit ferroelectric properties. Similarly, Nicolini [5] has reported that a material made of titanium dioxide behaves as a ferroelectric substance. It is of interest to note that both MnO_2 and TiO_2 crystallize in body centred tetragonal lattice with O—Mn—O and O Ti—O as the basis respectively. Further the central metal ion (Mn in MnO_2 and Ti in TiO_2) is surrounded by a somewhat distorted oxygen octahedron. Of the class of substances which crystallize in a similar structure and follow the above condition, SnO_2 appears prominent. It was therefore of great interest to study dielectric properties of SnO_2.

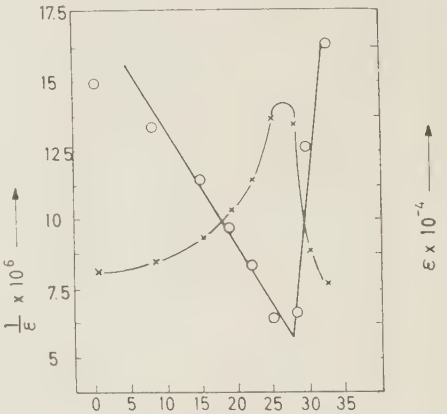

Fig. 1.

Employing essentially a similar method as reported by Volper, Koops, Verwey and Bhide *et al.* [1], it was

(1) J. Valasek: *Phys. Rev.*, **17**, 475 (1921).

(2) G. Busch and P. Scherrer: *Naturwiss.*, **23**, 737 (1935); E. Wainer and A. N. Salomon: *Titanium Alloy Mfg. Co. Elect. Rep.*, **8** (1942).

(3) V. G. Bhide, R. V. Damle and R. H. Dani: *Physica*, **25**, 579 (1959); V. G. Bhide and R. V. Damle: *Physica*, **26**, 33 (1960).

(4) J. N. Das: *Zeits. f. Phys.*, **151**, 345 (1958).

(5) L. Nicolini: *Nuovo Cimento*, **13**, 257 (1959).

found that the samples of SnO_2 (sintered ceramics and also compressed powder under very high pressures) exhibit an astonishingly high value of dielectric constant of the order of 10^5. Unlike other oxidic semiconductors such as Ni-Zn ferrites etc., the dielectric constant of SnO_2 is not so markedly dependent on the applied frequency in the audio frequency range. Although in the r.f. range the dielectric constant decreases with frequency, in a way similar to that reported by NICOLINI and BHIDE [3-5]. The dielectric constant ε of SnO_2 increases with the voltage applied to the specimen. ε-T (temperature) curves (Fig. 1) indicate that ε attains a maximum value at a certain temperature T_c (~ 298 °K) which fluctuates within small range from sample to sample and with the biasing field. At temperature above T_c, ε decreases in accordance with the Curie Weiss law $\varepsilon = C/(T - T_c)$. Furthermore, a dielectric hysteresis loop has been observed in SnO_2, (Figs. 2*a*, 2*b* employing a circuit similar to that of SAWYER and TOWER) [6] which shows beyond doubt, the existence of spontaneous polarization which is characteristic of every ferroelectric substance. In addition, these samples exhibit electromechanical coupling below T_c. These results suggest that similar to pyrolusite (MnO_2) and titanium oxide, SnO_2 seems to exhibit ferroelectric properties. Further work regarding transition at the Curie temperature is in progress.

Fig. 2*a*. — T 2 °C.

Fig. 2*b*. — $T = 30$ °C.

[6] C. B. SAWYER and C. H. TOWER: *Phys. Rev.*, **35**, 269 (1930).

On a Consequence of the Two-Centre Model of Cosmic Ray Jets.

E. M. Friedländer

Cosmic Ray Laboratory, Institute of Atomic Physics - Bucharest

(ricevuto il 28 Settembre 1960)

The two-cone structure of cosmic-ray jets has been given a consistent interpretation [1,2] by assuming that the mesons are radiated independently and isotropically from two «hot» centres moving away from each other with Lorentz factor $\bar{\gamma}$ in the c.m.s. of the colliding nucleons. In a previous paper [3] it has been shown that the value and the behaviour of $\bar{\gamma}$ can be explained, assuming the two centres to be the result of a pair of quasi independent pion-nucleon (nucleon-pion) collisions, involving individualized pions in the meson clouds of the two colliding nucleons. A similar model has been advanced independently by Yajima, Takagi and Kobayakawa [4] (*).

The purpose of this letter is to show that the concept of meson-nucleon collisions is not introduced ad hoc in the two-centre model, but that the basic assumptions of this model automatically imply a close relationship between $\bar{\gamma}$ and the structure of the collision partners.

We shall make use of the method of Birger and Smorodin [5] which yields the effective target mass M_t in terms of the quantities

$$A_i = E_i - p_i \cos\theta_i \,, \tag{1}$$

where E_i, p_i and θ_i are energies, angles and momenta of the secondaries, measured in the laboratory system:

$$M_t = \sum_i A_i \,, \tag{2}$$

the sum being extended over the whole jet, excepting the recoil nucleon. In order to connect these quantities with the two-centre model, it is useful to derive firstly the transformation formula for A from one Lorentz frame to another one. Let μ be the mass of the secondaries, γ their Lorentz factors ($\gamma = E/\mu$) and

$$\delta = \frac{A}{\mu} = \gamma - \sqrt{\gamma^2 - 1}\cos\theta \,. \tag{3}$$

(1) P. Ciok, T. Coghen, J. Gierula, R. Holynski, A. Jurak, M. Miesowicz, T. Saniewska, O. Stanisz and J. Pernegr: *Nuovo Cimento*, **8**, 166 (1958).

(2) G. Cocconi: *Phys. Rev.*, **111**, 1699 (1958).

(3) E. M. Friedländer: *Phys. Rev. Lett.*, **5**, 212 (1960).

(4) T. Yajima, S. Takagi and S. Kobayakawa: *Prog. Theor. Phys.*, **24**, 59 (1960).

(*) I am most grateful to prof. Miesowicz for the communication.

(5) N. Birger and Yu. Smorodin: *Zurn. Exp. Teor. Fiz.*, **37**, 1355 (1959).

It is easily shown that the value δ' of δ in a system C' moving with Lorentz factor γ_s with respect to the lab. frame is connected with the lab. system value δ by

$$\delta = \delta_s \cdot \delta' , \tag{4}$$

where δ_s is related to γ_s by an equation similar to (3) with $\theta_s = 0$. We shall now identify C' with the centre moving forward in the c.m.s. (lab. frame Lorentz factor γ_s^+). Owing to the isotropy of the angles θ' the average value of δ' is

$$\langle \delta' \rangle = \langle \gamma' \rangle , \tag{5}$$

where $\langle \gamma' \rangle$ is averaged over the C' spectrum of the secondaries. If the forward cone is to be treated as a separate jet ([1,2]), it is connected with a target mass M_t^+:

$$M_t^+ = \mu \sum_{j=1}^{n^+} \delta_j = \mu n_s^+ \delta_s^+ \langle \gamma' \rangle , \tag{6}$$

where n_s^+ is the total multiplicity of the forward jet. Similarly, for the centre moving backwards in the c.m.s.:

$$M_t^- = \mu n_s^- \delta_s^- \langle \gamma' \rangle . \tag{7}$$

Assuming forward-backward symmetry, we obtain from (6), (7) and (3):

$$M_t^+ / M_t^- = \delta_s^+ / \delta_s^- = \overline{\delta^2} , \tag{8}$$

where $\overline{\delta}$ is the δ-value pertaining to $\overline{\gamma}$. Since, obviously

$$M_t^+ + M_t^- = 1 , \tag{9}$$

(the nucleon mass being taken as unity) we have

$$M_t^+ = \overline{\delta^2} / (1 + \overline{\delta^2}) . \tag{10}$$

Thus, the value of $\overline{\delta}$, *i.e.* of $\overline{\gamma}$ turns out to be a direct measure of the effective target mass responsible for the formation of the forward jet. Similar arguments hold for the backward jet, mutatis mutandis.

We shall now use experimental data on $\overline{\gamma}$-values in order to obtain the distribution of effective target masses M_t^+. This has been done for 41 cosmic-ray jets produced by nucleons ($E \geqslant 10^{11}$ eV) and recorded and measured in the Prague laboratory and 21 jets produced by heavy primary nuclei ($\langle E \rangle \sim 10^{11}$ eV/nucleon) measured in our laboratory ([6]). The average values of M_t^+ for these two groups of jets turned out to be mutually consistent. The pooled distribution of M_t^+-values for all jets is shown in Fig. 1. This distribution shows a marked peak in the vicinity of the pion mass (*i.e.* 0.15 nucleon masses). The average value of M_t^+ is (1.13 ± 0.13) pion masses. This proves that at the moment of the collision, one pion is singled out in the proper field of each of the colliding nucleons, and suffers an inelastic collision with the bulk of the other nucleon.

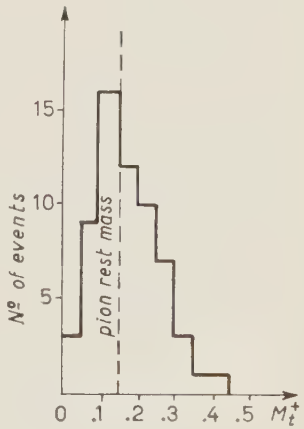

Fig. 1.

As pointed out by Birger and Smorodin ([5]), the sharpness of the peaking

([6]) E. Balea, E. M. Friedländer, C. Potoceanu and M. Sahini: *Compt. Rend. Acad. Sci. Paris*, **251**, 1487 (1960).

of the M_t^+-distribution provides a measure for the « degree of reality » of the target pion in the nucleon's pion cloud.

where n_s is the total visible multiplicity of the jet. The expected and observed values for $\sigma_{\lg\bar{\gamma}}$ are given in Table I.

TABLE I.

		Nucleon primary	Heavy primary	All jets
Average multiplicity		~ 14	~ 22	~ 16
$\sigma_{\lg\bar{\gamma}}$	expected	0.11	0.08	0.10
	observed	0.11 ± 0.01	0.07 ± 0.01	0.10 ± 0.01

We proceed now to show that the width of the peak in Fig. 1 can be accounted for mainly in terms of the statistical fluctuations involved in the estimation of $\bar{\gamma}$ from the angular distribution of each individual jet. Indeed, at high energies we have

$$\lg\bar{\gamma} \approx \tfrac{1}{2}(\lg\gamma_s^+ - \lg\gamma_s^-)\,. \tag{11}$$

Owing to isotropy in C', both $\lg\gamma_s^+$ and $\lg\gamma_s^-$ will obey gaussian distributions, with standard deviations

$$\begin{cases} \sigma_{\lg\gamma_s^+} = 0.39(n_s^+)^{-\frac{1}{2}}, \\ \sigma_{\lg\gamma_s^-} = 0.39(n_s^-)^{-\frac{1}{2}}. \end{cases} \tag{12}$$

Hence the distribution of $\lg\bar{\gamma}$ will also be a gaussian with standard deviation

$$\sigma_{\lg\bar{\gamma}} \approx 0.39 n_s^{-\frac{1}{2}} \tag{13}$$

These results prove that the width of the $\bar{\gamma}$ distribution – and hence of the observed (*i.e.* estimated) M_t^+-distribution — is due mainly to the normal fluctuations of the angular distribution. This implies a very narrow distribution of the true M_t^+-values, and hence [5] low kinetic energies of the cloud pions in the nucleon's proper fields. This justifies a posteriori the simplified approach to a pionic two-centre model [3] in which the incident nucleon and its cloud were assumed to have the same lab. system velocities.

* * *

I am very indebted to Dr. J. PERNEGR for kindly making available detailed data of the jets measured in the Prague laboratory.

Symmetry Operations for Strong and Weak Interactions.

V. Gupta

Tata Institute of Fundamental Research - Bombay

(ricevuto il 2 Ottobre 1960)

1. – Introduction.

The purpose of this note is to explore the consequences of G-conjugation [1] and S-symmetry [2] invariances for strong interactions linear and non-linear in the boson field. In Sect. **1** it is shown that these lead to parity conserving interactions for coupling of the $[\mathcal{N}\mathcal{N}\pi]$ type. In Sect. **2** it is shown how these results can be extended to K-meson couplings. Finally we discuss a new symmetry operation for weak interactions in Sect. **3**.

For the definition of charge conjugation C, time reversal T we follow Corinaldesi [3]. The transformation of bilinear forms in fermion fields is also listed in ref. [3] for the various couplings S, P, V, A, T.

2. – $[\mathcal{N}\mathcal{N}\pi]$ couplings.

In couplings of the type $[\mathcal{N}\mathcal{N}\pi]$, in general, an isotopic spin doublet $\begin{pmatrix}\psi_1\\ \psi_2\end{pmatrix}$ fermion field is coupled to a charged φ and neutral φ_0 boson field. We treat S and P and V and A couplings separately. For simplicity we will refer to the fermion doublet as nucleons and the boson field as pions.

2·1. *S and P interactions.* – The most general parity violating interaction Lagrangian [4] (with S and P couplings only) is $L=L_0+L_1$, where

$$(1)\qquad \begin{cases} L_0 = \sum_{r=0}^{\lambda} \{\overline{\psi}_1(g_r + ig'_r\gamma_5)\psi_1 + \overline{\psi}_2(f_r + if'_r\gamma_5)\psi_2\}\varphi_0^{m-2r}(\varphi\varphi^*)^r, \\ L_1 = \sum_{r=0}^{\lambda} \{\overline{\psi}_1(G_r + iG'_r\gamma_5)\psi_2\varphi_0^{m-2r-1}(\varphi\varphi^*)^r\varphi^* + \text{h.c.}\}. \end{cases}$$

(1) J. J. Sakurai: *Phys. Rev.*, **113**, 1679 (1958); S. Weinberg: *Phys. Rev.*, **112**, 1375 (1958); T. D. Lee and C. N. Yang: *Nuovo Cimento*, **3**, 749 (1958).

(2) T. D. Lee and C. N. Yang: *Phys. Rev. Lett.*, **4**, 307 (1960).

(3) E. Corinaldesi: *Nucl. Phys.*, **7**, 305 (1958).

(4) V. Gupta and S. N. Biswas: *Nuovo Cimento*, **16**, 971 (1960).

L_0 and L_1 involve the pion field « m » times. The coupling constants g_r etc. in L_0 are real and G_r etc. in L_1 are complex. Further, the upper limit, in the summation $\lambda = m/2$ in L_0 and $(m-2)/2$ in L_1 for even « m » and $\lambda = (m-1)/2$ for odd « m » in both L_0 and L_1.

It has been shown [4] that CP invariance secures parity conservation in p-p and n-n interactions (*i.e.* L_0). The TCP theorem would imply that these results are obtainable through T-invariance only and indeed this is the case. For p-n interactions, L_1, it was necessary to invoke invariance under both CP (or T) and charge symmetry C_s separately to make L_1 parity conserving [1,5]. C_s being given by $\psi_1 \rightleftarrows \psi_2$, $\varphi \rightleftarrows \varphi^*$, $\varphi_0 \rightleftarrows \varphi_0$. We wish to point out that invariance under the operation $S = TC_s$ is enough to make L_1 parity conserving. For, requiring $SL_1S^{-1} = L_1$, we obtain

$$G_r = G_r\xi\,, \qquad G'_r = -G'_r\xi\,, \tag{2}$$

where ξ is the total phase factor which arises from the T operation. It is clear that the two equations in (2) are incompatible unless G_r or G'_r vanish, thus, making L_1 parity conserving. The requirement of invariance under S is weaker than the requirement of invariance under T and C_s separately required [4,5] hitherto.

2·2. *V and A interactions.* – For vector (V) and axial vector (A) couplings between the nucleons and pions the interaction can be made parity conserving if the time reversal operation, T, is replaced by charge conjugation C. This has already been noted by Sakurai [1] for interactions linear in the pion field. We wish to point out that these results can be extended to the case of interactions non-linear in the pion field. In case of p-p, n-n interactions invariance under C and for p-n interactions invariance under $G = CC_s$ makes the interaction parity conserving. The proof follows in complete analogy to the S and P interactions.

3. – K-meson interactions.

In this section we consider the extension of the results for the pion-nucleon coupling to the interactions between baryons and K-mesons in the « doublet approximation » [6]. The general non-linear parity violating interaction Lagrangian (S and P couplings only) is given by $L_K = L_{K^0} + L_{K^+}$, where

$$L_{K^0} = \sum_{r=0}^{n} \Big[\{\overline{p}(g_r + ig'_r\gamma'_5)\Sigma^+ + \overline{n}(f_r + if'_r\gamma'_5)Y^0\} + \\ + \{\overline{Z}^0(G_r + iG'_r\gamma'_5)\Xi^0 + \overline{\Sigma}^-(F_r + iF'_r\gamma'_5)\Xi^-\}\Big](K^0\overline{K}^0)^r(K^+\overline{K}^+)^{m-r}K^0 + \text{h.c.}\,, \tag{3a}$$

$$L_{K^+} = \sum_{r=0}^{m} \Big[\{\overline{p}(h_r + ih'_r\gamma'_5)Z^0 + \overline{n}(j_r + ij'_r\gamma_5)\Sigma^-\} + \\ + \{\overline{\Sigma}^+(H_r + iH'_r\gamma'_5)\Xi^0 + \overline{Y}^0(J_r + iJ'_r\gamma'_5)\Xi^-\}\Big](K^0\overline{K}^0)^r(K^+\overline{K}^+)^{m-r}K^+ + \text{h.c.}\,. \tag{3b}$$

[5] G. Feinberg: *Phys. Rev.*, **108**, 878 (1957); S. N. Gupta: *Can. Journ. Phys.*, **35**, 1309 (1957); V. G. Soloviev: *Nucl. Phys.*, **6**, 618 (1958).

[6] A. Pais: *Phys. Rev.*, **110**, 574 (1958); **112**, 624 (1958).

(3*a*) and (3*b*) give the K^0-meson and K^+-meson interactions involving the K-meson $(2m+1)$ times. The coupling constants g_r, h_r etc. are complex and r' takes integral values. It is clear that if we define the symmetry operation (*) C_{K^0}: $N_1 \rightleftarrows N_2$, $N_3 \rightleftarrows N_4$, $K^0 \rightleftarrows \bar{K}^0$, $K^+ \rightleftarrows K^+$ then L_{K^0} becomes parity conserving if we demand its invariance under the operation $S_{K^0} = TC_{K^0}$. For the case of V and A couplings parity conservation is obtained by requiring invariance under CC_{K^0}. To make L_{K^+} parity conserving one can define instead of C_{K^0} the symmetry operators C_{K^+}: $N_1 \rightleftarrows N_3$, $N_2 \rightleftarrows N_4$, $K^+ \rightleftarrows \bar{K}^+$, $K^0 \rightleftarrows K^0$. Then invariance under TC_{K^+} makes L_{K^+} parity conserving.

It is clearly desirable to find a symmetry operation which can be applied both to L_{K^0} and L_{K^+} to give parity conservation. To be able to do this even in the linear case $(m=0)$ one has to start with an L_K which is charge independent in the Gell-Mann-Nishijima scheme and then rewrite it in the « doublet approximation » [see SAKURAI (1)]. The non-linear generalization of such a L_K in the « doublet approximation » involving the K-field $(2m+1)$ times is

$$(4) \qquad L_K = \sum_{r=0}^{m} \left[\{ \bar{N}_1 (g_r + i g_r' \gamma_5) N_2 + \bar{N}_3 (h_r + i h_r' \gamma_5) N_4 \} K^0 + \right.$$

$$\left. + \{ \bar{N}_1 (g_r + i g_r' \gamma_5) N_3 + \bar{N}_2 (h_r + i h_r' \gamma_5) N_4 \} K^+ \right] (K^0 \bar{K}^0)^r (K^+ \bar{K}^+)^{m-r} + \text{h.c.} .$$

Notice that L_K is not charge independent in the Gell-Mann-Nishijima scheme except for $m=0$. The coupling constants g_r, h_r etc. are complex. Requiring invariance of L_K under either TC_{K^0} or TC_{K^+} gives

$$g_r = \eta g_r , \qquad g_r' = -\eta g_r' ;$$

$$h_r = g_r \qquad \text{and} \qquad h_r' = g_r' ;$$

where η is the total phase factor which arises from the T operation. It is clear that for invariance we must have either $g_r = 0$ or $g_r' = 0$ thus giving a parity conserving L_K. For a non-linear L_K involving V and A couplings the modifications are straightforward. To obtain parity conservation the proofs go as above with T replaced by C.

4. – Weak interactions.

The weak interaction Lagrangian L_W, between four fermion fields ψ_A, ψ_B, ψ_C and ψ_D can be written in general as

$$(5) \qquad L_W = \sum_{ij} C_{ij} L_{ij}(AB; \bar{C}D) + \text{h.c.} .$$

(*) We use the notation that

$$N_1 \left(\begin{matrix} p \\ n \end{matrix} \right), \qquad N_2 \left(\begin{matrix} \Sigma^+ \\ \Gamma^0 \end{matrix} \right), \qquad N_3 \left(\begin{matrix} \Sigma^0 \\ \Sigma^- \end{matrix} \right), \qquad N_4 \left(\begin{matrix} \Xi^0 \\ \Xi^- \end{matrix} \right).$$

Transformations C_{K^0} and C_{K^+} have already been noted by SAKURAI (1) and G. FEINBERG and F. GÜRSEY: *Phys. Rev.*, **114**, 1153 (1959).

where $L_j(\bar{A}B;\bar{C}D)=(\bar{\psi}_A\Gamma_i\psi_B)(\bar{\psi}_C\Gamma_j\psi_D)$ and C_j are the various complex coupling constants; $i, j=S, P, V, A$ and T stand for the various possible couplings. Since L_{ij} has to be a scalar or pseudoscalar quantity it is understood that L_{SV} etc. are not included in the summation.

S-symmetry, TC_S, has been considered for weak interactions by Lee and Yang [2]. We consider the product

$$S_W = TC_W , \tag{6}$$

where the symmetry operation C_W is given by

$$\psi_A \rightleftarrows \psi_B , \qquad \psi_C \rightleftarrows \psi_D . \tag{7}$$

Requirement of the invariance of L_W under (6) gives

$$\eta C_{ii} = \quad C_{ii} , \qquad i = S, P, V, A, T;$$

and

$$\eta C_{ij} = \quad C_{ij} , \qquad i \neq j;\ i, j = V, A;$$

$$\eta C_{ij} = -C_{ij} , \qquad i \neq j;\ i, j = S, T, P;$$

The phase factor $\eta=\eta_A^*\eta_B\eta_C^*\eta_D$ arises from the phases associated with the fermion fields in the time-reversal operation. Clearly the last equation is incompatible with the first two. Thus taking (*) $\eta=1$, in particular, we find that L_W reduces to

$$L_W = \sum_i C_{ii}L_{ii} + C_{VA}L_{VA} + C_{AV}L_{AV} + \text{h.c.} . \tag{8}$$

Thus one can obtain the usual parity non-conserving V and A coupling, through the symmetry operation S_W, together with parity conserving S, T and P terms. Though the experiments show that V and A are really the dominant interactions, they do not, however, exclude an admixture of about 10% of T and possibly also about a few per cent of S interactions [7]. Thus the appearance of parity conserving S, T, P terms in L_W may not be altogether undesirable. For example, experimental evidence on the definite existence of Fierz interference terms would provide a test of the presence of S and T admixtures and possibly of S_W invariance.

It may be remarked that the requirement of the invariance of L_W under $G_W=CC_W$ would permit parity non-conserving terms involving S, T and P interactions only.

For weak interactions one would expect S_W to be more important than G_W because of the invariance under T of weak interactions. Of course, a possible objection to S_W, is that, the invariance under C_W of the free Lagrangian would require the same mass for all baryon pairs which are admitted and that all lepton pairs have equal mass.

* * *

I am very grateful to Prof. N. Dallaporta for helpful criticism and also to Drs. B. Banerjee, S. N. Biswas and D. Sankaranarayana for helpful comments.

(*) The choice $\eta=-1$ will give a purely pseudoscalar Lagrangian, involving S, T and P, and will not give parity non-conservation.

(7) C. S. Wu: *Rev. Mod. Phys.*, **31**, 783 (1959); J. S. Allen: *Rev. Mod. Phys.*, **31**, 791 (1959).

IL NUOVO CIMENTO Vol. XIX, N. 4 16 Febbraio 1961

Remark Concerning L. M. Falicov's Paper «The Theory of Photon Packets and the Lennuier Effect» (*Nuovo Cimento*, 16, 247, (1960)).

G. Beck

Centro Brasileiro de Pesquisas Fisicas - Rio de Janeiro

(ricevuto l'11 Novembre 1960)

In the quoted paper L. M. Falicov claims to give a theoretical explanation for a phenomenon reported by R. Lennuier. Radiation of narrow spectral width (Doppler width), emerging from initially excited atoms, passes through an appropriate filter which is supposed to cut the central region of the spectrum down to an insignificantly low intensity. Only the line wings reach a scattering atom at rest and interact with it outside the resonance region. According to current views, only the inciding frequencies should contribute to the scattered radiation.

No objection can be raised against Falicov's procedure to consider only the radiation which has already passed through the filter and which interacts with the scattering atom. It shall be pointed out, however, that it is not allowed to replace the spectral distribution λ_k by a «simple approximation to the real distribution» (p. 255), since λ_k is subject to the principle of causality and has, therefore, to be an analytic function whose poles have to be in one complex half plane.

1) The dispersion formula (18) has been derived by Falicov for the case of radiation which interacts with an atom assumed to be described, at $t=0$, by the ground state wave function of an *unperturbed* atom.

2) The same wave function of an atom which is placed in an external field, does not describe any longer an unexcited atom, but, due to the deformation of the wave functions by the external field, an atom which possesses a finite probability to be excited at $t=0$.

3) Only if the wave packet considered by Falicov would vanish for $t=0$ in the neighbourhood of the scattering atom, it could be claimed that this atom is, initially, unexcited. The spectral distribution, which Falicov assumes, does, however, not satisfy this requirement. The maximum of the obtained radiation at resonance frequency, does, therefore, not represent any scattered radiation, but radiation due to the initially assumed excitation of the scattering atom.

4) In order to find the correct condition to be imposed to λ_k we have to put in (A.1)

$$\sum_k H_{0k} \cdot \lambda_k \cdot \exp[i(\omega_0 - \omega_k)t] = 0 \quad \text{for} \quad t < 0 .$$

If this condition becomes satisfied, Falicov's formulae do no longer account for the phenomenon reported by Lennuier.

Nombre de mésons K^+ produits dans «Saturne» (*).

J. Teiger (**)

S.P.C.H.E., C.E.N. - Saclay

(ricevuto il 24 Novembre 1960)

Nous avons mesuré le nombre de mésons K^+ émis d'une cible interne du synchrotron à protons de Saclay, sous un angle de 35° avec la direction des protons incidents.

Le Tableau I donne les sections efficaces différentielles de production d'un méson K^+ de 0.6 GeV/c, par noyau cible, pour des cibles de C, de Cu et de Pb, et pour des protons incidents de 1.27 GeV à 2.92 GeV. Le Tableau I donne également le rapport entre les sections efficaces de production de K^+ et de π^+ de même impulsion.

Tableau I. – *Production de* K^+ *de* 0.6 GeV *à* 35°.
(Sections efficaces différentielles par noyau, en 10^{-9} bar/sr·MeV).

T_p en GeV		1.27	1.56	1.81	2.1	2.5	2.66	2.92
$\frac{d^2\sigma}{d\omega\, dT}$	C	17 ± 5	—	34 ± 7	62 ± 9	—	90 ± 13	114 ± 17
	Cu	50 ± 15	—	86 ± 17	136 ± 20	186 ± 25	316 ± 47	316 ± 47
	Pb	52 ± 15	70 ± 20	140 ± 28	235 ± 35	316 ± 47	525 ± 80	550 ± 83
$\frac{\pi^+}{K^+}$	C	69 ± 20	—	92 ± 18	89 ± 14	—	85 ± 12	66 ± 10
	Cu	61 ± 18	—	82 ± 16	52 ± 10	62 ± 10	85 ± 13	51 ± 29
	Pb	75 ± 22	99 ± 29	74 ± 15	69 ± 12	56 ± 9	56 ± 12	48 ± 8

La valeur absolue des sections efficaces dépend du calibrage absolu des électrodes d'induction. Nous estimons que ce calibrage peut être en erreur d'un facteur deux, mais qu'il est reproductible, pour l'ensemble des mesures, à environ 10 % près.

Pour une cible de Cu et pour des protons incidents de 2.72 GeV, nous avons mesuré aussi le nombre de mésons K^+ produits avec des impulsions de 0.7 GeV/c et de 0.8 GeV/c. Le Ta-

(*) Thèse présentée à la Faculté des Sciences de l'Université de Caen (no. 40, Avril 1960) (voir pour bibliographie). Publication de la méthode expérimentale à paraître dans *Nucl. Instr. and Methods*.

(**) Détaché de la Faculté des Sciences de l'Université de Caen.

bleau II donne le rapport des sections efficaces de production aux différentes impulsions.

Dans un faisceau secondaire focalisé et analysé en impulsion, les mésons K^+ ont été identifiés au moyen d'un télescope de compteurs sélectif en vitesse des particules. Il était composé de trois scintillateurs pour la définition géométrique d'un compteur Čérenkov à bande de vitesse ($n=1.5$; réflexion totale sur la face de sortie) et d'un compteur Čérenkov à seuil ($n=1.27$) en anticoïncidence. Un discriminateur d'amplitude sur la somme des impulsions provenant de deux scintillateurs fournissait une réjection supplémentaire des particules lentes.

A l'endroit des détecteurs, le faisceau était composé d'environ $2\cdot10^4$ protons, $3\cdot10^3$ π^+ et 6 K^+ pour 10^{10} protons incidents à la cible. La sélection électronique tenait compte des divers types de coïncidences fortuites qui pouvaient se produire avec des probabilités comparables aux taux des mésons K^+. Les contrôles ont montré que la sélection incluait moins de 10% d'évènements autres que des K^+ et qu'elle avait une efficacité de plus de 90%. Ces contrôles étaient basés sur les mesures suivantes:

— Temps de vol entre les scintillateurs;

— Efficacité des coïncidences en fonction de leur temps de résolution, du gain des photomultiplicateurs ou amplificateurs et du niveau de discrimination d'amplitude;

— Parcours dans le Cu des particules sélectionnées;

— Vie moyenne de désintégration des particules sélectionnées.

Tableau II. – *Production de* K^+ *de* 0.6, 0.7 *et* 0.8 GeV/c *à* 35°, *cible de* Cu, $T_p=2.72$ GeV, (Sections efficaces différentielles en unités arbitraires).

P_K en GeV/c	0.6	0.7	0.8
$d\sigma^2/d\omega dT$	1	1.66 ± 0.23	2.14 ± 0.3
π^+/K^+	85 ± 12	50 ± 7	27 ± 4

Une tentative d'interprétation du processus de production a surtout conduit aux conclusions suivantes:

Si la section efficace de production associée par un π sur un nucléon du noyau est égale à celle sur un proton libre, une fraction importante des K^+ observés doit être dûe à des π interagissant avec un nucléon avant de quitter le noyau.

Cependant, si tous les K^+ étaient créés dans ce processus par méson π intermédiaire, la variation du rapport π/K en fonction de l'impulsion de ces particules serait très différente de celle observée (Tableau II).

A Model of Hyperfragments.

G. Bhamathi (*) and S. Indumathi (**)
University of Madras - Madras

(ricevuto il 30 Novembre 1960)

1. – A model of hyperfragments.

At present the data on the interaction of the Σ and Ξ hyperons with the nucleons are very meagre. So far only a single event [1] involving a bound system of the Σ hyperon and a nucleon $\Sigma^-\mathcal{N}$ has been reported and no bound system involving a Ξ has been observed [2]. A study of the possible hyperfragments with the Σ and Ξ hyperons is made with a view to determine the Σ-$\mathcal{N}$ and Ξ-$\mathcal{N}$ potentials.

2. – Σ^--hyperfragments.

The Σ^- hyperfragments are analysed by postulating the equivalence of the Σ-p ($T=\frac{1}{2}$) and the Λ^0n system. It is of course well known that the Σ^- by exchanging pions with the proton can go over into a Λ^0 hyperon instantaneously. However we do not concern ourselves with the short lifetime of a Σ^- hyperfragment as we are interested only in the Σ^--$\mathcal{N}$ potentials.

The equations for the binding energy of the Σ^- hyperfragments in terms of its kinetic and potential energies can be written down [3]. Making use of the known binding energies for Λ^0 hyperfragments and the Λ^0-$\mathcal{N}$ potentials [4] the corresponding values for the Σ-hyperfragments can be obtained and are summarized in Table I.

The distribution of the pions originating from the decay of a Σ-hyperfragment should show the same asymmetry as that of a Λ^0 hyperfragment though the decay $\Sigma^-\to n+\pi^-$ does not possess any asymmetry. This is because the Σ-hyperfragment decays through a two-step process $\Sigma^-+p\to\Lambda^0+n$ and subsequently Λ^0 decays into a $p+\pi^-$ or $n+\pi^0$.

(*) Council of Scientific and Industrial Research Junior Research Fellow.

(**) University Grants Commission Junior Research Fellow.

(1) M. Baldo-Ceolin, C. Dilworth, W. F. Fry, W. D. B. Greening, H. Huzita, S. Limentani and A. E. Sichirollo: *Nuovo Cimento*, **7**, 328 (1958).

(2) D. H. Wilkinson, S. J. St. Lorant, D. K. Robinson and S. Lokanatan: *Phys. Rev. Lett.*, **3**, 397 (1959) and M. Baldo-Ceolin, A. Caforio, O. Fabbri, F. Farini, A. Ferilli, G. Miari and J. Schneps: *Nuovo Cimento*, **17**, 804 (1960) have observed events which can be interpreted as Ξ hyperfragments. But the evidence is not conclusive.

(3) R. H. Dalitz and B. W. Downs: *Phys. Rev.*, **110**, 958 (1958).

(4) S. Iwao and E. C. G. Sudarshan: *Phys. Rev. Lett.* (Feb. 1960).

TABLE I. – Σ^--*hyperfragments.*

Set *a*		Set *b*	
hyperfragments	binding energies	hyperfragments	binding energies
$\Sigma^{-3}\mathrm{H}$	unbound	$\Sigma^{-3}\mathrm{H}$	unbound
$\Sigma^{-4}\mathrm{H}$ ($\Sigma^{-4}\mathrm{He}$)	2.17 MeV	$\Sigma^{-4}\mathrm{H}$ ($\Sigma^{-4}\mathrm{He}$)	2.36 MeV
$\Sigma^{-5}\mathrm{H}$ ($\Sigma^{-5}\mathrm{He}$)	6.63 MeV	$\Sigma^{-5}\mathrm{H}$ ($\Sigma^{-5}\mathrm{He}$)	6.64 MeV
T_Σ	11.29 MeV	T_Σ	16.46 MeV
S_1^Σ	— 4.47 MeV	S_1^Σ	— 5.28 MeV
S_0^Σ	— 4.51 MeV	S_0^Σ	— 7.26 MeV

3. – Ξ^--hyperfragmen's.

The binding energies and Ξ-$\mathcal{N}$ potentials are calculated by considering the equivalence of $\Xi^-\mathrm{n}$ and $\Lambda^0\Sigma^-$ systems. It was possible to obtain a consistent set of solutions to these equations only if the spins of the Λ^0 and Σ^- were assumed to be in opposite directions. The values for the binding energies and Ξ-$\mathcal{N}$ potentials are summarised in Table II.

TABLE II. – Ξ^--*hyperfragments.*

Set *b*	
hyperfragments	binding energies
$\Xi^{-3}\mathrm{H}$	unbound
$\Xi^{-4}\mathrm{H}$ ($\Xi^{-4}\mathrm{He}$)	unbound
$\Xi^{-5}\mathrm{H}$ ($\Xi^{-5}\mathrm{He}$)	9.00 MeV
T_Ξ	19.38 MeV
S_1^Ξ	— 8.25 MeV
S_0^Ξ	— 3.63 MeV

The Ξ hyperfragment decays according to the scheme $\Xi + \mathrm{p} \to \Lambda^0 + \Lambda^0$. The correlation of the pions arising from the decay of these Λ^0-s has been worked out [5].

* * *

We are deeply indebted to Professor A. RAMAKRISHNAN for his constant guidance. We also with to thank Mr. A. P. BALANCHANDRAN and Mr. N. R. RANGANATHAN for interesting discussions. One of us (G.B.) is indebted to the C.S.I.R., Government of India and the other (S.I.) to the University Grants Commission for the award of fellowships.

[5] S. B. TREIMAN: *Phys. Rev.*, **113**, 355 (1959).

IL NUOVO CIMENTO Vol. XIX, N. 4 16 Febbraio 1961

Radiative Corrections to Electron-Electron and Electron-Positron Scattering.

G. Furlan and G. Peressutti

Istituto di Fisica dell'Università - Trieste
Istituto Nazionale di Fisica Nucleare - Sottosezione di Trieste

(ricevuto il 16 Dicembre 1960)

1. – We have recently calculated the contributions of the terms of order e^4 (radiative corrections) to the matrix element for the e^--e^- scattering (1). The purpose of this note is to continue and fulfill this previous work. Therefore we give and discuss here only numerical data (tables and plots) for Møller as for Bhabha scattering. We want to point out that we cannot directly compare our results with eventual experiments on e^--e^- or e^--e^+ scattering because we have calculated the contribution of the inelastic part (bremsstrahlung) only for the very particular case of an isotropic emission of soft photons (2). As we have verified in (1), these terms are sufficient to eliminate exactly the infrared divergences (3).

In this paper we intend to discuss, in evidence of the numerical data, the relative weight at different energies and angles of the corrections due to the various terms (photon self-energy, vertex parts, two-photon exchange) and give also the angular distributions so in C.M.S. as in the L.S. for both Møller and Bhabha processes.

2. – In (1) we have used for the expression of the differential cross-section of the three invariants $\varkappa$, μ and λ, whose expressions in C.M.S. and L.S. are respectively:

$$\left.\begin{aligned} \varkappa &= 2\gamma^2 - 1 \\ \mu &= \gamma^2(1 + \beta^2 \cos\theta) \\ \lambda &= \gamma^2(1 - \beta^2 \cos\theta) \end{aligned}\right\} \text{ C.M.S. ,}$$

(1) G. Furlan and G. Peressutti: *Nuovo Cimento*, **15**, 817 (1960). (Unfortunately this paper contains some mistakes and misprints. If someone wishes the correct results he can obtain it by writing directly to us).

(2) M. L. G. Redhead: *Proc. Roy. Soc.*, A **220**, 219 (1953). R. V. Polovin: *Žurn. Èksp. Teor. Fiz.*, **31**, 449 (1956) [translation: *Sov. Phys. J.E.T.P.*, **4**, 385 (1957)].

(3) A complete evaluation of the bremsstrahlung terms has been accomplished by Yung Su Tsai [*Phys. Rev.*, **120**, 269 (1960)] in connection with some experiments actually in progress at Stanford. He notes that σ_{hard} is very sensitive to experimental conditions.

$$\left.\begin{aligned} \varkappa &= \frac{\varepsilon_2}{m} = \gamma\,, \\ \mu &= \frac{\varepsilon_1'}{m} = \frac{\gamma(\gamma+1)-(\gamma-1)(\gamma+2)\cos^2\theta}{(\gamma+1)-(\gamma-1)\cos^2\theta} \\ \lambda &= \frac{\varepsilon_2'}{m} = \frac{\gamma(\gamma+1)+(\gamma-1)\cos^2\theta}{(\gamma+1)-(\gamma-1)\cos^2\theta} \end{aligned}\right\} \text{L.S.}$$

where γ is the energy of the incident electron in electronic masses and θ is the scattering angle.

The e^--e^- scattering in the lower order is described by two diagrams (direct scattering plus exchange scattering). The corrections to the order we have considered are due, for direct process, to a diagram of photon self-energy, to two vertex diagrams and to two diagrams describing two-photon exchange and as many graphs for the exchange processes.

We indicate the corresponding matrix elements with:

$$M_D^{(1)}, \quad M_{SE}^{(2)}, \quad M_V^{(2)}, \quad M_{T\,\mathrm{ph.}}^{(2)}, \quad M_{T\,\mathrm{ph.}}^{(2)'},$$

and the same for the exchange part, except with $p_1' \rightleftharpoons p_2'$, that is $\varkappa \rightleftharpoons \varkappa$, $\mu \rightleftharpoons \lambda$. So we can write for the absolute square of the total matrix element

$$|M|^2 = |M^{(1)}|^2 + 2\,\mathrm{Re}\{M^{(1)}M^{(2)}\} + |M^{(2)}|^2\,.$$

Neglecting the terms e^8, the contribution in α^3, as written in [1] formula (2), has ten finite quantities and an equal number for the exchange part. We can identify these first ten terms in this way:

$$|M_D^{(1)}|^2 + \mathrm{Re}\{M_D^{(1)}M_E^{(1)*}\} + 2\,\mathrm{Re}\{(M_D^{(1)}+M_E^{(1)})(M_{SE}^{(2)}+M_V^{(2)}+M_{T\,\mathrm{ph.}}^{(2)}+M_{T\,\mathrm{ph.}}^{(2)'})\}\,;$$

hereafter we will indicate them with I, II, III ... X.

III+IV represents the correction due to the photon self-energy, V+VI to the vertex part, VII+VIII+IX+X to two-photon exchange. Finally we will write

$$\mathrm{d}\sigma = \mathrm{d}\sigma^{(1)} + \frac{\alpha}{2\pi}\,\mathrm{d}\sigma^{(2)} = \mathrm{d}\sigma^{(1)}(1+\delta)\,.$$

For a convenient discussion of the numerical results we choose the situation where the correction has a maximum that is when direct and exchange terms are equal. This happens for $\mu=\lambda$ that is $\cos^2\theta=(\gamma+1)/(\gamma+3)$ in L.S. and $\cos\theta=0$ in C.M.S.

We can see that the total contribution of the diagrams with two-photon exchange is rather small, but at very low energies. In fact, in this case, their contribution is the only important one and its sign is negative. This seems to confirm the result that one obtains at the non relativistic limit where the correction is due only to these terms (see [2]). At high energies their sign is positive and their value, though small, is not at all negligible.

For the photon self-energy we can say that its contribution, always positive,

does not affect appreciably the value of the correction. To take into account other particles, even strongly interacting, for the vacuum polarization, does not modify appreciably this statement (4).

TABLE I. – *Møller scattering for $\mu=\lambda$ and at different energies in* MeV. *The α^2 terms are normalized to unity.*

ε_L (MeV)	ε_{CM} (MeV)	I+II	III+IV	V+VI	VII+...X	$\Sigma=1+\delta$
5	1.17	1	0.001567	0.001077	— 0.005592	0.997050
10	1.62	1	0.002383	— 0.002350	— 0.001534	0.998496
10^2	5.12	1	0.005663	— 0.030076	+ 0.008726	0.984310
10^3	15.8	1	0.009195	— 0.082921	0.016717	0.942992
10^4	50	1	0.012758	— 0.160501	0.024230	0.876486
10^5	158	1	0.016324	— 0.262733	0.031661	0.785252

Concluding, the only term really responsible for the value and sign of the correction is the vertex part. We may understand this easily because in the vertex part there appears a term (A_1 in (1)) that,at high energies, behaves as $\ln^2(2\lambda) \simeq \ln^2(q^2/m^2)$ compared with unity. [The same is true for radiative corrections to Compton scattering (5)].

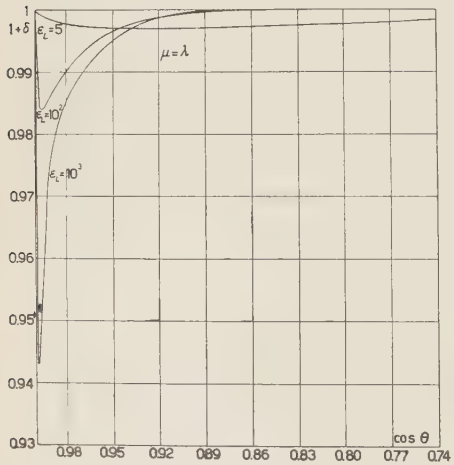

Fig. 1. – $(1+\delta)$ for electron-electron scattering as a function of the scattering angle at incident energies in L.S. of 5, 10^2 and 10^3 MeV.

We analyse now the dependence on the angle, for fixed energies, of the correction. For this purpose we plot $1+\delta$ as a function of the scattering angle θ in L.S. and in C.M.S., taking respectively for the energies the value $\varepsilon_L=5$, 10^2, 10^3 MeV in L.S. and $\varepsilon_{CM}=5$, 10, 10^2 in C.M.S. (see Fig. 1 and 2).

Looking at Fig. 1 we can see a peculiar behaviour of Møller scattering: in fact the effect in L.S. is at a maximum at very small angles (but at low energies), that is when the contribution of the direct terms and of the exchange terms become equal ($\mu=\lambda$, see also

(4) L. M. BROWN and F. CALOGERO: *Phys. Rev. Lett.*, **4**, 315 (1960).
(5) L. M. BROWN and R. P. FEYNMAN: *Phys. Rev.*, **85**, 231 (1952).

Table I). In the other part of the interval the contribution of the correction is almost non-existent.

Fig. 2 shows that on the contrary, in C.M.S. the dependence of radiative corrections on the angle is rather small: this result seems to confirm the one by YUNG SU TSAI.

(We have not included in our numerical calculations the contribution of soft photons).

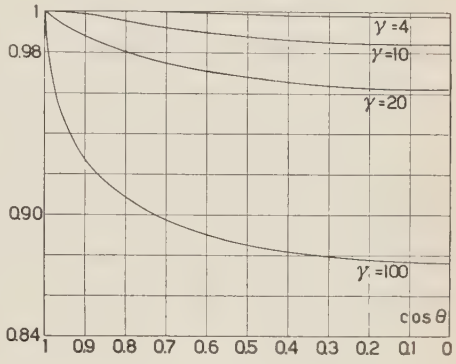

Fig. 2. – $(1+\delta)$ for electron-electron scattering as a function of the scattering angle at incident energies in C.M.S. of 2, 5, 10 and 50 MeV ($\varepsilon = m\gamma$). There the plot of the function for $\cos\theta$ negative (from 0 to -1) is simply the symmetric one of this above in respect to an axis passing across the point $\cos\theta = 0$ and parallel to the axis of ordinates.

3. – Now we want to discuss Bhabha scattering. It is well known that the essential difference between Møller and Bhabha processes lies in the fact that the exchange effect in the former case is replaced in the latter by an annihilation effect.

As is well known we can obtain Bhabha cross-section simply from Møller cross-section (formula (2) ([1])) by use of the following substitution law ([6]):

$$\lambda \rightleftharpoons \lambda, \qquad \mu \rightleftharpoons -\varkappa, \qquad \varkappa \rightleftharpoons -\mu\,. \tag{1}$$

This substitution causes a displacement of the poles, so that the integrals which occur, are, in general, to be recalculated following Feynman's prescriptions [see *e.g.* the conversion from Compton scattering to e^+-e^- annihilation into two γ ([7])]. In our case this is not always necessary, but we have again recalculated all the integrals confirming Feynman's rule.

TABLE II. – *Bhabha scattering for* $\cos\theta = 0$ *in L.S. and at different energies in* MeV. *The* α^2 *terms are normalized to unity.*

ε_L (MeV)	ε_{CM} (MeV)	I+II	III+IV	V+VI	VII+...X	$\Sigma = 1+\delta$
5	1.17	1	0.002015	— 0.001456	— 0.008302	0.992257
10	1.62	1	0.003115	— 0.007512	— 0.023905	0.971698
10^2	5.12	1	0.006704	— 0.043293	— 0.096927	0.866478
10^3	15.8	1	0.010268	— 0.103670	— 0.206270	0.700325
10^4	5	1	0.013828	— 0.188682	— 0.352519	0.472629

([6]) J. M. JAUCH and F. ROHRLICH: *The Theory of Photons and Electrons* (Cambridge, Mass., 1955).
([7]) L. M. BROWN and I. HARRIS: *Phys. Rev.*, **105**, 1656 (1957).

The meaning of the various terms in the cross-section is the same as for Møller scattering. For the discussion we follow the same order as in Sect. **2** in this paper.

We find a maximum effect of the radiative corrections at 90° in L.S. (that is 180° in C.M.S.). For different energies we have the Table II.

If we divide the contribution of every term into two parts, the former deriving from the scattering and the latter from the annihilation process, we can see that these two contributions are practically equal (but at very low energies).

Also for the Bhabha process the self-energy contribution is always positive and negligible. The vertex part is important and we can see that its sign and value are equal to those of Møller scattering. The interesting fact is that the contribution of two photon exchange graphs (VII+...X in Table II) is big and causes an enormous effect. Again we point out that we don't take into account the contribution of real photons (soft and hard). It would be very interesting to calculate this effect and verify if in this case the true correction is, as for Møller scattering ([3]), of some percents.

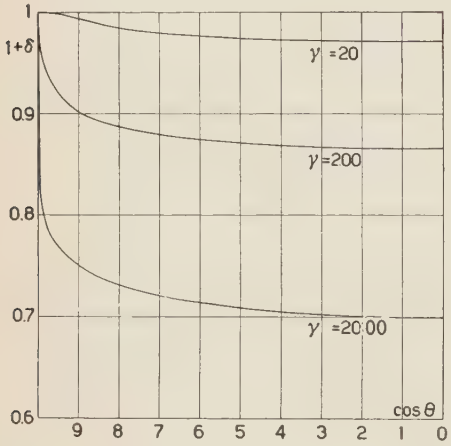

Fig. 3. – $(1+\delta)$ for electron-positron scattering as a function of the scattering angle at incident energies in L.S. of 10, 10^2 and 10^3 MeV.

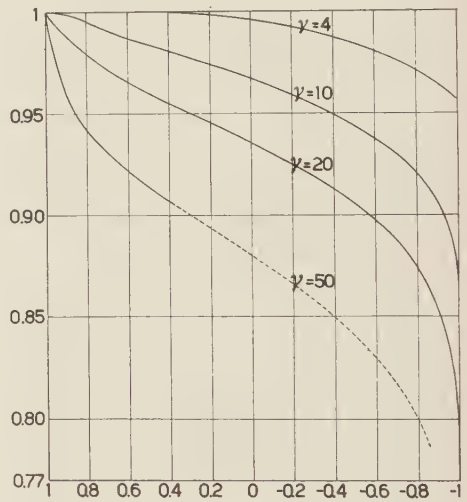

Fig. 4. – $(1+\delta)$ for electron-positron scattering as a function of the scattering angle at incident energies in C.M.S. of 2, 5, 10 and 25 MeV.

In Fig. 3 and 4 we plot $1+\delta$ as a function of the scattering angle in L.S. and C.M.S. at different energies.

* * *

The authors wish to thank Prof. P. Budini for helpful discussions and G. Bisiacchi for numerical calculations.

Note on the Polarization of Nucleons Scattered from Light Nuclei.

Y. Sakamoto

Yoshida College, University of Kyoto - Kyoto

(ricevuto il 29 Dicembre 1960)

For the incident energy of about 90 MeV, the experimental polarization of the proton scattered from ^{4}He differs from the one of ^{12}C at forward small angles, though the calculated results by the use of the optical model potential predict the same polarization for all α-particle type nuclei. Even for the incident energy of 150 MeV, small differences between the experimental data for the α-particle type nuclei are observed [1]. Here, it is important to note that in the interested angular region the polarization of p-^{4}He scattering is smaller than the one of p-^{12}C at about 90 MeV, while the former is larger than the latter at about 150 MeV.

In order to explain these differences, we take into account the charge distribution, instead of the point charge, for the target nucleus. In the present note, we use the Coulomb potential of the charge distribution defined by

$$V_C = \left(\frac{Ze}{r}\right) \mathrm{erf}\left(\frac{r}{a}\right),$$

where erf is the error function and a is the root mean square radius of the nucleus [2]. The results for the α-particle type nuclei are compared with the experimental data [3] in Table I. The experimental values are measured at $\theta_{lab}=5°$, and the calculated results are evaluated by using the Gammel-Thaler phase shifts of two-nucleon scattering at 156 MeV [4].

For the incident energy of about 90 MeV, we cannot obtain the polarization of p-^{4}He scattering smaller than the one of p-^{12}C in the interested angular region even if we take account of the charge distribution. Then, we investigate whether the effects of the pair correlations of nucleons in the nucleus explain the difference, or not.

The effects of the pair correlations of the nucleons decrease the absolute magnitudes of the central parts of the optical model potential; V_{CR} and V_{CI}, at 90 MeV [5]. V_{CI} shows stronger effects of the correlations than V_{CR}. The

[1] Y. Sakamoto: *Progr. Theor. Phys.*, **24**, 783 (1960).

[2] H. A. Bethe: *Ann. of Phys.*, **3**, 190 (1958).

[3] See ref. [1]. Ref. [1] gives the original references.

[4] J. L. Gammel and R. M. Thaler: *Phys. Rev.*, **107**, 291, 1337 (1957).

[5] A. K. Kerman, H. McManus and R. M. Thaler: *Ann. of Phys.*, **8**, 551 (1959).

stronger the correlation of pair nucleons, the smaller is V_{CI}. The spin-orbit parts of the optical model potential; V_{SR} and V_{SI}, are decreased by the effects of the correlations. V_{SI} shows stronger effects than V_{SR}. Then, the effects of the correlations give rise to a small polarization in the interested angular region at about 90 MeV. Since for the tightly bound ^{4}He one would expect the correlations to be larger than for ^{12}C, it seems that the difference of the polarizations of the protons scattered from ^{4}He and ^{12}C is explained by taking account of the effects of the correlations of nucleons in the nucleus.

The effects of the correlations on the optical model potential at 150 MeV are smaller than the ones at 90 MeV. The effects at 150 MeV do not play so important roles as the ones at 90 MeV. Then, the differences of the polarizations of the protons scattered from α-particle type nuclei at about 150 MeV are mainly caused by the charge distributions of the target nuclei.

TABLE I.

	point charge	p-^{4}He	p-^{12}C	p-^{16}O	p-^{40}Ca	n-^{12}C
experimental value		(43.7±1.9)% (149 MeV)	(42.0±2)% (135 MeV)	(37.2±3.5)% (155 MeV)	(28.3±1.9)% (155 MeV)	(22.0±8)% (155 MeV)
calculated	46.3%	45.6%	40.7%	39.1%	31.8%	22.9%

IL NUOVO CIMENTO Vol. XIX, N. 4 16 Febbraio 1961

Resonance Effects in Intermediate Boson Theory.

P. T. Matthews and A. Salam

Department of Physics, Imperial College - London

(ricevuto il 14 Gennaio 1961)

We propose here a neutrino experiment readily accessible to medium energy proton accelerators.

One of the most marked consequences of the extreme weakness of the weak interactions is the predominance by a factor of a million over the usual weak interaction processes of any effects which are of first order in the Fermi coupling constant. The first such effect to be considered theoretically [1] was the K_1^0 K_2^0 mass difference, for weak interactions allowing $\Delta S = 2$.

Other effects appear if the weak interaction is mediated by an intermediate boson, mass B, coupling g, related to the Fermi coupling constant, G, by

$$\frac{g^2}{B^2} = G = \frac{10^{-5}}{M^2},$$

where M is the nucleon mass and the final equality is an experimental result.

Consider any process

$$\alpha + \beta \to \delta + e + \nu,$$

in which the final leptons may be considered to come from the decay of a virtual intermediate boson. The matrix element is of the form

$$M(w) = F \frac{g^2}{(w^2 - B^2) - iB/\tau},$$

where w is the total energy of the leptons in their c.m. system, and τ is the lifetime of the intermediate boson. This is given by

$$\frac{B}{\tau} - \left(\frac{g^2}{4\pi}\right) B^2 \varrho - \lambda,$$

---

(1) L. Okun and B. Pontecorvo: *Zurn. Eksp. Teor. Fiz.*, **32**, 1587 (1957).

where ϱ is a factor of order 1 coming from the density of states, and hence

$$\lambda \simeq 1 \text{ (MeV)}^2 ,$$

for an intermediate boson of nucleonic mass. Thus the cross-section is proportional to

$$\sigma \sim \int |M|^2 w^2 \, \mathrm{d}w^2 = \int |F|^2 \frac{g^4}{(w^2 - B^2)^2 + \lambda^2} w^2 \, \mathrm{d}w^2 =$$
$$= |F|^2 g^4 \left[\log (w^2 - B^2) + \frac{B^2}{\lambda} \operatorname{tg}^{-1} \frac{w^2 - B^2}{\lambda} \right] .$$

If the range of integration is such as to include the interval $-30 < (w^2 - B^2)/\lambda < 30$, the process is dominated by the final term, giving

$$\sigma \simeq |F|^2 g^4 \frac{B^2}{\lambda} \pi = |F|^2 4\pi^2 g^2 \varrho .$$

If not, the final term gives a negligible contribution and

$$\sigma \simeq g^4 |F|^2 .$$

The first case, leading to a cross section larger by a factor of 10^6 arises whenever the initial energy is sufficient to create a real boson, and depends essentially on the existence of the intermediate particle. Particular cases of this effect have been noted by YANG and LEE ([2]).

Similar effects also occur for the integrated cross section in two body processes, when an intermediate boson can appear as a true resonance. The possibility of resonant scattering in

$$\bar{\nu} + e^- \to \bar{\nu} + \mu^- ,$$

has already been noted by GLASHOW ([3]). If neutral intermediate bosons exist, which are coupled to $(\bar{e}\mu)$ and $(\bar{\nu}\nu)$ pairs ([4]), there would be a similar resonance (at $E_{\text{lab}} \simeq 10^{12}$ eV) in change exchange e-μ scattering

$$e^- + \mu^+ \to e^+ + \mu^- .$$

The main point which we wish to make is that if the intermediate boson follows the renormalizable pattern proposed by TANIKAWA and WATANABE ([5]) there

---

([2]) T. D. LEE and C. N. YANG: *Phys. Rev. Lett.*, **4**, 307 (1960).

([3]) S. GLASHOW: *Phys. Rev.*, **118**, 316 (1960).

([4]) It has been remarked by LEE and YANG [*Phys. Rev.*, **108**, 1611 (1957)] that such a coupling is required if the Michel parameter is less than the value of $\frac{3}{4}$ predicted by the direct coupling of two component neutrinos. The present experimental data [M. M. BLOCK, E. FIORINI, C. KIKUCHI, G. GIACOMELLI and S. RATTI: *Proc. of* 1960 *High Energy Physics Conf.* (1960), p. 553] does not show any discrepancy within experimental errors.

([5]) Y. TANIKAWA and S. WATANABE: *Phys. Rev.*, **113**, 1344 (1959).

will be a resonance in the scattering

$$\nu + n \to p + e^-,$$

or

$$\nu + p \to n + e^+,$$

at quite low energies, ($E_{lab} \simeq 300$ MeV), readily accessible to medium energy proton accelerators, coming from the process

$$\nu + n \to B \to p + e^-,$$

where

$$B \geqslant 2\,300\ m_e .$$

If there is no resonance the cross-section is

$$\sigma = \frac{1}{2\pi} g^4 \left(\frac{p^2}{M^2}\right) \frac{1}{M^2},$$

where p is the c.m. momentum. Thus

$$\sigma \simeq 10^{-39}\ \text{cm}^2,$$

in the energy range considered.

If there is an intermediate particle

$$\sigma_R = \frac{1}{2\pi} \frac{g^4}{(w^2 - B^2)^2 + \lambda^2} p^2,$$

and the average cross section over an energy interval, Δ, which includes the resonance is

$$\bar{\sigma}_R = \sigma \frac{2\pi^2}{\varrho} \left(\frac{M}{\Delta}\right) \frac{1}{g^2}.$$

This gives rise to an average cross section of about 10^{-34} cm^2 for an energy interval of about 100 MeV which includes the resonance.

On the $e^+ + e^- \to \pi^0 + \gamma$ Process.

G. Furlan

Istituto di Fisica dell'Università - Trieste
Istituto Nazionale di Fisica Nucleare - Sottosezione di Trieste

(ricevuto il 16 Gennaio 1961)

In this note we want to discuss shortly the evaluation of the cross-section for the reaction $e^+ + e^- \to \pi^0 + \gamma$. As well known, this process will soon become possible using colliding beams of electrons and positrons and it would give some interesting information about the $\gamma\pi^0\gamma$ vertex. In the case where the two photons are real, (on the mass-shell) this vertex is directly related to the π^0 mean-life. There are however other processes which may allow a more complete determination of the form factor $\gamma\pi^0\gamma$, that is also for positive and negative values of the impulse transfer, when one photon becomes virtual, away from the mass-shell. We can cite to this end the photo-production of a π^0 in an external Coulomb field (momentum transfer space-like) and the production of the pair $\pi^0\gamma$ from the annihilation of e^+ and e^- (momentum transfer time-like). In the last case, as often discussed [1], the momentum transfer is, in c.m.s., $q^2 = -4\varepsilon^2$ and can allow the formation of resonanting intermediate states. Let us examine the structure of the matrix element and cross-section.

In the standard way we can write

$$(1) \qquad T_{FI} = (2\pi)^4 \delta(p_+ + p_- - q - k) \frac{e}{(p_+ + p_-)^2} \cdot \frac{m}{(2\pi)^3 \sqrt{\varepsilon\varepsilon'}} \langle kq \,|\, j_\mu(0) \,|\, 0 \rangle .$$

k, q are the momenta of the photon and of the pion respectively, p_+, p_- the momenta of the pair e^+e^-. From the Lorentz and gauge invariance we can write

$$(2) \qquad \langle kq \,|\, j_\mu(0) \,|\, 0 \rangle = \frac{\varepsilon_{\mu\nu\lambda\sigma} e_\nu k_\lambda q_\sigma}{(2\pi)^3 \sqrt{4\omega(q)\omega(k)}} e\boldsymbol{K}(\xi) ,$$

where $\xi = -(p_+ + p_-)^2 = 4\varepsilon^2$ and the fields are normalized to a spatial volume $(2\pi)^3$.

---

[1] N. Cabibbo and R. Gatto: *Phys. Rev. Lett.*, **4**, 313 (1960).

In the c.m.s.

$$\langle kq \,|\, j_k(0) \,|\, 0\rangle = \frac{\varepsilon}{(2\pi)^3} \frac{\delta_{kl}(\boldsymbol{e} \wedge \boldsymbol{k})_l}{\sqrt{\omega(q)\,\omega(k)}}\, e\boldsymbol{K}(\xi) \,.$$

Summing and averaging over the spins and polarizations we obtain

$$\frac{\mathrm{d}\sigma}{\mathrm{d}\Omega_k} = \frac{\alpha^2}{32}\left(\frac{\xi - m_\pi^2}{\xi}\right)^3 (1 + \cos^2\theta)\,|\boldsymbol{K}|^2 \,. \qquad (m_{\mathrm{el}}^2 \sim 0): \tag{3}$$

In order to evaluate $\boldsymbol{K}(\xi)$ we note that it is given by the dispersion relation

$$\boldsymbol{K}(\xi) = \frac{1}{\pi} \int_{4m_\pi^2}^{\infty} \frac{\operatorname{Im} \boldsymbol{K}(\xi')}{\xi' - \xi - i\varepsilon}\, \mathrm{d}\xi' ; \tag{4}$$

$\operatorname{Im} \boldsymbol{K}(\xi)$ may subsequently be analyzed studying the properties of $\operatorname{Im}[\langle kq \,|\, j_\mu(0) \,|\, 0\rangle]$. Inserting a complete system of real intermediate states we easily obtain

$$\operatorname{Im}[\langle kq \,|\, j_\mu(0) \,|\, 0\rangle] = -\frac{(2\pi)^4}{2(2\pi)^{\frac{3}{2}}} \frac{1}{\sqrt{2\omega_k}} \sum_\alpha \delta(p_\alpha - q - k) \,,$$

$$e_\nu \langle q \,|\, j_\nu(0) \,|\, \alpha\rangle \langle \alpha \,|\, j_\mu(0) \,|\, 0\rangle \,.$$

If we limit ourselves for simplicity to the two pion state (necessarily with l odd), we can write:

$$(2\pi)^3 \langle \pi^+\pi \,|\, j_\mu(0) \,|\, 0\rangle = \frac{e(p_{\pi^+} - p_{\pi^-})_\mu}{\sqrt{4\omega_+\omega_-}}\, F_\pi^*(\xi') \,, \qquad \xi' = -(p_{\pi^+} + p_{\pi^-})^2 ,$$

$$(2\pi)^3 \langle \pi^0 \,|\, e_\nu j_\nu(0) \,|\, \pi^+\pi^-\rangle = -\frac{i\varepsilon_{\nu\lambda\sigma\varrho} e_\nu k_\lambda (p_{\pi^+})_\sigma (p_{\pi^-})_\varrho}{\sqrt{8\omega(q)\omega_+\omega_-}(2\pi)^{\frac{3}{2}}\sqrt{2}}\, M(\xi', \eta') \,, \quad \eta' = -(p_{\pi^+} - k)^2 ,$$

$F_\pi(\xi)$ is the pion form-factor introduced by FRAZER and FULCO [2]. $M(\xi', \eta')$, related to the amplitude for the $\gamma + \pi \to \pi + \pi$ process, has been evaluated by H. S. WONG [3] in the hypothesis of a $\pi\pi$ resonance in the state $J = T = 1$ and his result is

$$M(\xi', \eta') \sim M_1(\xi') = \frac{A}{F_\pi(1)} \frac{1 + a}{\xi' + a} F_\pi(\xi') \,. \qquad \xi' > 4, \; m_\pi = 1 .$$

Using the data of Frazer-Fulco one obtains

$$a = 5.7 \,, \qquad F_\pi(1) = 1.08 \,,$$

A is a new coupling constant which can be derived *e.g.* from the π^0 mean-life.

---

[2] W. R. FRASER and J. R. FULCO: *Phys. Rev.*, **117**, 1909 (1960).
[3] H. S. WONG: *Phys. Rev. Lett.*, **5**, 70 (1960).

In this way WONG (*) finds

$$|A| \simeq 1.3e \,.$$

Taking into account these expressions and performing the integrations required we finally obtain

$$\text{Im}\, \boldsymbol{K}(\xi) = \frac{A(1+a)(\xi-4)^{\frac{3}{2}}}{F_\pi(1)(\xi+a)\sqrt{2\xi}} |F_\pi(\xi)|^2 \frac{1}{96\pi} \,. \qquad \xi = 4\varepsilon^2 > 4: \tag{5}$$

In conclusion our $\boldsymbol{K}(\xi)$ or the cross-section depends practically on three quantities: the position and the width, ξ_r and Γ, of the resonance which characterize $F_\pi(\xi)$ (and determine « a » and $F_\pi(1)$) and on the coupling constant A (that is on the π^0 mean-life if we assume that the $\gamma+\pi \to \pi+\pi$ reaction is the prominent intermediate process in the $\pi^0 \to 2\gamma$ decay. See (2)). The cross-section is of the order $10^{-28} \cdot \alpha^2 A^2 \sim 10^{-28}\alpha^3$ and it is interesting to see what are the effects of the form-factor $\boldsymbol{K}(\xi)$.

$\boldsymbol{K}(\xi)$ can be calculated from the (4) and taking $\xi = 2, 5, 10, 15$ (it corresponds to an energy of the incident electron in the c.m.s. $\varepsilon \simeq 98, 156, 220, 260$ MeV) we obtain the results of the following table. As we can see, when $\xi > 4$, $\boldsymbol{K}(\xi)$ has an

ξ	σ_{tot} (cm^2)	ξ	σ_{tot} (cm^2)
2	$2.449 \cdot 10^{-36}$	10	$2.029 \cdot 10^{-34}$
5	$2.345 \cdot 10^{-35}$	15	$0.641 \cdot 10^{-34}$

imaginary part which becomes important above all near the resonance ($\xi \sim 10$ see (3)). In this case the form-factor succeeds in increasing the total cross-section of a 10^2 factor (when compared to the $\xi = 2$ case). Then the cross-section decreases. As a comparison we note that the total cross-section for the reaction $e^+ + e^- \to \pi^+ + \pi^-$ is, at $\xi = 10$, $\sim 1.6 \cdot 10^{-31}$ cm^2, if we take into account the π form-factor. We can understand this difference by noticing that our cross-section contains, when compared to the $e^+ + e^- \to \pi^+ + \pi^-$ one, a term $\sim \alpha |F_\pi(\xi)|^2 \cdot g(\xi)$ which at $\xi = 10$ is really $\sim 10^{-3}$. Our situation is perhaps similar to that found by CALOGERO and BROWN (5) who studied the effect of the π-π interaction in the vacuum polarization for Møller and Bhabha scattering. Also in their work a term $\sim (\alpha |F_\pi(\xi)|^2)^2 f(\xi)$ should be considered and the result is an effect $< 1\%$ for a cross-section $\sim 10^{-32}$ cm^2, at 200 MeV in c.m.s.

As a conclusion we can say that the experimental difficulties (the products of the reaction to be revealed are practically three γ's) and the order of magnitude of

(*) A more general limitation $|A| < 2.5e$ has been found by J. S. BALL studying the effect of a π-π resonance in the photo-production (4).

(4) J. S. BALL: *Phys. Rev. Lett.*, **5**, 73 (1960).

(5) I. M. BROWN and F. CALOGERO: *Phys. Rev. Lett.*, **4**, 315 (1960).

the cross-section make this process one of the least probable ones to be revealed in the near future.

Moreover it will represent only a subsequent goal after a more detailed knowledge *e.g.* of the $\pi^+\pi^-$ production from the same e^+e^- annihilation, because our description depends completly on the features (and the existence) of the π-π interaction.

For a more complete evaluation we should take into account the contribution of the other intermediate states as the 3π state, $K\bar{K}$, $N\bar{N}$ state. Perhaps the more important will be the 3π state if there is also in this case the possibility of a bound state $T=0$, $J=1$ ([6]).

* * *

It is a pleasure to thank Professors P. Budini and S. Fubini for their encouragement.

([6]) G. F. Chew: *Phys. Rev. Lett.*, **4**, 142 (1960).

IL NUOVO CIMENTO Vol. XIX, N. 4 16 Febbraio 1961

Variation of the Rotatory Power in an Optical Antipode, Produced by 2 MeV Electrons.

A. Carrelli and F. Porreca

Istituto di Fisica Sperimentale dell'Università - Napoli

(ricevuto il 19 Gennaio 1961)

In this letter we relate shortly on some experiences in course by means of the beam of electrons accelerated by the microtron built in the Institute of Experimental Physics of the University of Naples.

Certain substances, showing rotatory power, have been bombarded with 2 MeV electrons. The average intensity of the beam, measured with a galvanometer attached to the target collecting electrons, is of 10^{-7} Amp. which corresponds to 5.10^{11} electrons/s. The cross-section of the beam is ~ 0.27 cm^2. The duration of the irradiation and the dose used in the various experiments have been measured by means of dosimetric pens.

Following substances were studied:

1) dextro-rotatory quartz and laevo-rotatory quartz;

2) alanine *d* and alanine *l*.

3) tartaric acid *d* and tartaric acid *l*.

4) ammonium tartrate *d*;

5) quinine and quinidine;

6) cinchonine and cinchonidine.

With the exception of quartz, the rotatory power, before and after the irradiation, has been measured in solution making sure of treating roughly the same quantity of the substance, in order to obtain from the beginning roughly the same value of the rotatory power for the various solutions.

The measuring instrument is a Laurent polarimeter and the experimental error which affects the measurements is $\pm 1'$.

The value of the angles α measured (before and after irradiation) does not fall below 30′ (with the only exception of alanine, whose α's are of about 10′). The experimental results obtained have shown that, with the exception of quartz whose crystals have presented a remarkable variation of optical transparence in the affected zone, which will be mentioned in another paper, the action of the electron beam produces an increase in the rotatory power value for only one of the two optical antipodes, which could be for certain substances « *l* » and for others « *d* ».

For each substance the experiments have been repeated several times: (in

particular, 21 times for tartaric acid *d* and 7 times for tartaric acid *l*).

The following table gives the qualitative indications of the results (it must be taken into account that quinidine and cinchonidine are optical antipodes of quinine and of cinchonine, respectively).

Substances which show α variation after bombardment	Substances which do not show α variation after bombardment
Alanine *d*	Alanine *l*
Tartaric acid *d*	Tartaric acid *l*
Ammonium tartrate *d*	Quarte *d* and quartz *l*
Quinine (*l*)	Quinidine (*d*)
Cinchonine (*l*)	Cinchonidine (*d*)

It must be noted that all the complex substances, except alanine which has only one asymmetric C atom, keep, in solution, practically unchanged and in the same ion form, the asymmetric molecular structure to which the type of optical activity is due.

The increasing effect is remarkable, as it is shown in the following table where $\Delta\alpha$, which is measured by 1′, represents the α increase, with respect to the value of the non-treated substance, at the same concentration c whose value is between 2.10^{-2} g/cm³ and 3.10^{-2} g/cm³ except for quinine and cinchonine whose c value is ten times less. The irradiation time is $1^{h}\,30^{min}$.

The $\Delta\alpha$ increase is relatively noticeable because, as a typical example, a solution of tartaric acid *d*, with $c=2.6\cdot10^{-2}$ g/cm³ after irradiation presents an $\alpha=56'$, that is, a $\Delta\alpha=13'$ in comparison with the value $\alpha=43'$ of the non-treated substance.

On the contrary its optical antipode, when subjected to the same irradiation, presents a variation $\Delta\alpha=\pm2'$ which means practically a variation $\Delta\alpha$ of the same order of magnitude as the experimental error.

Substances	$\Delta\alpha/c$ 1 cm³/g
Alanine *d*	$1.3\cdot10^{2}$
Tartaric acid *d*	$4.9\cdot10^{2}$
Ammonium tartrate *d*	$4.5\cdot10^{2}$
Quinine (*l*)	$20\cdot10^{2}$
Cinchonine (*l*)	$23\cdot10^{2}$

From the $\Delta\alpha$ value it is possible to arrive at the estimate of the molecular asymmetry induced by the irradiation, having first taken into account the fact that α is given by [1]

$$(8\pi^2/3)N\frac{n^2+2}{n\lambda_0}g\,,$$

where N is the number of particles per cm³, n is the refraction index, λ_0 the wave length and g *the molecular asymmetry*.

This action depends on the dose: indeed the $\Delta\alpha/c$ results, with good approximation and for at least 2^{h} irradiation, directly proportional to the dose.

The action varies in accordance with the incident beam energy and precisely, $\Delta\alpha/c$ decreases progessively, with the energy, until it vanishes completely at an energy value of about 0.5 MeV.

[1] M. Born: *Optik*, (Berlin, 1933), p. 412.

Finally it is to be noted that $\Delta\alpha$, of the measured substances in solution, varies with t, and exactly, decreases until it vanishes after a certain time interval Δt, which varies according to the different substances. This shows that the variation induced in the asymmetric group of the molecule vanishes with time.

It is our opinion that the temperature influences this tendency of the substance to return to its normal conditions, in the sense that a decrease of the temperature, in which this process is being carried out, would slacken its development. We have proved this, experimentally, by irradiating a sample of tartaric acid d and keeping it for a long period (12 hours) at dry ice temperature (~ -60 °C), and then measuring its rotatory activity.

The effect, that is the $\Delta\alpha$, of the substance subjected to this treatment, maintained itself for a much longer time compared to the one measured in the same irradiated substance which was kept twelve hours at room temperature before dissolving it and measuring its optical activity.

The work is progressing and we hope to give other information in a next paper.

IL NUOVO CIMENTO Vol. XIX, N. 4 16 Febbraio 1961

Photons Interaction with a Homogeneous Constant Magnetic Field.

A. Minguzzi

CERN - Geneva

(ricevuto il 20 Gennaio 1961)

1. – Analytici y properties in the variable $\sqrt{e^2 h_{\mu\nu} h_{\mu\nu}}$.

In the previous papers [1] we have studied the interaction of a photon field with a homogeneous and constant electromagnetic field obeying to the conditions $h_{\mu\nu}\tilde{h}_{\mu\nu} = 0$ (*), $h_{\mu\nu}h_{\mu\nu} > 0$.

It has been shown that to the order α and by using the Green functions exact in the $h_{\mu\nu}$ field [2] such an interaction can be described in terms of two indices of refraction, for which one can show to hold the dispersion relations in the photon energy, which are valid for the material media. The absorptive part of the index of refraction is connected with the existence of the process $\gamma \to e^+ + e^-$ and its threshold occurs at the photon energy $\omega = 2m$. We have also shown that for the frequencies under the threshold of the process $\gamma \to e^+ + e^-$ both indices of refraction can be developed in power series in $\sqrt{e^2 h_{\mu\nu}h_{\mu\nu}}$ which converge only asymptotically. We show now that when $\omega > 2m$, the development in power series of $\sqrt{e^2 h_{\mu\nu}h_{\mu\nu}}$, loses also this property, then it loses any meaning independently of the magnitude of $\sqrt{e^2 h_{\mu\nu}h_{\mu\nu}}$. In fact, if one had used the perturbative method not only on the α variable but also on the $\sqrt{e^2 h_{\mu\nu}\tilde{h}_{\mu\nu}}$ variable, the absorptive part of the refraction indices would have been identically zero because the Fourier transform of $h_{\mu\nu}$, $h_{\mu\nu}(k)$, is different from zero only at $\boldsymbol{k} = k_0 = 0$ and the process $\gamma \to e^+ + e^-$ is forbidden at each order; and this requires that the power series development in $\sqrt{e^2 h_{\mu\nu}\tilde{h}_{\mu\nu}}$ has zero radius of convergence. This result is related to the vacuum polarization due to a constant and homogeneous electric field. In a perturbative approach in the electric field variable no pair creation occurs and the vacuum is stationary; on the contrary a calculation which uses the Green function modified by the presence of the electric field shows at the same time the vacuum instability and the vanishing radius of convergence of the perturbative series in the electric field [2].

(*) $\tilde{h}_{\mu\nu} = \varepsilon_{\mu\nu\alpha\beta}h_{\alpha\beta}$, where $\varepsilon_{\mu\nu\alpha\beta}$ is the complete antisymmetric tensor of fourth rank.

(1) A. Minguzzi: *Nuovo Cimento*, **4**, 476 (1956); **6**, 501 (1957); **9**, 145 (1958).

(2) J. Schwinger: *Phys. Rev.* **82**, 664 (1951).

2. – Branch points of the indices of refrac ion.

From the integral expression of reference (1) the branch points of the index of refractions occur at the photon energies

$$\omega_n = 2\sqrt{m^2 + n\sqrt{e^2 h_{\mu\nu} h_{\mu\nu}}} \,. \tag{1}$$

On the other hand the energy levels of an electron in a magnetic field are

$$\pm\sqrt{p_\parallel^2 + m^2 + n\sqrt{e^2 h_{\mu\nu} \overline{h_{\mu\nu}}}} \,, \tag{2}$$

where $p_\parallel$ is the unquantized momentum along the direction of the magnetic field and n is a positive integer or zero. As it must be, from (2) follows (1) if one considers that the electron pairs interaction has been neglected, together with the possibility that more complicated processes than $\gamma \to e^+ + e^-$ contribute to the absorptive part.

3 – Time life of the process: $\gamma \to \gamma' + \gamma'$.

The results we have now discussed follow from the calculation of the vacuum polarization current in the order α^3. One can go on and calculate the terms of the vacuum current bilinear in the radiation field, $\langle j_\mu(x) \rangle_0$, which gives rise to a Hamiltonian of the form

$$H = \int \mathrm{d}^4 x : \langle j_\mu(x) \rangle_0 A_\mu(x) : ,$$

where $A_\mu(x)$ is the radiation field and this Hamiltonian is also responsible of the process $\gamma \to \gamma' + \gamma''$.

Unless the process $\gamma \to e^+ + e^-$ which cannot occur if one uses the perturbative theory, the process $\gamma \to \gamma' + \gamma''$ can occur without the intervention in the energy momentum balance of the constant and homogeneous field provided that the two end photons are emitted in the same direction of the initial photon; although this is far from being a convincing justification of the procedure, we will limit ourselves to the calculation of the S-matrix element of the transition $\gamma \to \gamma' + \gamma''$ in the lowest order of the external field. The phase space ϱ_N of N photons with energy E and momentum $\boldsymbol{Q}$ is (*)

$$\varrho_N = \lim_{m^2 \to 0} \int \prod_i \mathrm{d}^3 p_i \, \delta\Big(E - \sum_\tau \sqrt{p_\tau^2 + m^2}\Big) \, \delta\Big(\boldsymbol{Q} - \sum_\tau \boldsymbol{p}_\tau\Big) =$$

$$= \frac{\pi^{N-1} (E - |\boldsymbol{Q}|)^{3N-4}}{2^{N-1} (2N-1)!} \sum_0^m \frac{(4N-4-m)!}{(2N-2-m)!\,(3N-4-m)!} \left(\frac{2|\boldsymbol{Q}|}{E - |\boldsymbol{Q}|}\right)^m .$$

(*) This formula has been obtained by Dr. R. Hagedorn, to whom I express my thanks.

which shows that in the limit $E-|\boldsymbol{Q}|\to 0$, ϱ_N is different from zero only if $N=2$; *i.e.* the process in which a photon decays into N photons in the presence of external sources which do not contribute to the energy momentum balance has a phase space different from zero only if the final photons are two.

The matrix element of the process $\gamma\to\gamma'+\gamma''$ in the vacuum vanishes on account of the charge conjugation invariance, which entails the following transformation properties of the electrons propagator

$$\gamma\to\gamma^T, \qquad S_F(x)\to S_F^T(-x)\,, \tag{3}$$

where T means transposition.

In the presence of a constant and homogeneous electromagnetic field (3) is true only if the transposition is applied also to the tensorial indices; *i.e.* if the magnetic field is reversed. In terms of circular polarization we get the following squared matrix elements, where k, k', k'' are the components of the momenta of the three photons perpendicular to the direction of the magnetic field

$$\left|\langle \alpha k', \beta k'' | s | \alpha k\rangle\right|^2 = \frac{\pi^4}{648}\,\frac{e^8 h_{\mu\nu}h_{\mu\nu}}{2m^4\omega\omega'\omega''}\,|\boldsymbol{k}''|^2\,, \qquad \alpha\pm\beta,$$

$$\left|\langle \alpha k', \alpha k'' | s | \beta k\rangle\right|^2 = \frac{\pi^4}{648}\,\frac{e^8 h_{\mu\nu}h_{\mu\nu}}{4m^4\omega\omega'\omega''}\,|\boldsymbol{k}|^2\,,$$

where each of α, β denotes the two circular polarizations of the photons.

The fact that only the components of the momenta normal to the direction of the magnetic field is effective for the decay follows from the angular momentum conservation. In fact, if the photon field is propagating along the direction of the magnetic field the rotation invariance around the axis defined by the magnetic field direction implies that the angular momentum must balance among the three photons independently of the magnetic field, and if one analyses the photons in terms of circular polarization, he convinces himself that this is impossible.

The time life of the process τ is

$$\tau^{-1} = \frac{1}{3\pi}\,\frac{e^8 h_{\mu\nu}h_{\mu\nu}\omega}{2m^4(576\pi^2)^2}\,,$$

where one expects that this formula is true only when the photon energy w is small.

All that has been said depends critically on the fact that the photon mass is zero; the detection of the process

$$\gamma\to\gamma'+\gamma'',$$

in the case in which the external source does not contribute to the energy momentum balance, would be a proof of the zero mass of the photon.

LIBRI RICEVUTI E RECENSIONI

Physics of the Upper Atmosphere, edited by J. A. RATCLIFFE, Cavendish Laboratory, University of Cambridge, XI+586 pag., Academic Press, New York and London, 1960. $ 14,50.

Lo scopo che il libro si propone è di dare un quadro sufficientemente completo e aggiornato delle proprietà fisiche della atmosfera a quote superiori ai 60 km. Si tratta di un campo di ricerche che, se da molti anni era coltivato con metodi indiretti, oggi presenta attrattive del tutto particolari per l'avvento delle nuove tecniche di misurazione diretta con strumenti su razzi e satelliti e per la larga messe di risultati che se ne possono trarre.

La trattazione delle singole materie è affidata a ben noti specialisti. L'impressione che si trae dalla lettura del libro è decisamente favorevole; mentre da un lato costituisce, con l'abbondanza di dati numerici e di tabelle, un riferimento nel quale lo studioso trova informazioni rapide e documentate su specifiche questioni, dall'altro esso si presta ottimamente a fornire un panorama assai aperto a chi per la prima volta si interessa allo specifico genere di ricerche. La lettura riesce gradita anche a chi di geofisica in senso stretto non si occupa. È insomma un libro utile al ricercatore e allo studente. Lo scopo che il libro si proponeva si può dire ben raggiunto, anche se qua e là non mancano errori di stampa.

Diamo ora un breve schema della materia contenuta nel libro. I dodici capitoli in cui esso si suddivide trattano, rispettivamente, della termosfera e della atmosfera più esterna, delle proprietà e costituzione della atmosfera superiore, studiate sia con i metodi indiretti usuali che con la nuova tecnica dei razzi e dei satelliti, delle radiazioni ionizzanti del Sole, della luminescenza del cielo, dell'aurora polare, del suo spettro e della radioaurora, della ionosfera, degli effetti geomagnetici prodotti dalle correnti che fluiscono nell'alta atmosfera, degli sciami meteoritici; l'ultimo capitolo, infine, tratta dei primi risultati conseguiti nei suddetti campi di indagine durante l'anno geofisico internazionale 1957-1958.

La bibliografia che correda ciascun capitolo è vasta e ben rappresentativa.

F. MARIANI

R. M. FANO, L. J. CHU and R. B. ADLER – *Electromagnetic energy trasmission and radiation*, 620 p., rilegato, J. Wiley & Sons., New York, Londra, 1960.

I tre autori, insegnanti presso il Massachusetts Institute of Technology (M.I.T.), hanno raccolto in questo volume le notazioni di propagazione elettromagnetica che, nell'ambito del recente riordinamento degli schemi didattici della loro Scuola, si ritengono necessarie alla preparazione moderna di qualsiasi ingegnere elettrotecnico. Per rispondere a questi criteri didattici, la materia è classificata ed ordinata a diversi livelli

in modo da consentirne sia un esame agile e spedito che uno studio accurato ed approfondito.

Gli autori, che presuppongono nel lettore una adeguata preparazione sia matematica che sulle questioni fondamentali dell'elettromagnetismo, secondo l'impostazione da essi data in un volume a parte, esaminano via via tutti i problemi e gli schemi di propagazione dai più semplici ai più complessi partendo dalla nozione di circuito a costanti distribuite ed affrontando il comportamento a regime e transitorio delle linee non dissipative e dissipative; lo stesso criterio viene adottato per lo studio della propagazione nei mezzi materiali e guidata (onde piane nei mezzi dissipativi e non dissipativi, guide d'onda); l'ultimo capitolo dell'opera, che è corredata da esercizi e problemi su ogni argomento, è invece dedicato ai fondamenti di radiazione.

L'impostazione chiara e moderna degli argomenti trattati nell'opera, la cui veste tipografica è tra l'altro eccellente, la rendono particolarmente rispondente ai fini che le sono proposti.

F. Gasparini

L. D. Landau and E. M. Lifshitz – *Fluid Mechanics*. Un volume in 8° di pp. XII-536 con 119 figure. Pergamon Press, 1959. Prezzo rilegato scellini 105.

Il sesto volume del corso di fisica teorica di Landau e Lifshitz è dedicato alla meccanica dei fluidi come capitolo della fisica teorica. La trattazione è svolta con grande rigore matematico ma la chiarezza di esposizione, l'ottima traduzione e la notazione semplice e appropriata, ne fanno un testo adatto sia per uno studio ordinato della meccanica dei fluidi come per la consultazione dei singoli argomenti. Infatti la suddivisione dei capitoli e dei paragrafi è fatta in modo da tenere raggruppate le teorie complete dei fenomeni studiati. La trattazione comprende: il moto dei fluidi ideali e reali; il moto nelle vicinanze dei vincoli; la conduzione del calore nei fluidi; i fenomeni di diffusione e di superficie; la propagazione del suono e delle onde d'urto; il moto dei gas in una e due dimensioni; il moto dei fluidi a velocità supersoniche in presenza di corpi solidi; la dinamica delle combustioni nei fluidi; l'idrodinamica relativistica; la dinamica dei superfluidi; la teoria delle fluttuazioni nei fluidi. Non vi è cenno dei fenomeni idroelettrici e idromagnetici, ma una trattazione di questi fenomeni avrebbe richiesto troppo spazio data l'importanza e l'attualità dell'argomento. L'argomento è accennato nell'8° volume dello stesso corso di fisica teorica: *Electrodynamics of Continuous Media*. Le nozioni richieste per la lettura di questo volume sono quelle fondamentali della meccanica e della termodinamica; per la matematica, il calcolo differenziale e integrale, nonchè i rudimenti del calcolo delle variazioni.

C. Pedicino

R. M. Fano, L. J. Chu and R. B. Adler – *Electromagnetic fields, energy, and forces*, 520 pag., rilegato, J. Wiley & Sons, New York' Londra, 1960.

I tre autori, insegnanti presso il Massachusetts Institute of Technology (M.I.T.), hanno raccolto in questo volume le lezioni del corso a loro affidato, in base al recente sviluppo degli schemi didattici della loro scuola tendenti a dare agli allievi una preparazione equilibrata e moderna sugli argomenti fondamentali dell'Elettrotecnica.

Partendo dalle equazioni di Maxwell nella loro forma integrale e dalla forza di Lorenz agente sulla carica in movimento

in un campo magnetico, essi sviluppano la teoria in quattro stadi successivi: nel primo si ricavano le equazioni per i campi prodotti da cariche e correnti libere con determinate condizioni ai limiti, fornendo al lettore anche alcuni chiari complementi di analisi vettoriale; nel secondo viene trattata la polarizzazione elettrica e magnetica della materia in quiete considerando l'influenza di quest'ultima mediante opportune distribuzioni di cariche e correnti; nel terzo si introducono i concetti di energia elettromagnetica e di flusso di potenza interpretando il teorema di Poynting come la legge di conservazione dell'energia per il campo elettromagnetico; nel quarto infine si affrontano i problemi che insorgono quando vi è movimento relativo tra i componenti del sistema in esame senza valersi della teoria della relatività speciale. Va notato peraltro che, per completezza, in appendice gli autori presentano l'impostazione relativistica delle questioni esaminate.

Larga parte del testo (e questo ne costituisce senz'altro una particolarità di rilievo) è inoltre dedicata ai rapporti tra la teoria dei campi e la teoria dei circuiti, mettendo in evidenza le limitazioni proprie di quest'ultima che, come è noto, ignora le dimensioni fisiche dei componenti ma tiene conto solo del loro modo di interconnessione.

Ogni capitolo è corredato da numerosi esercizi e problemi nonchè da aggiornati riferimenti bibliografici.

Il libro è impostato su una visione accurata, chiara, moderna e completa dei problemi trattati e costituisce un'opera di indubbio pregio ed utilità.

Particolarmente curata è anche la veste tipografica.

F. GASPARINI

Direttore responsabile: G. POLVANI Tipografia Compositori - Bologna

Questo Fascicolo è stato licenziato dai torchi il 25-II-1961